



Norwegian University of
Science and Technology

Measurements of Young's Modulus on Rock Samples at Small Amplitude and Low Frequency

RockHard Deformations

Trygve Westlye Fintland

Master of Science in Physics and Mathematics

Submission date: June 2011

Supervisor: Steinar Raaen, IFY

Co-supervisor: Jørn Stenebråten, Sintef Petroleumsforskning AS

RockHard Deformations
MEASUREMENT OF YOUNGS MODULUS
ON ROCK SAMPLES AT SMALL
AMPLITUDE AND LOW FREQUENCY

Trygve Westlye Fintland

under supervision of

Jørn Stenebråten, SINTEF Petroleum Research AS

and

Steinar Raaen, Norwegian University of Science and Technology

June 20, 2011

I slit og stræv for eige gavn
i kamp og strid
vil studenten skriva seg eit namn
på tilmålt tid

Abstract

This thesis describes a new instrumental approach designed to measure the complex Young's modulus on cylindrical samples 1 inch in diameter 2 inch long and typically in the range of 1-70 GPa. Excitation frequencies are from 11 Hz to 167 Hz. The setup is based on the Forced Deformation Method (Batzle et al., 2006) and is capable of measuring phase and magnitude of the dynamic stress and strain. An actuator provides an oscillating force from one end of the plug. Strain is measured on the cylindrical side with three strain gages evenly spaced around the circumference. The lowest recordable magnitude of strain is in the order of 10^{-8} . Force is measured by a piezoelectric transducer. Values are < 10 N. Plug sample measurements of the Young's modulus values for Berea sandstone, Castlegate sandstone, Pierre shale, PEEK, and aluminium alloys (ALU-7075 and ALU-6061) are included. Reference material results are in accordance with published values. Some of the instrumentation needed is also given in detail in the previous work (Fintland, 2010).

Samandrag

Denne oppgåva gjev eit nytt instrumentelt oppsett utforma for målingar av kompleks Youngs modul på sylindriske prøvar ein tomme i diameter og to tommar lange som ligg i området 1-70 GPa. Eksitasjonsfrekvensar er frå 11 Hz til 167 Hz. Framstillinga er basert på den tvungne deformasjonsmetoden (Forced Deformation Method, Batzle et al., 2006) og kan måla fase og storleik av dynamisk kraft og tøyning. Ein aktuator yt ei oscillatorisk kraft frå den eine enden av pluggen. Tøyning blir målt på den sylindriske sida med tre strekkklappar jamnt fordelt kring midten. Den lågast målbare tøyinga er av 10^{-8} orden. Krafta blir målt med ein piezoelektrisk transdusar. Verdier er < 10 N. Målingar av Youngs modul på pluggar av Berea-sandstein, Castlegate-sandstein, Pierre-skifer, PEEK og to ulike aluminiumslegeringar (ALU-7075 og ALU-6061) ligg ved. Referansemålingar er i samsvar med publiserte data. Noko av instrumenteringa er òg gjeve i detalj tidlegare (Fintland, 2010).

Preface

Thank you SINTEF Petroleum Research AS, Trondheim and NTNU Institute of Physics by Steinar Raaen. I have received great help at both places. People have been open for discussion and have given me useful and good feedback. In particular my external mentor, Jørn Stenebråten has given me excellent support. He has prioritized his time both to explain and show me what I found hard to grasp. Looking back it would have been impossible to do this research without his feedback and continuous encouragement in the quest for the soft rock.

Rock has always been a building material for me. In our family's local farm, Fintland in Sirdalen my father and I put rock on rock such that "it settles by itself on the foundation". This time around the foundation is different. Steel and electronics surrounds it to extract the properties of the rock matrix. In the process of learning and understanding the structure and the theory, Rune M. Holt, Reidar Bøe and Tony Siggins have been great teachers.

Learning by doing has been a core part of this exercise. Big heavy machines have been operating to squeeze the sample tight. Master stone squeezer Eyvind Sønstebø helped me with the equipment.

The diversity in the exercise is great. I feel like I have done it all; reading, soldering, glueing, programming, writing and wondering. It has been a sincere pleasure being a part of this great team!

Forord

Takk til SINTEF Petroleumsforskning AS i Trondheim og NTNU Institutt for fysikk ved Steinar Raaen. Begge stader har alle dører har vore opne for meg både for diskusjon av problem og for nye innspel. Det er særleg ekstern rettleiar Jørn Stenebråten som har vore ein viktig støttespelar. I ein travel kvardag har han teke seg tid til både å forklara og å visa. I ettertid kan eg ikkje sjå korleis forskinga kunne vore gjennomført utan støtte og tilbakemeldingane eg har fått frå han i jakta på den mjuke steinen.

Stein har alltid vore eit byggemateriale for meg. På familiegarden Fintland i Sirdal lødde far, Kolbein Fintland, og eg stein slik at ”steinen la seg sjølv”. Denne gongen er grunnlaget for steinen annleis. Stål og elektronikk omkranser han for at eigenskapane til steingitteret kan studerast. I prosessen med å forstå struktur og teori har Rune M. Holt, Reidar Bøe og Tony Siggins utmerka seg som gode læremeistrar.

Læring på lab har vore ein sentral del av oppgåva. Store, tunge maskinar har vore i sving for å pressa prøven saman. Steinpressemeister Eyvind Sønstebø hjalp meg med utstyret, og me har drukke fleire kaffikoppar medan minerala blei most.

Mangfallet i oppgåva er stort. Her har eg hatt heile spekteret frå lesing lodding, liming, programmering, skriving og undring. Det har vore ei glede å få vera ein del av dette miljøet!

Mister du evnen til lek, da mister du livet.
(André Bjerke)

Contents

Abstract	v
Samandrag	v
Preface	vii
Forord	ix
Table of Contents	xiii
List of Figures	xviii
List of Tables	xxv
1 Introduction	1
2 Theory	3
2.1 The Elastic Domain	4
2.2 Poroelasticity	5
2.2.1 Porosity	5
2.2.2 Density	6
2.2.3 The Bulk Modulus	7
2.2.4 Biot's Theory	8
2.2.5 Young's Modulus E	10
2.2.6 Shear modulus G	11
2.2.7 Poisson's Number ν	12
2.2.8 The Wave Equation in Porous Media	13
2.2.9 Checking the Solutions in the Wave Equations	14
2.2.10 Relating Young's Modulus with Speed of Propagation	16
2.2.11 Dimensional Analysis of the Derived Expression for Speed	17
2.2.12 Shear Wave Velocity	17
2.3 Attenuation	17
2.3.1 The Attenuation $1/Q$	18
2.3.2 Dispersion	19
2.3.3 Cracks	19
2.4 Sensing Stress	22
2.4.1 The Piezoelectric Sensor	22
2.5 Sensing Strain	23
2.5.1 The Strain Gage	23
2.5.2 Wheatstone Bridge of Unequal Resistances, Differential Approach	23
2.5.3 Wheatstone Bridge of Unequal Resistances, Series Expanded	25

3	Equipment	29
3.1	Load Frames	29
3.1.1	The Manual Load Frame	29
3.1.2	The MTS Load Frame	31
3.2	Instruments	31
3.2.1	Hardware	31
3.2.2	Software	34
3.2.3	Drivers	35
3.2.4	Other	35
3.2.5	Interfaces and Connectors	36
3.3	Chemicals	37
4	Calibration	39
4.1	Force Sensor	39
4.1.1	Magnitude Conversion	39
4.1.2	Phase Conversion	40
4.2	Strain Gage	40
4.2.1	Magnitude Conversion	40
4.2.2	Phase Conversion	41
4.2.3	Strain Gage Wiring	41
4.2.4	Strain Gage Orientation	43
4.3	Epoxy	44
4.4	Temperature Sensor	45
4.5	Shielding of Setup	46
4.5.1	Ground Loops	47
4.5.2	Uninterruptible Power Supply	47
4.6	The time constant, t_c	47
5	Measurements	49
5.1	Sample Description	49
5.1.1	Aluminium	49
5.1.2	Berea Sandstone	51
5.1.3	Castlegate Sandstone	53
5.1.4	PEEK	53
5.1.5	Pierre Shale	55
5.1.6	Steel	56
5.2	Measurement Series Description	57
5.3	How to Conduct a Measurement - Step by step	58
5.3.1	How to Run a Measurement in LabVIEW	58

5.3.2	How to Interpret the Output of a Measurement	59
6	Post-Processing of Data	61
6.1	TDMS Logfile	61
6.2	MATLAB Scripts	61
6.2.1	RockHard Master Script - rockon - Running all sub-scripts necessary (rh1all.m → rh4sPhase.m) on the .tdms files present in folder	62
6.2.2	RockHard 1 - rh1 - Converting .tdms file to .mat file and setting constants	62
6.2.3	RockHard 2 - rh2phase and rh2fg2 - Calibrating the .mat file and calculating the Young's modulus	64
6.2.4	RockHard 3 - rh3 - Collecting data from various .mat files	64
6.2.5	RockHard 4 - rh4, rh4s and rh4sPhase - Plotting tools . .	65
6.2.6	Others	65
6.3	The Manual Load Frame	66
6.3.1	Curve Fitting	66
6.3.2	Exporting and Importing	67
6.3.3	Displaying	68
7	Sources of Errors	71
7.1	Error in Figures	71
7.2	Noise Floor	71
7.2.1	Systematic Error	72
7.2.2	Random Error	73
7.3	Time Constant	75
7.4	Non Parallel Surfaces and Stress	76
7.5	Temperature Correction	77
7.5.1	Temperature Coefficient of Resistance for Bondable Re- sistors	77
7.5.2	Gage Factor Variation with Temperatur	77
8	Results	79
8.1	The Manual Load Frame	79
8.2	The MTS Load Frame	80
8.2.1	The Cutoff Frequency	81
8.2.2	Aluminium 7075 and Aluminium 6061	82
8.2.3	Berea Sandstone	92
8.2.4	Castlegate Sandstone	96

8.2.5	PEEK	102
8.2.6	Pierre Shale	105
8.2.7	Steel	109
8.3	Direct and Indirect Measurements of Strain	109
8.4	Phase Measurements	109
8.4.1	Consistency Check	118
8.5	Results summary	119
9	Discussion	121
9.1	Instrumentation	121
9.2	Measurements	125
10	Conclusion	133
10.1	Further work	134
10.1.1	Hardware	134
10.1.2	Software	134
10.1.3	Chemical	135
10.1.4	Other	135
11	References	137
11.1	Creative Commons' References	141
A	The Resistivity of a Strain Gage	143
B	The Wheatstone Bridge	145
C	RockHard Scripts - rh* - Matlab scripts for post processing of .tdms files	147
C.1	rh1.m	148
C.2	rh1all.m	151
C.3	rh2.m	152
C.4	rh2phase.m	158
C.5	rh2fg2.m	164
C.6	rh3.m	167
C.7	rh3phase.m	170
C.8	rh4.m	174
C.9	rh4s.m	176
C.10	rh4sPhase.m	178

D	RockHard Functions - get* - Matlab functions for post processing of .tdms files	181
D.1	getChar.m	182
D.2	getNum.m	184
D.3	getTDMS.m	185
E	Other Scripts Modified by author - Matlab	188
E.1	ReadFile.m	189
F	Chemical Data Sheets	194
F.1	Acetone Data Sheet	195
F.2	Epoxy Data Sheet	201
F.3	Isopropanol Data Sheet	204
F.4	Marcol Laboratory oil Data Sheet	210
F.5	M-Bond 200 Adhesive	217
F.6	M-Bond 200 Catalyst Data Sheet	223
F.7	M-Prep Conditioner A	225
F.8	M-Prep Neutralizer 5A	230
F.9	Zap-a-gap CA+ Data Sheet	235
F.10	Zip Kicker Data Sheet	237
G	Hardware Data Sheets	239
G.1	Voltage filter	240
G.2	Temperature sensor LM35 TO-92	241
G.3	MTS Load Frame	245
G.4	Piezo Electric Sensor-PTZ5A	246
G.5	Scitex 420 Dual Phase Lock-In Amplifier	247
G.6	Strain Gage Item 17090	249
G.7	Strain Gage Item 3271	251
G.8	Strain Gage Instruction Bulletin B-127-14	253
G.9	UPS	257

List of Figures

1	Propagation of a single frequency wave. v is the wave velocity, λ is the wavelength, A is the area, l is the plug length, and s is the circumference (Manipulated by author from Figure 5).	3
2	Elongation of a metal: Illustration of offset yield point. 1: True elastic limit 2: Proportionality limit 3: Elastic limit 4: Offset yield strength, usually defined at $e=0.2\%$ S: Engineering stress e : Engineering strain A: Undeformed cross-sectional area P: Uniaxial load L: Undeformed length l: Elongation Reference: G. (Public Domain Licence, Section 11.1, Reference number: 1) . . .	4
3	Castlegate thin sections. (SINTEF Petroleum Research AS, Reidar Bøe)	6
4	Young's modulus. F is the force, A is the area, Δl is the displacement, l is the initial length (Manipulated by author from Figure 5)	11
5	Shear modulus. F is the force, A is the area, Δx is the displacement, l is the initial length, and θ is the displacement angle (Public Domain License, Section 11.1 Reference number 2) . . .	12
6	Poisson's number. F is the force, A is the area, Δl is the axial displacement, l is the initial length, Δs is the lateral displacement, s is the initial circumference (Manipulated by author from Figure 5)	12
7	Cracks in a Pierre shale. Surface is cleaned with alcohol. Fluid is emerging from the cracks. (SINTEF Petroleum Research AS, Reidar Bøe 2005)	19
8	The different techniques and their similarities. (Inspired by Hofmann, 2006, Reference number 25)	20
9	The Wheatstone bridge with supply voltage E_{in} , bridge voltage E_o , resistors R_1 and R_2 , length of sample L , diameter D , and one P-wave propagating through the rock. R_b and R_g consists of three strain gages coupled in series.	26
10	The Manual Load Frame.	30
11	A flow diagram of the measurements. See also Figure 12.	32
12	Instrumental setup. 'W' is the Wheatstone bridge (Section 2.5), 'C' is the Charge meter, 'PI' is the servo controller module of the actuator, 'Sci' is the lock-in amplifier, 'Wave' is a signal generator, 'DAQ' is the data acquisition unit, 'S' is the sample, 'P' is the pressure sensor, and 'A' is the actuator.	36

13	The single wire setup. (Stanford Research Instruments, User manual for Lock-in amplifier)	42
14	The double wires setup. (Stanford Research Instruments, User manual for Lock-in amplifier)	42
15	The configuration of the three strain gages when doing static one axial strain measurements. The two angles indicated are 120° and 240°.	43
16	Castlegate surface without epoxy.	44
17	Epoxy on a rough surface. (a) is a Castlegate sample (ML#222.3) before grinding the epoxy. (b) is a Berea sandstone (ML#318.1) after grinding.	45
18	The temperature sensor with corresponding wires. Output from the SHUNER contact.	46
19	The inside of the Faraday cage built to protect the Wheatstone bridge from electromagnetic noise. The chassis comes from an old hard drive.	47
20	The plug samples with attached strain gages.	50
21	The Berea sandstone texture. The grains are clearly visible. A 500 μm scale bar is shown in the lower right corner. (Churcher et al., 1991)	52
22	Castlegate thin section. Open and well connected pore network. A 200 μm scale bar is shown. (SINTEF Petroleum Research AS, Reidar Bøe 2005)	53
23	Chemical composition of PEEK.	54
24	The Pierre shale texture. The bigger piece is a mica flake. There is a tendency of orientation in the same direction as the flake. A 100 μm scale bar is shown in the lower left corner. (SINTEF Petroleum Research AS, Reidar Bøe 2005)	56
25	When fitting a sinusoidal curve to data points by the LSSE method, the aim is to minimize the area of the error (illustrated in red) to the model (black sinusoid) by adjusting the amplitude and phase of the sinusoid. The frequency is assumed given.	67
26	Data recorded in the Manual Load Frame	68
27	Strain in three gages mounted 120 degrees apart on an aluminium sample. Black line is their average.	76
28	The Manual Load Frame: Graphical output after MATLAB interpretation of easy.m. The file later transformed into rh*.m files (See Section 6)	79

29	The Manual Load Frame: Frequency specter of the force signal	80
30	Resonance frequencies in measurement system: Red curves: Relative perturbation of actuator (relative to max value) as a function of frequency. When reaching cutoff frequency divergence in the Young's modulus (blue curve, green curve, and yellow curve) occurs. Numerical values should not be extracted from the figure as it is intended as a cutoff frequency example only.	82
31	ALU-7075 (3Test) for increasing frequency: Perturbation (red curve); Young's modulus from strain gage (blue curve) and from actuator position (green curve). Strains of $\sim 11.5 \cdot 10^{-8}$ ($\sigma = 10.2 \cdot 10^{-9}$). $\bar{E}_{10 \text{ Hz} \rightarrow 99 \text{ Hz}} = 71.51 \text{ GPa}$ ($\sigma = 5.23$). From 3'rd measurement series. The error bars reflect max and min values within measurement interval.	84
32	ALU-7075 (5Test-200mV) for increasing frequency: Perturbation (red curve); Young's modulus from strain gage (blue curve) and from actuator position (green curve). Strains of $\sim 24.0 \cdot 10^{-8}$ ($\sigma = 7.39 \cdot 10^{-9}$). $\bar{E}_{11 \text{ Hz} \rightarrow 97 \text{ Hz}} = 70.36 \text{ GPa}$ ($\sigma = 0.72$). From 5'th measurement series. The error bars reflect max and min values within measurement interval.	85
33	ALU-7075 (5Test-300mV) for increasing frequency: Perturbation (red curve); Young's modulus from strain gage (blue curve) and from actuator position (green curve). Strains of $\sim 36.6 \cdot 10^{-8}$ ($\sigma = 10.1 \cdot 10^{-9}$). $\bar{E}_{11 \text{ Hz} \rightarrow 97 \text{ Hz}} = 70.43 \text{ GPa}$ ($\sigma = 0.57$). From 5'th measurement series. The error bars reflect max and min values within measurement interval.	86
34	ALU-7075 (5Test-400mV) for increasing frequency: Perturbation (red curve); Young's modulus from strain gage (blue curve) and from actuator position (green curve). Strains of $\sim 49.6 \cdot 10^{-8}$ ($\sigma = 16.5 \cdot 10^{-9}$). $\bar{E}_{11 \text{ Hz} \rightarrow 97 \text{ Hz}} = 70.52 \text{ GPa}$ ($\sigma = 0.44$). From 5'th measurement series. The error bars reflect max and min values within measurement interval.	87
35	ALU-7075, relative signal response measured at 49Hz	88
36	ALU-6061 (4Test) for increasing frequency: Perturbation (red curve); Young's modulus from strain gauge (blue curve) and from actuator position (green curve). Strains of $\sim 7.90 \cdot 10^{-8}$ ($\sigma = 6.09 \cdot 10^{-9}$). $\bar{E}_{11 \text{ Hz} \rightarrow 97 \text{ Hz}} = 70.61 \text{ GPa}$ ($\sigma = 4.72$). From 4'th measurement series. The error bars reflect max and min values within measurement interval.	90

37	ALU-6061 (5Test) for increasing frequency: Perturbation (red curve); Young's modulus from strain gauge (blue curve) and from actuator position (green curve). Strains of $\sim 13.99 \cdot 10^{-8}$ ($\sigma = 3.26 \cdot 10^{-9}$). $\bar{E}_{11 \text{ Hz} \rightarrow 97 \text{ Hz}} = 69.86 \text{ GPa}$ ($\sigma = 1.23$). From 5'th measurement series. The error bars reflect max and min values within measurement interval.	91
38	Dry Berea sandstone, ML#318.1.1 (3Test) for increasing frequency: Perturbation (red curve); Young's modulus from strain gauge (blue curve) and from actuator position (green curve). Strains of $\sim 7.07 \cdot 10^{-8}$ ($\sigma = 3.38 \cdot 10^{-9}$). $\bar{E}_{13 \text{ Hz} \rightarrow 99 \text{ Hz}} = 22.02 \text{ GPa}$ ($\sigma = 1.03$). From 3'rd measurement series. The error bars reflect max and min values within measurement interval.	93
39	Dry Berea sandstone, ML#318.1.2 (5Test-1) for increasing frequency: Perturbation (red curve); Young's modulus from strain gauge (blue curve) and from actuator position (green curve). Strains of $\sim 26.74 \cdot 10^{-8}$ ($\sigma = 8.43 \cdot 10^{-9}$). $\bar{E}_{13 \text{ Hz} \rightarrow 99 \text{ Hz}} = 20.49 \text{ GPa}$ ($\sigma = 0.17$). From 5'th measurement series. $t_c = 30$ seconds. The error bars reflect max and min values within measurement interval.	94
40	Dry Berea sandstone, ML#318.1.2 (5Test-2) for increasing frequency: Perturbation (red curve); Young's modulus from strain gauge (blue curve) and from actuator position (green curve). Strains of $\sim 12.78 \cdot 10^{-8}$ ($\sigma = 3.53 \cdot 10^{-9}$). $\bar{E}_{11 \text{ Hz} \rightarrow 97 \text{ Hz}} = 21.16 \text{ GPa}$ ($\sigma = 0.22$). From 5'th measurement series. $t_c = 30$ seconds. The error bars reflect max and min values within measurement interval.	95
41	Dry Castlegate sandstone 222.3.1 (3Test) for increasing frequency: Perturbation (red curve); Young's modulus from strain gauge (blue curve) and from actuator position (green curve). Strains of $\sim 5.54 \cdot 10^{-8}$ ($\sigma = 5.72 \cdot 10^{-9}$). $\bar{E}_{19 \text{ Hz} \rightarrow 99 \text{ Hz}} = 13.88 \text{ GPa}$ ($\sigma = 1.17$). From 3'rd measurement series. The error bars reflect the max and min within the very interval.	97
42	Dry Castlegate sandstone 222.3.2 (4Test) for increasing frequency: Perturbation (red curve); Young's modulus from strain gauge (blue curve) and from actuator position (green curve). Strains of $\sim 5.62 \cdot 10^{-8}$ ($\sigma = 1.86 \cdot 10^{-9}$). $\bar{E}_{11 \text{ Hz} \rightarrow 97 \text{ Hz}} = 11.50 \text{ GPa}$ ($\sigma = 0.17$). From 4'th measurement series.	98

43	Dry Castlegate sandstone 222.3.2 (5Test-1) for increasing frequency: Perturbation (red curve); Young's modulus from strain gauge (blue curve) and from actuator position (green curve). Strains of $\sim 20.0 \cdot 10^{-8}$ ($\sigma = 6.01 \cdot 10^{-9}$). $\bar{E}_{11 \text{ Hz} \rightarrow 97 \text{ Hz}} = 11.82 \text{ GPa}$ ($\sigma = 0.14$). From 5'th measurement series.	99
44	Dry Castlegate sandstone 222.3.2 (5Test-2) for increasing frequency: Perturbation (red curve); Young's modulus from strain gauge (blue curve) and from actuator position (green curve). Strains of $\sim 11.3 \cdot 10^{-8}$ ($\sigma = 0.32 \cdot 10^{-9}$). $\bar{E}_{11 \text{ Hz} \rightarrow 97 \text{ Hz}} = 11.98 \text{ GPa}$ ($\sigma = 0.32$). From 5'th measurement series.	100
45	Dry Castlegate sandstone 222.3.2 (5Test-3) for increasing frequency: Perturbation (red curve); Young's modulus from strain gauge (blue curve) and from actuator position (green curve). Strains of $\sim 5.64 \cdot 10^{-8}$ ($\sigma = 1.78 \cdot 10^{-9}$). $\bar{E}_{11 \text{ Hz} \rightarrow 97 \text{ Hz}} = 12.16 \text{ GPa}$ ($\sigma = 0.27$). From 5'th measurement series.	101
46	PEEK03 (3Test) for increasing frequency: Perturbation (red curve); Young's modulus from strain gauge (blue curve) and from actuator position (green curve). Strains of $\sim 12.7 \cdot 10^{-8}$ ($\sigma = 4.15 \cdot 10^{-9}$). $\bar{E}_{10 \text{ Hz} \rightarrow 99 \text{ Hz}} = 4.47 \text{ GPa}$ ($\sigma = 0.12$). From 3'rd measurement series.	103
47	PEEK03, signal response measured at 89Hz. This is an example of the selection process when the signals cannot maintain the constant value. This was mainly a problem in early measurement series. Y-axis is relative scale.	104
48	Saturated Pierre shale ML#192.02.12 (4Test-3), measured after some hours of initial loading, increasing frequency: Perturbation (red curve); Young's modulus from strain gauge (blue curve) and from actuator position (green curve). Strains of $\sim 4.18 \cdot 10^{-8}$ ($\sigma = 1.56 \cdot 10^{-9}$). $\bar{E}_{10 \text{ Hz} \rightarrow 99 \text{ Hz}} = 3.99 \text{ GPa}$ ($\sigma = 0.15$). From 4'th measurement series.	106
49	Saturated Pierre shale ML#192.03.10 (4Test-1): Perturbation (red curve); Young's modulus from strain gauge (blue curve) and from actuator position (green curve). Strains of $\sim 13.8 \cdot 10^{-8}$ ($\sigma = 9.20 \cdot 10^{-9}$). $\bar{E}_{10 \text{ Hz} \rightarrow 99 \text{ Hz}} = 3.05 \text{ GPa}$ ($\sigma = 0.193$). From 4'th measurement series.	107

50	Saturated Pierre shale ML#192.03.10 (4Test-3): Perturbation (red curve); Young's modulus from strain gauge (blue curve) and from actuator position (green curve). Strains of $\sim 15.8 \cdot 10^{-8}$ ($\sigma = 5.53 \cdot 10^{-9}$). $\bar{E}_{10\text{ Hz} \rightarrow 99\text{ Hz}} = 2.31\text{ GPa}$ ($\sigma = 0.095$). From 4'th measurement series. NOTE! The strain gages got replaced after the measurements in Figure 49. The sample was also partly damaged at this time.	108
51	Difference in phase of stress and strain in Aluminium (blue), Berea (red), and Castlegate (green). Even though the curves may be noisy the tendency is clear.	110
52	Berea ML#318.1.1: Difference in phase of stress and strain at different strain levels. Low strain $12.8 \cdot 10^{-8}$ (blue curve), high strain $26.7 \cdot 10^{-8}$ (green curve).	111
53	Castlegate ML#222.3.2: Difference in phase of stress and strain at different strain levels. Low strain $5.64 \cdot 10^{-8}$ (blue curve), medium strain $11.3 \cdot 10^{-8}$ (green curve), high strain $20.0 \cdot 10^{-8}$ (red curve).	111
54	ALU-7075, Phase to frequency	112
55	The Castlegate sample ML#222.3.2: Aluminium corrected phase difference and attenuation.	114
56	The Castlegate sample ML#222.3.2 (high strain): Attenuation as defined in Section 2.3, aluminium corrected.	115
57	The Berea sample ML#318.1.1: Aluminium corrected attenuation.	115
58	The Castlegate sample ML#222.3.2: The measured strain in the Castlegate is about $11 \cdot 10^{-8}$	116
59	The Castlegate sample ML#222.3.2: The measured strain in the Castlegate is about $20 \cdot 10^{-8}$	117
60	The Berea sample ML#318.1.1:	117
61	ALU-7075 Young's modulus over frequency consistency check; The measurement in 'a' was repeated without dismantling to check for consistency.	118
62	Castlegate sample measured twice. Before (light blue line) and after (purple line) installation of the UPS.	122
63	ALU-7075: Frequency average of Young's modulus (11-97 Hz, prime numbers) to strain in sample. The error bars represent the standard deviation.	126

64	Berea sandstone: Frequency average of Young's modulus (11-97 Hz, prime numbers) to strain in sample. The error bars represent the standard deviation.	128
65	Castlegate sandstone: Frequency average of Young's modulus (11-97 Hz, prime numbers) to strain in sample. Only samples from the 5TestSeries are included for regression. Other points are plotted in purple with their respective standard deviations. .	129
66	The Wheatstone bridge with supply voltage, V_s , bridge voltage, V_g , resistor;s R_A to R_D , length of sample, L , diameter, D , and one axial force F	145

List of Tables

1	Numeric example values of the full scale amplifier ranges, FS, on the lock-in amplifiers measuring force, strain and position. The limits have been empirically settled. ϵ is the measured strain in the sample.	39
2	P-wave and S-wave ultrasonic frequency speeds measured previously by SINTEF Petroleum Research AS, Jørn Stenebråten. . .	49
3	Dimensions of samples used for testing. The assumed measurement error is ± 0.02 mm.	51
4	Chemical composition of Aluminium alloy 6061 (AMS 4117) and 7075 (AMS 4122)	51
5	Mineral composition of Berea sandstone, weight percentages (Churcher et al., 1991).	52
6	Standard properties of PEEK (Searle et al., 1985)	54
7	Ultrasonic wave-speeds and calculated isotropic elastic constants for PEEK450G (Rae et al., 2007)	54
8	Mineral composition of Pierre shale, weight percentages (Bøe R. 2005)	55
9	Corrections for diameter values found in measurement files. . . .	71
10	Pierre shale (ML#192.02.12) time dependence.	105
11	Results. Average values of E on the range 10-99 Hz (9 sample values, evenly spaced) with indicated strain values. Δ is the standard deviation. Any * indicates the frequency range going from 13-97 Hz (19 samples, prime numbers) Any @ indicates the limited range {11, 17, 23, 29} Hz. In the case of off-scale spikes they have been suppressed. Castlegate and Pierre were the only samples tested with a uniaxial static stress of 5 MPa, the rest were on 10 MPa.	119

1 Introduction

One of the most successful methods for mapping and understanding the subsurface is the seismic survey. From its infancy in 1924 (Musgrave, 1967) it has ever improved and is now the name of the game when exploring and developing new oilfields. In recent years technology has improved both in dimensions and resolution. The information is not only about the rock matrix, but also to some degree the fluid and saturation levels (Hilterman, 1990). Originally the main application was mapping large structures as salt domes (Zimmerman, 1968), but seismic is now even used to study possible flow barriers (Vienot et al., 1998), time laps effects and compaction (Barkved et al., 2005). To increase the resolution a more detailed description of the intrinsic properties of the rock is needed. The velocity of the propagating wave depends mainly on the elastic stiffness and the density of the rock (Fjær et al., 2008). The density of the rock is again dependent on the rock's composition and the density of the components. The stiffness is not necessarily independent of amplitude and frequency (Johnson et al., 1996), but average values are often used. This averaging may be good enough up to a certain resolution. To further enhance it, dependencies in greater detail must be known.

In a non isotropic material, the behavior of the rock may be substantially different than theoretical predictions. Possibly there may be frequency, amplitude and stress dependence (Johnson et al., 1996). Several apparatus setups are possible for low frequency measurements of elasticity and attenuation, many originating from material testing of metals and ceramics. According to Batzle et al. (2006) there are two main experimental methods to determine low-frequency elasticity behavior: resonance and stress-strain measuring.

The principle behind the resonating bar is to put the sample into vibration by a sinusoidal force at one modulus of vibration. The mode could be lengthwise, flexural or torsional each having its own elasticity modulus (Young's modulus or shear modulus). The frequency of resonance, the density, and the geometrical dimensions of the sample is needed to calculate the modulus. The decay time when removing the driving force can be used to settle the attenuation. The width of the resonance frequency peak can also be used. This technique has a history of application going back to Johnson in 1970 and Winkler et al. in 1979 and from then on several times in the 80's and 90's. (Tittmann et al., (1980), Clark (1980), Murphy (1982), Bulau et al., (1983), Guyer et al., (1995)). One of the drawbacks with this technique is the need for a relatively large sample with specific dimensions as pointed out by Johnson.

The other approach, as described by Batzle et al. is the stress-strain measur-

ing. This is a straight forward and easy to understand setup, but when dealing with small signals and stiff materials, things anyhow tend to complicate. A static load is applied to a column consisting of the sample, a force meter, an actuator, and some sensor to measure the strain. The static load level is settled on two conditions: maintaining the sample in the elastic domain (not driving it to fracture or permanent deformation), and applying sufficient force to make the column rigid enough for wave to propagate, and minimize the effect of the boundaries. The ideal condition would be to apply the maximum static load within the elastic domain, since this minimizes the effect of the contact surfaces.

Static values and dynamic values of elasticity may be different (Ostrovsky, 2001). A wave propagating through a rock will experience the dynamic value of elasticity.

If the magnitude of perturbation is great enough or if the rock is not perfectly elastic hysteresis occurs and leaves behind a rock with different characteristics (Mckavanagh and Stacy, 1974). For strains greater than 10^{-5} there is a strong amplitude dependency (Gordon and Davis, 1968). Thus the magnitude of the perturbational wave should be scaled properly to produce strain values in the sample much smaller than 10^{-5} , to be amplitude independent.

2 Theory

A seismic wave propagates through the bedrock and is reflected back to the surface. The reflective pattern is different depending on the density, layout and elastic properties of the rock. The pattern may also be dependent on the frequency and the amplitude used in the initial wave. The subsurface rock may both disperse and attenuate the wave. The propagation of energy that a wave represents excite the molecules in various ways when propagating through a solid. In general they can be either described by longitudinal displacement, a P-wave, or an excitation transverse to the direction of propagation, an S-wave. Both are illustrated in Figure 1. When crossing a boundary in the sub surface, a change in properties, a P-wave may partly convert into an S-wave and both are in co-existence.

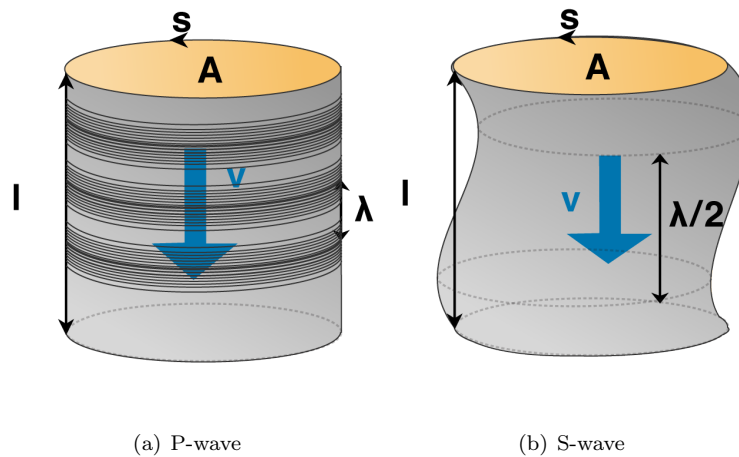


Figure 1: Propagation of a single frequency wave. v is the wave velocity, λ is the wavelength, A is the area, l is the plug length, and s is the circumference (Manipulated by author from Figure 5).

2.1 The Elastic Domain

If the material is said to be elastic, it implies that it can return to its initial state by itself when the applied stress is removed. If the material behaves plastically, it does not return in state, but remains in the final state when the applied stress is removed. As always there are situations where the materials partly return in state. It is then said to be plasto-elastic. If the deforming force is great enough the material breaks and is permanently damaged. Figure 2 summarizes this for the case of stretching a metal. The principles will be the same as when compacting a rock.

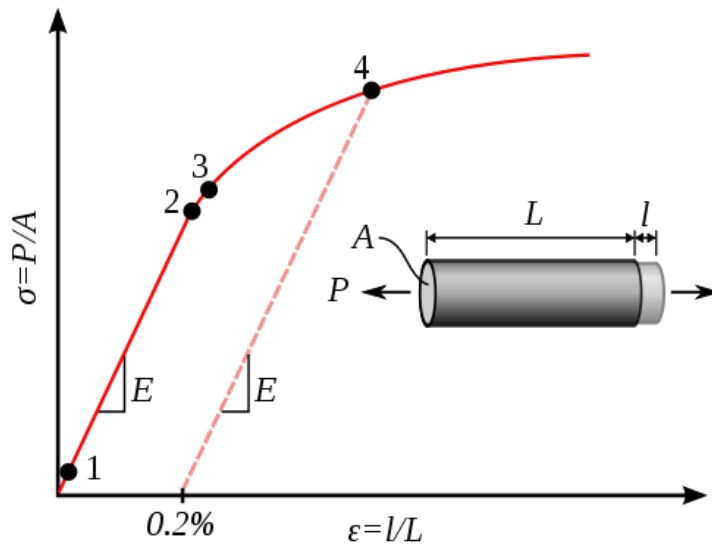


Figure 2: Elongation of a metal: Illustration of offset yield point. 1: True elastic limit 2: Proportionality limit 3: Elastic limit 4: Offset yield strength, usually defined at $\epsilon=0.2\%$ S: Engineering stress ϵ : Engineering strain A: Undeformed cross-sectional area P: Uniaxial load L: Undeformed length l: Elongation Reference: G. (Public Domain Licence, Section 11.1, Reference number: 1)

For porous materials plasto-elastic behavior is common. The first time compacting the sample it deforms a bit before acting elastically. This is usually a first time effect only when applying a static stress, and will therefore have no impact on the dynamic measurements after steady-state in the static uniaxial stress is reached. All samples are assumed tested in the elastic domain.

The effect of hysteresis, or plastic deformation within the elastic domain, has been studied by among others (Yale et al., 1995). They found the hysteresis (the area of the hysteresis loop) to be related to the difference in the static and dynamic value of the Young's modulus.

2.2 Poroelasticity

Much of the theory derived in this section is based on the works of Gasmann (1951) and Biot (1956). The presentation and notation is to some extent based on Fjær et al. (2008) and Bautmans (2009).

2.2.1 Porosity

The definition of bulk porosity is given as

$$\phi = \frac{V_v}{V_b}, \quad (1)$$

where V_v is the void occupied volume, while the V_b is the bulk volume (typically measured by a caliper). There are several techniques for measuring porosity. One is to saturate the sample with a liquid or a gas of known density, and use the difference of weight before and after saturation.

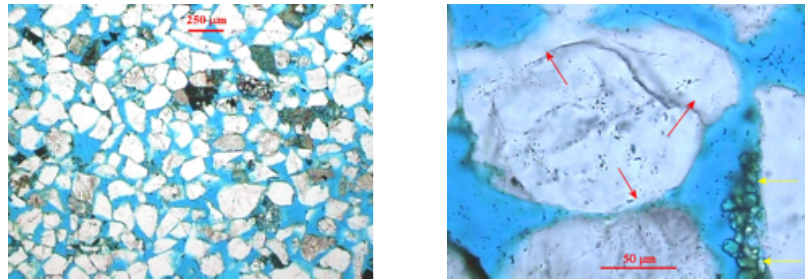
Porosity may be inter or intra granular. In clastic sedimentary rocks 'inter granular' means that the grains are still in place, while the voids are around the grains (Example Figure 3 where grains are white, and voids are blue). The inter granular porosity is often said to be connected, meaning that by going from one pore to another no matrix needs to be crossed.

Intra granular porosity rock within the domain of reservoir rock is typically oolites eroded away. What remains are isolated voids without connectivity or with a micro pore network that needs geological time to saturate the voids. The network is therefore non-connected and have poor permeability.

In clastic sedimentary rocks the two types of porosity cannot be in co-existence. In carbonate rock they can. The explanation for this lays in the depositional origin. Clastic sedimentary rocks are grains of sand and fragments eroded from the mountains, then compacted to form a solid matrix. Both matrix and grains are said to be of syndepositional origin, it was there in the first place, while cement partly filling the voids is of post-depositional origin, an after effect.

In a carbonate rock the process is different. The matrix is a coral reef that may undergo both diagenesis (chemical alteration) and bioturbation (animals i.e. excavating cavities).

A shale (a clastic sedimentary rock with mud, a mix of tiny fragments and clay minerals) is said to have micro-porosity. The overall porosity may still be high, but the voids are so tiny that the permeability (ease of flow) is very low. The shale in an oil reservoir is often the impermeable trap collecting the oil migrating from a source rock into a reservoir rock.



(a) Overview thin section photo of Castlegate sandstone. There exists an open, continuous and moderately to well-connected pore network (blue). A $250\ \mu\text{m}$ scale bar is shown.

(b) Detailed photo of Castlegate sandstone showing quartz cement (red arrows) and tiny, brownish crystals of siderite (yellow arrows). A $50\ \mu\text{m}$ scale bar is shown.

Figure 3: Castlegate thin sections. (SINTEF Petroleum Research AS, Reidar Bøe)

Silt and clay are terms used if the size of the grains is small: diameter less than $1/256\ \text{mm}$ for clay, diameter less than $1/16\ \text{mm}$ for silt (Wentworth 1922 and Bates and Jackson, 1987). The permeability is generally poor the smaller the grain size (not taking into account fractures etc.).

Figure 3 shows an example of inter-granular porosity in a thin section of a clastic sedimentary rock. The section is $30\ \mu\text{m}$ thick and is saturated with epoxy before placed in the microscope. The white grains are mainly quartz with tiny fragments of partly dissolved feldspar. The blue epoxy fills the voids in the rock showing the inter granular network. Any dark section may be a patch of clay. The grains are close to the same size, meaning that the sorting has been good. Both the feldspar and the clay weaken the rock and make it harder for compressional waves to propagate.

Apart from the mineralogy, the general behavior of the rock (elastic response, failure stress etc.) depends heavily on the non solid parts of the rock, thus the pore system and the layout.

2.2.2 Density

The general definition of the bulk density of any material is given as

$$\rho = \frac{m}{V} \quad (2)$$

where m is the mass of the object, and V is the volume it occupies. When considering a two phase system, for instance a saturated clastic rock, two densities can be given, the dry ρ_{dry} and the wet ρ_{wet} . The dry density uses the mass of the matrix in the expression given above (Equation 2). No fluid is assumed

in the pores since air or any gas saturation is considered of negligible density as compared to the matrix. The wet density takes into account the weight of the fluid (often being water, oil or brine). Assuming the pores to be partly saturated S by any fluid 'fl' of non-negligible density ρ_{fl} , the expression of the overall density is given as

$$\rho_{\text{wet}} = (1 - \phi)\rho_{\text{m}} + \phi \rho_{\text{fl}}S, \quad (3)$$

where ϕ is the porosity as defined earlier, and ρ_{m} is the material density.

The effective density for low acoustic frequencies may differ slightly from the density given in Equation 3 in a porous medium. By considering incompressible, viscous flow of fluid, the size of particles and pores can contribute when the wavelength of any propagating wave is of the same order. This can be further investigated by looking at the fluid's resistance to the oscillations of a rigid sphere. The effective compressibility is the volume-average of the component's compressibility. The acoustic properties could then be derived from the effective compressibility and the effective density. For further reading (Ament, 1953) is recommended.

2.2.3 The Bulk Modulus

The general expression for the bulk modulus is given as

$$K = V \frac{\partial p}{\partial V}. \quad (4)$$

Consider some particles submerged in a liquid in a container of volume V . The particles may be in contact with each other but they are not consolidated, they do not stick together. By reducing the volume adiabatically, pressure increases. A particle is moved a distance $\vec{u} = (u_x, u_y, u_z)$ which is from now on called the displacement vector. For any external stress a single phase fluid system would have the volumetric change

$$\epsilon_{\text{vol,fluid}} = \nabla \cdot \vec{u}_{\text{molecule}} = -\frac{dV_{\text{fluid}}}{V_{\text{fluid}}}, \quad (5)$$

where $\vec{u}_{\text{molecule}}$ would be the displacement of a molecule within the liquid, and $\epsilon_{\text{vol,fluid}} = \epsilon_{x,\text{fl}} + \epsilon_{y,\text{fl}} + \epsilon_{z,\text{fl}}$ (Fjær et al., 2008). Being a two phase system the total deformation $\epsilon_{\text{vol,tot}}$ is a volumetric weighted sum over the components.

$$\epsilon_{\text{vol,tot}} = \frac{V_{\text{fl}}}{V_{\text{tot}}} \epsilon_{\text{vol,fl}} + \frac{V_{\text{s}}}{V_{\text{tot}}} \epsilon_{\text{vol,s}} = \frac{\sigma_b}{K_{\text{effective}}}, \quad (6)$$

where σ_b is the bulk stress and $K_{\text{effective}} = \sigma_b/\epsilon_{\text{vol}}$ is the effective bulk modulus. Using the expression for porosity ϕ and that $V_s + V_{\text{fl}} = V_{\text{tot}}$, Equation 6 transformes into

$$\phi \frac{\sigma_{\text{fl}}}{K_{\text{fl}}} + (1 - \phi) \frac{\sigma_s}{K_s} = \frac{\sigma_b}{K_{\text{effective}}}, \quad (7)$$

where the deformation of each component is expressed in terms of its own bulk modulus K . Since the stress is assumed uniform, σ 's cancel out

$$\frac{1}{K_{\text{effective}}} = \phi \frac{1}{K_{\text{fl}}} + (1 - \phi) \frac{1}{K_s}. \quad (8)$$

2.2.4 Biot's Theory

The theory of poroelasticity is based upon the published work of Maurice Biot (1905-1985) in the period (1935-1962). Other important contributors in its infancy years are Fritz Gassmann and Yakov Frenkel. The theory is based on: Darcy's law (fluid flow through matrix), Navier-Stokes equation (viscous flow), and linear elastic theory (solid matrix).

A two component medium is considered isotropic, porous and permeable. The components are: a solid 's' being the matrix and a fluid 'fl' filling the pores. Any nonlinear effects are discarded. The deformation in the solid is expressed in terms of the volumetric change

$$\epsilon_{\text{vol},s} = \nabla \cdot \vec{u}_s = -\frac{dV}{V}, \quad (9)$$

where \vec{u}_s is a displacement vector and V is the volume. The ratio of displaced fluid volume to total volume ξ can be given relative to the displacement of the solid

$$\xi = \phi \nabla \cdot (\vec{u}_s - \vec{u}_{\text{fl}}), \quad (10)$$

or by the ratio of the displaced volume ΔV_{fl} minus ΔV_{p} relative to the total volume V_{tot} . ΔV_{fl} is the change of volume in the fluid, ΔV_{p} is the change of volume in the pore.

$$\begin{aligned} \xi &= \frac{\Delta V_{\text{p}} - \Delta V_{\text{f}}}{V_{\text{tot}}} \\ &= \frac{\Delta V_{\text{p}}}{V_{\text{tot}}} \frac{V_{\text{p}}}{V_{\text{p}}} - \frac{\Delta V_{\text{f}}}{V_{\text{tot}}} \frac{V_{\text{p}}}{V_{\text{p}}} \\ &= \phi \left(\frac{\Delta V_{\text{p}}}{V_{\text{p}}} - \frac{\Delta V_{\text{f}}}{V_{\text{p}}} \right) \end{aligned} \quad (11)$$

where $\phi = V_{\text{p}}/V_{\text{tot}}$ If assuming the sample is initially fully saturated with con-

nected pores, $V_f = V_p$,

$$\begin{aligned}\xi &= \phi \left(\frac{\Delta V_p}{V_p} - \frac{\Delta V_f}{V_f} \right) \\ &= \phi \left(\frac{\Delta V_p}{V_p} - \frac{\Delta p_f}{K_f} \right),\end{aligned}\quad (12)$$

if

$$K_f = V_f \frac{\partial p_f}{\partial V_f} \approx V_f \frac{\Delta p_f}{\Delta V_f}.$$

The effect of an external stress on a volume element is balanced by partly the matrix of the rock, and partly by a hydrostatic fluid pressure p_f . The classic theory of Hooke (1678) did not take into account the presence of any pore fluid. Biot (1956) modified it to describe a linear stress-strain relationship for a two phase system dependent on: ϵ , ξ , tensor elements σ_i and τ_{ij} , and the fluid pressure p_f . The tensors can be listed as

$$\sigma_i = \lambda \epsilon_{\text{vol}} + 2G\epsilon_i - C\xi, \quad (13)$$

$$\tau_{ij} = 2G\Gamma_{ij}, \quad (14)$$

$$p_f = C\epsilon_{\text{vol}} - M\xi, \quad (15)$$

with λ and G being the Lamé parameters, and C and M additional elastic moduli. G is also known as the shear modulus (Section 2.2.6). Subscript i and ij denotes x, y, and z in a rotary fashion, if $i = x$ then $j = y$ etc. Summing over the indexes gives

$$\begin{aligned}\bar{\sigma} &= \frac{\Sigma_i \sigma_i}{3} = \frac{\Sigma_i (\lambda \epsilon_{\text{vol}} + 2G\epsilon_i - C\xi)}{3} \\ &= \lambda \epsilon_{\text{vol}} + \Sigma_i \left(\frac{2G\epsilon_i}{3} \right) - C\xi \\ &= K\epsilon_{\text{vol}} - C\xi,\end{aligned}\quad (16)$$

where $K = \lambda + \frac{2G}{3}$ in undrained condition. Equation 15 and Equation 16 are together called Biot-Hooke's law for isotropic stress. To get a better understanding of it, one may use two examples (Fjær, 2008). The notation is adapted, language modified and some parts are left out.

Example 1 The sample is drained, meaning no fluid is in the pores, or the fluid is free to move maintaining hydrostatic pressure, $\Delta p_f = 0$.

$$\Delta\sigma = \left(K - \frac{C^2}{M}\right)\epsilon_{\text{vol}} = K_{\text{fr}}\epsilon_{\text{vol}} \quad (17)$$

$$\xi = \frac{C}{M}\epsilon_{\text{vol}}. \quad (18)$$

The K_{fr} is here defined as the drained bulk modulus (framework modulus). C/M controls the pore and bulk volume change and can be simplified

$$\Delta V_{\text{p}} = \frac{C}{M}\Delta V = \alpha\Delta V, \quad (19)$$

where α is often referred to as the Biot coefficient.

If considering the grains incompressible, only the pore space will deform and $\Delta V_{\text{p}} = \Delta V \Rightarrow \alpha = 1$. Compressible grains mean $\Delta V_{\text{p}} < \Delta V \Rightarrow \alpha < 1$.

Example 2 The sample is now undrained, there is fluid in the pores but it is confined in the sample thus cannot escape. The fluid increment is thus $\xi = 0$ and

$$\Delta\sigma = K\epsilon_{\text{vol}}\Delta p_{\text{f}} = \frac{C}{K}\Delta\sigma. \quad (20)$$

K is now the undrained bulk modulus. The ratio C/K determines the increase in pore pressure.

Through different manipulation of the above relations one may reach the Biot-Gassmann equation relating the different bulk moduli

$$\frac{K}{K_{\text{s}} - K} = \frac{K_{\text{fr}}}{K_{\text{s}} - K_{\text{fr}}} + \frac{K_{\text{fl}}}{\phi(K_{\text{s}} - K_{\text{fl}})} \quad (21)$$

where K_{s} is the bulk modulus of the solid grains, K_{fr} is the bulk modulus of the drained rock (framework) and K_{fl} is the bulk modulus of the fluid.

Especially K_{fr} depends on the microstructure (porosity and layout) of the rock, see Section 2.2.1. Shear waves do not propagate in a fluid, thus the shear wave modulus is identical in both the drained and undrained sample (Biot, 1956). For further reference Holt (2004) and Fjær et al. (2008) is recommended.

2.2.5 Young's Modulus E

Young's modulus E is defined as the stress σ over the strain ϵ in a uniaxial setup (Figure 4). Stress is the force per area in the direction of the force. Strain is

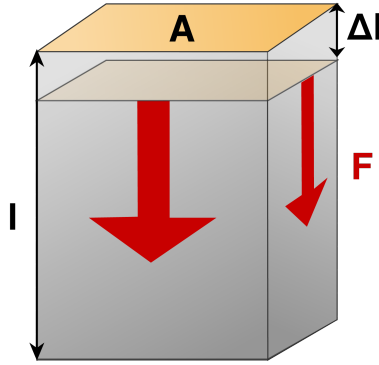


Figure 4: Young's modulus. F is the force, A is the area, Δl is the displacement, l is the initial length (Manipulated by author from Figure 5)

the relative decrease in length $\Delta l = l - \hat{l}$ to the original length l .

$$E = \frac{\sigma}{\frac{l-\hat{l}}{l}} = \frac{\sigma}{\frac{\Delta l}{l}}. \quad (22)$$

Relations commonly used:

$$E = 2K(1 - 2\nu) \quad (23)$$

$$E = 2G(1 + \nu), \quad (24)$$

where K is the bulk modulus, G is the shear modulus and ν is the Poisson's number.

2.2.6 Shear modulus G

The shear modulus is the materials response to shear deformation. It is also called the modulus of rigidity and is defined as

$$G = \frac{\tau_{xy}}{2 \cdot \Gamma_{xy}} = \frac{\tau_{xy}}{\gamma_{xy}} = \frac{F/A}{\Delta x/l} = \frac{F/A}{\tan \theta}, \quad (25)$$

where $\Gamma_{xy} = \frac{1}{2} \tan \theta$ and the variables are defined from Figure 5. In the small angle approximation $\tan \theta \approx \theta$ if θ is given in radians, and

$$G = \frac{F}{A \cdot \theta}.$$

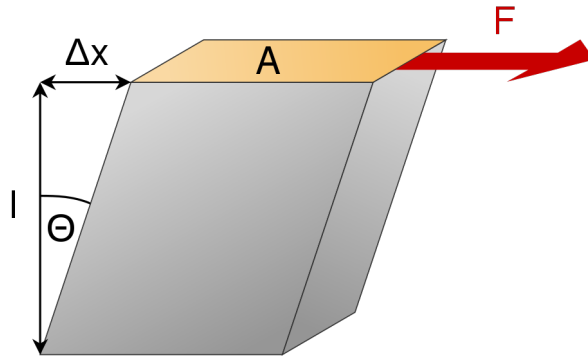


Figure 5: Shear modulus. F is the force, A is the area, Δx is the displacement, l is the initial length, and θ is the displacement angle (Public Domain License, Section 11.1 Reference number 2)

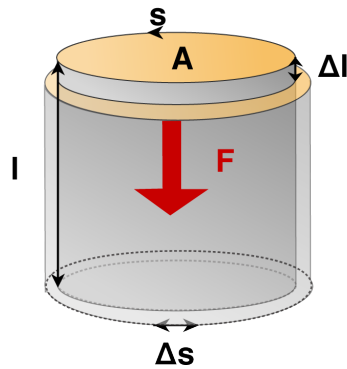


Figure 6: Poisson's number. F is the force, A is the area, Δl is the axial displacement, l is the initial length, Δs is the lateral displacement, s is the initial circumference (Manipulated by author from Figure 5)

2.2.7 Poisson's Number ν

Poisson's number is defined as

$$\nu = -\frac{\epsilon_{\text{lateral}}}{\epsilon_{\text{axial}}}. \quad (26)$$

and deals with the lateral expansion due to relative axial contraction. By definition it is a dimensionless number. On a cylindrical sample, the Poisson's ratio explains the increase in circumference due to the applied uniaxial stress (Figure 6).

2.2.8 The Wave Equation in Porous Media

Starting with Newton's law in one dimension

$$(1 - \phi) \rho_s \frac{\partial^2 u_{x,s}}{\partial t^2} + \phi \rho_f \frac{\partial^2 u_{x,f}}{\partial t^2} = \frac{\partial \sigma_x}{\partial x}, \quad (27)$$

where the result is a description of the longitudinal motion. Differentiating with respect to x and putting the time differentiation outside gives

$$\frac{\partial^2}{\partial t^2} \left((1 - \phi) \rho_s \frac{\partial u_{x,s}}{\partial x} + \phi \rho_f \frac{\partial u_{x,f}}{\partial x} \right) = \frac{\partial^2 \sigma_x}{\partial x^2}. \quad (28)$$

The next step is to replace with the previously derived quantities and the relation for density:

$$\xi = \phi \frac{\partial}{\partial x} (u_{x,s} - u_{x,f}) \quad (10)$$

$$\epsilon = \frac{\partial u_{x,s}}{\partial x} \quad (29)$$

$$\sigma_x = \lambda \epsilon_x + 2G \epsilon_x - C \xi \quad (13)$$

$$\rho = \phi \rho_f + (1 - \phi) \rho_s \quad (30)$$

and by multiplying (10) with ρ_f , and (29) with (30) and replacing with corresponding terms in 28 what is left is

$$\boxed{\frac{\partial^2}{\partial t^2} (\rho \epsilon_x - \rho_f \xi) = \frac{\partial^2 (\lambda \epsilon_x + 2G \epsilon_x - C \xi)}{\partial x^2}}, \quad (31)$$

This is the first wave equation and there are two unknowns, ϵ and ξ . In order to evaluate them further, another expression is needed for the force acting on a volume element. This can be found in consolidation theory (Bautmans, 2009) and when inserted in Newton's law it gives

$$\frac{\partial^2}{\partial t^2} (\rho_f u_{x,f}) = \nabla p_f - \frac{\eta}{\tilde{k}} \phi \left(\frac{\partial \vec{u}_f}{\partial t} - \frac{\partial \vec{u}_s}{\partial t} \right), \quad (32)$$

with \tilde{k} being the permeability. By differentiating with respect to x and simplifying to one dimension

$$\frac{\partial}{\partial x} \left(\frac{\partial^2}{\partial t^2} \rho_f u_{x,f} \right) = \frac{\partial^2 p_f}{\partial x^2} - \frac{\eta}{\tilde{k}} \phi \frac{\partial}{\partial x} \left(\frac{\partial \vec{u}_f}{\partial t} - \frac{\partial \vec{u}_s}{\partial t} \right), \quad (33)$$

recognized once again a wave equation. Previously known relations are identified

$$\frac{\partial}{\partial x} \left(\overbrace{\frac{\partial^2}{\partial t^2} (\rho_f \epsilon_x - \rho_f \xi / \phi)}^{\frac{\partial^2}{\partial t^2} (\rho_f \epsilon_x - \rho_f \xi / \phi)} \right) = \frac{\partial^2 p_f}{\partial x^2} - \frac{\eta}{\tilde{k}} \phi \overbrace{\frac{\partial}{\partial x} \left(\frac{\partial \vec{u}_f}{\partial t} - \frac{\partial \vec{u}_s}{\partial t} \right)}^{-\partial \xi / \partial t}, \quad (34)$$

and using that $p_f = C\epsilon_{\text{vol}} - M\xi$

$$\boxed{\frac{\partial^2}{\partial t^2} (\rho_f \epsilon_x - \frac{\rho_f}{\phi} \xi) = \frac{\partial^2}{\partial x^2} (C\epsilon_x - M\xi) + \frac{\eta}{\tilde{k}} \frac{\partial \xi}{\partial t}}. \quad (35)$$

with unknowns for ξ and ϵ in both (31) and (35). The standard solutions to any wave equation of this type are

$$\epsilon_x = \epsilon_{x0} e^{i(\omega t - kx)} \quad (36)$$

$$\xi_x = \xi_o e^{i(\omega t - kx)} \quad (37)$$

where $\omega = 2\pi f$ is the angular frequency in radians per second, and $k = 2\pi/\lambda$ is the wave number in inverse meters.

2.2.9 Checking the Solutions in the Wave Equations

The solutions are checked by differentiating ϵ_x and ξ with respect to time t and distance x

$$\ddot{\epsilon}_x = -\omega^2 \epsilon_x \quad (38)$$

$$\ddot{\xi} = -\omega^2 \xi \quad (39)$$

$$\dot{\xi} = i\omega \xi \quad (40)$$

$$\frac{\partial^2 \epsilon_x}{\partial x^2} = -k^2 \epsilon_x \quad (41)$$

$$\frac{\partial^2 \xi}{\partial x^2} = -k^2 \xi. \quad (42)$$

Equations (38) to (42) are inserted into (31) and (35) and reorganized

$$\left(\frac{\omega^2}{k^2} \rho - \lambda - 2G \right) \epsilon_{x,o} + \left(C - \frac{\omega^2}{k^2} \rho_f \right) \xi_o = 0, \quad (43)$$

$$\left(\frac{\omega^2}{k^2} \rho_f - C \right) \epsilon_{x,o} + \left(\frac{\omega^2}{k^2} \frac{\rho_f}{\phi} + M + \frac{i\omega\eta}{k^2 \tilde{k}} \right) \xi_o = 0. \quad (44)$$

The term ω/k is recognized as being the phase velocity v_p , and the expression simplifies to

$$(v_p^2 \rho - \lambda - 2G) \epsilon_{x,o} + (C - v_p^2 \rho_f) \xi_o = 0, \quad (45)$$

$$(v_p^2 \rho_f - C) \epsilon_{x,o} + \left(v_p^2 \frac{\rho_f}{\phi} + M + i \frac{v_p \eta}{k \tilde{k}} \right) \xi_o = 0. \quad (46)$$

Biot (1956) introduced a function $F(\kappa)$ to deal with non Poiseuille flow (behaving non laminar): $\kappa = \sqrt{\omega/\nu}$. κ is here a frequency parameter with ν being the viscosity and ω as defined earlier. This implies that $\eta \rightarrow \eta F(\kappa)$ in (46). This modification is generally used to cope with higher frequencies (Tsiklauri, 2001), and may not be necessary for the low frequency range. Another modification introduced by Biot (1956) is the tortuosity $\tilde{\tau}$ of the pore channel network. This is the ratio between the length of the pore L to the distance between the endpoints C

$$\tilde{\tau} = \frac{L}{C}.$$

Any straight line L will have tortuosity equal to 1 over the distance $L = C$. The other extreme is a circle with infinite tortuosity. According to Bautmans (2009) a typical sandstone value would be in the range of 2-3. The tortuosity influences the term dealing with the geometry of the rock $\rho_f/\phi \rightarrow \rho_f \tilde{\tau}/\phi$. To obtain v_p^2 in all terms the substitution of $v_p = \omega/k$ is used. The two modified solutions (45) and (46) are expressed in matrix notation

$$\begin{pmatrix} (v_p^2 \rho - \lambda - 2G) & (C - v_p^2 \rho_f) \\ (v_p^2 \rho_f - C) & \left(v_p^2 \frac{\rho_f \tilde{\tau}}{\phi} + M + i \frac{v_p \eta F(\kappa)}{\omega \tilde{k}} \right) \end{pmatrix} \begin{pmatrix} \epsilon_{x,o} \\ \xi_o \end{pmatrix} = 0. \quad (47)$$

To solve this set of equations make the determinant be zero. Non-trivial solutions capable of expressing the P-wave velocity v_p are given in terms of the other factors. Equation 47 have only one term being frequency dependent, the imaginary part in the bottom right corner. The low frequency limit $\omega \rightarrow 0$ is of interest. If any infinite number times a constant should be finite, then the constant needs to be zero.

$$\lim_{\omega \rightarrow 0} \overbrace{(v_p^2 \rho - \lambda - 2G)}^{finite} \cdot \left(\overbrace{v_p^2 \frac{\rho_f \tilde{\tau}}{\phi} + M}^{finite} + i \overbrace{\frac{v_p \eta F(\kappa)}{\omega \tilde{k}}}^{infinite} \right) + \overbrace{(C - v_p^2 \rho_f)^2}^{finite} = 0 \quad (48)$$

To make the imaginary part of Equation 48 equal to zero, the first braced expression must itself be zero

$$(v_p^2 \rho - \lambda - 2G) = 0, \quad (49)$$

if $\{\eta, F\} \neq 0$ and $\tilde{k} \neq \infty$. Rewriting and using $\lambda = K - 2G/3$ gives

$$\begin{aligned} v_p &= \sqrt{\frac{\lambda + 2G}{\rho}} \\ &= \sqrt{\frac{K + 4G/3}{\rho}}. \end{aligned} \quad (50)$$

2.2.10 Relating Young's Modulus with Speed of Propagation

To relate the speed of propagation to the elasticity and density of the rock first assume that the rock is homogeneous isotropic. Since both shear waves and longitudinal waves propagate in the medium, both of their elastic moduli are taken into account. This is different from when dealing with fluids since shear waves cannot propagate and the expression gets simpler. The compressional wave velocity in dry rock is given by

$$v_p = \sqrt{\frac{K + 4G/3}{\rho}}, \quad (50)$$

where K is the bulk modulus, G is the shear modulus and ρ is the density. Shear modulus is the sample's resistance against shear deformation. There is a close link between the different elasticity constants. By using $E = 3K(1 - 2\nu)$ and $E = 2G(1 + \nu)$, Equation 50 yields

$$\begin{aligned} v_p &= \sqrt{\frac{\frac{E}{(1-2\nu)} + 4\frac{E}{2(1+\nu)}}{3\rho}} \\ &= \sqrt{\frac{E}{3\rho} \left(\frac{1}{(1-2\nu)} + \frac{2}{(1+\nu)} \right)} \\ &= \sqrt{\frac{E}{\rho} \frac{(1-\nu)}{(1-2\nu)(1+\nu)}}, \end{aligned} \quad (51)$$

where ν is Poisson's ratio.

2.2.11 Dimensional Analysis of the Derived Expression for Speed

A straight forward approach to check the validity of any expression is to do a dimensional analysis of its constituents. The velocity expressed in SI units yields meters per second. E has the dimension of Pascal, or Newton per meter squared. Applying Newton's law gives E in dimensions of $\text{kg} \cdot \text{m}/\text{s}^2/\text{m}^2$. ρ is of dimension kg per meter cubed, thus the kg cancels out. Poisson's number is dimensionless and under the square root remains m^2/s^2 ,

$$\text{dimension} \left(\sqrt{\frac{\overset{\text{N/m}^2}{E} \overset{(1-\nu)^0}{(1-\nu)^0}}{\underset{\text{kg/m}^3}{\rho} \overset{(1-2\nu)(1+\nu)^0}{(1-2\nu)(1+\nu)^0}}} \right) = \sqrt{\frac{\text{m}^2}{\text{s}^2}} = \text{m/s}.$$

The dimension is correct as stated for velocity.

2.2.12 Shear Wave Velocity

The shear wave velocity is given by the expression

$$v_s = \sqrt{\frac{G}{\rho}}. \quad (52)$$

Combining Equation 51 and Equation 52 and applying standard relations of the dynamic elastic moduli, it is rewritten to

$$E_{\text{dynamic}} = \rho v_s^2 \frac{3v_p^2 - 4v_s^2}{v_p^2 - v_s^2}, \quad (53)$$

an expression that just depends on the speed of the P-wave v_p and the S-wave v_s together with the density ρ . The discussion of the difference in the dynamic and the static Young's modulus is left for Section 2.3.3.

2.3 Attenuation

When evaluating the bar velocity there is also a related curve of attenuation attached to it. The attenuation $1/Q$ is the inverse of the Quality Factor Q and is the tangent to the phase difference α of the strain and force measurements. In an elastic material, no attenuation, the phase difference between stress and strain is zero and the attenuation is also zero. In a purely viscous material, a Newtonian fluid, the phase difference is 90 degrees and the attenuation is infinite.

2.3.1 The Attenuation $1/Q$

The expression for the attenuation is given by

$$\frac{1}{Q} = \tan \alpha, \quad (54)$$

where α is defined as the phase angle between the force and the strain. $1/Q$ will then be a dimensionless quantity describing the attenuation of wave energy in the rock. The Q and the Young's modulus are related. If expressing the Young's modulus in complex notation, taking into account the time delay between the maximum stress and strain, then $1/Q$ is the ratio of the imaginary and real part of Young's modulus. The stress is expressed as

$$\sigma(t) = \sigma_o \sin(\omega t)$$

with σ being the maximum stress amplitude and $\omega = 2\pi f$ the cycle frequency. It will propagate a sinusoidal strain to the sample with a phase lag α

$$\epsilon(t) = \epsilon_o \sin(\omega t - \alpha).$$

The term $\epsilon_o = \sigma_o/|E|$ is recognized where E is the complex Young's modulus. Integration of the stress over the strain gives the energy that goes into the system

$$\int \sigma d\epsilon = \int \sigma \dot{\epsilon} dt \quad (55)$$

$$= \int \omega \frac{\sigma_o^2}{|E|} \sin(\omega t) \cos(\omega t - \alpha) dt \quad (56)$$

$$= \cos \alpha \cdot \frac{\sigma_o^2}{|E|} (\sin^2(\omega t)) + \sin \alpha \cdot \frac{\sigma_o^2}{|E|} \left(\frac{t}{2} - \frac{1}{4\omega} \sin(2\omega t) \right) \quad (57)$$

The first term is said to be in phase, meaning the elastic energy stored in the material. The second term is the energy that is converted into heat, thus lost, in the system. Integrating over a period gives the average elastic energy

$$\bar{W} = 1/T \int_0^T \cos \alpha \cdot \frac{\sigma_o^2}{|E|} \sin^2(\omega t) dt, = \frac{1}{4} \frac{\sigma_o^2}{|M|} \cos \alpha$$

where $T = 2\pi/\omega$. This is valid for all values of Q , not only the small angle approximation. Because of the sine and cosine orthogonality, there is a 180 degree cyclic behavior meaning adding or subtracting any multiple of 180 degrees at the phase does not change the physical interpretation.

The lost energy over one cycle can also be found by integrating in the same manner and is given by

$$\delta W = \frac{\pi \sigma_o^2}{|E|} \sin \alpha. \quad (58)$$

These expressions are in accordance with Paffenholtz and Burkhardt (1989) and O'Connell and Budiansky (1978). The maximal stored energy is found by optimizing Equation 57 in the first term

$$W_{\max} = \frac{1}{2} \frac{\sigma_o^2}{|E|} \cos \alpha, \quad (59)$$

and from there on the $1/Q$ can be expressed as

$$\frac{1}{Q} = \frac{1}{4\pi} \frac{\delta W}{\bar{W}} = \frac{1}{2\pi} \frac{\delta W}{W_{\max}} = \frac{\Im(E)}{\Re(E)} = \tan \alpha. \quad (60)$$

2.3.2 Dispersion

If the velocity of a wave is frequency dependent $v = v(f)$ it is called dispersion. Hofmann (2006) goes into greater detail on this topic.

2.3.3 Cracks

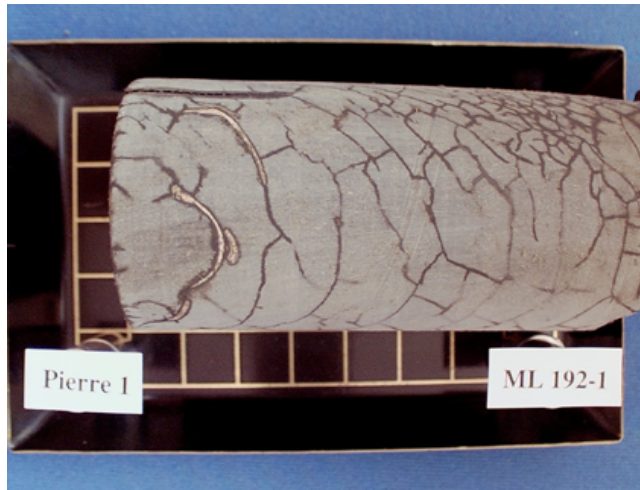


Figure 7: Cracks in a Pierre shale. Surface is cleaned with alcohol. Fluid is emerging from the cracks. (SINTEF Petroleum Research AS, Reidar Bøe 2005)

The static value of the Young's modulus is not necessarily equal to the

dynamic one. The dynamic modulus is typically recorded during logging at site by acoustic measurement techniques with frequencies in the kHz area. In a laboratory it can be measured by the use of ultrasonic equipment, or any other wave propagating setup. The static value is obtained by loading the rock reading off the values of stress and strain. The slope of the curve determines elastic parameters. Figure 8 places this experiment in relation to other.

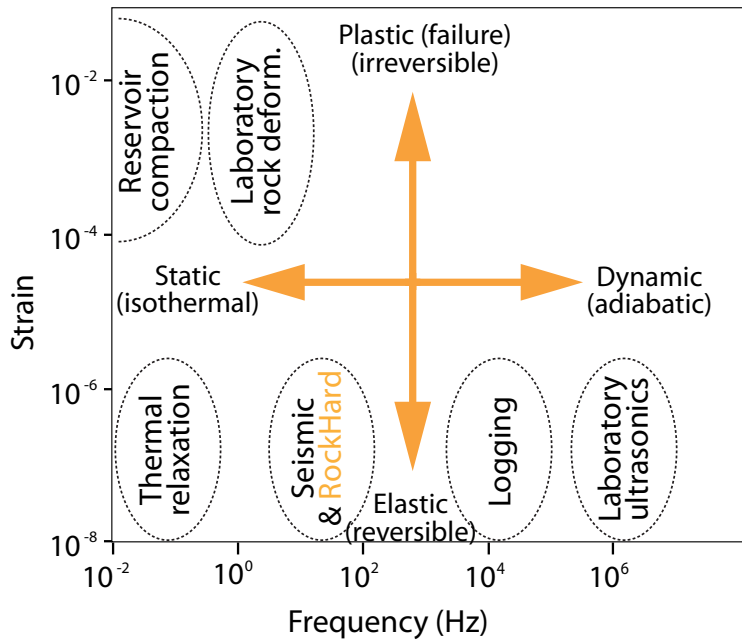


Figure 8: The different techniques and their similarities. (Inspired by Hofmann, 2006, Reference number 25)

When measuring on rocks and materials containing cracks and cavities these inhomogeneities may cause a difference in the results according to which technique is used to measure the modulus. The ratio of static and dynamic measurements of compressibility in several granites was reported by Simmons et al. (1965) to be about 0.5 at atmospheric pressure, and close to unity at pressures of 300MPa and above. King (1969) had similar results when looking at Berea and Boise sandstone, but tests included a confining pressure which at the time is not present in the RockHard setup.

Olsen (2007) made a summary of research done in this topic in his PhD thesis. The description that follows is based on Olsen's (2007) overview. Unfortunately the author did not have access to all his references, but refers the interested reader to Olsen's publication (2007). For matter of completeness both

references are given in (Section 11) even though Olsen (2007) is mainly used as a source.

Cheng and Johnston (1981) found correlation factors between the dynamic and static values depending on stress levels. The static measurements were from strain gauges and the dynamic ones from ultrasonic pulse transmission. They suggest plastic deformation during loading may cause the difference of static and dynamic results, because this deformation does not occur in dynamic measurements. The closing of (micro-)cracks under high confining pressures is also listed as a possible explanation.

Montmayeur and Graves (1985) did not obtain any evident correlation between static and dynamic values when measuring Young's modulus by the use of LVDT's and acoustic P and S-wave propagation.

Van Herden (1987) settled a relationship to $E_s = aE^b$, where a and b are coefficients specific for the different rock types. The values were obtained by ultrasonic and strain gauge measurements on dry sandstones. The ratio E_d/E_s varied from 1-3.

Jizba et al. (1990) narrowed down the ratio of dynamic and static bulk modulus values for dry sandstones of porosity (0.2% \rightarrow 12%) to 1.1 to 1.6. The technique of measuring was strain gauges and acoustic velocities. They also found dependence to clay content and stress level in the interval 5-125 MPa.

Tutuncu and Sharma (1992) confirmed the observations of Jizba et al. (1990) concerning clay content, and Cheng and Johnston's proposal of micro cracks was said to have a larger influence on the static value of Young's modulus. Observations were made on fully water saturated samples with the use of LVDTs and ultrasonic pulse transmission. Stress levels corresponded to in situ stress for the rocks.

Tutuncu et al. (1994) found that for increasing strain, the Young's modulus decreased. As stress levels rise, the Young's moduli (static and dynamic) approach each other, but for low stress values the static one is lower. Dry sandstone samples were among others used for the experiment.

Yale and Jamieson (1994) found the dynamic Young's modulus to be 15% to 70% higher than the static modulus with the difference being greatest on softer samples.

Yale et al. (1995) found that the ratio between static and dynamic Young's modulus on a saturated sandstone depends on the porosity. The ratio is about 2 for high porosity, and 1.1 for lower porosity. Quartz cementation was said to have an impact.

Plona and Cook (1995) found the static value to be 3-5 times lower than

the dynamic Young's modulus when operating with a large loading cycle on dry sandstone. For high stresses the dynamic approaches the static one.

Tutuncu et al. (1998) obtained a ratio of 1-6 between dynamic and static measurements of Young's modulus on a saturated sandstone. They observed that if the strain amplitude increases for a static test, static Young's modulus decreases.

Fjær (1999) suggests non-elastic deformation to be an explanation of the difference in values. Failure in the rock at low stress levels is not observed in measurements and may explain the difference.

Wang (2000) puts the limit at 15 GPa saying that there is good correlation above this value, and limited below. In hard rocks the difference in strain amplitude have less impact. Wang therefore suggests this difference to be an explanation of why the static and dynamic values do not correlate well.

Al-Tahini et al. (2004) pointed out the influence of quartz cementation to explain the difference.

Li and Fjær (2008) used the assumption of plastic deformation at the grains contacts at low stress levels when building a DEM (Discrete Element Method) numerical model to simulate weak sandstones. With increasing stress, the formation of micro cracks is the dominating cause for any deviation.

Learning that several researchers suggests better correlation for high static pressures, values of 10MPa for strong sandstones and 5MPa on weaker samples are used. They are assumed to be sufficient to close off cracks, while still maintaining elastic properties in the rock.

2.4 Sensing Stress

2.4.1 The Piezoelectric Sensor

The piezoelectric effect was first discovered by Curie in 1880, but its application in industrial sensor technology only spans the last 50-60 years. The piezoelectric sensor reacts to compression with a charge buildup. Even though it is compressed, the deflection is very small due to the inherent high modulus of elasticity. The charge is measured by the charge meter that in turn converts it into Newtons with appropriate calibration. The main benefit of this system is its extreme linearity and its insensitivity to electromagnetic noise and radiation. Thermal effects may influence as a change in the internal resistance of the sensor. Because the sensor relies on charge buildup, the best application is for dynamic measurements. This makes it an excellent choice in regard to measure the complex Young's modulus.

2.5 Sensing Strain

2.5.1 The Strain Gage

Strain gages measure the ohmic change caused by longitudinal unidirectional strain in the sample (See Appendix A). By converting this change of resistance into a voltage, a signal that can be processed electronically is obtained. In the small signal range, the ohmic change is assumed linear for metallic strain gages. The strain gages used in RockHard are made of constantan making them less susceptible for temperature fluctuations. Temperature changes may still be of significant importance, but may be corrected for as stated by strain gage manufacturer Vishay[®]. Semi-conductor strain gages may have greater sensitivity for a smaller range, but this is to the cost of linearity. The constantan strain gages provided reasonably good results even without thermal calibration.

2.5.2 Wheatstone Bridge of Unequal Resistances, Differential Approach

To convert a change in resistance to a change in voltage, a Wheatstone bridge can be used. The standard bridge of equal resistances is derived in Appendix B, here a derivation of unequal resistances follows. A simple voltage divider is given by

$$\frac{E_{\text{out}}}{E_{\text{in}}} = \frac{R_{\text{g}}}{R_1 + R_{\text{g}}} \quad (61)$$

To apply this to the Wheatstone bridge it must first be balanced. This is done by making sure that the resistance in the left leg is equal to the resistance in the right leg. Also the ratio of the two resistances in each leg must be equal, $R_{\text{left}}^{\text{upper}}/R_{\text{left}}^{\text{lower}} = R_{\text{right}}^{\text{upper}}/R_{\text{right}}^{\text{lower}}$.

The voltage divider is first applied to the right leg only. R_{g} represents the strain gage resistance of 1050Ω (three strain gages of 350Ω coupled in series). R_1 is a single 350Ω resistor. To get an estimate of the voltage output E_{out} when changing the resistance an amount ΔR , a differential expression is given

with respect to R_g

$$\begin{aligned} \frac{\partial}{\partial R_g} \left(\frac{E_{\text{out}}}{E_{\text{in}}} \right) &= \frac{\partial}{\partial R_g} \left(\frac{R_g}{R_1 + R_g} \right) \\ &= \left(\frac{1}{R_1 + R_g} \right) + R_g \frac{\partial}{\partial R_g} \left(\frac{1}{R_1 + R_g} \right) \\ &= \frac{R_1 + \cancel{R_g}}{(R_1 + R_g)^2} - \frac{\cancel{R_g}}{(R_1 + R_g)^2} \\ &= \frac{R_1}{(R_1 + R_g)^2} \end{aligned}$$

and an infinitesimal approximation gives

$$\frac{\Delta E_{\text{out}}}{E_{\text{in}}} = \frac{R_1 R_g}{(R_1 + R_g)^2} \frac{\Delta R_g}{R_g} \quad (62)$$

with ΔR_g being the total change in resistance over the three strain gages and R_g their total resistance. Since

$$\frac{\Delta \tilde{R}_g}{\tilde{R}_g} = k \frac{\Delta L}{L}, \quad (63)$$

where k is the gage factor, one can combine the two equations and end up with an expression for the output as related to the strain $\Delta L/L$. Here the tilde denotes one individual strain gage with resistance of 350Ω . Note that the factor of 3 cancels out in the substitution

$$\frac{\Delta E_{\text{out}}}{E_{\text{in}}} = \frac{R_1 R_g}{(R_1 + R_g)^2} \frac{k \Delta L}{L} \quad (64)$$

or numerically expressed in terms of strain

$$\epsilon = \frac{\Delta L}{L} = \frac{16}{3k} \frac{\Delta E_{\text{out}}}{E_{\text{in}}}. \quad (65)$$

This is almost the same expression as for the classic quarter bridge of equal resistances as given in Appendix B.

To get an idea of magnitudes let us assume

$$L = 50 \text{ mm}$$

$$k = 2.11$$

$$E_{\text{in}} = 10 \text{ V}$$

$$\Delta E_{\text{out}} = 100 \text{ nV}$$

then the deformation would be equal to about a nano meter and the strain would be in tens of nanoscale. To apply it to the signal recorded, the input on the DAQ card is first converted to yield the peak to peak value instead of the rms. Any expansion and sensitivity must also be accounted for. As stated by Stanford Research the output of the SR850 DSP is given by

$$\begin{aligned} V_{\text{out}}^{\text{rms}} &= \left(\frac{V_g^{\text{rms}}}{\text{sensitivity}} - \text{offset} \right) \cdot \text{Expand} \cdot 10 \text{ V} \\ &= \frac{V_g^{\text{rms}}}{2 \cdot 10^{-6} \text{ V}} \cdot 10 \text{ V} = 5 \cdot 10^6 \cdot V_g^{\text{rms}} \end{aligned} \quad (66)$$

where for our case both the offset and the expansion is not in use. Since the instrument operates in rms mode an additional multiplication of $2\sqrt{2}$ is needed to get the peak to peak value. The sensitivity as stated here is the full scale given in the upper right corner of the display, for our application typically 2 um for strain measurements.

By combining equation (65) and (66) putting $\Delta E_{\text{out}} = 2\sqrt{2} \cdot V_g^{\text{rms}}$, it gives the final expression

$$\begin{aligned} \frac{\Delta L}{L} &= \frac{16 \cdot 2\sqrt{2} \cdot V_{\text{out}}^{\text{rms}}}{3k \cdot 5 \cdot 10^6 E_{\text{in}}} \\ &= 142.985 \cdot 10^{-9} \cdot V_{\text{out}}^{\text{rms}}. \end{aligned} \quad (67)$$

This is under the assumption that the full scale resolution of the lock-in amplifier is set to 2 uV, the gage factor k is 2.11 and the input voltage E_{in} is 10 V.

The main approximation in this equation is the step from infinitesimal to differential values. As long as the values are small of magnitude, this relation is true, but as value increase reliability is questionable. It would be useful to compare this differential result to the one of series expansion given in Section 2.5.3.

2.5.3 Wheatstone Bridge of Unequal Resistances, Series Expanded

Instead of differentiating the expression for the voltage divider, as given in Equation 61, an alternative way is to do a series expansion of it to the order specified. Some approximations are intrinsic also in this approach, but the result may be useful for comparison to the differential result (Equation 67).

From the principle of a voltage divider and superposition the general expression for the potential between the two legs of the bridge is reached

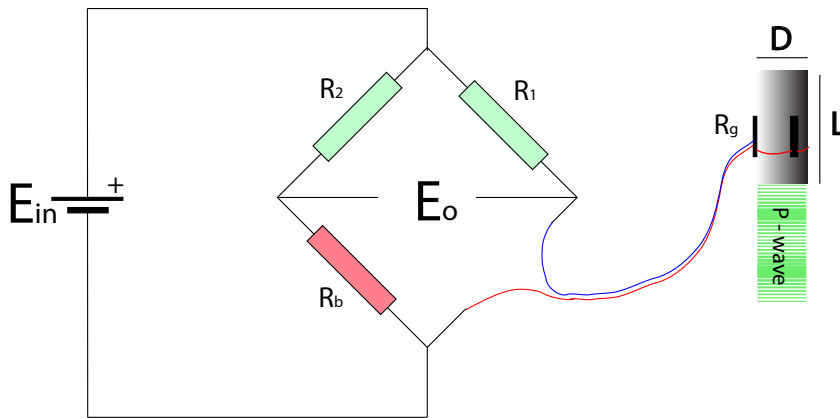


Figure 9: The Wheatstone bridge with supply voltage E_{in} , bridge voltage E_o , resistors R_1 and R_2 , length of sample L , diameter D , and one P-wave propagating through the rock. R_b and R_g consists of three strain gages coupled in series.

$$\frac{E_o}{E_{in}} = \left(\frac{R_g}{R_1 + R_g} - \frac{R_b}{R_2 + R_b} \right),$$

where the names are according to Figure 9.

By expanding $R_g = R_{1050} + \Delta R_{1050}$ and setting $3R_1 = 3R_2 = 3R_{350} = R_b = R_{1050}$ the result yields

$$\begin{aligned} \frac{E_o}{E_{in}} &= \left(\frac{R_{1050} + \Delta R_{1050}}{R_{350} + R_{1050} + \Delta R_{1050}} - \frac{R_{1050}}{R_{350} + R_{1050}} \right) \\ &= \left(\frac{1 + X}{(1/3 + 1 + X)} - \frac{3}{4} \right) \\ &= 4/3 \left(\frac{1 + X}{(1 + 3X/4)} - 1 \right) \\ &= \frac{3}{4} \left((1 + X) \left(1 - \frac{3}{4}X + \left(\frac{3}{4}X \right)^2 - \dots \right) - 1 \right) \\ &= \frac{3}{4} \left(-\frac{3}{4}X + X - \frac{3}{4}x^2 + \left(\frac{3}{4} \right) x^2 + \dots \right) \\ &\approx \frac{3}{16}X - \frac{9}{64}X^2. \end{aligned} \tag{68}$$

where $X = \Delta R/R$ and when assuming that $|X| \ll 1$. The voltage E_o is proportional to the relative change in ohmic resistance $\Delta R/R$. The numerical term in the first order is $3/16$. This is close, but actually a bit lower than the classic ‘‘Quarter bridge’’. The first term is identical to the first order of the differential approach (Section 2.5.2), as expected. The first correcting term of second order is included. For further discussion on the orientation of the strain gages, see Section 4.2.4.

3 Equipment

A lot of hardware needs to be synchronized and operated to do low frequency testing of low amplitude perturbation. The equipment is sectioned in three main groups: The load frame applying the static uniaxial stress to the sample, the instruments and sensors acquiring data together with the software analyzing it, and the chemicals used to prepare the samples and glue the gages. They are mutually dependent and care must be taken in configuration and analyzing the implication of each one. More information about the instruments can be found in (Fintland, 2010) and in Appendices.

3.1 Load Frames

Two load frames were used in the setup: The Manual Load Frame for primary calibration and testing, and the MTS frame capable of two ton force for accurate measurements and final calibration. The MTS frame is by far superior to the manual one, both in accuracy and rigidity. In order to document the process, both frames have their own subsection below, even though all published data come from the MTS frame.

3.1.1 The Manual Load Frame

The Manual Load Frame is a hydraulic jack as shown in Figure 10 and it was used in the early stages of development. It is oil pressured which makes the system non rigid in nature and absolute measurements difficult. Nevertheless the apparatus provides some useful data for rough calibration and for verifying the general the idea behind the setup. The piston of the jack is bigger than of the plug, making it necessary to convert the pressure given at the pressure gauge into actual pressure on the sample. The conversion factor is about 3.14 thus a pressure of 2 MPa read off at the pressure gauge corresponds to an applied pressure of 6.28 MPa on the plug sample.

To avoid the effects of misalignment (See Section 7.4) a globe joint was used underneath. The placement of the joint was done due to practical circumstances and is not ideal. This is because the weight of the ball will make the friction of the joint greater than what would have been the case if it was hanging freely. Nevertheless it improves the setup to some degree and is good enough for the purpose of initial testing. Because of this compensation, only one strain gage was used for the strain measurements in this setup.

The force was measured directly from the charge meter, but corrected for drift. For large perturbations ($\sim 200 \text{ nm}_{pp}$) at uniaxial pressures of about 5



Figure 10: The Manual Load Frame.

MPa, the dataset came out clean enough to read without the need of filtering. When lowering the perturbation and increasing the static pressure, the need for band-pass filtering was immediate. The lowest calibrated range on the sensitive force sensor (Section 3.2.1) is 100N. Signals are typically of about $0.1 \rightarrow 1$ N and are not in need of any heavy amplification. In this stage the lock-in is therefore used primarily as a band-pass filter for extracting the signal on the frequency of perturbation. When later going down to strains of order 10^{-8} on soft materials, amplification of force also becomes important.

Another direct advantage of using the lock-in amplifiers is that any DC component on the input is effectively removed and thereby removing the low frequency drift as experienced both in the Manual Load Frame, but also to some degree in the MTS when the sample is consolidating. One of the downsides when introducing filters and amplification to the system is the increased complexity of the signal path. It may be hard to keep track of all the changes it undertakes

on its way from source to graph. Instruments are calibrated by using standard reference materials.

3.1.2 The MTS Load Frame

The MTS Frame is a computer controlled load frame capable of delivering up to two ton force. The main advantage of this system is the increased rigidity since the crossbow is lowered by the use of screws instead of hydraulic controlled pistons as is the case for the Manual Load Frame (Section 3.1.1). The precision of the bow is good down to the micrometer, but below, the noise picked up in the control system makes it non static and fluctuating. This can be further controlled by the use of LVDTs (Linear Variable Differential Transformer), but here as well there is a lack of precision, and the benefit may be questioned. LVDTs were not used in RockHard.

The computer operating the MTS can keep the force or position actively controlled to compensate for drift (by the use of sensors on the crossbow and/or LVDTs). But it is not the low frequency drift that is the main difficulty, more any sudden changes due to electrical noise on the actual frequency. The best solution may here be to cut power to the MTS, but at power breakdown the force drops momentarily about 2000 N. The risk of any sudden impact altering or fracturing the rock is present and should be treated with care.

3.2 Instruments

The amount of instruments required for the task may seem overwhelming. By first studying Figure 11 and Figure 12 it may be easier to get the big picture. Remember that all instruments should operate at a UPS or a smoothed supply voltage. The strain circuit (Figure 11) can benefit of having its own.

3.2.1 Hardware

The PC was used for practically all measurements on the other hardware. The Macintosh was mainly used for making illustrations, for educational purposes and for report writing.

- Actuator
Physik Instrumente, P-235.1s
Single axis, range 0-15 μm , (See data sheet in (Fintland, 2010)).
- Actuator controller
Physik Instrumente, E-471.20 HVPZT, E-517, E-509.X1, (See data sheet in (Fintland, 2010)).

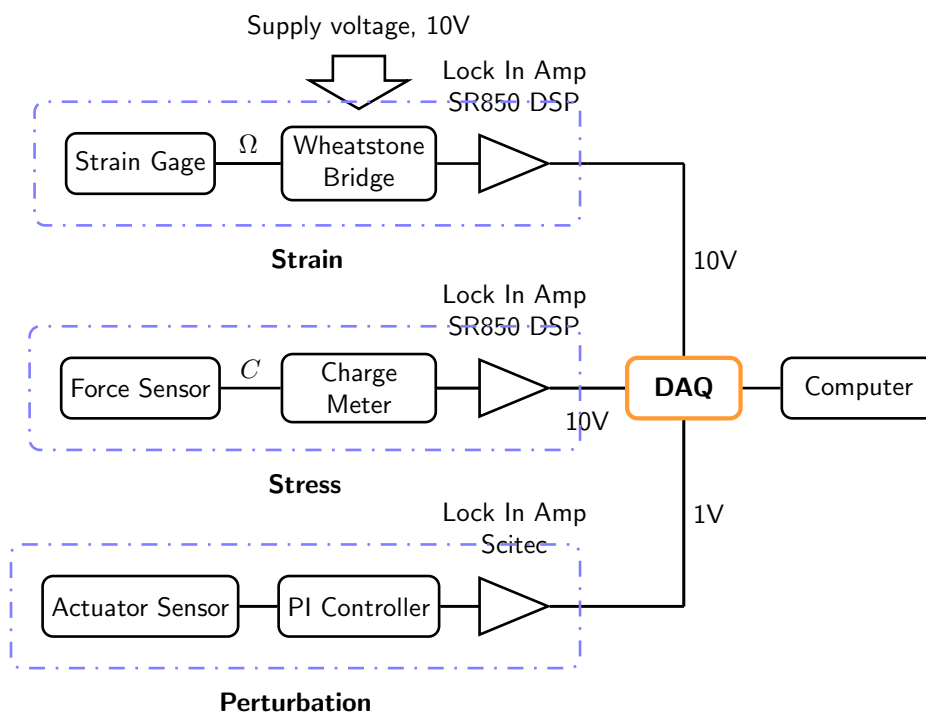


Figure 11: A flow diagram of the measurements. See also Figure 12.

- Charge meter
Kistler, 5015, (See data sheet in (Fintland, 2010)).
- GPIB-card
Agilent Technologies, 82350B PCI GPIB, (See data sheet in (Fintland, 2010)).
- I/O-card
National Instruments, PCI-6034E all inputs with block BNC-2110, (See data sheet in (Fintland, 2010)).
- Load Frame
MTS 2/M, 10kN load frame, (Appendix G.3).
- Lock-in amplifier, force and strain
Stanford Research Systems, SR850 DSP Lock-In Amplifier , (Appendix G.5).
- Lock-in amplifier, actuator position
Scitec, 420 Dual Phase Lock-In Amplifier , (See data sheet in (Fintland, 2010)).
- Mac
2.4GHz Intel Core 2 Duo
2GB 667MHz DDR2 SDRAM
- Oscilloscope
Tektronix, TDS2004B, (See data sheet in (Fintland, 2010)).
- PC
Dell Optiplex 760 Intel(R) Core(TM) 2 Duo CPU
E8400 @ 3.00 GHz
2.99GHz, 3,25GB of RAM
- Press force sensor (PFS)
Kistler, 9323AA, 0...10kN, (See data sheet in (Fintland, 2010)).
- Supply voltage filter,
APC, LINE-E1200I (used on actuator controller module)
(Appendix G.1)
- Temperature sensor,
TO-92, LM35DZ/NOPB
(Appendix G.2)

- UPS,
APC, Smart-UPS 19" 750 VA 480 W 2HE, SUA750RMI2U, 2 pieces
(Appendix G.9)
- Wave generator
Agilent 33220A, 20MHz Function / Arbitrary Waveform Generator, (See
data sheet in (Fintland, 2010)).

3.2.2 Software

PC:

- Agilent Technologies, Agilent IO Control v. 15.0.10528.0
- Botkind, Allway Sync v.11.2.2
- Drop box, Drop box v.0.7.101
- Google docs (Cloud environment)
- MATLAB R2010b, 32-bit, v.7.11.0.584
 - Sinefit
YangQuan Chen, 17 Jul 2003
<http://www.mathworks.com/matlabcentral/fileexchange/3730-sinefit>
 - hline and vline
Brandon Kuczenski, 9'th November 2001
Matlab Central File#1039
 - Keep
David Yang, 10'th August 1999
Matlab Central File ID#181
 - Reading and Writing TDM/TDMS Files in MATLAB
National Instruments
 - RockHard scripts
by author
(Section /refsec:postprocessing)
 - Shade area between two curves
John Bockstege, 30'th November 2006
Matlab Central File ID#13188
- Microsoft, Office (Word, Excel, Powerpoint)

- Microsoft, Windows XP SP3
- National Instruments, LabVIEW 2010
- T. Teranishi, Terra Term Pro v.2.3 For Windows 95/NT

Mac:

- Adobe, Acrobat 8 Professional v.8.0.0
- Adobe, Illustrator CS3 v.13.0.0
- Apple, OS X v.10.6.4
- Drop box, Drop box v.0.7.101
- Google docs (Cloud environment)
- MATLAB R2009b, 64-bit, v.7.9.0.529
- Microsoft, Office 2008 (Word v.12.2.0, Excel v.12.2.0, Powerpoint v.12.2)
- National Instruments, LabVIEW 2010 v.10.0 (32-bit)
- Richard Koch, TeXShop v.2.18

3.2.3 Drivers

- Actuator: E517_All_VIs.vi (From CD)
- Lock-in amplifier: sr850.llb (From web-page of manufacturer)
- Press force sensor: 5015_V1-33.llb (From CD)
- Wave generator driver: agilent_33xxx_series.zip (From web-page of manufacturer)

3.2.4 Other

The strain gages are of same or very similar resistive properties. The conducting parts are all made out of constantan.

- General Purpose Strain Gages,
Vishay[®] Micro-Measurements & SR-4
350 ± 0.3% Ω
Item code: 17090. Appendix G.6 (Used on most samples)

- General Purpose Strain Gages,
Vishay[®] Micro-Measurements & SR-4
 $350 \pm 0.3\% \Omega$
Item code: 3271. Appendix G.7. (Used on steel sample)

3.2.5 Interfaces and Connectors

The setup of the equipment is according to Figure 12. The power supply is not shown here. The mains power line voltage is smoothened through a UPS before being fed to the different instruments. There is serial connection between the charge meter and the PC, and USB to the signal generator, the controller of the actuator, and oscilloscope. There is a possibility to include GPIB communication to the lock-in amplifiers, but mainly the settings have been set on the instruments themselves, or even extracted from a 3.5" floppy disk. For further details see (Fintland, 2010, Section 5.1.5).

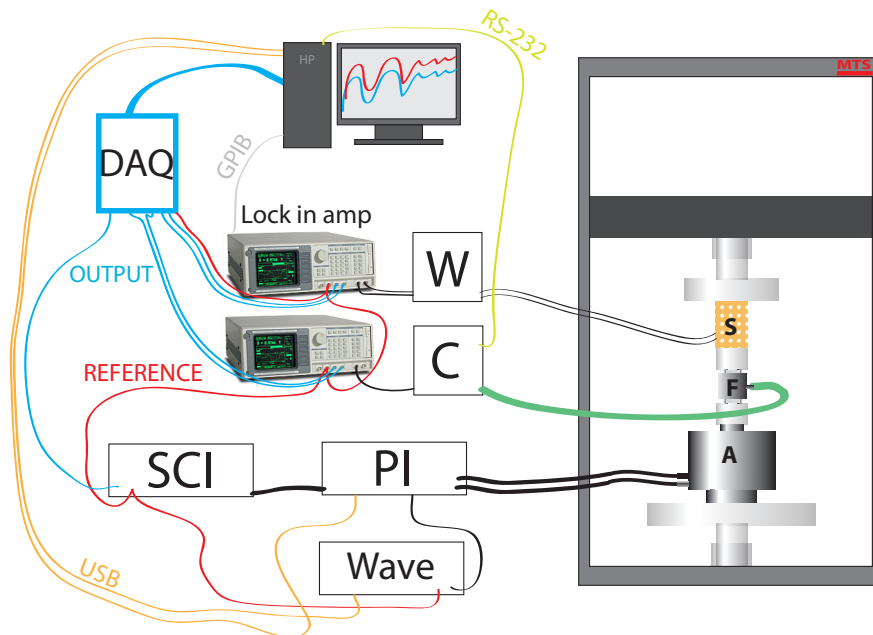


Figure 12: Instrumental setup. 'W' is the Wheatstone bridge (Section 2.5), 'C' is the Charge meter, 'PI' is the servo controller module of the actuator, 'Sci' is the lock-in amplifier, 'Wave' is a signal generator, 'DAQ' is the data acquisition unit, 'S' is the sample, 'P' is the pressure sensor, and 'A' is the actuator.

3.3 Chemicals

To attach the strain gages to the surface of the samples a series of chemicals were needed both for cleaning, preparing and bonding. In an alphabetic order they are:

- Acetone (Appendix F.1)
- Catalyst, Vishay[®] (Appendix F.6)
- Conditioner A, MN5A-1, Vishay[®] (Appendix F.7)
- Epoxy, Loctite 3430 A&B Hysol (Appendix F.2)
- Isopropanol (Appendix F.3)
- Marcol Laboratory oil (Appendix F.4)
- M-Bond 200 Adhesive, Vishay[®] (Appendix F.5)
- Neutralizer 5A, MCA-1, Vishay[®] (Appendix F.8)
- Zap-a-gap[®] CA+ (Green Label), Zap[®] glue (Appendix F.9)
A cyanoacrylate adhesive used on the oily shale surface
- Zip Kicker[®] (CA Accelerator), Zap[®] glue (Appendix F.10)
An accelerator sprayed on the glue to speed up the adhesive process.

All strain gages were installed according to VISHAY[®] Instruction Bulletin B-127-14 (Appendix G.8)

4 Calibration

With the lock-in amplifiers the full scale of each one needs to be set depending on the strength of the input signal and the desired sensitivity. As a general rule the average input signal should be about halfway of the full scale, but it may be set less if the fluctuations are big. The easiest way of making sure that the sensitivity is set correctly is through the use of the oscilloscope, and making a manual check for a typical frequency. Some general guidelines for setting the full range may be found in Table 1.

Table 1: Numeric example values of the full scale amplifier ranges, FS, on the lock-in amplifiers measuring force, strain and position. The limits have been empirically settled. ϵ is the measured strain in the sample.

E GPa	ϵ 10^{-9}	FS-strain nV	FS-force mV	FS-position. mV
< 10	~ 50	≤ 500	10	10
< 10	~ 150	500	20	10
~ 70	~ 110	500	500	30

4.1 Force Sensor

4.1.1 Magnitude Conversion

The piezoelectric crystal in the force sensor induces a charge in the charge meter when compacted. The amount of charge to make up one Newton has been factory calibrated to the numerical value 9.551 pC/N when operating from 0...100 N. This is the lowest given calibrated scale. To transfer the signal to the computer an analog value between -10 V and 10 V is used. 10 V would correspond to full scale of the measurements. To summarize: The charge Q is proportional to a force F which in turn makes up a voltage U which is fed to the lock-in amplifier whose output is $V_{\text{force}}^{\text{rms}}$ that can be related linearly to the force in question

$$Q \propto F \propto U \propto V_{\text{force}}^{\text{rms}}. \quad (69)$$

The lock-in equation relating U and $V_{\text{force}}^{\text{rms}}$ is given as Equation 66. We end up with

$$F = 10 \text{ N/V} \cdot U_{\text{toLockIn}}^{\text{pp}} = 10 \text{ N/V} \cdot 2\sqrt{2} \cdot \frac{V_{\text{force}}^{\text{rms}} \cdot \text{sensitivity}}{10 \text{ V}}, \quad (70)$$

where $V_{\text{force}}^{\text{rms}}$ is the channel signal on the DAQ card.

4.1.2 Phase Conversion

If including the phase β when logging the output of the lock-in amplifier's channel 2 is given by

$$\beta = \frac{U(\text{Lock in, ch 2, output})}{10V} \cdot 180^\circ \quad (71)$$

this is under the assumption that the lock-in is set to output phase on channel 2 without any offset and standard expansion. The range of Channel 2 is $\{-10 \text{ V}, 10 \text{ V}\}$ providing a phase range of $\{-180^\circ, 180^\circ\}$. Each lock-in amplifier gives the phase as compared to the reference of the signal generator. If assuming the reference phase being equal, the difference of their respective absolute values will make up the difference in phase of the stress and strain. The phase value will be extracted from the output of the two amplifiers by the same equation (Equation 71), and their difference decides the relative phase difference

$$\alpha = \beta_{\text{stress}} - \beta_{\text{strain}} - 180^\circ \cdot n, \quad (72)$$

where $n \in \mathbb{Z}$.

4.2 Strain Gage

When measuring on low frequencies with low amplitude, the noise makes a generous contribution. The circumstances requires the use of lock-in amplifiers to extract the weak signal from the strain gages. The gain of the amplifiers may be up to 160 dB and it goes without saying that noise of the measured frequency will be amplified accordingly. This makes it hard to measure at the power line frequency of about 50 Hz (and multiples of this one). But at frequencies different from 50 Hz on the other hand, results are very useful.

4.2.1 Magnitude Conversion

The strain gage is sensitive to a change in resistivity ΔR . Over the Wheatstone bridge this change in resistance generates a voltage difference V_g that in turn is fed to the lock-in amplifier for further analysis. The output is linearly proportional to the input, and the relation of the strain and the measured voltage is expressed in the following,

$$\frac{V_g}{V_s} \approx \frac{x}{4}, \quad (73)$$

where V_g is the output of the Wheatstone bridge, V_s is the supply voltage and x is the relative change in resistance $\Delta R/R$. The overall expression for the strain is given as

$$x = \frac{\Delta R}{R} = k \frac{\Delta L}{L} \approx \frac{2.1 \Delta L}{L}, \quad (74)$$

where k is the gage factor given by manufacturer and $\Delta L/L$ is the strain. The output of the lock-in amplifier is the rms value of the voltage amplitude so the peak to peak value would be $2\sqrt{2}$ times greater than what the display reads. We recall Equation 66 and get

$$V_{\text{out}}^{\text{rms}} = \left(\frac{V_g^{\text{rms}}}{\text{sensitivity}} - \text{offset} \right) \cdot \text{Expand} \cdot 10 \text{ V}, \quad (66)$$

$$= \frac{V_g^{\text{rms}}}{0.5 \cdot 10^{-6} \text{ V}} \cdot 10 \text{ V} = 2 \cdot 10^7 \cdot V_g^{\text{rms}}, \quad (66a)$$

where the parameters should be self explanatory. The sensitivity is the full scale (upper right corner on the lock-in's display). Combining Equation 73, 74, and 66a give

$$\frac{\Delta L}{L} = \frac{x}{2.1} = \frac{4V_g}{2.1V_s} = \frac{4 \cdot 2\sqrt{2} \cdot V_g^{\text{rms}}}{2.1 \cdot V_s} = \frac{4 \cdot 2\sqrt{2} \cdot V_{\text{out}}^{\text{rms}}}{2.1 \cdot V_s \cdot 2 \cdot 10^7} \quad (75)$$

$$\approx 2.7 \cdot 10^{-8} \cdot V_{\text{out}}^{\text{rms}} \quad (76)$$

A numerical example with a full scale of 500 nV is provided. The full scale must be optimized to every sample depending on its stiffness, and the magnitude of perturbation. Some typical values for full scales are given in Table 1.

4.2.2 Phase Conversion

The lock-in amplifiers measuring stress and strain are identical. Given the same settings for phase output, the conversion is equal to Section 4.1.2.

4.2.3 Strain Gage Wiring

The signals from the strain gage are very small and thus the noise impact is substantial. The lock-in amplifier filters most of the noise with a different frequency than the source, but what remains is the noise of equal frequency. This may be changing and dependent on the amount the wiring to and from the strain gage picks up. In general the shorter the wire, the lesser the noise. But nevertheless a bit of wiring is necessary and the optimal design arises as

the next question. There are two main ways to cope with it: The single wire, or the dual wire setup.

The single wire, as illustrated in Figure 13, has the benefit that any noise affecting both the core of the coax cable and the surrounding conducting web will influence equally and thereby be rejected by looking at the difference. Any noise affecting just the outer web will not be rejected and may create erroneous readings. Since the physical distance between the core and the web is small (less than a millimeter), any noise will usually affect both core and web, but possibly with different magnitudes.

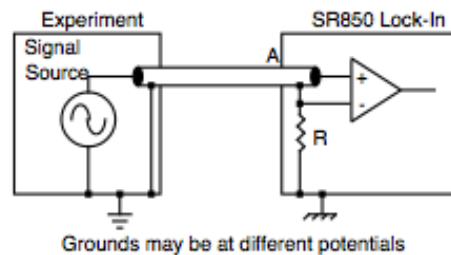


Figure 13: The single wire setup. (Stanford Research Instruments, User manual for Lock-in amplifier)

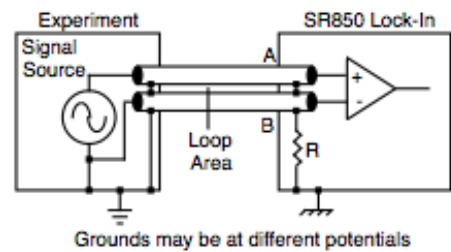


Figure 14: The double wires setup. (Stanford Research Instruments, User manual for Lock-in amplifier)

As already mentioned; a different approach is to transmit the signal in two different wires and ground both of the conducting webs, as seen in Figure 14. This will create good shielding, but if the cables are physically far apart, it is less likely that noise will affect both conductors in equal amount, thus reducing the common mode rejection ratio (CMRR).

Both of the setups have been tested. In order to avoid ground loops, the dual wire setup was grounded either at the lock-in or at the signal source (supply voltage). The double wires turned out to be the best option when shielding the cables and connections. Thermal noise proved to have an impact on the

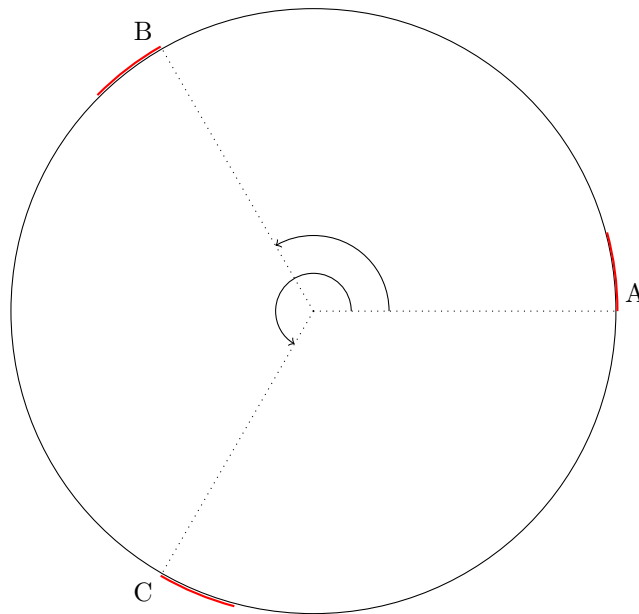


Figure 15: The configuration of the three strain gages when doing static one axial strain measurements. The two angles indicated are 120° and 240° .

measurements. This is caused by heating in the strain gages when the current is flowing. It could be avoided by using a half bridge (Section 2.5) since the thermal change of resistance has the same effect on both legs of the circuit. This again introduces other complications and possible error sources.

4.2.4 Strain Gage Orientation

In Figure 4.2.4 the cylindrical sample is seen from the short side in a cross section midway on the long side. The three strain gages are oriented 120 degrees apart. The reasoning behind the setup of the strain gages may seem wrong since the use of averaging over three gages does not increase the resolution of a quarter bridge. In fact it gets worse than when using a single strain gage. To answer the question one must look in the nature of the problem, namely orienting the sample. Because of non parallel surfaces in the MTS frame (Section 7.4), one side reads compaction and the other one expansion. Taking the average over several strain gages compensate for this. As the amount of information collected increases the average is assumed to converge to the true value.

Coherent with the increased amount of strain gages other problems arise. The sample has limited surface area and the surface may need to be smoothed with epoxy if it is of rough texture (Section 4.3). Alternatives to the configuration used are many. If using three strain gages, as before, another possible way

is to use a half bridge (with better resolution) applying two gages on one leg and one other on the second leg with equal dummy resistors. The exact increase of resolution would have to be calculated, but it is roughly about the double of the present setup. This would require many wires going back and forth between the sample and the bridge making it more possible to pick up noise on their way, and the layout was abandoned due to its complexity.

By using four strain gages each 90 degrees apart, a half bridge with two and two in series would make sense. A full bridge needs both compaction and expansion (both sides of a beam) and since the effects of compaction in this case is due to misalignment one would try to minimize them rather than reinforce them. The full bridge setup is therefore not particularly useful in this context. The decision of making use of only three strain gages was based upon the empirical results upon testing. The wiring and bridge configuration were after that optimized to fit. A main guideline throughout the setup is to keep it as simple as possible whilst still producing reasonable and reproducible results in accordance with theory.

4.3 Epoxy



Figure 16: Castlegate surface without epoxy.

When applying epoxy to smooth the rough surface of a sandstone sample, the layer of epoxy may alter the characteristics of the rock. Epoxy is supposed to make the rock stiffer, but the effect is yet to be quantified. It is also not known if there is any frequency dependence related to the epoxy.

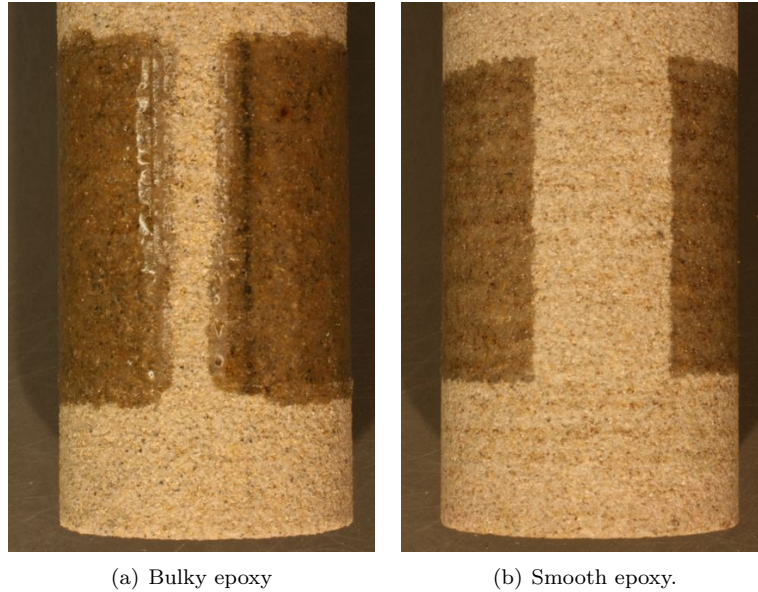


Figure 17: Epoxy on a rough surface. (a) is a Castlegate sample (ML#222.3) before grinding the epoxy. (b) is a Berea sandstone (ML#318.1) after grinding.

Figure 16 shows a rock surface before application of any epoxy. The different constituencies show up on the rough surface. Filling epoxy in the cavities is a continuous process of applying and grinding it off to produce an ever smoother surface. In Figure 17(a) the epoxy has been applied without having been grinded. In Figure 17(b) the sand grains are in level with the epoxy and the surface is smoothed to be perfect for strain gage attachment. Excessive grinding may reduce the cross sectional area of the sample and must be corrected for.

4.4 Temperature Sensor

Figure 18 shows temperature sensor developed to measure ambient temperature close to the sample. The sensor requires an input voltage of 4 to 20 V on the wire '5'. The wire labeled '0' should be grounded together with the other ground wire of the coax cable. The output is from the SHUNER contact. This has common ground with '0' wire input. The output in mV is ten times the temperature in Celsius independently of the provided input voltage.

$$U_{\text{output}}^{\text{SHUNER}} = 0 \text{ mV} + 10 \text{ mV}/^{\circ}\text{C} \cdot T. \quad (77)$$

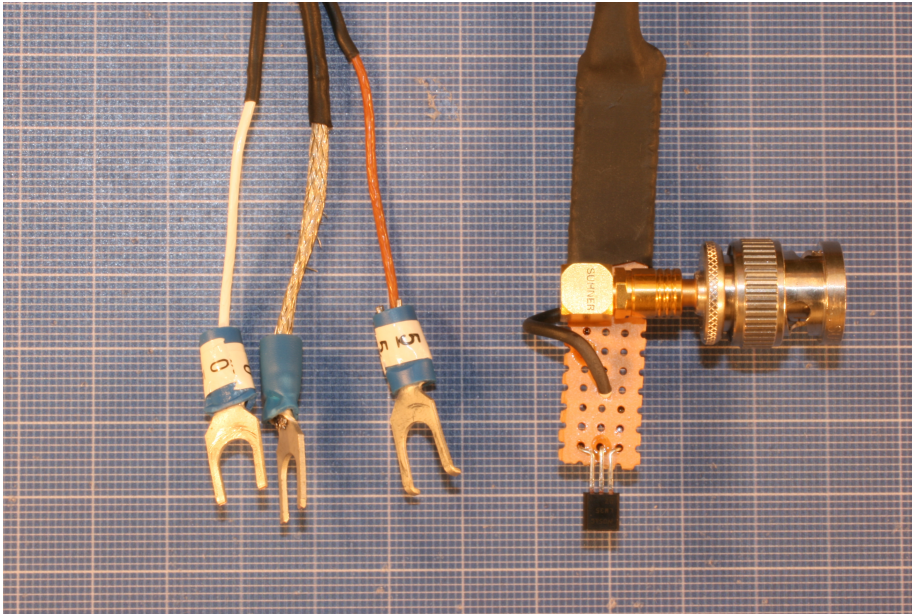


Figure 18: The temperature sensor with corresponding wires. Output from the SHUNER contact.

For a temperature of 23°C the output will then be 0.23V . The linearity is excellent for our purposes since the sensor is optimized for room temperature.

Due to practical circumstances the temperature sensor was removed from system to make room for measurement of phase. In principle there is no problem in measuring both, but the code in both LabVIEW and MATLAB must be modified to 6-channel input instead of 5-channel input.

4.5 Shielding of Setup

To make the best possible analog conditions for measuring weak signals (μV and less) some heavy shielding was needed to avoid big fluctuations in the lock-in amplifier. Cables were replaced by coaxial cables where the outer web was grounded. To shield the Wheatstone bridge itself a Faraday cage out of an old hard drive chassis was built, Figure 19. This proved to be an extremely effective way of doing it. The lock-in got a much smoother signal with a reduced amount of spurs and noise. By having a cleaner input, the output was more continuous and unambiguous.

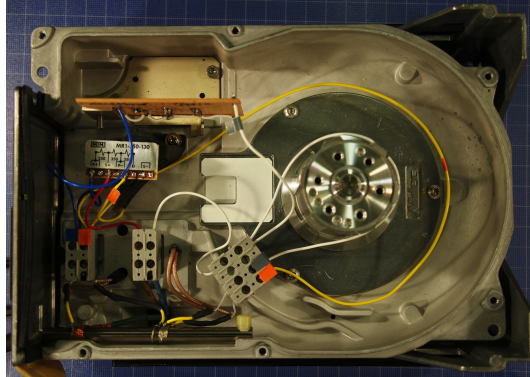


Figure 19: The inside of the Faraday cage built to protect the Wheatstone bridge from electromagnetic noise. The chassis comes from an old hard drive.

4.5.1 Ground Loops

Ground loops may be a problem when having excessive grounding. If a wire is put to ground in both ends, a current can propagate the cable and influence the measurements. This was avoided by grounding the wires in one end only, and by setting any abundant device ground to float.

4.5.2 Uninterruptible Power Supply

Since the lock-in amplifier in theory is influenced by all its inputs, also fluctuations of the supply voltage from the mains power line may show up on measurements. This was especially evident in the first phases of testing when doing low strain values. By installing an uninterruptible power supply (UPS) there is a buffer between the mains power line and the amplifier. The voltage delivered to the amplifier comes from the battery of the UPS and is to be treated as constant both in phase and amplitude. This is a great advantage and showed good improvements when operating at high gains.

The UPS has the possibility to power many instruments at the same time. Both the signal generator, the lock-in amplifiers, and the supply voltage to the Wheatstone bridge got smoothed power from the UPS.

The effect of smoothing by the use of UPS can later be seen in the measurements (Section 5) by comparing Figure 41 and Figure 42.

4.6 The time constant, t_c

The time constant t_c is a setting on each of the lock-in amplifiers defining for how long the integral should run. If the time constant is long, the response to

any impact will be slow. This is a useful feature if the signal is noisy since any long time constant will average out the error and produce a steady output. A problem when $t_c \gg 1$ s is the time it takes for the signal to rise and stabilize on the true value. Usually it takes 2-4 time constants before reaching any semi-constant value. For the samples included in this report $t_c \in \{3, 10, 30\}$ s. It is recommended using $t_c = 3$ sec when setting the full scales of the equipment. The general trend seems to be the stiffer the sample, the higher the time constant. With total measurement times of 200-300 seconds the numbers stand in great contrast to the values needed for steel (See Section 5.1.6).

5 Measurements

The plug samples (Aluminium, PEEK, sandstones and shale) are all previously investigated for their elastic properties at SINTEF. This has been done by mounting them in the MTS frame at a given confining pressure, and then send ultrasonic pulses of P and S-waves. The speed of a compressional and shear wave in the material is determined by measuring the time of arrival of the signature waveform over the known distance. A simple workbench version was tried. In order to preserve the specimens for later testing no sirup/honey was applied to the rock surface, and it was therefore hard to make an S-wave propagate.

The values presented in Table 2 are therefore based on previous measurements done under good conditions, on samples from the same block. The Young's moduli are calculated from Equation 53.

Table 2: P-wave and S-wave ultrasonic frequency speeds measured previously by SINTEF Petroleum Research AS, Jørn Stenebråten.

Sample ML#	ρ g/cm ²	uniaxial stress MPa	v_p m/s	v_s m/s	E GPa
ALU-6061	2.70	2	6466	3146	71.88
ALU-7075	2.81	2	6288	3107	72.62
Berea ML#318	2.14	5	2990	1970	18.54
Castlegate ML#222.1	1.96	5	2970	1680	13.99
PEEK03	1.32	5	2563	1129	4.64
Pierre ML#192.2	2.33	5	2370	901	5.35

5.1 Sample Description

The dimensions of the plugs are given in Table 3. In any calculation they are assumed isotropic and homogenous. To gain a better understanding of the composition and texture of the materials, each material has its own subsection.

5.1.1 Aluminium

The aluminium samples ALU-6061 and ALU-7075 are of known alloys with composition given in Table 4. Judging from the chemical composition, the properties of the alloys may be somewhat different. They are both one inch in diameter cylindrical plugs 2 inch long, with three strain gages attached 120 degrees apart. End pieces are kept clean and there is no evident outer damage. The attachment process of the strain gages is as prescribed by VISHAY[®] using

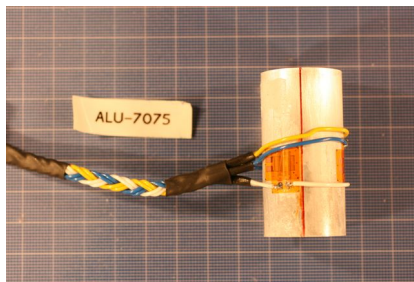
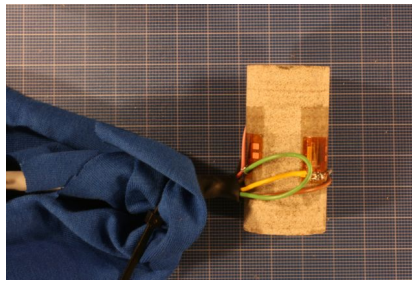
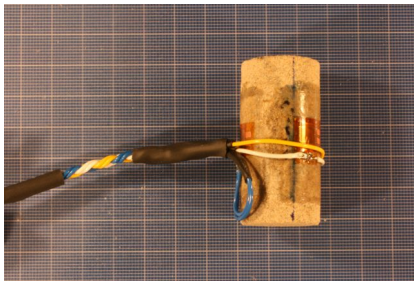
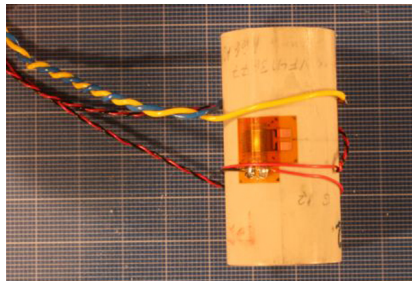
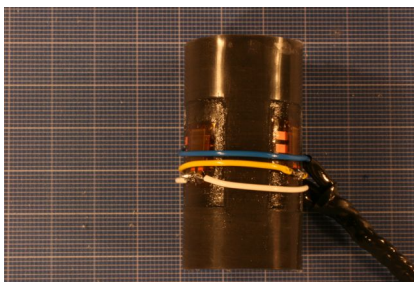
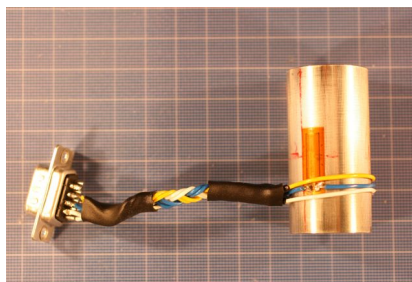
(a) ALU-7075, $\varnothing = 1''$, $l = 2''$ (b) Berea sandst., $\varnothing = 1''$, $l = 2''$ (c) Castlegate sandst., $\varnothing = 1''$, $l = 2''$ (d) PEEK, $\varnothing = 1''$, $l = 2''$ (e) Pierre shale, $\varnothing = 1''$, $l = 2''$ (f) Steel, $\varnothing = 1''$, $l = 2''$

Figure 20: The plug samples with attached strain gages.

Table 3: Dimensions of samples used for testing. The assumed measurement error is ± 0.02 mm.

Material	ML#/sample	diameter mm	length mm
Aluminium	6061	25.41	50.83
Aluminium	7075	25.41	50.82
Berea (sandstone)	318-01-01	25.31	50.64
Castlegate (sandstone)	222.3.1	24.50	50.51
Castlegate (sandstone)	222.3.2	24.90	50.76
PEEK	03-166	25.41	50.82
Pierre (shale)	192.1	25.41?	50.82?
Steel		25.41	50.82

Table 4: Chemical composition of Aluminium alloy 6061 (AMS 4117) and 7075 (AMS 4122)

Alloy		Si	Cu	Mg	Zn	Cr	Mn	Fe	Ti	Al
6061	Min	0.40	0.15	0.8	-	0.04	0.15	-	-	Rem
	Max	0.80	0.40	1.2	0.25	0.35	0.40	0.7	0.15	Rem
7075	Min	-	1.2	2.1	5.1	0.18	-	-	-	Rem
	Max	0.40	2.0	2.9	6.1	0.28	0.30	0.50	0.20	Rem

their recommendations on grinding, preparation, neutralizing and gluing (Section 3.3 and Appendix G.8). The bulk density values are table values (Jeng et al., 1997 and The Aluminium Association Inc. 2006)

$$\rho_{6061} = 2.70 \text{ g/cm}^3 \qquad \rho_{7075} = 2.81 \text{ g/cm}^3. \quad (78)$$

The samples used for testing are referred as: ALU-6061 and ALU-7075. In early test series also Aluref03-166 was used. Since the alloy of this sample is not known, it was later rejected for further testing.

5.1.2 Berea Sandstone

Berea sandstone is a quartzose clastic rock with geographical origin in the USA. The sorting and grain size of the Berea siliclastic may vary depending on the depth in the outcrop layering. The general tendency in the Berea layers is the deeper the coarser, and the more poorly sorted (Churcher et al., 1991). By visual inspection of the samples used for testing, they were found to be typical of the Upper Berea unit. It is finer grained, well sorted, and with closely spaced

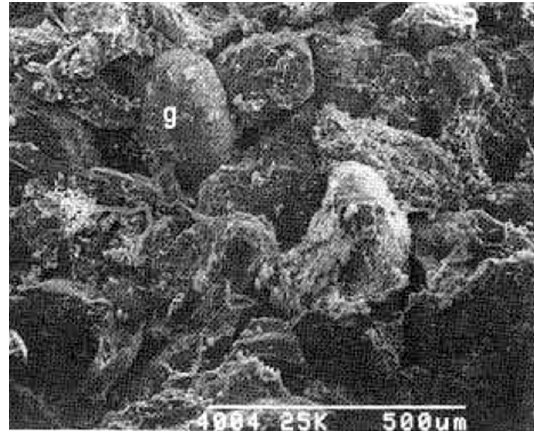


Figure 21: The Berea sandstone texture. The grains are clearly visible. A $500\ \mu\text{m}$ scale bar is shown in the lower right corner. (Churcher et al., 1991)

planar layers. Some ordinary values are extracted from literature (Churcher et al., 1991) and presented in Table 5.

Table 5: Mineral composition of Berea sandstone, weight percentages (Churcher et al., 1991).

Qtz	K-fsp	Plag	Chl	Kaol	Ill	Smect	Calc
85-90	3-6	1-2	tr	2-6	(tr)	-	6-8

Abbr.: Qtz = quartz, K-fsp = potassium feldspar, Plag = plagioclase feldspar, Chl = chlorite, Kaol = kaolinite, Ill = illite, Smect = smectite, Calc = calcite
tr = traces (small amount)

The surface of the Berea is quite rough because of the large grain structure compared to clay. A SEM picture Figure 21 shows it. One may clearly see the round grains packed and partly cemented. As a consequence of this rough surface, epoxy is needed in order to make the strain gage stick evenly to the bulky surface and sense the strain (See Section 4.3).

The attachment process of the strain gages is as prescribed by VISHAY[®] using their recommendations on grinding, preparation, neutralizing and gluing (Section 3.3 and Appendix G.8). The there gages are mounted on an epoxy surface (Section 4.3) evenly spaced around the circumference.

The Berea sample used for testing may be referred to as: 318.01.01. In one occasion a typing error named the sample 310 instead of 318. There is no sample 310 subject for testing, so this number should be read as 318.

5.1.3 Castlegate Sandstone

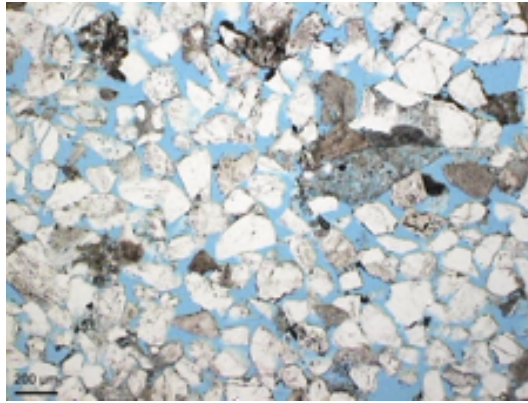


Figure 22: Castlegate thin section. Open and well connected pore network. A 200 μm scale bar is shown. (SINTEF Petroleum Research AS, Reidar Bøe 2005)

The Castlegate sandstone generally has a higher amount of feldspar than the Berea sandstone. According to Fjær (2009) the anisotropy is relatively low and a normal porosity is at about 28.8%, with mineral composition of 70 % quartz and 30 % feldspar. Figure 22 shows a well connected pore network where consolidation is poor. By comparing the the Berea and the Castlegate sandstone hands on, this observation is confirmed. The Berea sandstone sticks more together, particles do not come off as easy as with the Castlegate sandstone in dry condition.

The attachment process of the strain gages is as prescribed by VISHAY® using their recommendations on grinding, preparation, neutralizing and gluing (Section 3.3 and Appendix G.8). The gages are mounted on an epoxy surface (Section 4.3) 120 degrees apart near the centre of the sample.

The Castlegate samples used for testing may be referred to as: ML#222.1.1 and ML#222.1.2

5.1.4 PEEK

The semicrystalline polyetheretherketone (PEEK) is a high performance, high temperature crystalline thermoplastic. It is suitable for testing mainly because of its excellent load bearing properties over long periods of time. The resistance to dynamic fatigue is outstanding at room temperature (Searle et al., 1985). Judging from its first appearance in literature in the 1980's it is a quite recent material.

Various standard properties were found. In the sake of completeness two

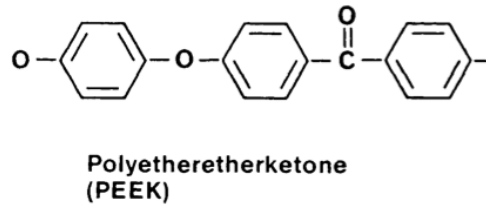


Figure 23: Chemical composition of PEEK.

deviating tables are displayed: Table 6 and Table 7.

Table 6: Standard properties of PEEK (Searle et al., 1985)

ρ g/cm^3	TS@20° MN/m ²	TS@150° MN/m ²	EB @20° %	FM @20° GN/m ²	FM @150° GN/m ²	HDT °
1.320	93	37	> 100	3.6	2.2	165

Abbr.: TS = Tensile Strength, EB = Elongation to Break, FM = Flexural Modulus, HDT = Heat Distortion Temperature.

Since the data given in Table 6 are quite old and may not be up to date, a second reference (Platt, 2003) and (Ratner et al., 1996) is provided in Table 7 for comparison. The values are not the same in the two tables. This may be due

Table 7: Ultrasonic wave-speeds and calculated isotropic elastic constants for PEEK450G (Rae et al., 2007)

ρ g/cm^3	v_p m/s	v_s m/s	E GPa	ν	G GPa	K GPa
1.28	2590 ± 10	1130 ± 10	4.6	0.38	1.7	6.6

Abbr.: ρ =density, v_p =p-wave speed, v_s =s-wave speed, E =Young's modulus, ν = Poisson's ratio, G =shear modulus, K =bulk modulus.

to material development or improved measurement techniques. Since Table 7 is more recent and corresponds to the values measured by SINTEF (Table 2), this and the SINTEF ones will be used for later reference. The Young's modulus measured in Table 7 have no given load information. Since the numbers are quite similar to the ones of Table 2, the load value is assumed equal.

PEEK may in many applications replace metal in manufacturing. It is in use in aerospace, transportation, electronics, medical equipment and food processing industry. Peek is also often used as bearings. It has a high resistance to different kinds of radiation, acids and temperature fluctuations. (Melo et al., 2002, Rae et al., 2007).

The attachment process of the strain gages is as prescribed by VISHAY® using their recommendations on grinding, preparation, neutralizing and gluing (Section 3.3 and Appendix G.8). The gages are mounted 120 degrees apart near the centre of the sample.

The PEEK plug sample used for testing may be referred to by: PEEK03-162

5.1.5 Pierre Shale

The Pierre shales have ML# 192.2.12 and ML#192.3.10. A sample with ML#192.1 was XRD analyzed at SINTEF Petroleum Research in 2005 by R. Bøe. Even though every sample is different, an overview of the main characteristics is obtained by looking at Table 8. The smectite makes the shale soft and is the main component.

Table 8: Mineral composition of Pierre shale, weight percentages (Bøe R. 2005)

Qtz	K-fsp	Plag	Chl	Kaol	Ill	Smect	Calc	Sid	Dol	Pyr
7.4	0.3	1.8	7.9	8.7	15.2	57.8	0.2	0.1	0.1	0.5

Abbr.: Qtz = quartz, K-fsp = potassium feldspar, Plag = plagioclase feldspar, Chl = chlorite, Kaol = kaolinite, Ill = illite, Calc = calcite, Sid = siderite, Dol = dolomite/ankerite, Pyr = pyrite.

Apart from the mineralogical composition, the texture of the rock is of importance. In general shales do not have much texture and the scale of the grains is very small. A SEM image reveals this in Figure 24.

The density of the Pierre shale has been settled by two different methods to get an estimate for both the dry density and the wet density (Section 2.2.2). To get the dry density Bøe used the ratio between the weight after drying and the total sample volume. The bulk wet density was determined as the ratio between the weight before drying and the total sample volume. The sample volume was in turn determined by the buoyancy method: the ratio between the weight of displaced water and the water density.

$$\rho_{wet} = 2.400 \text{ g/cc} \qquad \rho_{dry} = 2.209 \text{ g/cc} \qquad (79)$$

The shale is the only sample analyzed with a saturation. The sample itself was encapsulated in a teflon sleeve to prevent it from drying out when exposed to air. While stored it was kept in an oil filled container. When attaching the strain gages, some holes had to be cut in the teflon sleeve. Care was taken to avoid having the sample dry out, and a special glue (3.3) was used to make

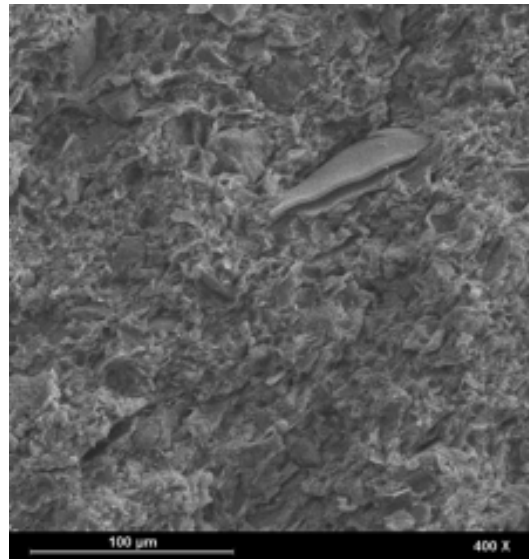


Figure 24: The Pierre shale texture. The bigger piece is a mica flake. There is a tendency of orientation in the same direction as the flake. A $100\ \mu\text{m}$ scale bar is shown in the lower left corner. (SINTEF Petroleum Research AS, Reidar Bøe 2005)

the gage stick to the oily surface. Before applying the adhesive, the surface was cleaned with a gentle rub of acetone. The positioning of the strain gages were as always about 120 degrees apart, evenly spread around the circumference centre on the sample.

Some problems arose during mounting and measuring the shales. The wires put a shear moment on the fragile shale making it partly fractured. In some cases the strain gage came loose with a small coating of clay underneath. By replacing the wires with slimmer and more flexible ones, the situation seemed to better. The importance of effective assembly was evident since this was the only sample with saturation.

5.1.6 Steel

The steel plug was used initially for testing. Because of its very high rigidity ($\sim 200\ \text{GPa}$), it demands very different amplification gains, integration times and perturbations than the soft rocks. Measurements are only mentioned for curiosity (Section 6.3.3) and should not be given much attention.

5.2 Measurement Series Description

In the Manual Load Frame setup the measurements were not divided into measurement series.

In the MTS Load Frame several series of measurements were conducted following the different improvements and changes of the equipment. At the time of publishing the fifth series (5TestSeries) is in the making. Measurements from first and second series were conducted while still measuring on steel with a HF/LF setup, making the dataset big (about 1.8 million measurements over a two hours). This was the limit for what MATLAB could handle in graphics and great effort was made to simplify the setup. By rejecting steel as a reference, the integration time could be reduced down to seconds, and the measurement time down to minutes. Many measurements were conducted after these new standards in the third measurement series. The measurements started to converge towards the table values found in literature, and more samples were added (Castlegate for instance). Analogue improvements were continuously implemented (For instance the Faraday cage) and the noise got lower. When taking the leap from the third measurement series to the fourth two important changes are worth mentioning: Phase measurements were once again implemented after having been absent since the first series, and UPS' were set to smoothen the supply voltage of most of the electronics. In the fifth measurement series integration time was increased to 30 seconds with a total measurement time of 300 seconds. The perturbations are also in general quite high.

Not only hardware followed the evolution of the series. Software adapted and improved both in collecting and displaying the data. A downside of changes in any software is the loss of backwards compatibility. This was often the case in RockHard since major changes made it hard to support vintage data. Looking at the data obtained in early measurement series one may question their importance. All files described in `rockon.m` (Section 6.2.1) are working from the fourth measurement series where phase measurements were integrated.

In general the latest measurement series should be given the most attention, but data from third, fourth and fifth series are presented.

5.3 How to Conduct a Measurement - Step by step

5.3.1 How to Run a Measurement in LabVIEW

1. Make sure that wires are connected according to Figure 12.
2. Switch on all instruments about one hour prior to any measurements. This will help them reach thermal equilibrium and make the measurements better.
3. The sample should be 1 inch in diameter and 2 inch long. Check the dimensions and write down the exact length and diameter. It should have three strain gages glued at its sides to measure the axial deformation (Section 4.2.4). The wires from the gages should go to a 9 pin delta connector. The gage is connected to one pin on the first row and one on the second row. Check earlier samples for the exact wiring. (The wiring to make them in series is implemented in the lead wire from the Wheatstone bridge.
4. The sample is loaded in the MTS Load Frame according to Figure 12. The boom is lowered (TestWorks) to the desired static load and the sample is connected to the Wheatstone bridge.
5. If the lock-in amplifiers have been disconnected from power, recall basic settings from the 3.5" floppy drive (file '5015' for the force, '850' for the strain).
6. Push [Meas] on the Kistler Charge Meter to start feeding the force signal to the lock-in amplifier measuring force (LIA-Y). Set an output of the signal generator (signal strength $\in \{10, 50\}$ mV; frequency $\in \{10, 100\}$ Hz should suffice) and switch the output on. Set integration times to a reasonable value (3-10 seconds) and adjust the gain of the amplifiers till the signal is midway on the scale. (The oscilloscope can be used for that task: max scale of LIA-X (strain) and LIA-Y (force): 10V; Scitec max 1V).
7. Switch off the perturbation signal (Push [Output] on signal generator) and push [Meas] on the Charge Meter to make the instruments ready to be computer controlled.
8. Start up RockHardDeformations_master.vi (RockHard master file) and fill in all the fields according to the settings found in previous step.

9. Make sure that the actuator runs in open loop and that its position is set within the allowed interval as given in the RockHard master file. (Adjust the 'Control Input' on the PI actuator controller unit if needed.)
10. Remember to also set the perturbation voltage, the frequencies and the sampling times.
11. Run RockHard!
12. LabVIEW will output the result of the (completed) previous measurement in the graphics pane in the upper left corner of the RockHard master file. The .tdms files will appear in the path specified as LabVIEW starts to access them.
13. When completed close LabVIEW and follow the guide for post processing in MATLAB (Section 5.3.2).

5.3.2 How to Interpret the Output of a Measurement

1. Open MATLAB (32-bit version!)
2. Navigate to the folder containing the .tdms measurement files. (Default: c:\RockHard*TestSeries\)
3. Make sure that c:\RockHard\RockHardPostProcessing\ is included in PATH.
4. Type 'rockon' and hit [enter]
5. Several steps will now execute. The process is finished when the four graphs are displayed full screen.
6. The process is very memory demanding and should therefore be left to finish. If any problems are experienced, please restart computer to clear memory and repeat this section.
7. Hit any key to exit the graphs. All plots have been exported to the measurement's root folder.

6 Post-Processing of Data

6.1 TDMS Logfile

The .tdms binary file that comes as an output of the LabVIEW RockHard master program contains several types of data. The measurements are coded in a binary fashion making it hard to interpret in any third party software such as MATLAB. A script called ReadFile.m developed by National Instruments have a certain level of support for the transfer, but it depends on the use of .dll libraries thus making it a Windows dependent platform. Even though the measurement data are extracted (to MEASUREMENTS variable in MATLAB) by the use of the script, the metadata containing information about the measurement process (settings from instruments etc.), are not easily imported. Therefore the need of special tailored scripts is evident.

These customized scripts are found in Appendix C with some of their functions given in Appendix D. All scripts and functions are documented well and could be explained by typing in the MATLAB command window: 'help [name of function]'. An explanation of the way to use the script and its inputs and outputs will appear.

NOTE! An important thing to remember is that ALL SCRIPTS MUST RUN FROM THE ROOT FOLDER OF THE MEASUREMENTS! This is basically the folder containing the .tdms files. Since the scripts are folder independent, they are located in the C:\RockHard\RockHardPostProcessing folder. THAT PATH MUST BE INCLUDED IN THE MATLAB PATH BEFORE ANY EXECUTION OF SCRIPTS. The standard path of RockHard is: C:\RockHard.

6.2 MATLAB Scripts

To be able to analyze the data stored in the overall .tdms log files provided by LabVIEW, quite a lot of calculation is needed. It is beneficial to use scripting in MATLAB since the calculations are often repeated. The master script is named rockon.m and it will execute all the other scripts in the proper manner. The sub scripts (they are invoked from rockon.m) documented here are named rh1* to rh4* with increasing level of operation (* meaning wildcharacter). rh1 and rh2 deals with individual files while rh1all, rh2all, rh2fg2, rh3* and rh4* demands a group. rh1 needs to be prior to rh2 etc. The files are not to be treated as laminated master code, more a way of attack where individual configurations may be necessary. For the same reason quite a lot of old code and thoughts are included in comments. This may be an inspiration to the person modifying it providing ideas and making it easier to understand.

6.2.1 RockHard Master Script - rockon - Running all sub-scripts necessary (rh1all.m → rh4sPhase.m) on the .tdms files present in folder

This master script is a great simplification of the analyzing of data from RockHard Deformations. It was developed quite late (somewhere in the 4'th measurement series) and may therefore not be completely backwards compatible. Nevertheless it should have no problem in running on all new measurement series with a 5 channel input: stress (magnitude and phase), strain (magnitude and phase) and position (magnitude).

The steps in rockon.m are best described by reading on the different modules themselves either in the sections that follows (Section 6.2.2 to Section 6.2.5), in the Appendices (Appendix C and Appendix D) or by typing 'help [name of rh-script] in the Matlab command window.

6.2.2 RockHard 1 - rh1 - Converting .tdms file to .mat file and setting constants

The MATLAB script rh1.m (Appendix C.1) is the first step of post-processing. The idea of this step is to extract the data embedded in the .tdms file and store it in a .mat file for easy access afterwards. For this task there is dependency on the library published by National Instruments which supports the basic import. The library is build on the use of .dll files thus only MS Windows compatible. Unfortunately this library is not able to out of the box import the settings of RockHard.

Reading the binary file as a text-file worked to some extent since some of the data were stored as text. Much binary data needed to be rejected and the functions getChar.m (Appendix D.1) and getNum.m (Appendix D.2) were developed for the task. getChar.m imports the binary file as a single text-string (as much as max-length of a string) together with a keyword which is the title of the field that is to be imported. The keyword needs to exactly match the name of field given in the source code of LabVIEW RockHard master program (not necessarily the same as what is on the front panel, but in source code. Any whitespace must be removed from the name. Relative from the position of the keyword the value can be extracted by suppressing the binary data that lie between the name of field and value of field. This is all taken care of by the function and the returned output is a string containing the value of field.

The getNum.m uses the getChar.m with an additional casting of type to make the value a double. This casting is essential when further interpreting the field buy boolean logics and mathematical operations.

Both functions are operated by the script `getTDMS.m`. This script contains all the name of fields that should be extracted from the `.tdms` file. If by any chance more fields should be included, this is where to include them. The input to the script is the `.tdms` file and the output is a struct containing the data.

The struct is ordered as a collection of data with a specific structure. It is best explained by an example. After having run `rh1*.m` type `master.waveGenerator.frequency` in the command window. This will output the frequency of the wave generator, namely the frequency of perturbation. 'master' is here the super-node name or the name of the struct itself. Adding '.' gives access to under-nodes. After typing the punctuation mark one may hit [tab] on the keyboard to get an overview of the different under-nodes. If hitting [enter] after typing 'master' the structure of the master is given as screen output.

Information is not only extracted from the contents of the `.tdms` file. The filename is also of importance since this contains information about the full range of the lock-in amplifiers, measurement time, frequency etc. Any filename of the `.tdms` file must therefore be on the template made by RockHard master program. Any extra information may be appended at the end of the file, just before the file extension. Examples of data extracted from file name are:

- Strain gage lock-in amplifier full range
The script searches for the string '_x' and 'nV_' and imports what is located between them.
- Force lock-in amplifier full range
The script searches for the string '_y' and 'mV' and imports what is located between them.
- Position lock-in amplifier full range
The script searches for the string 'scitec' and, after position of 'scitec', searches for 'Hz_' and imports what is located between them.
- Frequency The script searches for the string 'mVpp_' and 'mV_' and imports what is located between them.

Strictly speaking much of the information provided in the file name could be extracted from the contents of the file. But extraction from filename is a way to access information fast without having to import the file, and in some situations it may be beneficial. For backwards compatibility the information provided in the struct is sometimes copied to variables within the MATLAB workspace.

rh1all The script `rh1all.m` executes `rh1.m` on all `.tdms` files contained in folder by providing their path as the variable 'filepath' in consecutive order depending

on their filename, or sometimes after the time of creation, the latter option may be commented away in final setup.

6.2.3 RockHard 2 - rh2phase and rh2fg2 - Calibrating the .mat file and calculating the Young's modulus

The script rh2phase.m (Appendix C.4) continues where rh1.m left. The raw data extracted in rh1.m are now calibrated and the Young's modulus for that specific perturbation and frequency is calculated. The script also outputs one .pdf file reflecting the signals measured. They are plotted relative to their maximum value to show any abnormal behavior in either of the three channels measuring magnitude. The only new variables input to the script are 'mStart' and 'mEnd' being the start and the end of the interval for calculation. Both numbers are in percent ($\in \{1 - 100\}$) of the measurement time. 'mStart' < 'mEnd', and their standard values are set to hence 70 and 100 if no other value is provided within the workspace. The data outside the range of mStart and mEnd are rejected in terms of calculation. Calculations of the Young's modulus and the phase of force and strain is executed.

rh2all When several '.mat' files are present rh2all.m calls the rh2phase.m to run over all files in folder. The values used for 'mStart' and 'mEnd' is extracted from the mStartEndList.csv file. If the file is not present it will be created with standard values.

rh2fg2 and rh2 These files have been replaced by the rh2all.m file and rh2phase.m, but they are left in the repository for backwards compatibility. Their usage is much the same as the files they replaced. Refer to source code (Appendix C.5 and Appendix C.3) for further explanation.

6.2.4 RockHard 3 - rh3 - Collecting data from various .mat files

The MATLAB script rh3phase.m (Appendix C.6) is all about grouping the data that rh2phase.m (or rh2all.m) produced. The code given in the appendix extracts some data from the .mat files and plots them in various sub-plots. The plots are usually operating on a linear scale and are therefore best used for data spanning a limited frequency range or perturbation range. Error bars indicate the max/min values of the measured values within the measurement zone (between mStart and mEnd). Running the script gives a collection of variables with the prefix 'total' which is a label of data extracted from several

.mat files. The plots are written to a .pdf file at the end of runtime and the variables remains in memory but are not stored in any .mat file.

There is a graphical output from rh3. This is a collection of sub-plots with the standard of plotting stress/frequency, strain/frequency, indirectly measured Young's modulus/frequency, directly measured Young's modulus/frequency. This graphical output is then stored in measurement root catalog with the default name of 'summary.pdf'.

rh3 It contains much of the same functionality as rh3phase, but it does not contain any calculation of phase. It has therefore been replaced by rh3phase.m for all practical purposes, but is left in the repository for limited backwards compatibility.

6.2.5 RockHard 4 - rh4, rh4s and rh4sPhase - Plotting tools

The MATLAB scripts rh4.m (Appendix C.8), rh4s.m (RockHard 4 Small, Appendix C.9) and rh4sPhase.m (RockHard 4 Small Phase, Appendix C.10) do not import any data from any file, so they are all dependent on rh3phase.m running just before. rh4.m is to be thought of as a pure plotting environment for already collected data. The output is the frequencyDependence.pdf file giving the Young's modulus and the perturbation in the same plot over frequency on a logarithmic scale. It was originally constructed to plot from 10-8009 Hz, with a frequency grid of 34 of quasi logarithmic distribution and should be treated thereafter. To plot for a lesser frequency span the rh4s.m file should be used. Input how many of your measuring points that should be plotted on a linear scale (default of 18 points if sum of x values are below 35000 Hz). rh4sPhase.m plots the absolute phase of the force and the strain, the difference in phase of the two, and the attenuation $1/Q$. When running the script input how much Young's module and how much deformation is expected. If the values 'y1Max' and 'y2Max' are present in workspace input is suppressed.

6.2.6 Others

Several other script files was developed when making plot for this report. Some of them would classify for further usage, one being **rhMean.m** which can be run after rh3*.m. The script extracts the mean values and standard deviations of the Young's modulus and the strain. The code is scarcely documented, but should be self explanatory.

6.3 The Manual Load Frame

At first the experimental setup only contained one lock-in amplifier and thus the sine signal recorded from the other instruments needed some more interpretation. One general approach to extract parameters from noisy data is to optimize a model to them, and read of the values from the model. There are different ways of optimizing the model depending on the number of unknowns and the linearity of the system. A commonly accepted solution is to minimize the sum of the square errors (SSE) between the model and the actual data. This will provide a set of values for the unknowns for which the square distances from the model to the data points are optimized. Any burst may have a significant impact on the fitting since each datapoint is given equal importance. Initially the sine signals recorded did not show the tendency of bursts, and LSSE was therefore applied. This technique was used for interpreting several signals before the conversion using three lock-in amplifiers. One of the main drawbacks of this way of doing it was the need for a high sampling rate over a long time since the dataset contained both high frequency sine waves and low frequency lock-in amplifier signals. If the data are very noisy the readings were very erroneous with limited reliability.

6.3.1 Curve Fitting

Figure 25(a) and Figure 25(b), show that the increased amplitude of the sine wave makes the error between the model and the data smaller. To implement this general idea into MATLAB the additional Optimization Toolbox and the work of (Chen, 2003) was used with some adjustments. One of these modifications was fixing the frequency to the known frequency of the perturbational wave. This greatly improved the reliability of the predicted values.

Although the fit may be good for various cases, problem arises when dealing with data where other frequencies have influenced. This may create an envelope on the signal which in turn requires the use of filtering before processing the data. The R value will indicate if the fit is reasonable or not.

The Coefficient of Determination R^2 tells us about the correlation between the observed data and the model. It tells us if the model fits or not. If the value is 1 all the data can be explained from the model. There is no correlation if the value is equal to 0. Mathematically it can be expressed as

$$R^2 = 1 - \frac{\text{SSE}}{\sum_i (y_i - \bar{y})^2},$$

where y_i is the measured data, \bar{y} is the average, $\text{SSE} = \sum_i (y_i - f_i)^2$, and f_i is

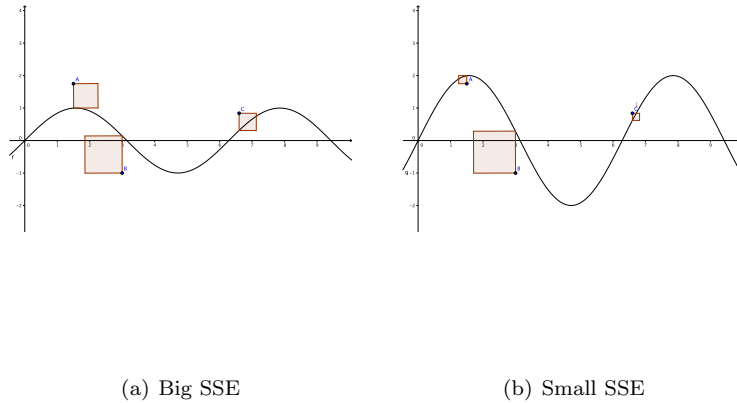


Figure 25: When fitting a sinusoidal curve to data points by the LSSE method, the aim is to minimize the area of the error (illustrated in red) to the model (black sinusoid) by adjusting the amplitude and phase of the sinusoid. The frequency is assumed given.

the model data. This is a demonstration of how to filter a noisy sinusoid in a MATLAB environment, after the implementation of the three lock-in amplifiers and going extremely small in phase, this way of doing it had no application. Similar techniques were previously used (Bautmans, 2009) when attempting to construct low frequency setups.

6.3.2 Exporting and Importing

The dataset of the Manual Load Frame consisted of both high and low frequency measurement data. The high frequency data are the direct signals measured, and the low frequency data are the signal from the lock-in amplifiers which ideally should turn into DC-signals.

One problem when having signals that deviates in frequency is how to configure the sampling. To catch the high frequency signal a sampling speed twice the high frequency is required. The low frequency is irrelevant of sampling frequency, but demands a long measuring time. By doing both at the same time the recorded amount of data may be huge and the post processing hard. One way to overcome this was to include several more lock-in amplifiers to convert the HF data into the same environment as the LF set. Before this option was available, about 1.8 million lines of data were recorded in every measurement cycle producing binary files of up to a 100 MB each. An example of measurements

from the early setup is Figure 26

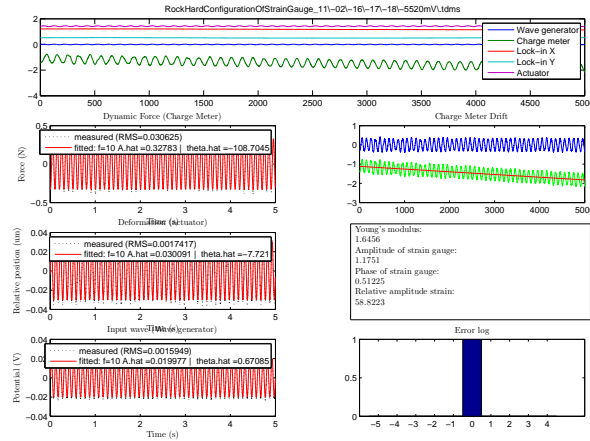


Figure 26: Data recorded in the Manual Load Frame

6.3.3 Displaying

When measuring for a short period of time, or with a low sampling rate, the raw data can be easily plotted for all the measured interval. This is very helpful in order to identify sources of errors which may show up as drift, peeks or deep canyons on an else-wise smooth curve. For instance the crane in the workshop has a heavy influence and can easily be identified on the plot of the raw data of the lock-in amplifiers. But when the amount of data approaches millions of readings and the file size is close to a hundred MB, all wide range graphics are labour intensive and may cause the program to run out of runtime memory and eventually crash. To cope with this dilemma a new set of tools were implemented in the file `easy.m` emphasizing the numerical back-end on the low frequency data, and avoiding heavy plotting. This file later turned into `rh1.m` and `rh2.m` when doing the transfer to the MTS. (Section 6.2.2 and Section 6.2.3). The output of the early script `easy.m` is given in Figure 26. There is some resemblance to the layout of `rh3.m` and `rh3Phase.m`.

The idea of using the the lock-in amplifier to filter the signals of strain and stress is that with sufficient time of integration t_c what remains is a DC-component telling the value. Just as the charging of a condensator the system needs some time to reach this near constant value. The higher the t_c the longer the time. But the lower the t_c the worse signal to noise ratio. When first starting measuring on aluminium and steel using a t_c of 300 s to 1ks in the MTS frame, a

near constant value was reached after about 0.6 hours, depending on the peak to peak magnitude of the perturbational P-wave. For steel the measurement time should therefore be at least an hour in order to have a certain determinational ground, and to make possible the identification of external shock events (such as the crane).

Since steel is outside the scope of this instrumental setup, one later focused on softer samples with integration times of about 3-10 seconds and total measurement times of 200 seconds. This provided useful results for samples going up to about 70 GPa.

7 Sources of Errors

7.1 Error in Figures

In several test series the diameter and the length of the sample was assumed hence 1" and 2" without confirming it with a caliper. The number is afterwards stored in a binary fashion in the .tdms file making it hard to edit. If importing raw data and measurement data one should check that the variable 'crossArea' is the correct area as derived from Table 3. This mainly applies to the Castlegate samples. All numbers in this thesis have been corrected for this error. Graphs are not corrected since the error is hardly visible on the plot. A list of dimensions used for calculation and the corrections needed is provided in Table 9. The biggest error found was about 4%, but this value was a single case. When propagating the 4% error in diameter to the circular cross sectional area, it turns into 7%.

Table 9: Corrections for diameter values found in measurement files.

Plug	TestSeries	\varnothing in .tdms mm	\varnothing actual mm	\varnothing error %
ALU-6061	4Test	25.45	25.41	0.2
	5Test	25.40	25.41	0.0
ALU-7075	3Test	25.40	25.41	0.0
	4Test-1	25.45	25.41	0.2
	4Test-2	25.45	25.41	0.2
	5Test-1	25.40	25.41	0.0
	5Test-200	25.40	25.41	0.0
	5Test-300	25.40	25.41	0.0
	5Test-400	25.40	25.41	0.0
ML#318.1.1	3Test	25.42	25.31	0.4
	5Test-1	25.40	25.31	0.4
	5Test-2	25.40	25.31	0.4
ML#222.3.1	3Test	25.42	24.50	3.7
ML#222.3.2	4Test	24.45	24.90	-1.8
ML#222.3.2	5Test-1	25.03	24.90	0.5
ML#222.3.2	5Test-2	25.03	24.90	0.5
ML#222.3.2	5Test-3	25.03	24.90	0.5
PEEK-03-166	3Test	25.42	25.41	0.0
Pierre (shale)	192.1	25.45	-	-

7.2 Noise Floor

The development of the measuring system has been an ongoing process and it has continuously improved in reliability and complexity. Some of the setup has

also developed differently than anticipated. To settle a noise floor for all the different vintage data would be near an impossible task since there has been so many modifications bettering the results. Most of the final error can be said to be random error in the fluctuations of the semi DC signal from the lock-in amplifiers. To estimate the error one needs to look at each sample by itself and analyze the fluctuations of the output on the lock-in amplifier.

7.2.1 Systematic Error

- Gain of amplification is too low/high

If the gain is set too low the response of the amplifier will make the output shoot up way above the true value due to the integration aspect. Depending on the time constant of integration it will integrate itself back to the true values in amplitudes close to where it started. It may be beneficial to run the equipment with a low gain in order to get consistent files when measuring on both stiff and soft materials or if there is heavy frequency dependence of very different values. In general any underestimation of gain should be avoided. Not only the resolution of the output is reduced, but also the time before reaching any constant DC-value, if possible since it takes several time constants for the amplifier to integrate its way back again. With too high gain the output signal may be cropped.

- High frequency filtering on the charge meter

The Kistler 5015 Charge Meter has a built in low pass filter to remove any high frequency noise. By the use of the lock-in amplifier this filter is not really necessary. Just make sure that it is not set to filter the frequencies one is about to measure (learned the hard way!). It could possibly be set to a value well above measurement range, or disabled.

- Intrinsic instrument error (Lock-in amplifiers are old)

Any electronic component have a limited lifetime. As the amplifiers are quite old (possibly from the 80's) time wears them. When feeding the same signal to both with identical wires they generally behave uniquely even though they eventually tend to settle on the same value. One of the row of buttons on the lock-in measuring force is not functioning. The workaround for this is through the use of a 3.5" floppy disk and setting the settings on the one working and recall them on the defective device.

- Low frequency noise (Mains power line frequency of 50 Hz for instance.)
Operates with huge gain on the strain measurements the whole system is very susceptible for noise. The filtering in the lock-in amplifier is generally

very good, but any noise with components of the measuring frequency will have an impact. When addressing the systematic low frequency error, the mains power line frequency of 50 Hz is a good example.

- Numerical error in post processing
As the complexity of the system is ever increasing it may be hard to keep a clear picture of all the signal modifications. Numerical errors can occur systematically. An example of this may be setting values wrong in the MATLAB scripts (full ranges, gains, cross sectional area, and conversions).
- Unbalanced bridge for given static load
The Wheatstone bridge should initially be balanced, meaning that no current should be flowing when there is no perturbation. This may not always be the case since the static load may induce a higher resistance in one of the legs. With any flowing current follows thermal heating and non-linearity. This issue is more relevant for bigger strains and the manufacturer provides more information regarding this topic.
- Wire crosstalking
Maxwell's equations shows that an electromagnetic field is also prominent when sending any alternating signal through a wire. This field will influence any nearby wire and possibly impact its signal. This is particularly the case when dealing with wires with poor insulation (non coax cables) and high voltages. Crosstalking may not only occur in wires. Also the DAQ-card is subject to this problem. If the grounding is not properly done any port may influence any other one. This proved to be a problem with the signals from the lock-in amplifiers on the range $\{-10V, 10V\}$ while other signals were far weaker.

7.2.2 Random Error

- Attenuation of signal
The signal output of the actuator propagates not only in the sample, but also through the rest of the components. Generally speaking the components have been chosen among the most rigid ones to make the least losses, but still they may be significant, especially when measuring on stiff samples such as metals. Since the strain is the most difficult value to measure a general guideline is to try to keep the measured strain values in the order of 10^{-8} by adjusting the other parameters.
- Boundary surface losses

When going from one material to a different one the boundary itself dissipates energy. If the connection between the materials is good, there may be less energy loss than in a loose setup where the boundary surfaces may end up vibrating air molecules rather than the adjacent sample.

- Cross sectional area measurement

The diameter is measured with a digital slide caliper expressing the result down to a hundred of a mm. Any error is magnified through the calculations of the area after the law of propagation of errors. It is questionable whether the cross sectional diameter is constant. Generally speaking the drilling is accurate to justify the assumption. If applying epoxy (Section 4.3) caution must be taken not to grind away too much of the rock and thereby altering the diameter of the sample.

- Electromagnetic noise

Any wire may act as an antenna. By making sure that every wire is grounded and avoid ground loops, the effect is minimized. Electronics such as the Wheatstone bridge is shielded in a Faraday cage built out of the chassis of an old hard drive providing an excellent shield when grounded.

- Grains and impurities on surface

When applying the static uniaxial load to the sample, any grains and particle on the surface may be squeezed into it and affect the sample and the dissipated energy in the boundary. Surfaces are generally cleaned and kept free of contact to any possible contaminator.

- Ground loops

If a wire is grounded in both ends, it effectively works as an antenna making it possible for current to pass through. With any current comes an electromagnetic field that may alter the signal and induce noise. By grounding in one end only this effect is minimized.

- Human error

The possibility of human error is present in any setup. The error could be both systematic or random.

- Impurities on contacts (corrosion, grease and bad connection)

If the contacts of the wires are not clean, the signal may have problems coming through. Stains of fat and dust may be cleaned through the use of acetone or spirits.

- Intrinsic instrument error (Lock-in amplifiers are old)
The vintage electronic components may introduce a systematic error or a random one.
- Length of sample measurement
The length is measured with a slide gage. After testing this length is reduced because of the plasto-elastic effect (Section 2.1). The resolution of the slide gage is one hundred of a mm.
- Misalignment of sample
If the sample is not centered, the uniaxial stress may put a greater load on one of the sides making the strain non uniform. Please read Section 7.4 for further assessment of the issue.
- Mains power line fluctuations
Any burst on the mains power line may influence the electronics handling the measured signals. By using battery powered UPS systems this error has been minimized. After installation of the UPS's the signals behaved far better without that much fluctuations as earlier (See Section 4.5.2).
- Temperature fluctuations
Almost any instrument is influenced by big alterations in temperature. Prior to measuring the instruments are switched on to be able to reach thermal equilibrium. Otherwise the temperature in the laboratory is fairly constant at 22.9° C.
- Very low frequency noise (trains, cars, cranes etc)
Much of the testing has been done during night-time to minimize the effects of external low frequency noise contributors such as traffic and crane operating in the laboratory. The crane have proven itself to have a big impact on the strain signal.
- Wire crosstalking
The wire crosstalking may appear random (from bursts) or systematic.

7.3 Time Constant

Often the lock-in amplifier is not able to hold the near DC output for an infinite time. The reason for this is still unknown, but one possibility lies in the massive amplification. Any noise can contribute substantially and if the magnitude is high enough, the DC-signal will be heavily offset and depending on the inte-

gration time, it takes a while of low noise environment to once again reach a DC-output.

7.4 Non Parallel Surfaces and Stress

If the contact surfaces between the plug and the load frame are not parallel, the tension will not be uniformly distributed throughout the plug. A measurement of the strain on one side may give a completely different reading than on the other side. This is more evident the more rigid the material is, and steel is then the prime example. In order to get a correct calculation of the Young's modulus, the average strain over three different strain gages each mounted 120 degrees apart, is used (see Figure 4.2.4).

Because of an uncalibrated instrument, no exact numerical value could be extracted at this time. The tendency remains clear and can be explained from Figure 27. The equipment can handle pressures up to 10 MPa without any

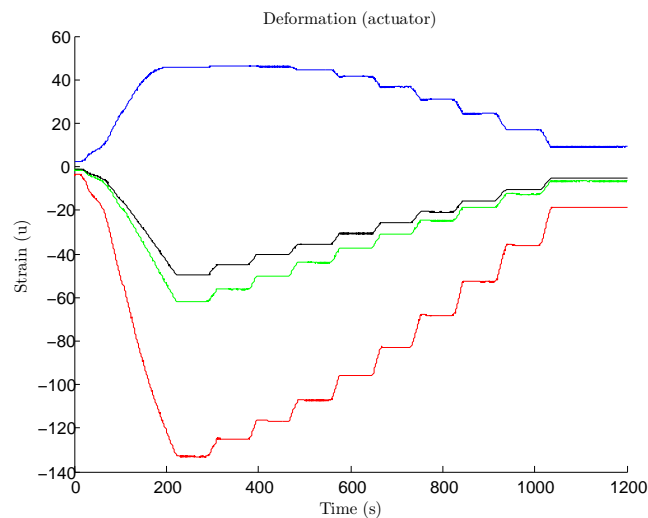


Figure 27: Strain in three gages mounted 120 degrees apart on an aluminium sample. Black line is their average.

permanent damage so the measurements in Figure 27 were done at several static stresses starting from 10 GPa stepping 2 GPa downwards reaching 1 GPa. One of the strain gages shows a positive value (extension instead of compaction) while the others shows deviating negative values (compaction).

7.5 Temperature Correction

Since the current flowing through the strain gage meets some resistance, heat will be produced and in turn alter the resistance due to thermal effects. This effect can be minimized by balancing the bridge properly. A balanced bridge will not send any current if there is no strain. Since the deformations in question are very small (nano scale) even at maximum perturbational compaction the strain and thus the current is small. Thermal effects in the strain gages have therefore been assumed small at the frequency of perturbation.

7.5.1 Temperature Coefficient of Resistance for Bondable Resistors

The manufacturer of the strain gages, Vishay[®], gives the following expression for the thermal output of strain gages on 1018 steel

$$\text{Thermal output}(\mu\epsilon) = a_0 + a_1T + a_2T^2 + a_3T^3 + a_4T^4$$

where the coefficients are given for Celsius temperature and are foil dependent.

7.5.2 Gage Factor Variation with Temperature

The alloys used in resistance strain gages typically show a change in gage factor with temperature. The error due to this effect can often be small and therefore ignored. In some circumstances, depending on the alloy, the temperature and the requirement for accuracy, it must be corrected for. According to Vishay[®]¹ a temperature change of $\pm 50^\circ\text{C}$ on an A alloy strain gage should in general not require any correction on the strain gage. The Designation System used by Vishay[®]² tells the alloy number A to be constant, and the gage factor variation is then assumed to be negligible for the range of operation in this experiment. Temperature is still logged and can be used for correction if the assumption does not hold.

¹Vishay[®] Tech Note TN-504-1

²Vishay[®] document number 11501, March 31'st 2005

8 Results

The results are best from the MTS Load Frame (Section 8.2), but to show the workflow some general trends the Manual Load Frame is also included (Section 8.1). Any numerical value should be extracted from the MTS Results Summary (Section 8.5).

8.1 The Manual Load Frame

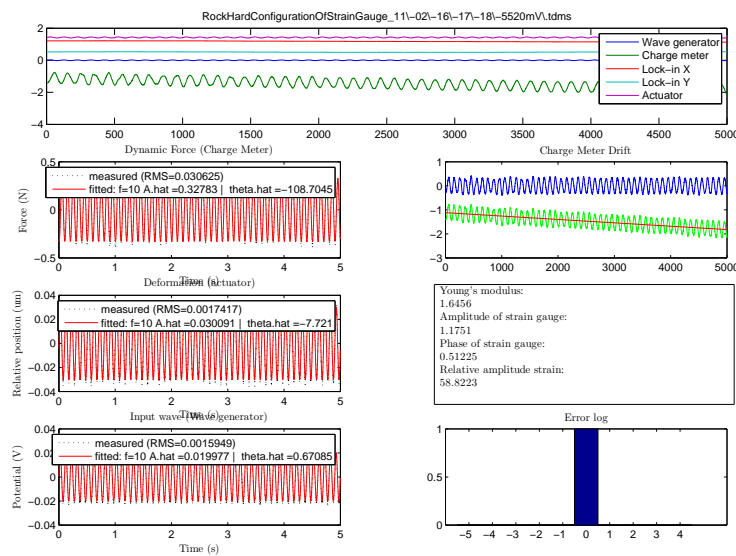


Figure 28: The Manual Load Frame: Graphical output after MATLAB interpretation of easy.m. The file later transformed into rh*.m files (See Section 6)

The recordings done in this setup show a clear tendency of quasi linear force decay (Figure 28, second one from the top, on right side) during even the shortest sampling time. The pressure drop in the cylinder of the piston is the obvious cause. This is also easily confirmed by the pressure meter mounted on top. A simple correction for this is to fit a linear model (red curve) to the data (green curve) and subtract the model from the measurements (blue curve, still second upper right plot in Figure 28). The actuator ran in closed loop at low frequency. A frequency analysis was done on the force signal, Figure 29, to determine whether there are other impacting frequency. One had in mind of detecting a somewhat stronger signal for the power line frequency at 50 Hz

which looked like it was making an envelope on the applied signal. Judging from Figure 29 the result was not as conclusive as anticipated.

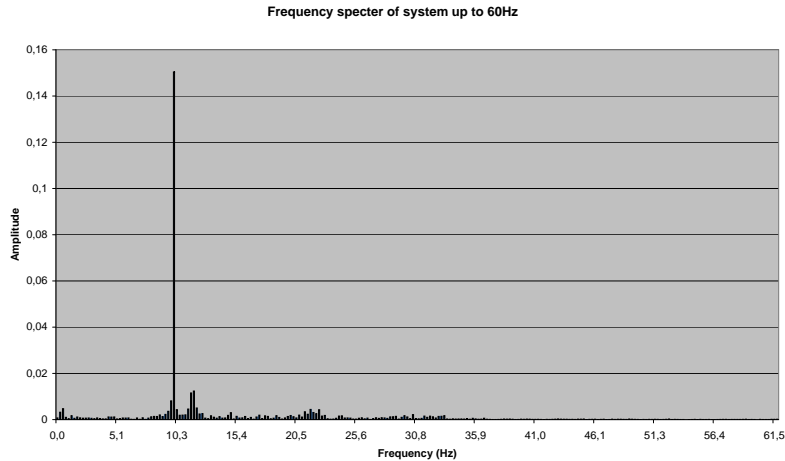


Figure 29: The Manual Load Frame: Frequency specter of the force signal

The numerical measurements done for this setup shows a general tendency of being too low in estimation of the Young's modulus. For instance steel gets values of about 40 GPa while the table value is about 200 GPa. This indicates that a lot of energy from the perturbational wave is dissipated into the frame itself without deforming the sample. With dynamic stress of about 600 Pa (static being about 5 MPa) the strains obtained were on the order of 10^{-7} measuring on Peek03. This gave a Young's module estimate of about half the static value. Any numbers produced from this setup were afterwards rejected because of lack of accuracy.

8.2 The MTS Load Frame

The main aim of the RockHard setup is to get reliable and reproducible results within the range of seismic frequencies, focusing on 10-100 Hz. One may be tempted to ask for the limit when keeping the perturbation (from the signal generator) constant. The results of doing a semi-logarithmic sweep of selected frequencies from 10 Hz to 8.009 kHz are shown for most samples. An extraction of the data going from 10 Hz to 245 Hz is plotted on a linear scale. Depending

on the measurement series (Section 5.2) also the phase difference between force and strain (or attenuation) may be displayed.

To gain a better resolution of frequencies prime numbers were swept going from 11 Hz to 167 Hz for certain samples. Prime numbers were chosen to reduce the impact of any multiple of a lower frequency. The plots are sectioned according to sample material and plug number. Please note the measurement series number of the test. The higher the number, the better the quality. Some low quality data have been included to illustrate instrumental improvements. The values published in the summary (Section 8.5) should be used when referring the values of the materials.

8.2.1 The Cutoff Frequency

The limit of the setup before going into oscillation, here described as the cutoff frequency (magnitude decay of $1/\sqrt{2}$), is dependent on the rigidity of the sample in place, the rigidity of the instruments (Load Frame etc), and far less dependent on the peak to peak magnitude of perturbation. For several materials it was found to be around 245 Hz, perturbations in the range 5.2 nm_{pp} to 27.4 nm_{pp}, among these the Castlegate and the Berea sandstone. For aluminium samples the result was lower, ranging from 150 Hz to 250 Hz.

The effect of frequency cutoff was first studied with the Berea sample shown in Figure 30. The instruments at this stage were not calibrated and the test was conducted in a crude manual way so any numerical value of Young's modulus cannot be extracted from the figure. Nevertheless the tendency is clear. As amplitude drops and frequency increases, the Young's modulus gets into heavy oscillations. The yellow curve, being Young's modulus of the perturbation at 5.2 nm_{pp}, is showing the same pattern as the stronger perturbation of 22.4 nm_{pp}, but it is shifted towards the left. The blue curve is a scaled curve of the Young's modulus calculated from the actuator. The actuator curve is scaled by matching the constant level for the low frequencies to the left in the diagram.

One clearly sees that the oscillations are frequency and not amplitude dependent. This is because a lower in magnitude perturbational wave produces the same results as a higher one. This may be an indication that the cutoff frequency is acting as a limit before resonance within the system itself occurs.

The experiment illustrated in Figure 30 was conducted in a manual way reading of the different instruments at different frequencies to check for any non linearity as for increase in perturbation frequency. The process was then automated into LabVIEW and MATLAB where the results were plotted in a similar fashion for different materials. Figure 31, Figure 38, Figure 41, and

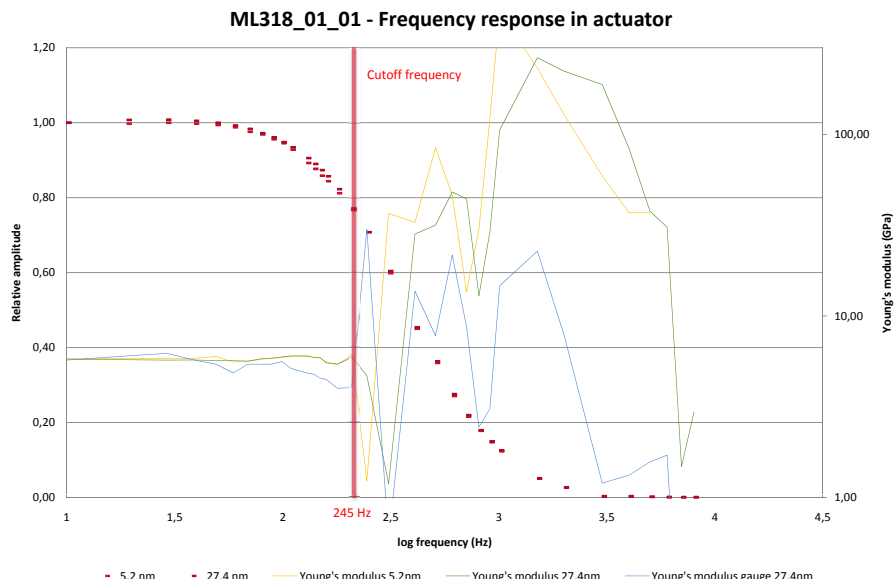


Figure 30: Resonance frequencies in measurement system: Red curves: Relative perturbation of actuator (relative to max value) as a function of frequency. When reaching cutoff frequency divergence in the Young's modulus (blue curve, green curve, and yellow curve) occurs. Numerical values should not be extracted from the figure as it is intended as a cutoff frequency example only.

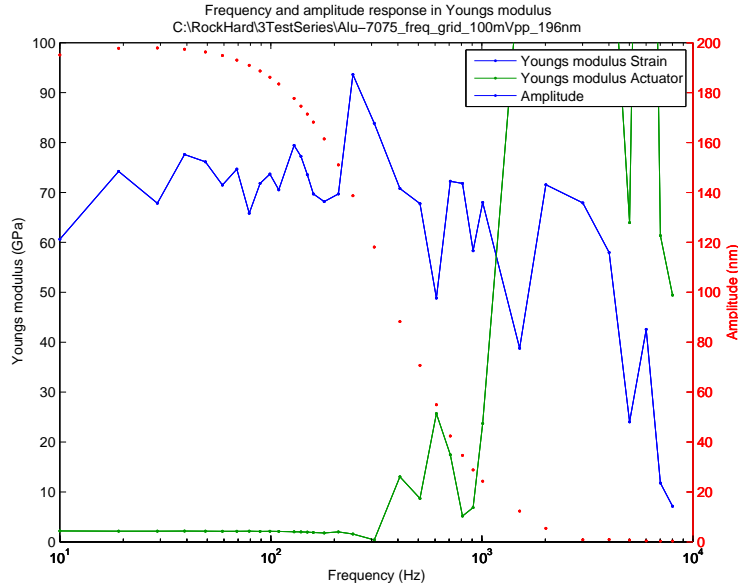
Figure 46 show when compared to Figure 30 that the Young's modulus axis is non-logarithmic, and absolute differential perturbation is plotted instead of the relative one. The position of the two axis was also interchanged mainly due to esthetic reasons.

8.2.2 Aluminium 7075 and Aluminium 6061

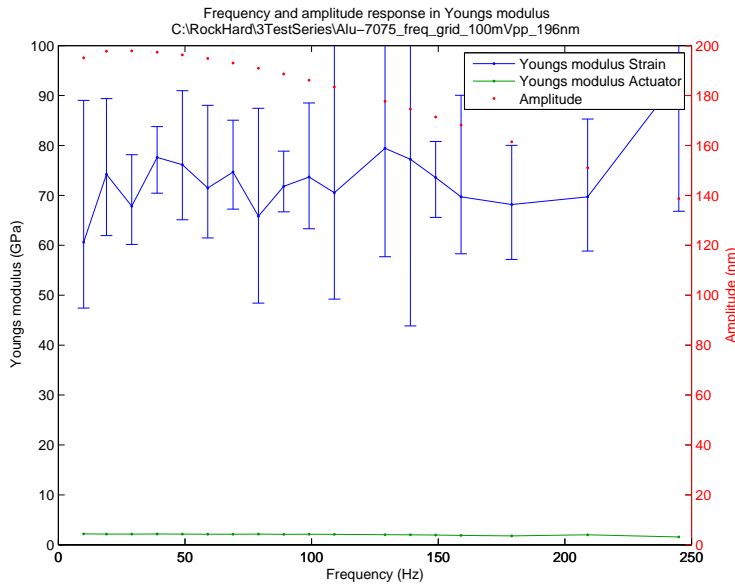
When doing the calibration of the equipment it is useful to have reference materials to check the accuracy and the results of measurements. Since the aim is to measure rocks typically in the range of 10 to 40 GPa, the reference samples should at least span this area. The reference materials should have a predictable, preferably linear response. It should be isotropic and homogeneous with small thermal effects. Encountering these properties in the area of interest may be a challenge. A common material to use is aluminium with a Young's modulus typically of 60 to 75 GPa depending on the alloy. Figure 31 shows a typical measurement series for a given perturbation at various frequencies. In (b) the same data are enlarged and plotted with its respective error bar (max/min value) on a linear axis. It is evident that the uncertainty is big and it is hard to give a precise value. This is mainly because of the extremely weak signal measured

on the strain gage, and the limited time of integration on the lock-in amplifier. In this series the integration time on each amplifier was set to 3 seconds with a total measurement time of 200 seconds. The value displayed in the plot was either the value that seemed most constant in the spectrum, or the average value of the last 30 percent of the measurement time. When choosing to do an average over an interval, the max and the min of the same interval is reflected in the error bars. They are peak values and may reflect spikes just as well as continuous variation. Small error bars are not necessarily tantamount to small variation in the 200 seconds, but may also reflect that a near constant value within that very interval was chosen instead of the overall mean. Their value should therefore be treated with care. The standard deviation would maybe be more appropriate in this context, but since the plots were initially used for error mitigating, the extreme values were of more importance. The standard deviation over the lower frequencies' Young's modulus values is given in Section 8.5.

Figure 31 shows a frequency sweep of semi-logarithmic character. For frequencies up to about 200 Hz there is indication of a linear trend. The measurement comes from the 3rd measurement series, which is an explanation for the noise level present in Figure 31(b). Figure 31(b) shows the same data as Figure 31(a), but this time on a linear scale for values below 250 Hz. The error bars are high, indicating much fluctuation within the interval. Based on these observations of quality issues the data could be reject. In the 5th measurement series the recorded data were smoother with lesser error bars due to analogue and measurement improvements. In Figure 32, being from the 5th measurement series, a strong driving perturbation of about 400 nm (200mV) was used to obtain a smooth and consistent output with a low noise level. The strain recorded in the sample was about $2.4 \cdot 10^{-7}$ which would be in the same range as Spencer et al. (1994) and Batzle et al. (2006). The phase still contains substantial amount of noise. To reduce the noise in the phase, the perturbation was yet again increased in Figure 33. The driving peak to peak value of the actuator is now 600 nm inducing a strain of $36 \cdot 10^{-8}$ in the sample. While the standard deviation of the Young's modulus $f \in \{11, 97\}$ Hz was about 0.72 GPa, it is now down to 0.57. Figure 33(b) shows that the noise is less than in Figure 32(b). The highest perturbation used for ALU-7075 is given in Figure 34. Here 400 mV is the peak to peak output of the signal generator. This makes the actuator move 800 nanometer. The induced strain in the sample is recorded to $49.6 \cdot 10^{-8}$ with a standard deviation of $1.65 \cdot 10^{-8}$, when averaged over $f \in \{11, 97\}$. Figure 34(b) shows that the random fluctuations that were

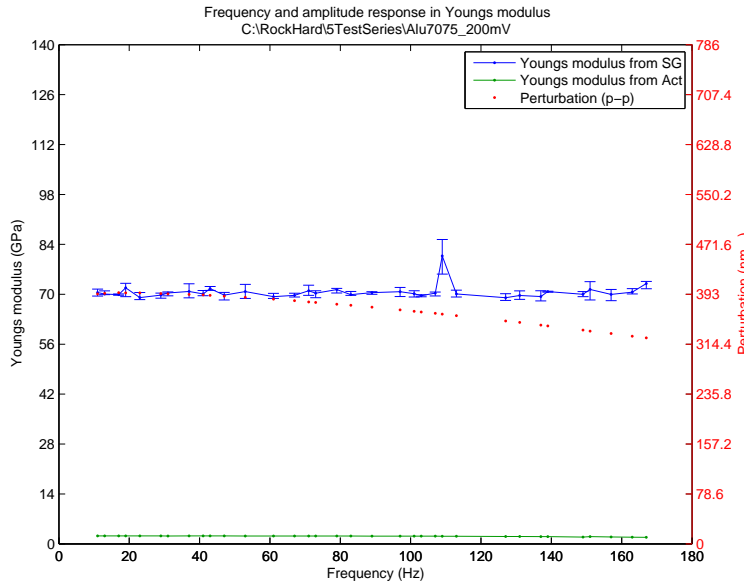


(a) Increasing frequencies of perturbation on a logarithmic scale.

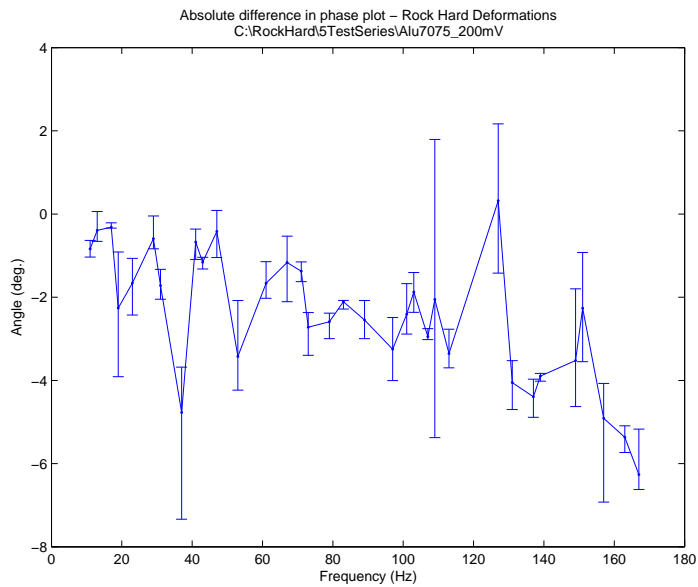


(b) Extraction of (a) on a linear scale.

Figure 31: ALU-7075 (3Test) for increasing frequency: Perturbation (red curve); Young's modulus from strain gage (blue curve) and from actuator position (green curve). Strains of $\sim 11.5 \cdot 10^{-8}$ ($\sigma = 10.2 \cdot 10^{-9}$). $\bar{E}_{10 \text{ Hz} \rightarrow 99 \text{ Hz}} = 71.51 \text{ GPa}$ ($\sigma = 5.23$). From 3'rd measurement series. The error bars reflect max and min values within measurement interval.

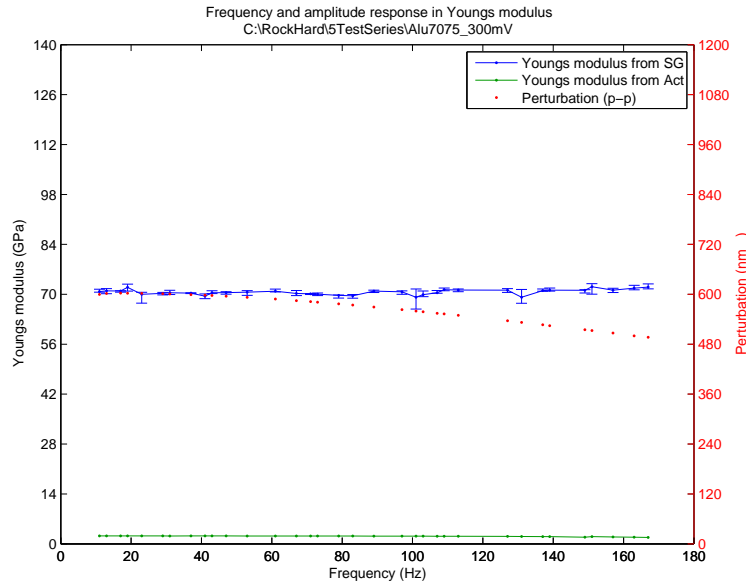


(a) Increasing frequencies of perturbation on a linear scale.

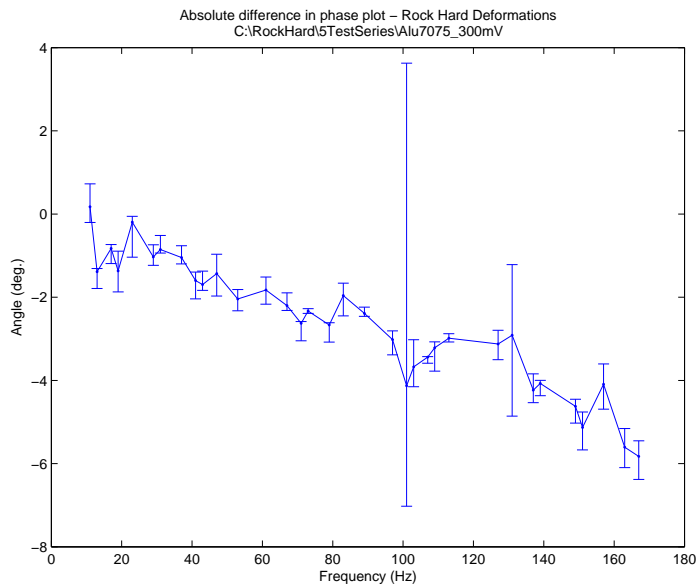


(b) The corresponding phase of (a) without any correction.

Figure 32: ALU-7075 (5Test-200mV) for increasing frequency: Perturbation (red curve); Young’s modulus from strain gage (blue curve) and from actuator position (green curve). Strains of $\sim 24.0 \cdot 10^{-8}$ ($\sigma = 7.39 \cdot 10^{-9}$). $\bar{E}_{11 \text{ Hz} \rightarrow 97 \text{ Hz}} = 70.36 \text{ GPa}$ ($\sigma = 0.72$). From 5’t measurement series. The error bars reflect max and min values within measurement interval.

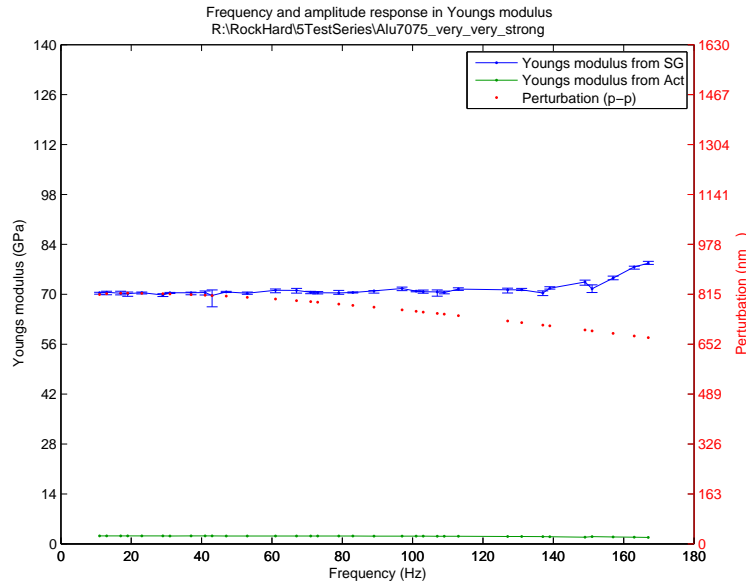


(a) Increasing frequencies of perturbation on a linear scale.

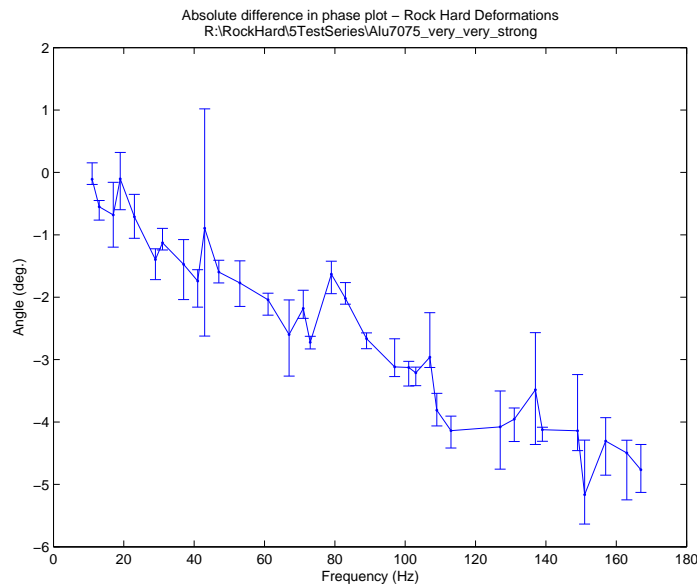


(b) The corresponding phase of (a) without any correction.

Figure 33: ALU-7075 (5Test-300mV) for increasing frequency: Perturbation (red curve); Young's modulus from strain gage (blue curve) and from actuator position (green curve). Strains of $\sim 36.6 \cdot 10^{-8}$ ($\sigma = 10.1 \cdot 10^{-9}$). $\bar{E}_{11 \text{ Hz} \rightarrow 97 \text{ Hz}} = 70.43 \text{ GPa}$ ($\sigma = 0.57$). From 5'th measurement series. The error bars reflect max and min values within measurement interval.



(a) Increasing frequencies of perturbation on a linear scale.



(b) The corresponding phase of (a) without any correction.

Figure 34: ALU-7075 (5Test-400mV) for increasing frequency: Perturbation (red curve); Young's modulus from strain gage (blue curve) and from actuator position (green curve). Strains of $\sim 49.6 \cdot 10^{-8}$ ($\sigma = 16.5 \cdot 10^{-9}$). $\bar{E}_{11 \text{ Hz} \rightarrow 97 \text{ Hz}} = 70.52 \text{ GPa}$ ($\sigma = 0.44$). From 5'th measurement series. The error bars reflect max and min values within measurement interval.

present in both Figure 33(b) and Figure 32(b) are much less now. There is also a clear linear decay of the phase ('Angle' on graph, related to attenuation) as frequency increases.

As an example of the process of choosing an average value at each frequency, take a look at Figure 35. The initial peak is caused by the lock-in amplifier integrating its way to the true value. The amplification level may seem incorrect, but this time it was set due to the ease of post-processing files with the same settings. The signals are here given in comparison to their maximum value to see the response of the lock-in, but also to check for abnormal behavior or bursts. Ideally they should all converge to a sharp DC signal. We see that the strain gage signal continues to fluctuate and settling a numerical value is hard. By increasing the time constant of the lock-in amplifiers, some of these fluctuations will die out. This again requires longer measurement times and, if many frequencies are due for observation, it will be a time consuming process. When operating with a long integration time other problems arises as well (See Section 7.3). For high frequencies the hardware specification of the amplifiers may not allow as long integration times as one would like. This is particularly a problem for frequencies above 100 Hz and when sweeping a large spectra. While sweeping one would like to have the conditions more or less the same for the series and therefore restrain oneself to shorter integration times to avoid the possibility of ambient noise influencing (crane operating etc.).

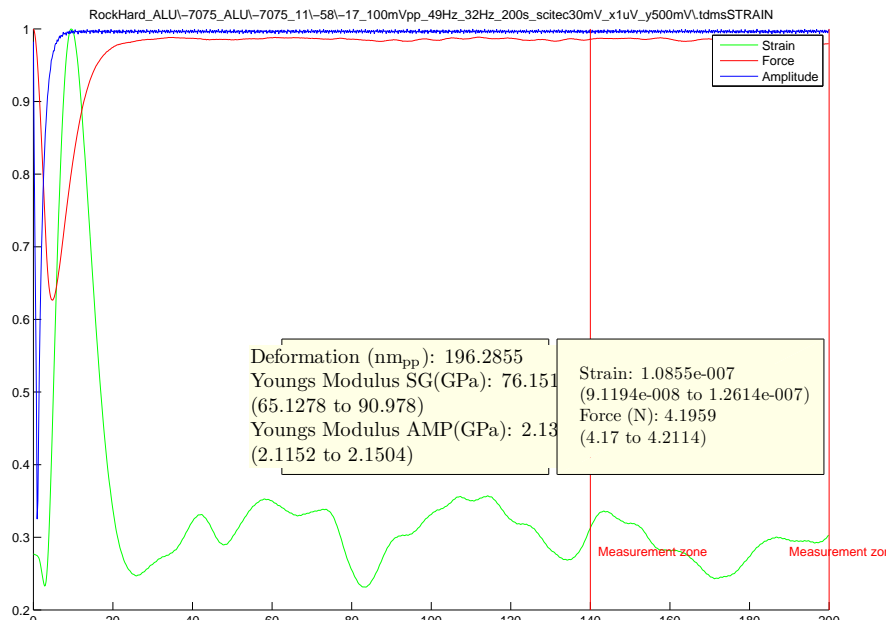
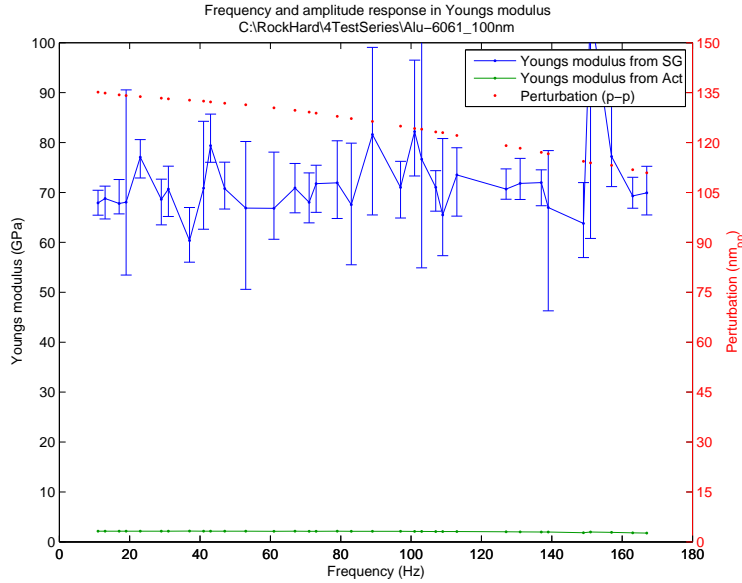
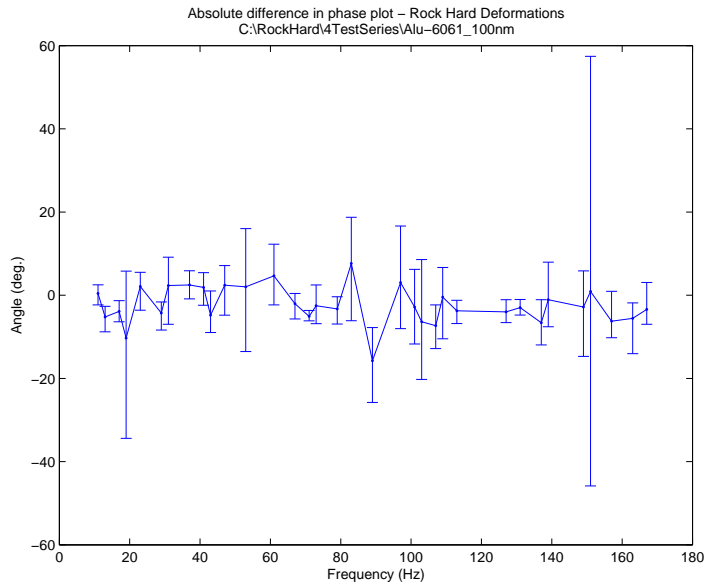


Figure 35: ALU-7075, relative signal response measured at 49Hz

The alloy ALU-6061 was measured in Figure 36 and in Figure 37 in both phase and magnitude.

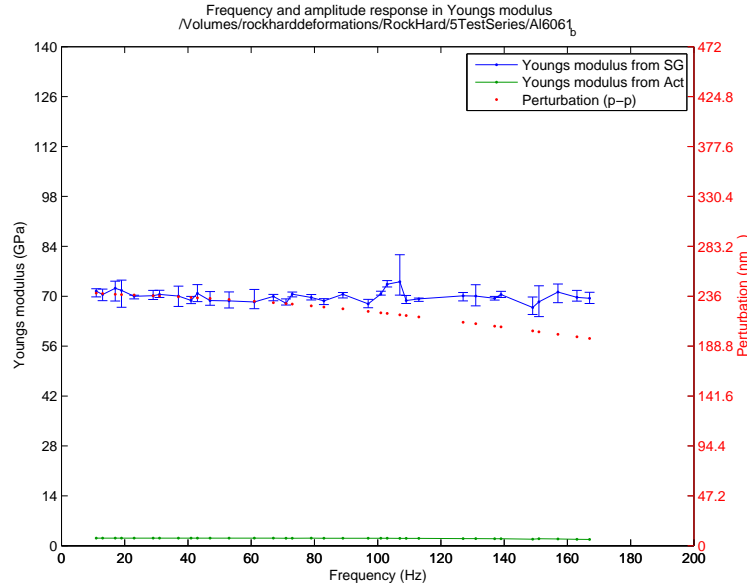


(a) Increasing frequencies of perturbation on a linear scale.

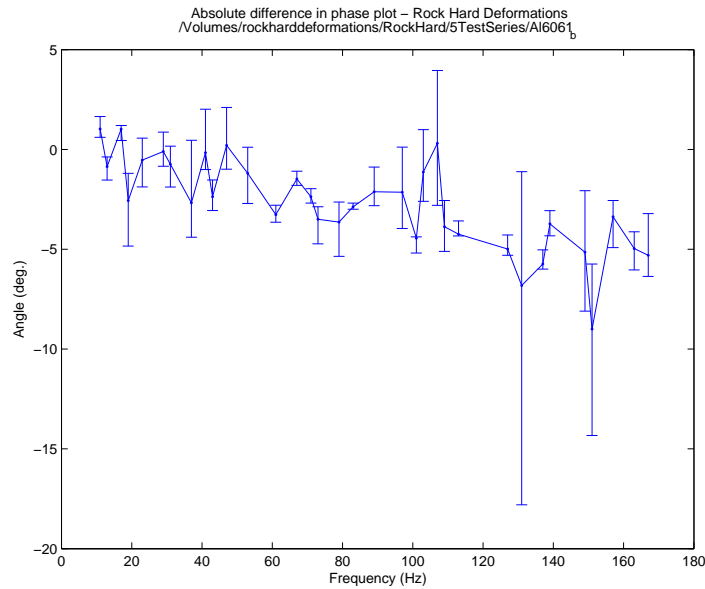


(b) The corresponding phase of (a) without any correction.

Figure 36: ALU-6061 (4Test) for increasing frequency: Perturbation (red curve); Young's modulus from strain gauge (blue curve) and from actuator position (green curve). Strains of $\sim 7.90 \cdot 10^{-8}$ ($\sigma = 6.09 \cdot 10^{-9}$). $\bar{E}_{11 \text{ Hz} \rightarrow 97 \text{ Hz}} = 70.61 \text{ GPa}$ ($\sigma = 4.72$). From 4'th measurement series. The error bars reflect max and min values within measurement interval.



(a) Increasing frequencies of perturbation on a linear scale.



(b) The corresponding phase of (a) without any correction.

Figure 37: ALU-6061 (5Test) for increasing frequency: Perturbation (red curve); Young's modulus from strain gauge (blue curve) and from actuator position (green curve). Strains of $\sim 13.99 \cdot 10^{-8}$ ($\sigma = 3.26 \cdot 10^{-9}$). $\bar{E}_{11 \text{ Hz} \rightarrow 97 \text{ Hz}} = 69.86 \text{ GPa}$ ($\sigma = 1.23$). From 5'th measurement series. The error bars reflect max and min values within measurement interval.

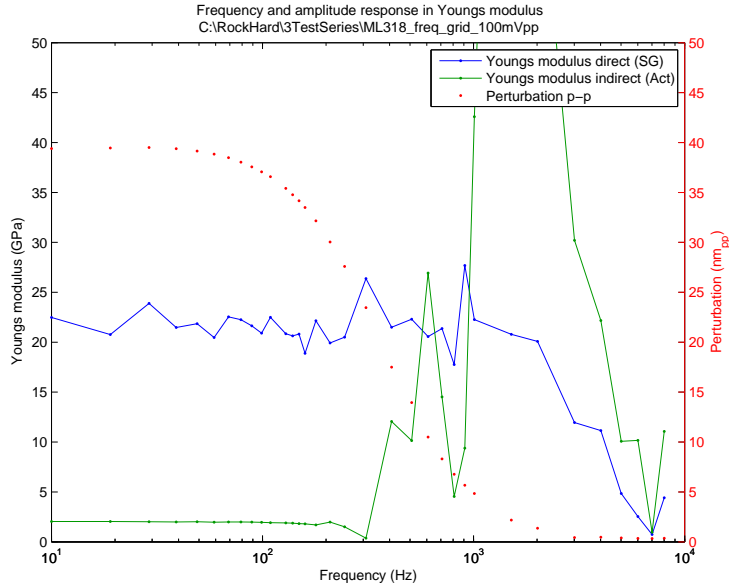
8.2.3 Berea Sandstone

The Berea Sandstone was subject to testing several times. The same sample (ML#318.01.01) was used for all tests thus any plastic deformation should only influence the first set of measurements which is not published here due to poor quality. The data collected from the sample comes from various measurement series. The oldest presented in this report (Figure 38) originates from 3TestSeries meaning it may be quite noisy and offset in value (Section 5.1). Even though the values may be non consistent in this particular measurement, there is a constant trend for values between 21 ~ 24 GPa up to the cutoff frequency. Strains are about $7 \cdot 10^{-8}$. The peak to peak movement of the actuator is given on the right side with a smooth decay starting from about 40 nm_{pp}. The cutoff frequency of the peak to peak displacement of the actuator is at about 230 Hz (Figure 38(b)). The time constant t_c is 3 seconds and the measurement time is 200 seconds for the 3TestSeries. Data from the 4TestSeries was rejected due to possible interchange of samples. In the 5TestSeries the integration time t_c was increased to 30 seconds with a total measurement time of 300 seconds.

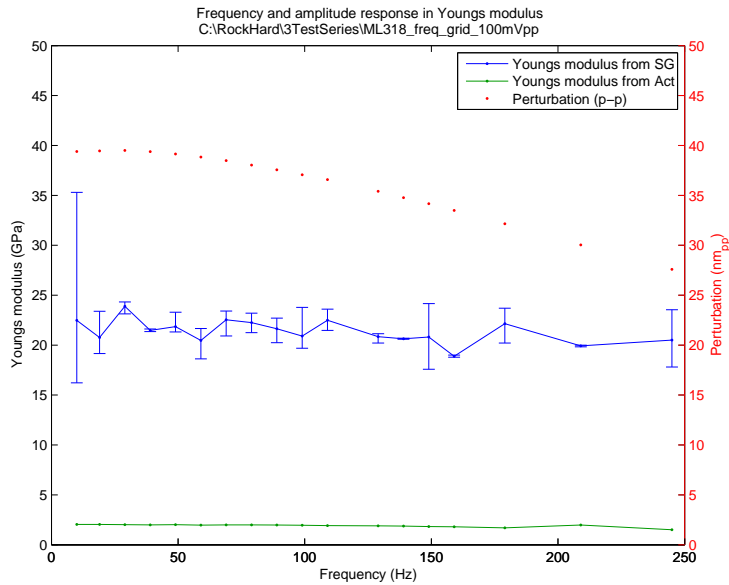
Figure 38 shows the results from the 3TestSeries plotted on both a semi-logarithmic axis (a) and an extraction on a linear axis (b). The blue line seems constant for higher frequencies than what seemed to be the case for the aluminium sample. That may be an indication of the sample stiffness influencing on the cutoff. The green curve, being based on the calculated strain from the actuator, goes into oscillation at about 200 Hz.

Figure 39 originates from the 5TestSeries and contains measurements at prime number frequencies starting at 11 Hz and ending at 167 Hz. The values can thus be plotted straight on a linear scale, as seen in (a). Compared to Figure fig:fdepberea the trend seems very much more constant. There are hardly any fluctuations, and the error bars are tiny. The strain values used to obtain the results should be checked. In Figure 39 the strains measured in the strain gage were about 3-4 times bigger than in Figure 38, and the time constant in Figure 39 was as big as 30 seconds giving plenty of time for averaging and noise cancellation. In Figure 38 the time constant was 3 seconds giving room for much more sudden fluctuations.

Figure 40 has much of the same setup as Figure 39, but the perturbational amplitude has here been reduced to about 70 nm_{pp} whilst Figure 39 contained the double. Strain levels are closer to the ones from the 3TestSeries, but the noise level is much better. The phase measurements in Figure 40(b) shows more noise than Figure 39(b), which is mainly due to the lower perturbation. The same can be said about the Young's modulus.

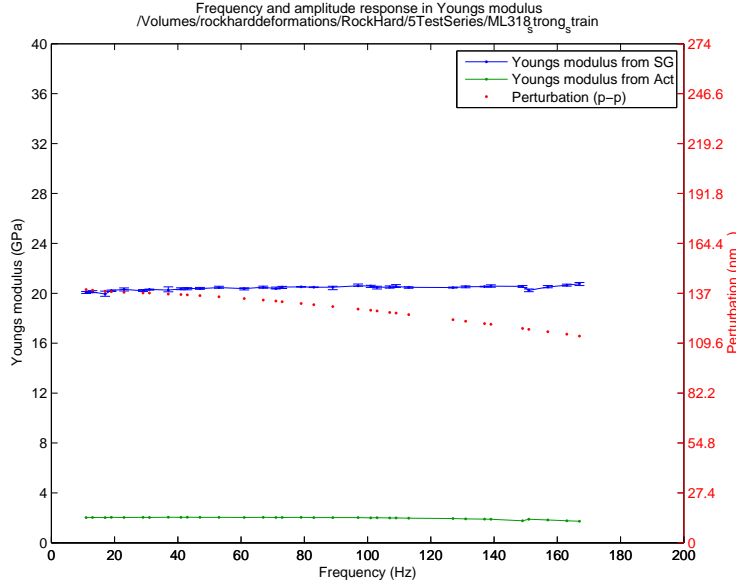


(a) Increasing frequencies of perturbation on a logarithmic scale.

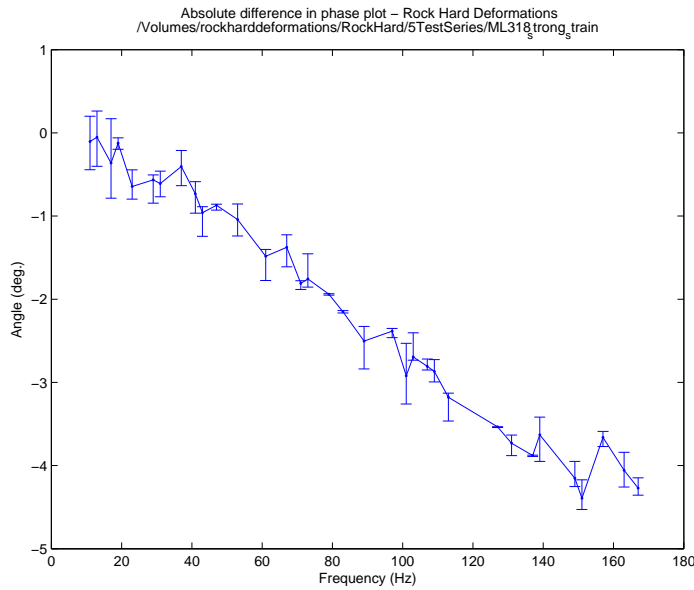


(b) Extraction of (a) on a linear scale.

Figure 38: Dry Berea sandstone, ML#318.1.1 (3Test) for increasing frequency: Perturbation (red curve); Young’s modulus from strain gauge (blue curve) and from actuator position (green curve). Strains of $\sim 7.07 \cdot 10^{-8}$ ($\sigma = 3.38 \cdot 10^{-9}$). $\bar{E}_{13 \text{ Hz} \rightarrow 99 \text{ Hz}} = 22.02 \text{ GPa}$ ($\sigma = 1.03$). From 3’rd measurement series. The error bars reflect max and min values within measurement interval.

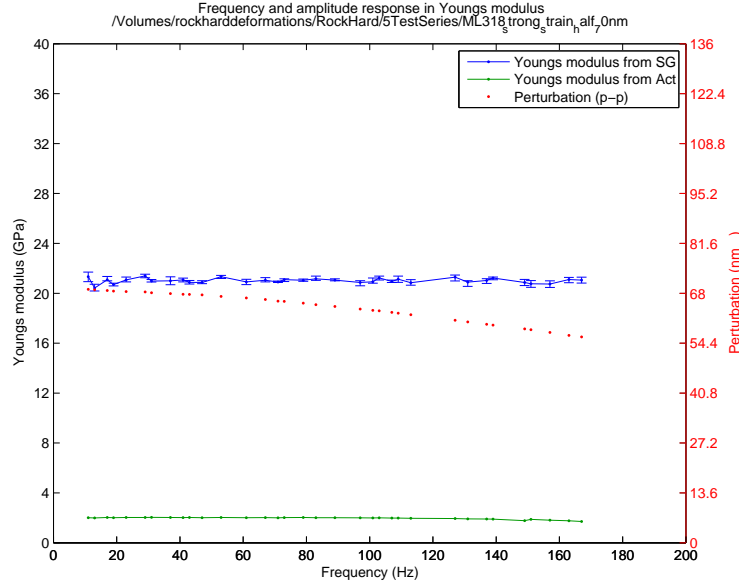


(a) Increasing frequencies of perturbation on a linear scale.

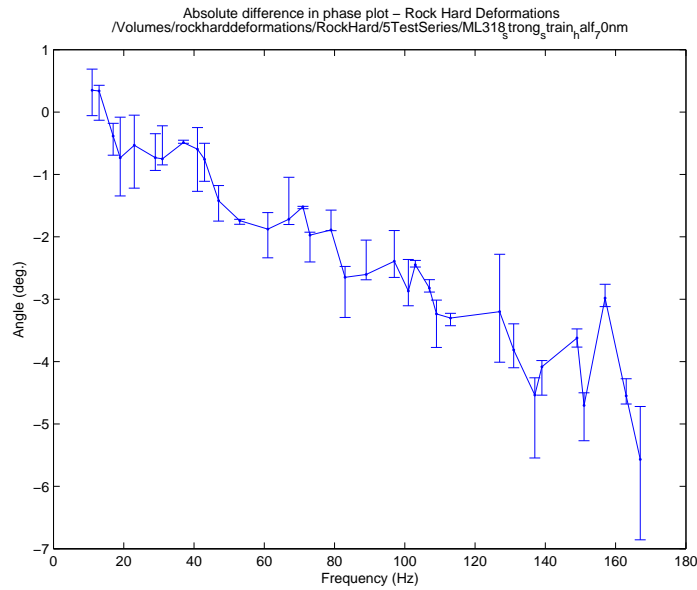


(b) The corresponding phase of (a) without any correction.

Figure 39: Dry Berea sandstone, ML#318.1.2 (5Test-1) for increasing frequency: Perturbation (red curve); Young’s modulus from strain gauge (blue curve) and from actuator position (green curve). Strains of $\sim 26.74 \cdot 10^{-8}$ ($\sigma = 8.43 \cdot 10^{-9}$). $\bar{E}_{13 \text{ Hz} \rightarrow 99 \text{ Hz}} = 20.49 \text{ GPa}$ ($\sigma = 0.17$). From 5’tth measurement series. $t_c = 30$ seconds. The error bars reflect max and min values within measurement interval.



(a) Increasing frequencies of perturbation on a linear scale.



(b) The corresponding phase of (a) without any correction.

Figure 40: Dry Berea sandstone, ML#318.1.2 (5Test-2) for increasing frequency: Perturbation (red curve); Young’s modulus from strain gauge (blue curve) and from actuator position (green curve). Strains of $\sim 12.78 \cdot 10^{-8}$ ($\sigma = 3.53 \cdot 10^{-9}$). $\bar{E}_{11 \text{ Hz} \rightarrow 97 \text{ Hz}} = 21.16 \text{ GPa}$ ($\sigma = 0.22$). From 5’t measurement series. $t_c = 30$ seconds. The error bars reflect max and min values within measurement interval.

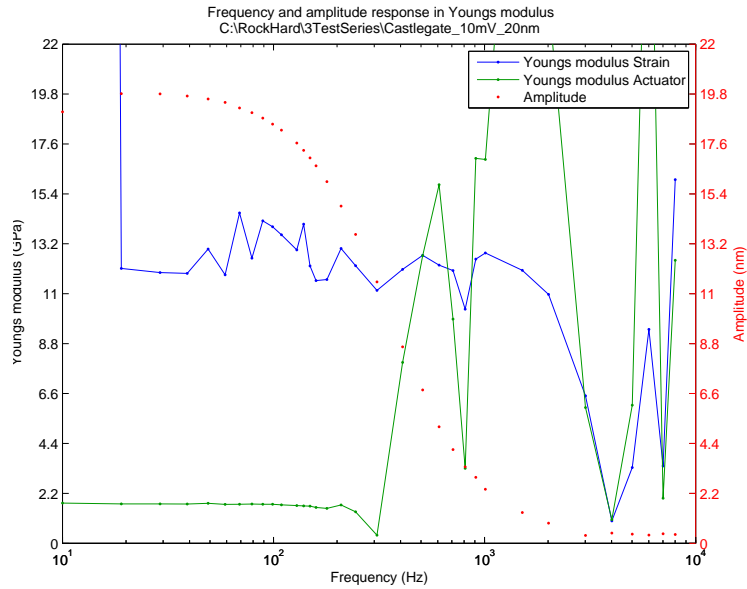
8.2.4 Castlegate Sandstone

The Castlegate sample was tested most thoroughly of the clastic samples. In the process of grinding off the excess epoxy on sample ML#222.1.1 the author got a bit carried away and therefore reduced the diameter to 24.4 cm. This causes a 7% decrease in the area which has been corrected for when calculating the Young's modulus. Unfortunately it is not corrected for in the plots in Figure 41. The true mean and its standard deviation is thus given as numerical values below. The data shown in Figure 41 are acquired before installation of the UPS (Section 4.5.2) and shows quite inconsistent values in the area $12 \rightarrow 15$ GPa.

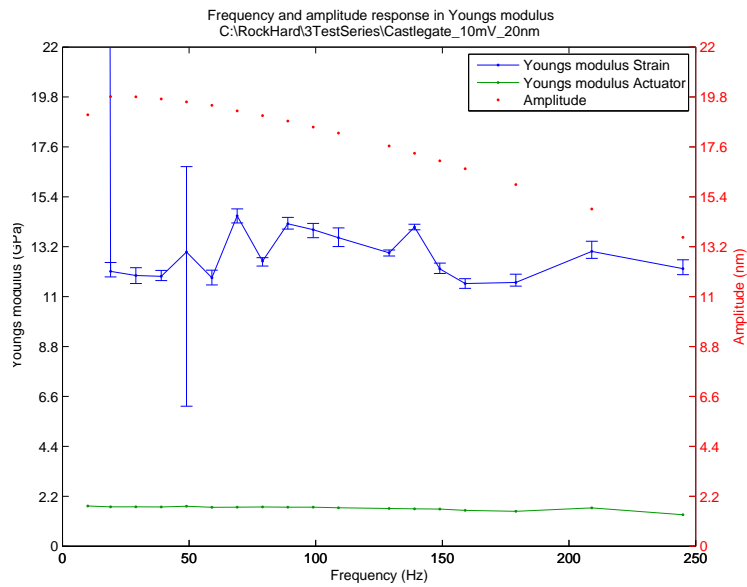
Figure 41 shows as usual the semilogarithmic values from 10 Hz to 8009 Hz. What seems to be a measurement error shows up at 10 Hz. The errors are as always quite big as is custom of the 3TestSeries. The cutoff frequency comes at about 200 Hz judging from the green curve, a bit later looking at the blue one (Figure 41). The error at 49 Hz is severe based on the measurements done for Figure 41(b).

Measurements from the 4TestSeries are displayed in Figure 42. The sample is now replaced with ML#222.3.2 instead of ML#222.3.1 which was the one tested in Figure 41. The strain values are similar ($5.62 \cdot 10^{-8}$ in this and $5.54 \cdot 10^{-8}$ in the one before) and the improvement from the 3TestSeries is obvious. While the standard deviation of frequencies $19 \rightarrow 99$ Hz were 1.17 GPa in Figure 41(b), it is now down to 0.17 GPa.

In Figure 43 the perturbation is much greater, about $20.0 \cdot 10^{-8}$. This makes the error in both Young's modulus and phase minimal. As the data come from the 5TestSeries the integration time is increased to 30 seconds and the measurement time is 300 seconds. The same conditions applies to both Figure 44 and Figure 45, but these have smaller strains.

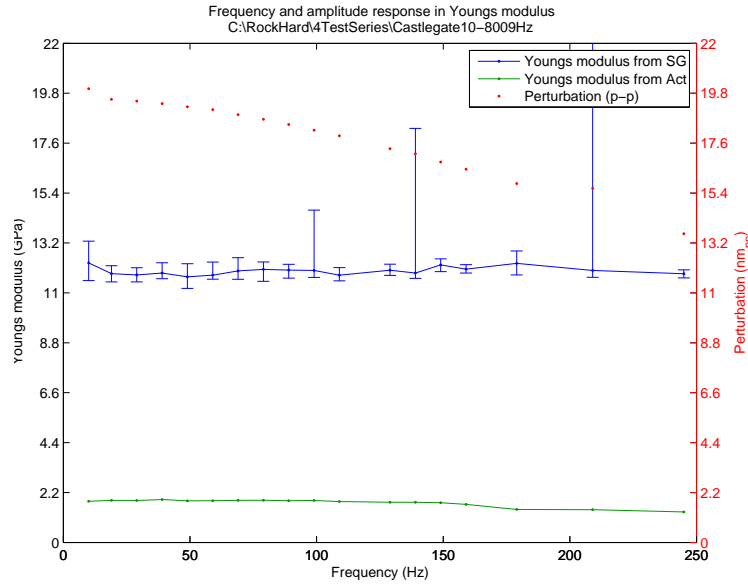


(a) Increasing frequencies of perturbation on a logarithmic scale.

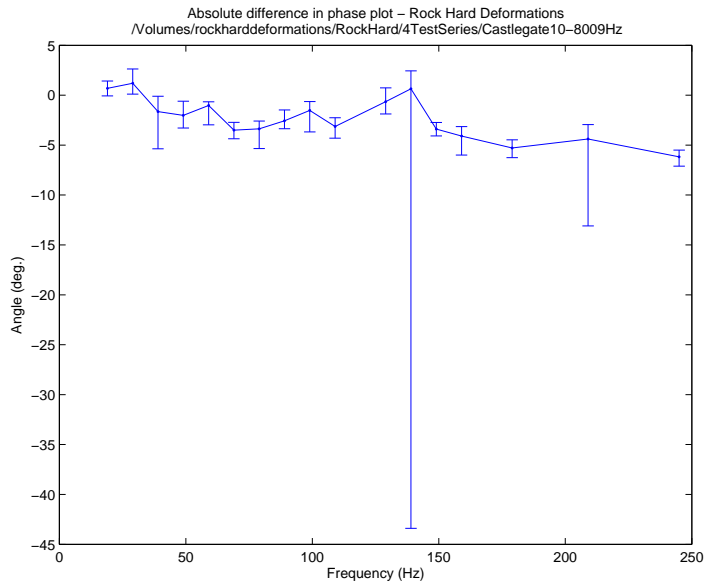


(b) Extraction of (a) on a linear scale.

Figure 41: Dry Castlegate sandstone 222.3.1 (3Test) for increasing frequency: Perturbation (red curve); Young's modulus from strain gauge (blue curve) and from actuator position (green curve). Strains of $\sim 5.54 \cdot 10^{-8}$ ($\sigma = 5.72 \cdot 10^{-9}$). $\bar{E}_{19\text{ Hz} \rightarrow 99\text{ Hz}} = 13.88\text{ GPa}$ ($\sigma = 1.17$). From 3'rd measurement series. The error bars reflect the max and min within the very interval.

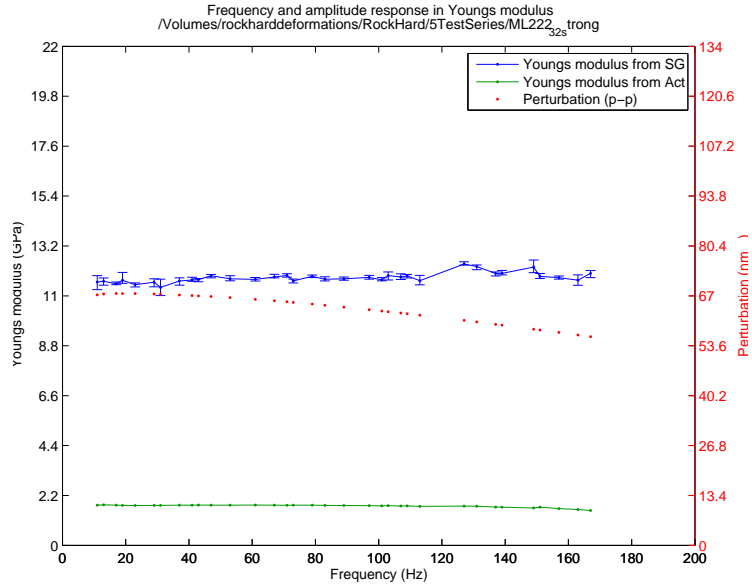


(a) Dry Castlegate sandstone. Measurement done with the use of UPS smoothening on supply voltage.

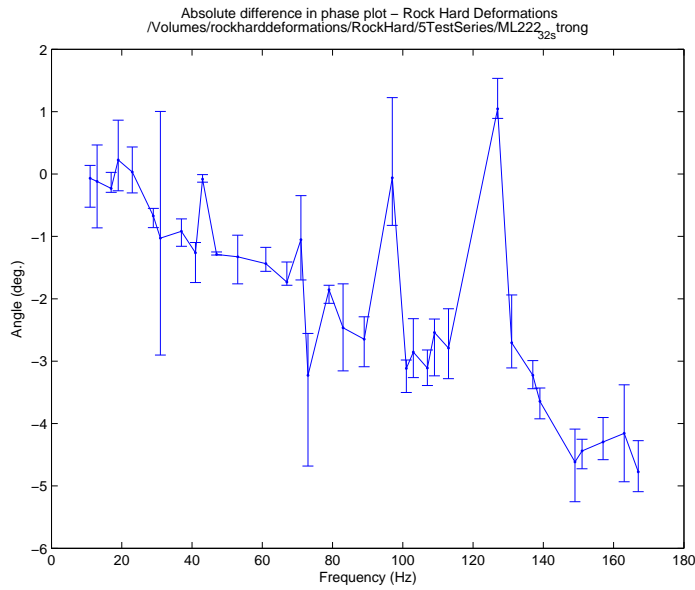


(b) The corresponding phase of (a) without any correction.

Figure 42: Dry Castlegate sandstone 222.3.2 (4Test) for increasing frequency: Perturbation (red curve); Young's modulus from strain gauge (blue curve) and from actuator position (green curve). Strains of $\sim 5.62 \cdot 10^{-8}$ ($\sigma = 1.86 \cdot 10^{-9}$). $\bar{E}_{11 \text{ Hz} \rightarrow 97 \text{ Hz}} = 11.50 \text{ GPa}$ ($\sigma = 0.17$). From 4'th measurement series.

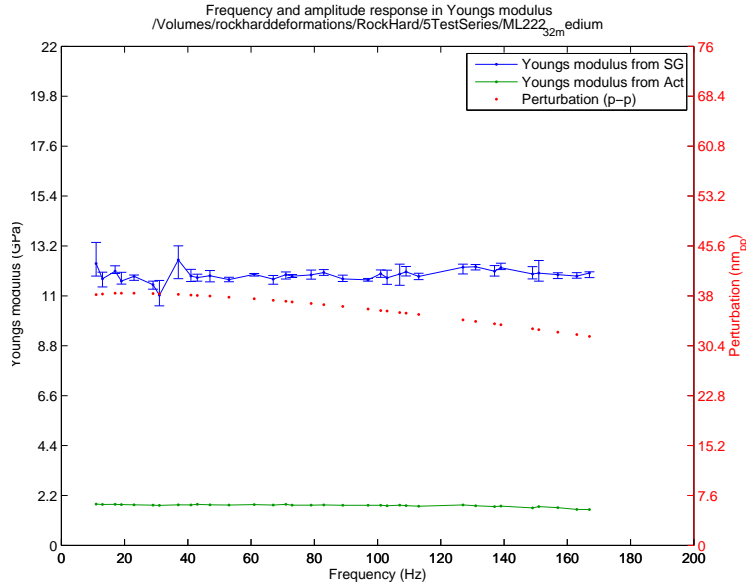


(a) Increasing frequencies of perturbation on a linear scale.

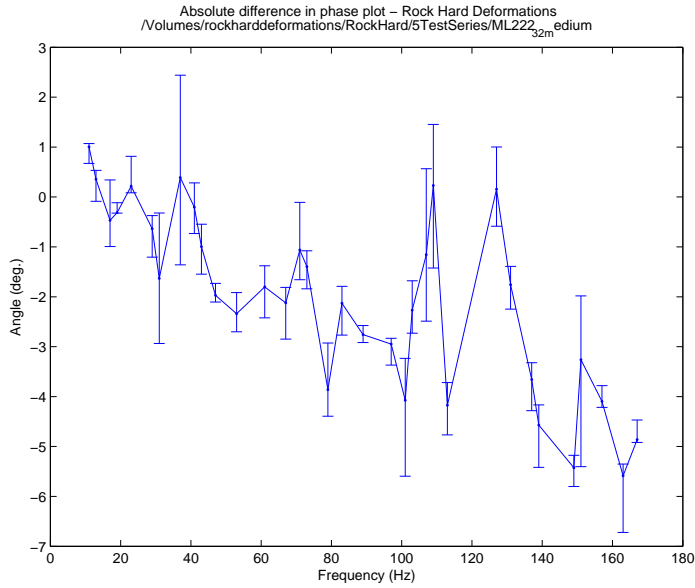


(b) The corresponding phase of (a) without any correction.

Figure 43: Dry Castlegate sandstone 222.3.2 (5Test-1) for increasing frequency: Perturbation (red curve); Young's modulus from strain gauge (blue curve) and from actuator position (green curve). Strains of $\sim 20.0 \cdot 10^{-8}$ ($\sigma = 6.01 \cdot 10^{-9}$). $\bar{E}_{11 \text{ Hz} \rightarrow 97 \text{ Hz}} = 11.82 \text{ GPa}$ ($\sigma = 0.14$). From 5'th measurement series.

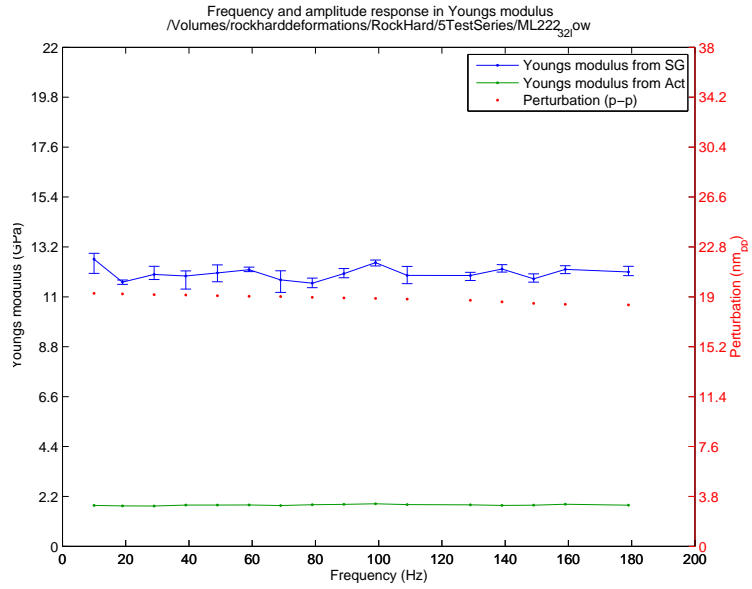


(a) Increasing frequencies of perturbation on a linear scale.

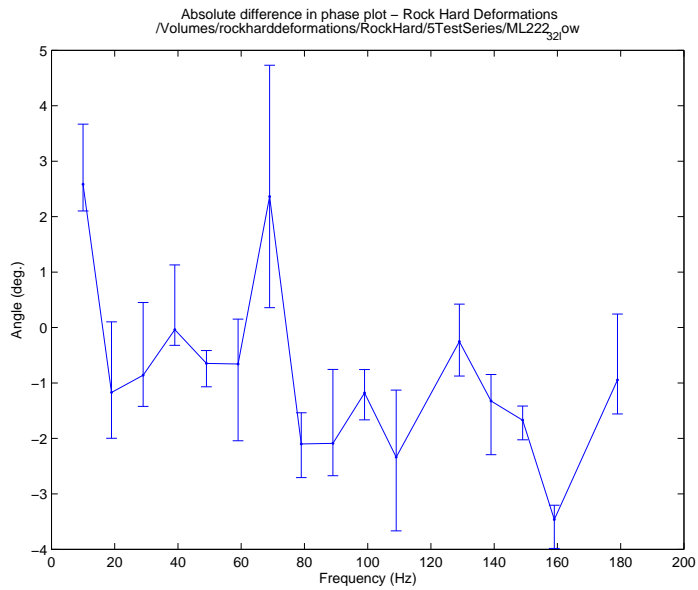


(b) The corresponding phase of (a) without any correction.

Figure 44: Dry Castlegate sandstone 222.3.2 (5Test-2) for increasing frequency: Perturbation (red curve); Young's modulus from strain gauge (blue curve) and from actuator position (green curve). Strains of $\sim 11.3 \cdot 10^{-8}$ ($\sigma = 0.32 \cdot 10^{-9}$). $\bar{E}_{11 \text{ Hz} \rightarrow 97 \text{ Hz}} = 11.98 \text{ GPa}$ ($\sigma = 0.32$). From 5'th measurement series.



(a) Dry Castlegate sandstone. Measurement done with the use of UPS smoothening on supply voltage.



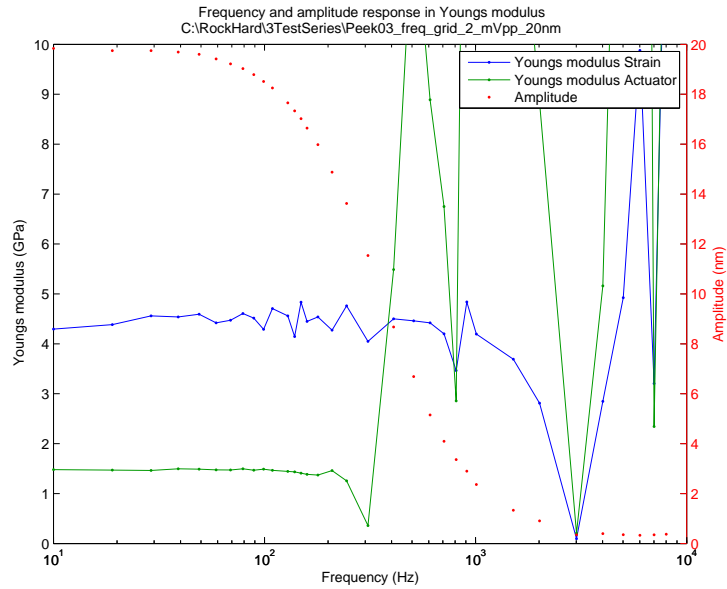
(b) The corresponding phase of (a) without any correction.

Figure 45: Dry Castlegate sandstone 222.3.2 (5Test-3) for increasing frequency: Perturbation (red curve); Young's modulus from strain gauge (blue curve) and from actuator position (green curve). Strains of $\sim 5.64 \cdot 10^{-8}$ ($\sigma = 1.78 \cdot 10^{-9}$). $\bar{E}_{11 \text{ Hz} \rightarrow 97 \text{ Hz}} = 12.16 \text{ GPa}$ ($\sigma = 0.27$). From 5'th measurement series.

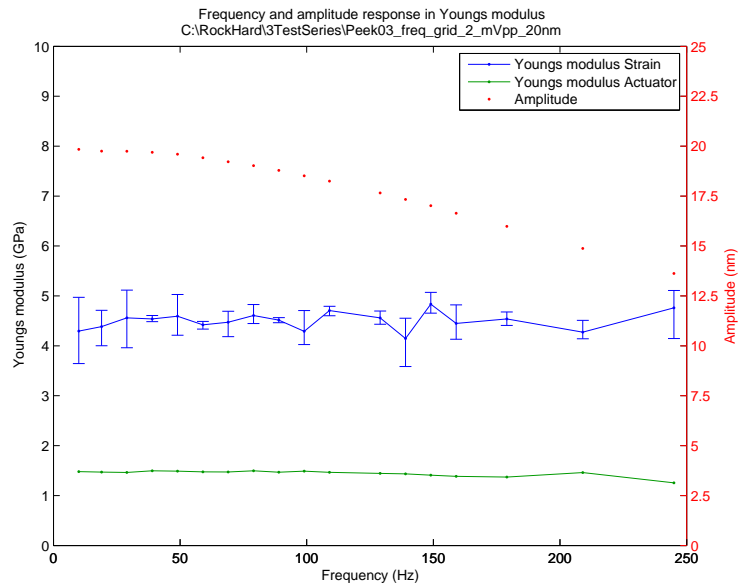
8.2.5 PEEK

To examine the other end of the scale PEEK (Polyetheretherketone) was used. It is an organic polymer thermoplastic with a static Young's modulus from 3.9 GPa (Kuo et al., 2005). The dynamic is given to 4.6 GPa (Rae et al., 2007), and 4.64 GPa (SINTEF, Table 2). The test was carried out in the third measurement series with the possibility of substantial noise. Even though the measurements originates from an early series, the values are remarkably smooth. A possible explanation for this may be that the material is very soft, and a quite strong perturbation was used providing a strain of $12.7 \cdot 10^{-8}$. The mean value of E on the interval 10 Hz to 99 Hz is 4.47 GPa ($\sigma = 0.12$) having a mean strain on the same interval of $12.7 \cdot 10^{-8}$ ($\sigma = 4.15 \cdot 10^{-9}$). Since the value of E has a low standard deviation, the PEEK was not subject for more testing.

The frequencies of 10 to 250 Hz all seem quite constant with some possible abnormal behavior at multiples of the mains power line frequency at 50 Hz. Figure 47 shows an example of the selection process for the values displayed in 46. The most constant value was chosen, and the interval was set narrow. The time constant is 3 seconds and the measurement time is 200 seconds.



(a) Increasing frequencies of perturbation on a logarithmic scale. Notice the strong irregular behavior for high frequencies.



(b) Extraction of (a) on a linear scale. The error bars reflect max and min values within measurement interval.

Figure 46: PEEK03 (3Test) for increasing frequency: Perturbation (red curve); Young's modulus from strain gauge (blue curve) and from actuator position (green curve). Strains of $\sim 12.7 \cdot 10^{-8}$ ($\sigma = 4.15 \cdot 10^{-9}$). $\bar{E}_{10 \text{ Hz} \rightarrow 99 \text{ Hz}} = 4.47 \text{ GPa}$ ($\sigma = 0.12$). From 3'rd measurement series.

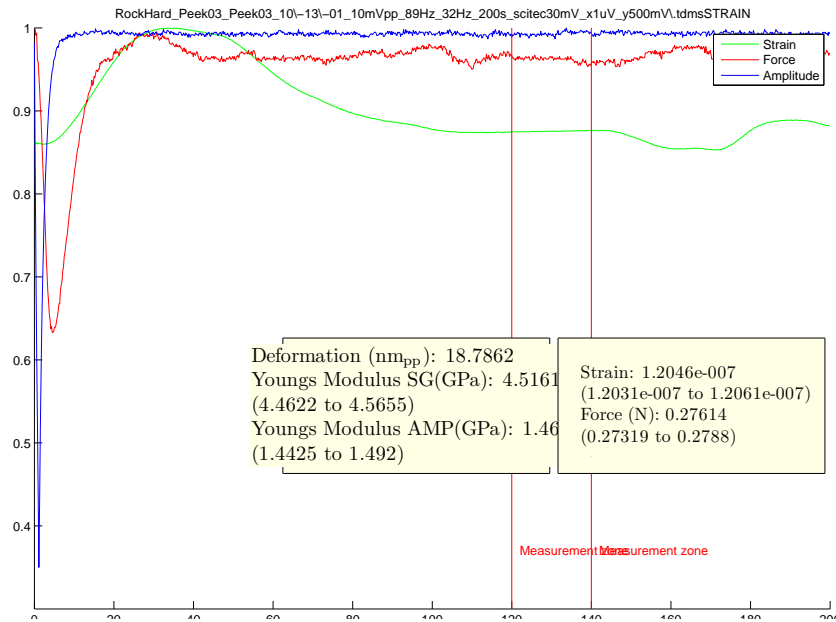


Figure 47: PEEK03, signal response measured at 89Hz. This is an example of the selection process when the signals cannot maintain the constant value. This was mainly a problem in early measurement series. Y-axis is relative scale.

8.2.6 Pierre Shale

The Pierre shale showed a strong tendency of stiffening as it consolidated and dried during measurements. Table 10 shows Young's modulus for selected frequencies at certain times of sample ML#192.02.12.

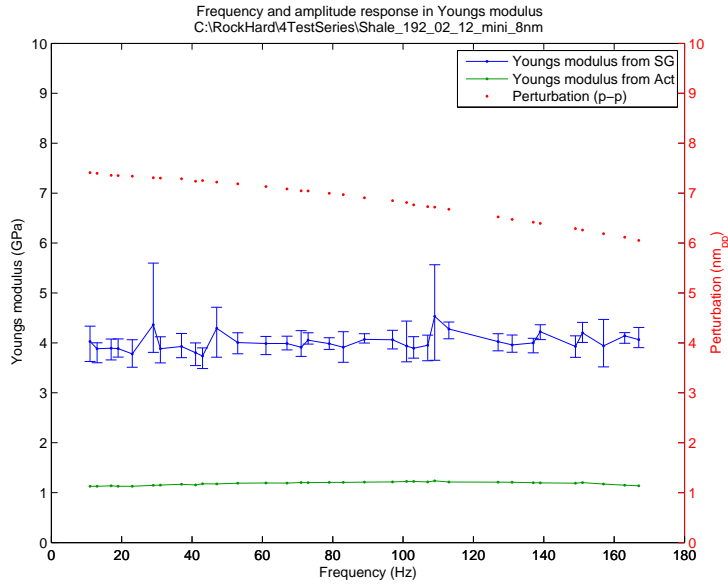
Table 10: Pierre shale (ML#192.02.12) time dependence.

Time hh:mm:ss	Frequency Hz	E GPa	Perturbation mm _{pp}
16:22:43	17	2.01 ± 0.2	19.43
16:29:23	23	2.30 ± 0.15	19.41
16:32:43	29	2.32 ± 0.2	19.40
16:46:13	17	2.45 ± 0.2	19.51
16:52:53	23	2.43 ± 0.1	19.42
16:56:13	29	2.47 ± 0.1	19.38
19:04:26	17	3.20 ± 0.1	19.47
19:11:06	23	3.19 ± 0.1	19.43
19:14:26	29	3.19 ± 0.1	19.40

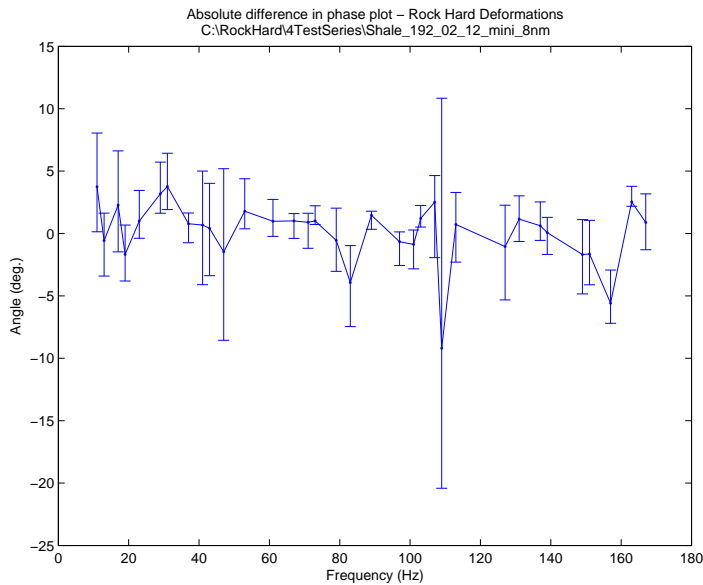
Figure 48 shows a late measurement when values seemed to stabilize to some extent. The measurements are from the 4TestSeries with good analogue conditions, but the time constants used for testing were set to 3 seconds which seem quite low judging from the dataset obtained. There were some problems with the strain gages on sample ML#192.03.10 where the shear moment of the wires made the strain gage come partly loose tearing off a block of the sample. New and smaller strain gages of equal properties as the former ones were mounted at the partly damaged sample. The first test (before damaging) is Figure 49 and the one after is Figure 50.

The measurement series of which Table 10 is based (ML#192.02.12) were restarted before completion to get a faster re-sampling of the same frequencies and thus is not displayed in the same manner as the other ones.

Measurement '192_03.10_about6nm' was rejected because the strain gages did not have sufficient contact to the surface.

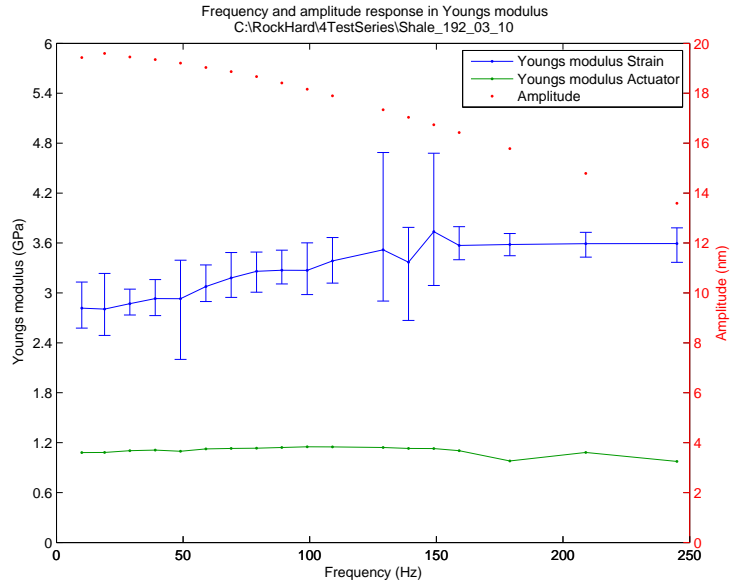


(a) Increasing frequencies of perturbation on a linear scale.

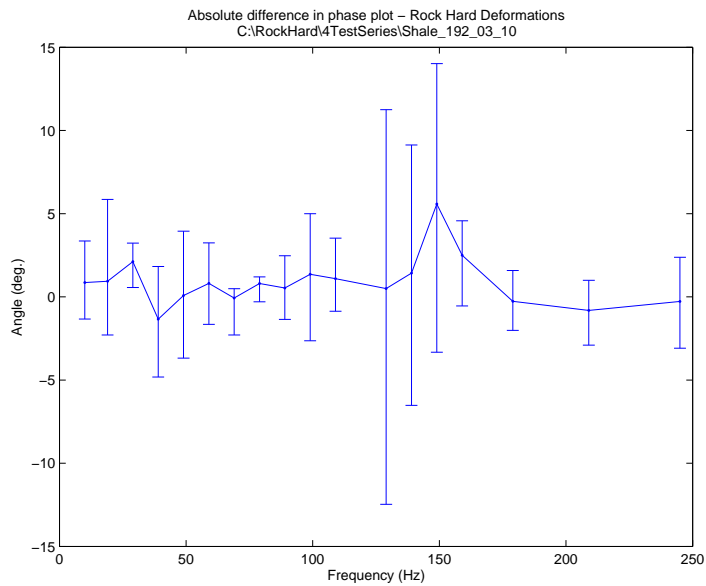


(b) The corresponding phase of (a) without any correction.

Figure 48: Saturated Pierre shale ML#192.02.12 (4Test-3), measured after some hours of initial loading, increasing frequency: Perturbation (red curve); Young's modulus from strain gauge (blue curve) and from actuator position (green curve). Strains of $\sim 4.18 \cdot 10^{-8}$ ($\sigma = 1.56 \cdot 10^{-9}$). $\bar{E}_{10\text{ Hz} \rightarrow 99\text{ Hz}} = 3.99\text{ GPa}$ ($\sigma = 0.15$). From 4'th measurement series.

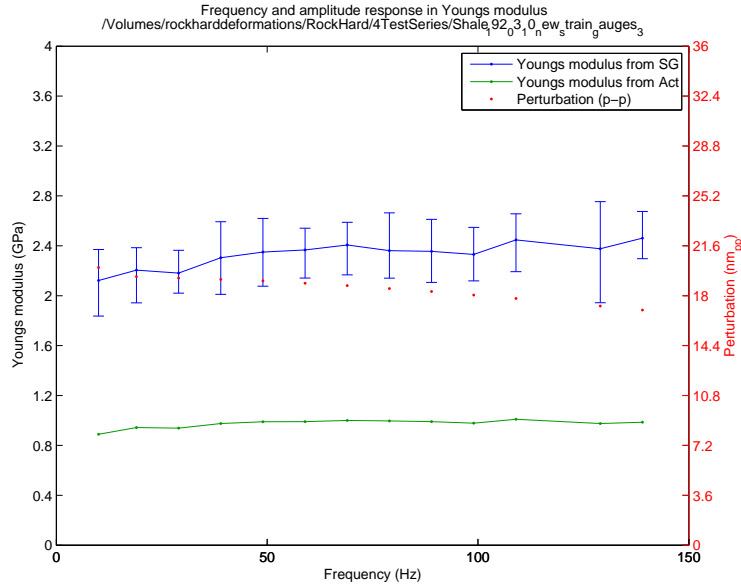


(a) Increasing frequencies of perturbation on a linear scale.

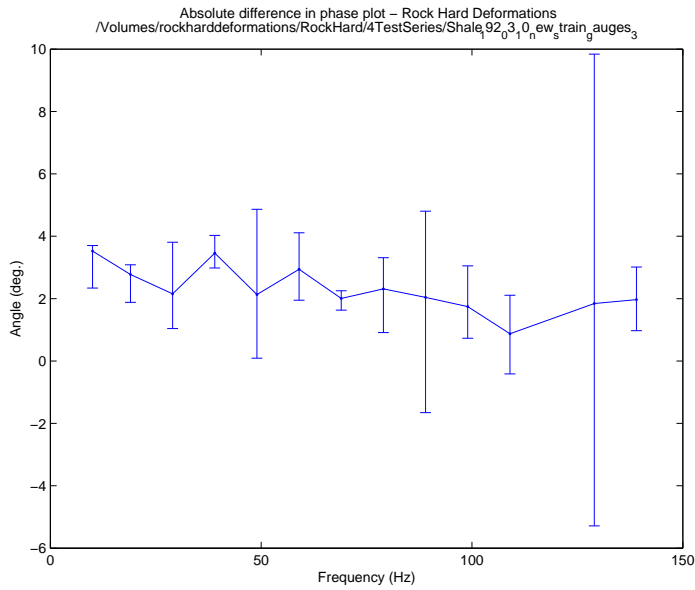


(b) The corresponding phase of (a) without any correction.

Figure 49: Saturated Pierre shale ML#192.03.10 (4Test-1): Perturbation (red curve); Young’s modulus from strain gauge (blue curve) and from actuator position (green curve). Strains of $\sim 13.8 \cdot 10^{-8}$ ($\sigma = 9.20 \cdot 10^{-9}$). $E_{10 \text{ Hz} \rightarrow 99 \text{ Hz}} = 3.05 \text{ GPa}$ ($\sigma = 0.193$). From 4’t measurement series.



(a) Increasing frequencies of perturbation on a linear scale.



(b) The corresponding phase of (a) without any correction.

Figure 50: Saturated Pierre shale ML#192.03.10 (4Test-3): Perturbation (red curve); Young’s modulus from strain gauge (blue curve) and from actuator position (green curve). Strains of $\sim 15.8 \cdot 10^{-8}$ ($\sigma = 5.53 \cdot 10^{-9}$). $\bar{E}_{10\text{ Hz} \rightarrow 99\text{ Hz}} = 2.31\text{ GPa}$ ($\sigma = 0.095$). From 4’t measurement series. NOTE! The strain gages got replaced after the measurements in Figure 49. The sample was also partly damaged at this time.

8.2.7 Steel

Values fluctuating around $180 \sim 200$ GPa were obtained (at strains down to $2 \cdot 10^{-8}$). Since the settings of the equipment were so different than what was the case with operation within the normal range ($1 \sim 70$ GPa), the steel plug was abandoned for further and more precise testing. The time settings used to obtain results on steel were time constants of $300 \sim 1000$ s and measurement times of up to 2 hours. It goes without saying that when measuring on several different perturbations and frequencies it is a tedious process with many possible factors influencing the final result.

8.3 Direct and Indirect Measurements of Strain

When measuring the strain in soft materials one assumes most of the deformation to go straight in the sample. The deformation going into the rest of the system may be treated as a constant since the overall rigidity of it is higher than the rigidity of the sample. Bearing this in mind the strain could have been measured anywhere in the system and not necessarily directly on the sample. The actuator is equipped with a sensor registering its position at all times. This sensor is calibrated down to the nanometer and could possibly be used for the purpose of indirect measurements. Any compaction in the rock will then show up as an expansion on the actuator. By applying it straight over the length of the sample one obtains the green curve in all figures showing the Young's modulus. This needs further assessing to be of use.

8.4 Phase Measurements

In the measurements that follow, certain analog improvements were implemented and have an influence on the results. One major contributor is the smoothening of the power supply through UPS'. These greatly reduced the noise of the output signal and made them far more DC-like. Section 4.5.2 contains further details.

The phase difference in force and strain was included in logging from the 4TestSeries. Referring to 'phase', it is the phase (angle, in degrees) of the force relative to source minus the phase (angle, in degrees) of the strain relative to source that is illustrated. The general trend is an increase in phase difference as frequency goes up (Aluminium: Figure 36(b), Figure 37(b); Berea: Figure 39(b), Figure 40(b); Castlegate: Figure 42(b), Figure 43(b), Figure 44(b)). When looking at the figures it may not seem like they have any striking similarity. The reason for it being hard to spot any similarity is the different range of the

y-axis. Some error bars are big and to cope with that, the y-axis are scales accordingly. If plotting all curves mentioned above in the same plot (Figure 51), they all seem to follow the same trend in decay. If calculating this trend

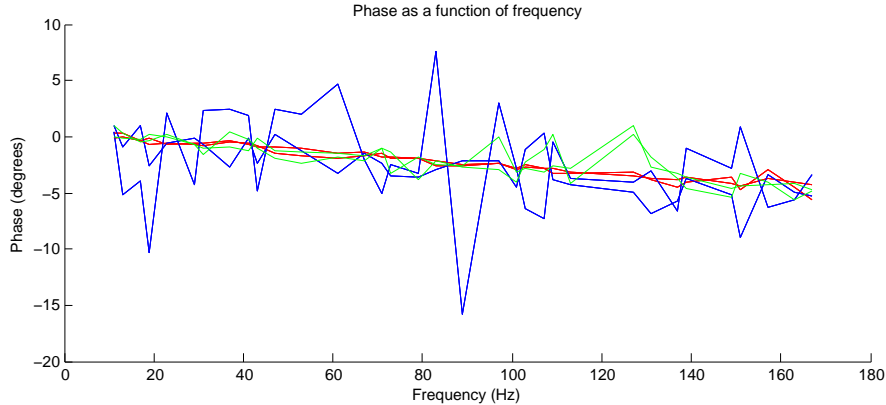


Figure 51: Difference in phase of stress and strain in Aluminium (blue), Berea (red), and Castlegate (green). Even though the curves may be noisy the tendency is clear.

line from the least square errors method (Section 6.3.1) and from the data series of the cleanest Berea sample, it is given by

$$\alpha = -0.029f + 0.29, \quad (80)$$

where f is given in Hz and α in degrees.

The aluminium shows up in Figure 51 with a lot of noise. The higher the strain, the lesser the noise. To obtain a good flat signal for aluminium, strain values of the order 10^{-7} must be used. Figure 54 shows ALU-7075 with a strong perturbation providing a high value for the strain, up to $5 \cdot 10^{-7}$. In Figure 53 the phases of three different strains are plotted for the Castlegate sample (ML#222.3.2). The same tendency of high strain low noise repeats. Doing a linear curve fit of the least noisy one (red curve, Figure 53), gives

$$\alpha = -0.028f + 0.34, \quad (81)$$

where f is given in Hz and α is in degrees. This is fairly consistent with Equation 80 for Berea.

To get the attenuation within the sample itself, one needs to know the system attenuation. Through discussion with Tony Siggins (CSIRO Earth Science & Resource Engineering, Australia) a decision was made of subtracting the alu-

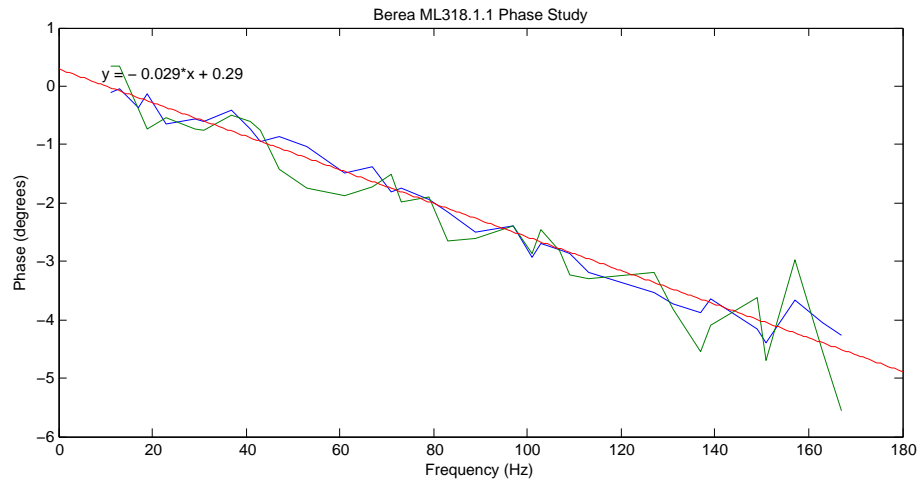


Figure 52: Berea ML#318.1.1: Difference in phase of stress and strain at different strain levels. Low strain $12.8 \cdot 10^{-8}$ (blue curve), high strain $26.7 \cdot 10^{-8}$ (green curve).

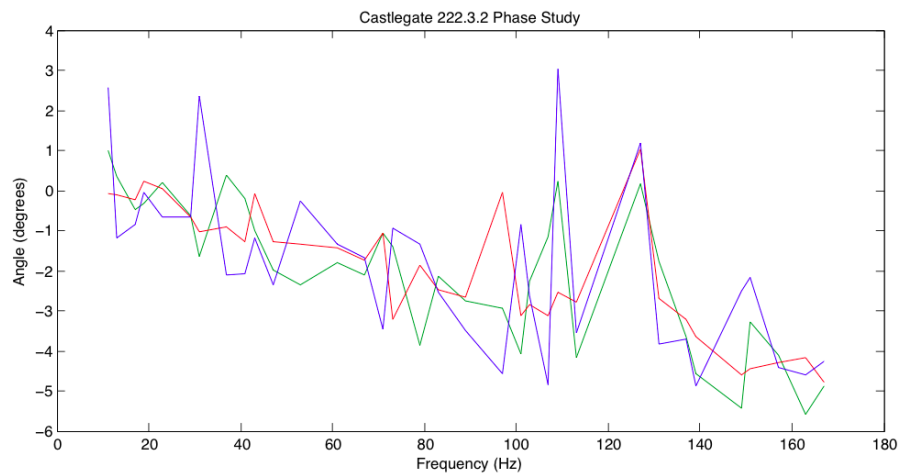


Figure 53: Castlegate ML#222.3.2: Difference in phase of stress and strain at different strain levels. Low strain $5.64 \cdot 10^{-8}$ (blue curve), medium strain $11.3 \cdot 10^{-8}$ (green curve), high strain $20.0 \cdot 10^{-8}$ (red curve).

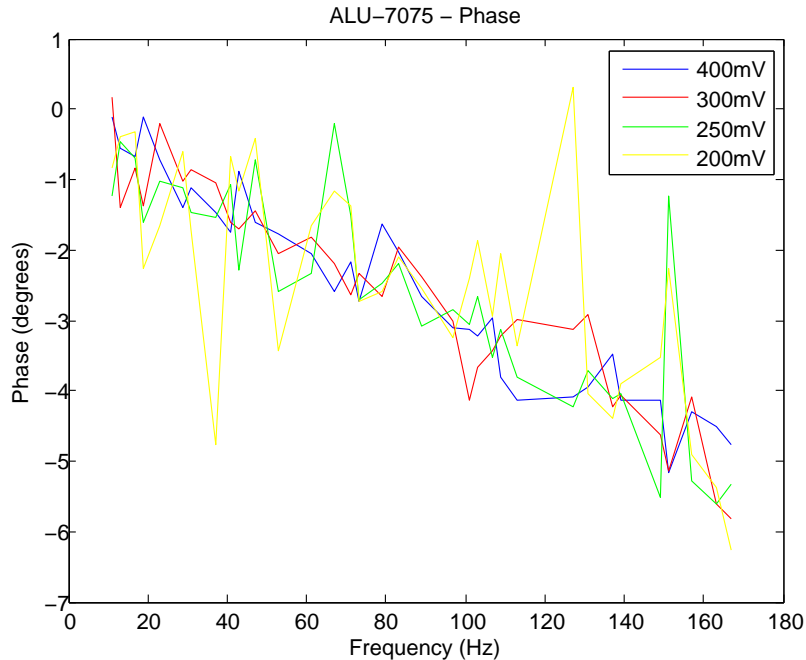


Figure 54: ALU-7075, Phase to frequency

minium phase from the other phases and then look at the difference. The main problem with this way of doing it is that the aluminium has a quite noisy dataset for low strains (See blue lines in Figure 51 and Figure 54). This may result in inconsistent measurements that are hard to evaluate.

Assuming that the system attenuation is linear for all frequencies, one approach would be to do a linear curve fit to the aluminium data (Figure 54), and subtract this fit from the other series. Another possibility would be to run an aluminium test with a very high strain to mitigate the error. Figure 54 shows that the phase's oscillatory behavior repeats some of the pattern at other strain levels, but in general it appears random. The randomness indicates that any linear model should do fine. If fitting a straight line to the curve with the highest strain (blue curve, Figure 54), the expression that is left is

$$\alpha = -0.0301 \cdot f. \quad (82)$$

This curve was deliberately forced to start from origin. A problem with linear curve fitting is that there may be an amplitude dependent attenuation in the

system that does not show up. By subtracting a linear model, the result may not be as conclusive as anticipated.

The general pattern from Figure 55 repeats in Figure 56, but is not identical. The same ALU-7075 data were used in both cases.

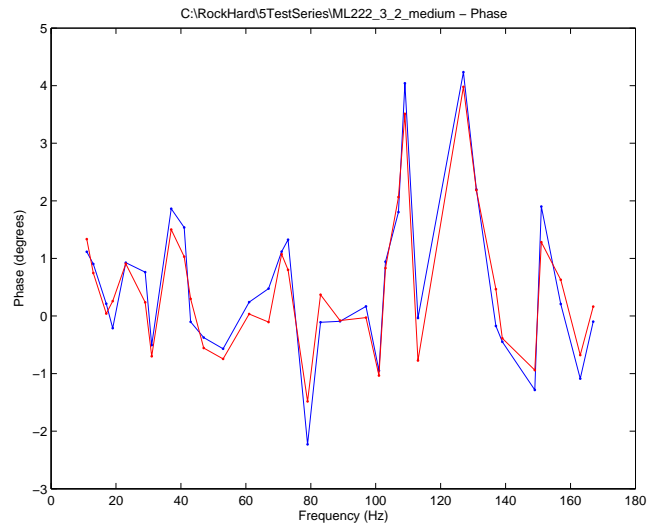
To correlate the results over different rocks, Figure 57 presents a Berea sample with the same steps as described for the Castlegate. From Figure 57 much of the same tendency as for the Castlegate is prominent, but the magnitudes are not as big as in the Castlegate.

Just as an example of the values obtained by the method outline above, have a look at Figure 55, where both a linear model (red curve, using Equation 82) and the absolute value (blue curve) of aluminium ALU-7075 were subtracted from the Castlegate sample's phase. Judging from Figure 55(a) the two curves match to a good extent. The deviations should be interpreted as random noise. Since the phase is very small: $\tan(\alpha) \approx \alpha$, the attenuation $1/Q$ ends up as merely a rescaling of y-values (Figure 55(b)).

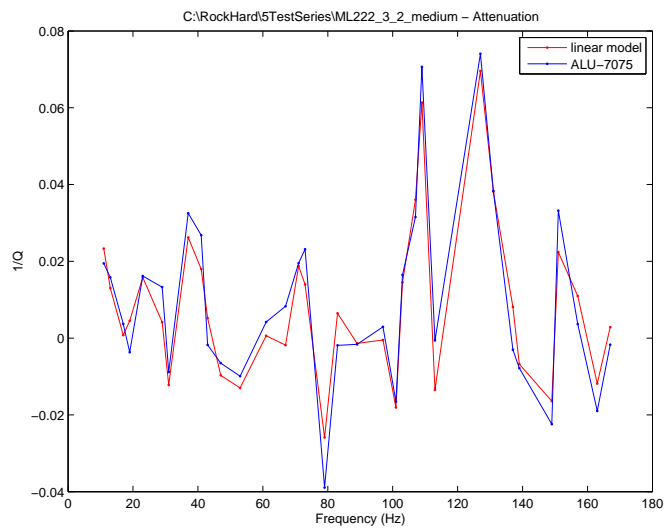
The two curves correlate nicely for high strains in ALU-7075. If trying to go lower in strain on the aluminium sample, the behavior is different. For strain values comparable to the values induced in the Castlegate, namely about $20 \cdot 10^{-8}$, the aluminium sample has a great oscillatory pattern. By plotting both the subtraction of the similar-in-strain ALU-7075 (blue curve, strain about $20 \cdot 10^{-8}$) and the strong-in-strain ALU-7075 (green curve, strain about $50 \cdot 10^{-8}$) together with the linear model (red curve), one obtains Figure 58. The shaded area between the two curves is what is random error for low strains. For low frequencies the strong-in-strain model is following the linear model more closely. The similar-in-strain model follows the same peaks as the others, apart from near 50 Hz, a frequency that is susceptible to noise from the power lines.

The strong-in-strain model correlates best to the linear model for both low and high frequencies. At 131 Hz the values of strong-in-strain and similar-in-strain model deviate substantially. This point showed up in the previous measurements (Figure 42(b)) as an abnormal value.

To get better reference one may take a look at the Castlegate with a higher strain value in the same type of plot, Figure 59. Many of the same trends of Figure 58 show up. Around 97 Hz all three models are together, and in general the strong-in-strain ALU-7075 is closer to the linear model. A similar trend shows up in the Berea sample, Figure 60. One may draw the conclusion that a clean aluminium sample (meaning low in noise, high in strain) should be used to subtract from the phase of the samples. The linear model based on solemnly the slope of decay in the aluminium sample has corresponding values to the



(a) Blue line: The absolute phase of ALU-7075 (strain of $5 \cdot 10^{-7}$) was subtracted from the absolute phase of the sample. Red line: The linear trend (Figure 54) in the phase of ALU-7075 (strain of $5 \cdot 10^{-7}$) was subtracted from the absolute phase of the sample.



(b) The attenuation $1/Q$ of (a) as defined in Section 2.3.

Figure 55: The Castlegate sample ML#222.3.2: Aluminium corrected phase difference and attenuation.

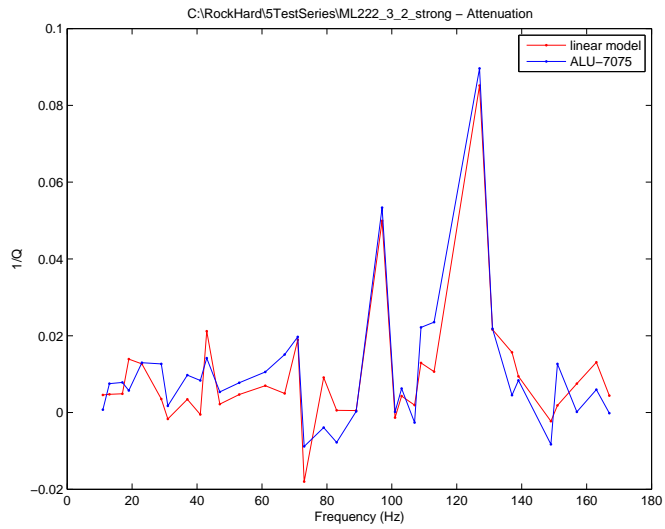


Figure 56: The Castlegate sample ML#222.3.2 (high strain): Attenuation as defined in Section 2.3, aluminium corrected.

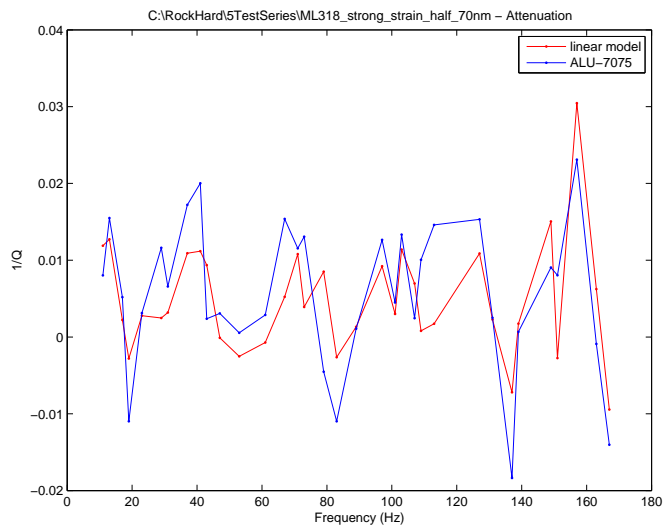


Figure 57: The Berea sample ML#318.1.1: Aluminium corrected attenuation.

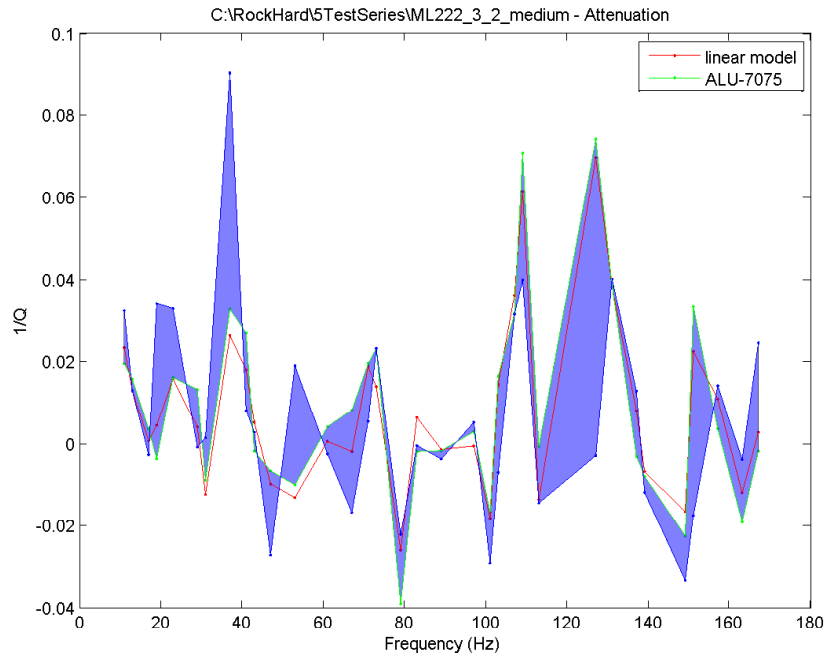


Figure 58: The Castlegate sample ML#222.3.2: The measured strain in the Castlegate is about $11 \cdot 10^{-8}$.

strong-in-strain model.

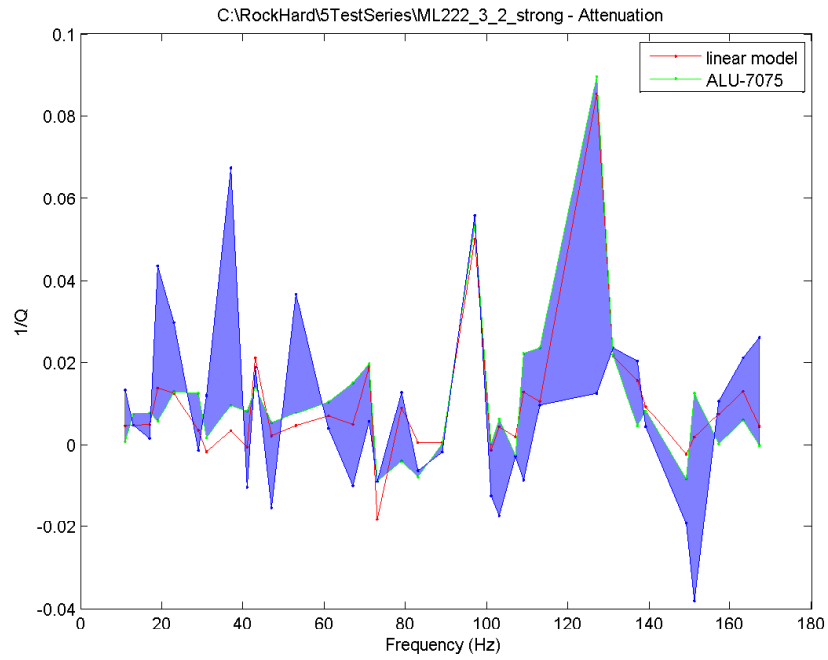


Figure 59: The Castlegate sample ML#222.3.2: The measured strain in the Castlegate is about $20 \cdot 10^{-8}$.

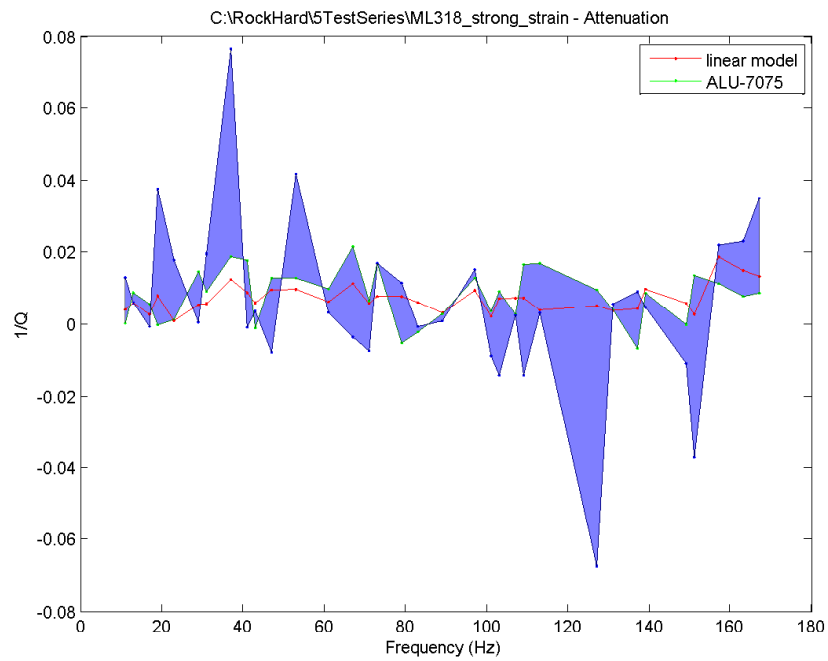


Figure 60: The Berea sample ML#318.1.1:

8.4.1 Consistency Check

The setup is based on a lot of averaging to obtain numerical values for very weak signals. With this in mind one may rightfully ask the question of whether the measurements are repeatable, and if one obtains the same values the second time around. Table 11 contains one repeated experiment (within the same measurement series) of ALU-7075 (4Test-1) and (4Test-2). Strain values are exactly the same to the second decimal, and Young's modulus values are only different in the first decimal. They are both well within the standard deviations of each other. In this consistency test, the static load frame was unloaded between the tests, and the sample rotated 180 degrees. The aim was to check both the averaging done by the lock-in amplifiers, but also the averaging done by the strain gages. There is a similar trend of behavior when comparing the two tests over frequencies (Figure 61). Multiples of 50 Hz are dominating to some greater extent in Figure 61(a).

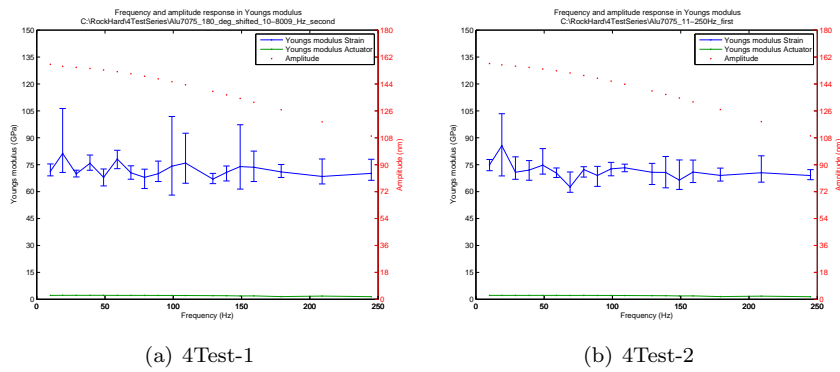


Figure 61: ALU-7075 Young's modulus over frequency consistency check; The measurement in 'a' was repeated without dismantling to check for consistency.

8.5 Results summary

Vast amounts (> 100 hours) of measurement results have been rejected in the development process of RockHard. The cause of rejection is often that analogue improvements make room for higher quality data with better resolution. None of the data from 1TestSeries and 2TestSeries are included due to quality enhancements in later series.

Table 11: Results. Average values of E on the range 10-99 Hz (9 sample values, evenly spaced) with indicated strain values. Δ is the standard deviation. Any * indicates the frequency range going from 13-97 Hz (19 samples, prime numbers) Any @ indicates the limited range {11, 17, 23, 29} Hz. In the case of off-scale spikes they have been suppressed. Castlegate and Pierre were the only samples tested with a uniaxial static stress of 5 MPa, the rest were on 10 MPa.

Sample#	E GPa	ΔE GPa	ϵ 10^{-8}	$\Delta\epsilon$ 10^{-9}
ALU-6061* (5Test)	69.86	1.22	14.0	3.26
ALU-6061* (4Test)	70.61	4.72	7.90	6.09
ALU-7075* (5Test-400mV)	70.52	0.44	49.6	16.5
ALU-7075* (5Test-300mV)	70.43	0.57	36.6	10.1
ALU-7075* (5Test-1)	69.83	1.06	30.4	9.58
ALU-7075* (5Test-200mV)	70.36	0.72	24.0	7.39
ALU-7075 (3Test)	71.51	5.23	11.5	10.2
ALU-7075 (4Test-1)	72.81	5.82	9.07	6.49
ALU-7075 (4Test-2)	72.98	4.51	9.07	5.62
Berea* ML#318 (5Test-1)	20.49	0.171	26.7	8.44
Berea* ML#318 (5Test-2)	21.16	0.2216	12.8	3.53
Berea ML#318 (3Test)	22.02	1.03	7.07	3.38
Castlegate ML#222.3.1 (3Test)	13.88	1.17	5.54	5.72
Castlegate* ML#222.3.2 (5Test-1)	11.82	0.14	20.0	6.01
Castlegate* ML#222.3.2 (5Test-2)	11.98	0.32	11.3	3.83
Castlegate* ML#222.3.2 (5Test-3)	12.16	0.27	5.64	1.78
Castlegate* ML#222.3.2 (4Test)	11.50	0.17	5.62	1.86
PEEK03 (3Test)	4.47	0.12	12.7	4.15
Pierre@ ML#192.2.12 (4Test-1)	1.77	0.898	15.1	5.43
Pierre* ML#192.2.12 (4Test-2)	3.36	0.128	12.9	4.51
Pierre* ML#192.2.12 (4Test-3)	3.99	0.15	4.18	1.56
Pierre ML#192.3.10 (4Test-3)(new SG)	2.31	0.095	15.8	5.53
Pierre ML#192.3.10 (4Test-1)	3.05	0.193	13.8	9.20

9 Discussion

The setup is continuously evolving as challenges and new ideas emerges. Documenting every single step of the process extensively would be an impossible task within the timeframe available. The report is focused on key issues of improvement such as the shielding of noise and smoothening of the output. The aim of the task may be said to be double; both building an instrumental setup capable of producing measurements of great precision in the low frequency range and at low strain levels, but also measure standard materials to confirm it. The same duality is found in this discussion: one for the instrumentation (Section 9.1) and one for the measurements (Section 9.2).

9.1 Instrumentation

The Manual Load Frame was rendered useless for all practical purposes, and this discussion will therefore solemnly focus on the results obtained from the MTS frame.

Shielding of noise One of the most important aspects of the setup is the shielding of both electromagnetic and low frequency noise. Many steps have been carried out to reach the setup described in this report. A topic that may not have been properly discussed is the positioning of the equipment itself. It is always a good idea to have the instruments located close to the zone of measuring to avoid long wires that are susceptible to pick up noise. The setup was also roughly divided into a high/normal voltage (HV) and an ultra low voltage (ULV) zone. The ULV zone includes the instruments concerning strain measurements and are operating on its own UPS. Even though it is now mentioned as ULV there is still supply voltages to the instruments within the zone, operating at 230 V. The cables are physically separated to optimize the situation within each zone. The shielding of the fluctuations on the mains power line was done by the use of UPS. An example of the effect can be seen in Figure 62 where a Castlegate sample was measured before and after the installation of the UPS.

Orientation of sample The orientation of the sample has proven to be of great importance to the result. The setup is averaging over three strain gages in a quarter Wheatstone bridge. This configuration was chosen due to practical circumstances. Spencer et al. (1994) used the configuration of totally 6 transducers. Two measuring axially and four laterally. One downside by using just two sensors in axial direction, is the issue of the contact surface and non-

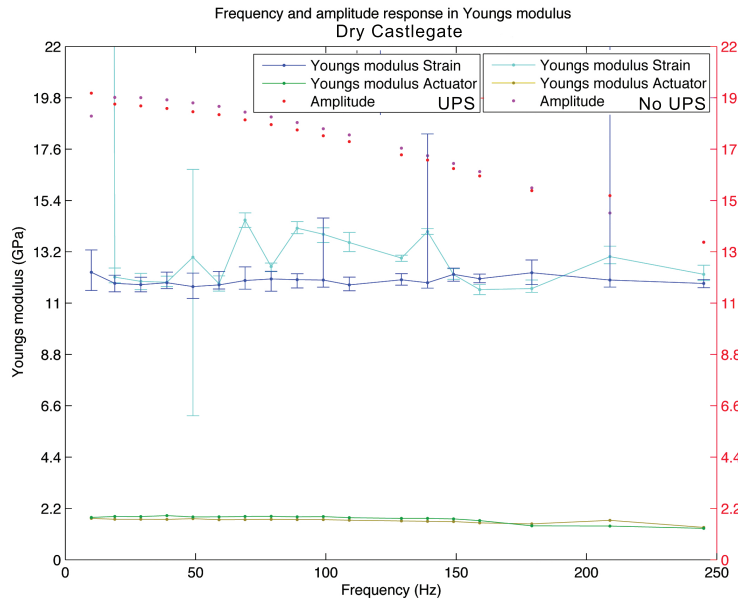


Figure 62: Castlegate sample measured twice. Before (light blue line) and after (purple line) installation of the UPS.

uniformness of the sample. A positive aspect of Spencer et al.'s setup (1994) is the possibility to also measure Poisson's number by taking into account the lateral expansion. The main reason for not including this measurement in the RockHard setup, is the lack of lock-in amplifiers. By including Poisson's number an additional amplifier must be provided and logged.

Sensor configuration For the sensor configuration of axial deformation, a better solution than the one used would be to include one more strain gage and then use them two and two in series over a half bridge. This would enhance the resolution while maintaining the averaging. The strain gages in series need to be diagonally opposite to make the averaging correct. The rest of the bridge needs to be changed accordingly. This approach was to a certain extent implemented by

Epoxy The epoxy applied on the surface on the Castlegate and the Berea sandstone is assumed to stiffen the sample by filling some of the vugs. Unfortunately the timeframe did not permit any further investigation of this issue.

Low strains If going too low in strains ($< 10^{-8}$) the amplifiers needed longer integration time and measurement time. The lowest strains obtained, with

measurement times of 200 seconds ($t_c \in \{3 - 10 \text{ sec}\}$), were on the order of $1.5 \cdot 10^{-8}$, but the noise and the oscillations in phase implies that strain values $\sim 5 \cdot 10^{-8}$ should be used to get steadier signals. If comparing to Spencer et al. (1994) and Batzle et al. (2006 and 2010) the strain values used is an order of magnitude lower. Batzle et al. say that strains of order 10^{-7} to a good extent replicates the effects of the seismic wave, but the RockHard setup is capable of doing it even better, down to ten times lower for soft rocks. In the strain values of Spencer et al. (1994) and Batzle et al. (2006), the signal to noise ratio improves and the standard deviation is smaller. The strain amplitude was also found to have a substantial impact on the elastic properties with inverse proportionality to E .

Since the aim of the setup is getting measurements of Young's modulus at low perturbations and low amplitudes in a uniaxial deformational setup, it is a challenge to find experiments having done exactly the same. Often measurement of Poisson's ratio are available and what is published is the speed of the P-wave (Spencer et al., 1994). To use a confining pressure to stiffen the sample is also a common setup (King 1969), but would not be directly comparable of a uniaxial test. An idea for further development of the setup is to include a confining pressure. This would not only make it easier to compare the results to published literature, but would also replicate the effect of the surrounding bedrock since that will exert a uniform stress on the sample in all angles. By making such a confining pressure vessel further shielding is possible. The vessel itself may act as an additional Faraday cage if grounded correctly, giving a complete shield to all of the measurement chain, starting with the sample and ending at the computer. To obtain even better results this is a quite straight forward way to go being both easy to implement, and based on previous experience, presumably highly effective.

To be able to compare the measurements of the Young's modulus, the recorded data in the ultrasonic range (Table 2) are used. These have been done on plugs from the same block as the samples described (Section 5.1). Effort was made to do ultrasonic measurements on the same samples as recorded in the RockHard setup. To preserve the samples for later testing no sirup was used. Problems were experienced when trying to record a clean S-wave, and thereby setting the Young's modulus. Some deviations are therefore expected when comparing the measurements in Section 9.2.

The Cutoff Frequency For all samples abnormal behavior was obtained for frequencies above 250 Hz. In some stiff materials (Aluminium, Figure 31(b))

it seemed to start even lower, maybe as low as 200 Hz. The cause of the oscillatory off scale behavior is not settled, but it could be due to resonance frequencies within the system. The reasoning for this assumption is that the range of frequencies where it occurs seem fairly constant, and quite independent of perturbational amplitude. A theory about the actuator at high frequencies not being able to follow the peak to peak value was for a long time considered plausible. After further testing at lower amplitudes, the theory was later abandoned. Testing indicated that perturbation had a small impact on the start position of the section, but other factors (such as resonance) have a larger influence. This phenomenon is a limiting factor when trying to link the low frequency measurement with the ultrasonic one since the range of the equipment goes from Hertz to about 200 Hz. The sub Hertz area should be within range, but then the Scitec Lock-In Amplifier needs replacement. It has a lower limit of 10 Hz.

Comparing the frequency range to the setup of Batzle et. al. (2006) one learns that the range of RockHard Deformations is rather limited. Batzle et. al. (2006) claim obtainable frequencies of about 2500 Hz before encountering resonances in the mechanical system. Paffenholz et al. (1989) had a similar setup with a range of {0.03 Hz, 300 Hz}, but strains just down to 10^{-6} . Spencer et al. (1994) developed a setup in the range {0.2 Hz, 155 Hz} with strains near 10^{-7} . The load frame used (Section 3.2.1) is of electromechanical construction and is capable of delivering up to 10 kN. To further investigate the limits of the setup a stiffer electromechanical load frame may help.

9.2 Measurements

Aluminium Two alloys of aluminium were tested at 10 MPa, ALU-6061 and ALU-7075. Both showed Young's moduli of about 70 GPa, with ALU-7075 having a mean of about 71.2 GPa, while ALU-6061 was slightly below on about 70 GPa (Table 11). The P-wave and S-wave velocities measured at SINTEF are $v_p = 6288$ m/s and $v_s = 3107$ m/s for ALU-7075, and $v_p = 6466$ m/s and $v_s = 3146$ m/s for ALU-6061 at 2 MPa. $\rho_{\text{ALU-7075}} = 2.81$ g/cm³ (Table 2) makes $E_{\text{ALU-7075}} = 72.62$ GPa and $E_{\text{ALU-6061}} = 71.88$ GPa. The match is good, but one should also keep in mind that the standard deviation is substantial on these measurements when averaged over frequencies (10 → 99Hz and strains). The strains induced by perturbation are about 10^{-7} for these tests, which match the values used by Batzle et. al. (2006) and Spencer et al. (1994). The higher the strain, the lesser the standard deviation over frequency. The strain in the sample seem to impact substantially on the measurement.

One may question whether the values obtained at low frequency should be expected to fall over or under the values at ultrasonic frequencies. Fjær (2009) shows the dynamic to be higher than the static value, implying that the RockHard setup should possibly output lower values than what is measured in the ultrasonic range. The strain relation dependency illustrated in Figure 63 shows that a crucial factor to evaluate may be the strain induced by the ultrasonic equipment.

To estimate the strain output of the transducer used for ultrasonic testing, one may do a small numerical calculation based on the data sheet of PZT5A (Appendix G.4). The displacement coefficient is typically given to be 350 pm/V and operates at 200 V. Assuming a width of about 2 mm of the sensor gives

$$\frac{350 \text{ pm/V} \cdot 200 \text{ V}}{2 \text{ mm}} = 3.5 \cdot 10^{-5}. \quad (83)$$

This strain level is well above the values used in this setup. It may be doubtful if this actually represents the strain in the rock since there are severe losses in the contact surfaces. Nevertheless it is an indication of the capability of the RockHard setup to measure at small signal scale, and that the numerical value obtained at ultrasonic frequencies may represent strain levels quite different than the ones assessed in RockHard Deformations.

In Figure 63 the ALU-7075 results of Table 11 are plotted. For the measurements located to the left in the diagram the sample was in the load frame with the same static stress all the time. The only change between these measurements is alterations in the perturbational wave amplitude. Since the orientation

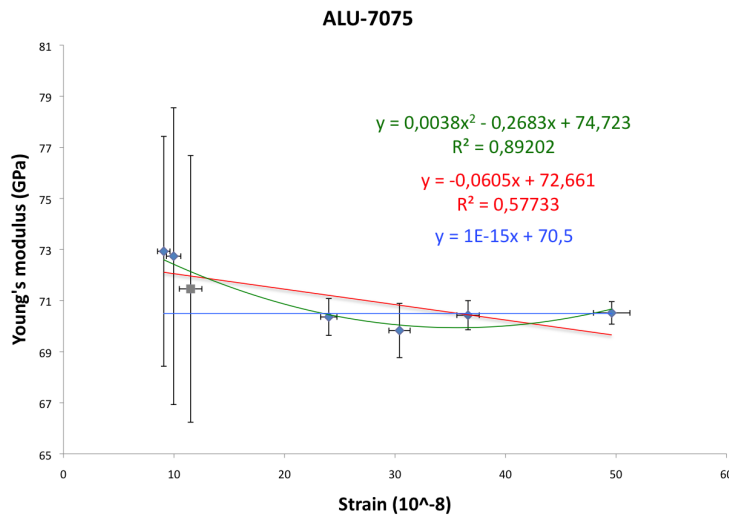


Figure 63: ALU-7075: Frequency average of Young's modulus (11-97 Hz, prime numbers) to strain in sample. The error bars represent the standard deviation.

and the position of the sample is identical in these three situations, one may easily identify the shift downwards in Young's modulus as strain increases, even though the standard deviation is quite big for such small strain levels on a stiff materials as aluminium. This may not necessarily be a material property since a constant line would go well within the error bars of the plot. Being within the linear elastic region of the sample, E should be independent of the amplitude, and a constant model would thus be of a better fit.

The values obtained for aluminium are so close to the ultrasonic ones that there is no point in addressing the difference any further at this time. A polynomial model was also implemented to get a better fit to the measured points. Since the most likely situation for aluminium would be a constant value, this model rejected.

Berea sandstone The values of ML#318.1.1 obtained in the low frequency setup clearly depend on the strain in the sample (Figure 64). For strains in the area of where Spencer et al. (1994) and Batzle et. al. (2006) conducted their research ($\sim 10^{-7}$), and at a uniaxial static stress of 10 MPa, values of about 20 \rightarrow 21 GPa are obtained for the Young's modulus, with a standard deviation of about 0.2 GPa (5TestSeries). The ultrasonically measured value for 5 MPa uniaxial stress is 18.54 GPa, using a $\rho_{Berea} = 2.14 \text{ g/cc}$. The match is poor, but a repeated experiment confirms the RockHard low frequency value. The uniaxial stresses are different and may explain the deviation.

Comparing to the ultrasonic values previously measured (Table 2) one notice that the low frequency value actually is substantially higher than the ultrasonic one. King (1969) measured a Berea sandstone with a changing hydrostatic confining pressure. At about 5 MPa the same values as given in Table 2 was obtained. E is shown to increase fast as of increase in hydrostatic pressure. At about 10 MPa King (1969) measured the Young's modulus to about 24 GPa.

A measurement with confining pressure is not directly comparable to a uniaxial one, since the confining pressure stiffens the rock. With this in mind, the range of values in the confining pressure case indicate that both of the Young's moduli at a uniaxial static stress are correct for their respective stress level. The Castlegate sandstone shows better correlation to ultrasonic values than the Berea sandstone. In the Castlegate sandstone both the ultrasonic and the seismic frequency Young's modulus measurements were carried out at the same uniaxial static stress, 5 MPa.

Figure 64 shows the linear trend of the three measuring points, all with uniaxial static stress of 10 MPa. The second order trend line shows better correlation to the measured points. Neither of these are considered to reflect reality to a high level of accuracy, but they show the trend of decreasing values of Young's modulus to an increase in strain.

More measuring points at different strain levels would be of interest to better the models. The value located the leftmost in the diagram comes from an early measurement series (3Test) where instrumental error still could have been influencing. It is recommended conducting the experiment once again for verification. An ultrasonic measurement of the very sample (ML#318.1.1) at a uniaxial stress of 10 MPa is also highly recommended.

The measurement as described above was endeavored undertaken, but was not completed. Part of the reason for this was to preserve the samples for further low frequency testing (avoid contamination by sirup).

Attenuation measurements in the Berea sandstone are inconclusive. Numeri-

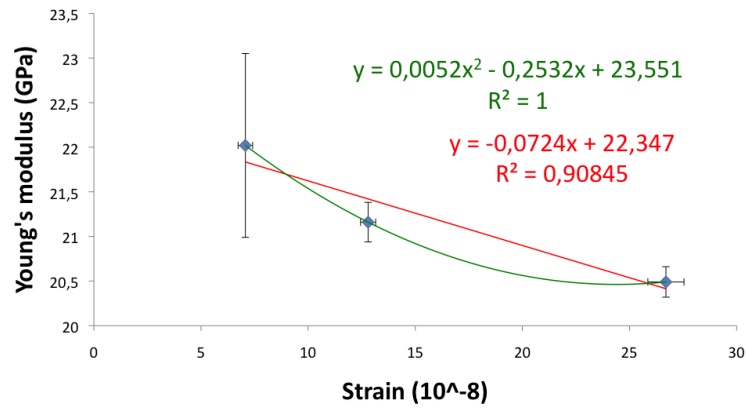


Figure 64: Berea sandstone: Frequency average of Young's modulus (11-97 Hz, prime numbers) to strain in sample. The error bars represent the standard deviation.

cal values close to zero confirm that the measurements are in the elastic domain. Noise makes negative values present.

Castlegate sandstone In the Castlegate sample ML#222.3.2 there is less decrease in the Young's modulus due to increase in strain than what is found in the Berea sandstone. This may be due to dealing with a softer material where the influence of strain is not as big as in harder ones, such as in the more consolidated Berea sample. The trend of decreasing stiffness to an increase in strain confirms the observations done by Tutuncu et al. (1994). The values over both frequency (Figure 42 to Figure 45) and amplitude (Figure 65) show small deviation and are fairly consistent in value. Young's modulus is about 12 GPa for strains close to 10^{-7} . The phase for increasing frequency (Figure 53) has

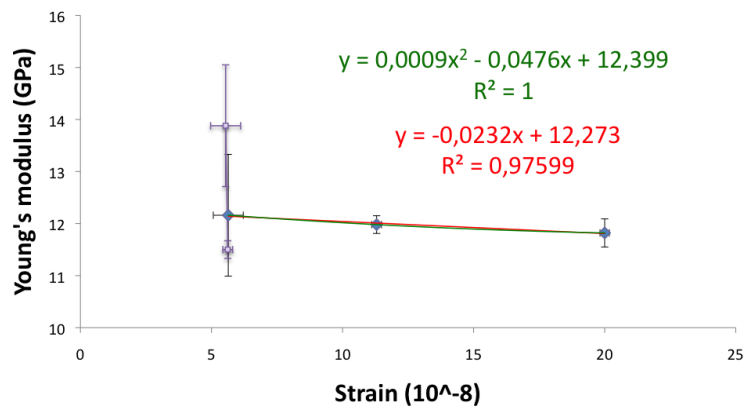


Figure 65: Castlegate sandstone: Frequency average of Young's modulus (11-97 Hz, prime numbers) to strain in sample. Only samples from the 5TestSeries are included for regression. Other points are plotted in purple with their respective standard deviations.

random noise of about one degree. The higher in frequency, the more negative the relative phase (relative phase or just 'phase' is defined as the phase of the force with respect to the reference signal minus the phase of the strain with respect to the reference signal).

The Castlegate (ML#222.1) has previously been measured in the ultrasonic range (Table 2) at the same uniaxial static stress (5 MPa) to have $E_{\text{dynamic}}^{\text{US}} = 13.99$ GPa. This value is above the low frequency values for ML#222.3.2 ranging from $E_{\text{dyn}}^{\text{LF}} \in \{11.50 \pm 0.17, 12.16 \pm 0.27\}$ GPa for strains $\sigma \in \{20.0 \pm 0.6, 5.62 \pm 0.19\} \cdot 10^{-8}$. The ML#222.3.1 shows the value $E_{\text{dyn}}^{\text{LF}} = 13.88 \pm 1.17$ GPa, but being from 3TestSeries it is a low quality data set with high standard deviation.

PEEK The PEEK values shown in Figure 46 and Table 11 are from the third measurement series meaning their noise level may be higher than in the final setup. The data previously measured at SINTEF are: $v_p = 2563$ m/s, $v_s = 1129$ m/s, and $\rho_{\text{PEEK}} = 1.32$ g/cm³ for a clean sample without fiberglass etc. Calculating the Young's modulus from these numbers gives the value of 4.64 GPa which matches perfectly to what one would expect judging from Figure 46(a) and Table 11.

Pierre shale The Pierre shale shows a strong time lapse effect in the Young's modulus. When loaded with a uniaxial stress the elasticity value increases. The first minutes it increases fast, then more slowly reaching a near constant value after some hours (Table 10). There are at least two plausible explanations for this: increased consolidation and drying when exposure to air.

When removing the sample from the load frame one notices that the sleeve is now longer than the plug even though they were initially equal. This is a non-ambiguous indication of plastic deformation. The sleeve is not pushed during testing since the actuator attached piston match the one inch plug and therefore slides on the inside of the sleeve if properly aligned. The amount of plastic compaction is by visual inspection estimated to some tenths of a mm.

Since the setup does not have any confining pressure and the sample is initially water saturated, some of the fluid will be pushed out due to the uniaxial stress. With a fluid exposed to air, some drying will occur, especially at high temperatures. This effect may also have an impact on the elastic response of the rock, presumably make it stiffer, and increase the Young's modulus. The magnitude is not yet known, but Table 10 shows increasing values when time goes by time, just as expected.

At ultrasonic frequency the Young's modulus is measured to 5.35 GPa (Table 2) at 5 MPa uniaxial stress. This is above the final value measured in Rock-Hard (ML#192.2.12: 3.99 ± 0.15 GPa), set after 2.75 hours. Having ultrasonic frequency measurements higher than seismic ones is expected. According to Hornby et al. (1995) (cited by Sarker et al. (2010)) P-wave velocity from ultrasonic measurements was very much higher than from the sonic log. Duranti et al. (2005) (cited by Sarker et al. (2010)) concluded that increasing frequency resulted in increasing stiffness when measuring on shale samples from seismic to ultrasonic frequencies. But Sarker et al. (2010) found no significant difference on Mancos shale measured at seismic and ultrasonic frequencies. In the Rock-Hard setup the two plugs used for respectively ultrasonic and seismic frequency measurements come from the same block (ML#192), but are not identical. The

difference found in Young's modulus may therefore be due to plug heterogeneity and different level of consolidation in the samples.

Sample ML#192.03.10 experienced problems with the strain gages' contact to the surface of the shale. The shear force of the wires soldered to the gages made the gages come loose tearing off a large fragment of the shale. It is evident that the removal of such a big fragment (about the size of the strain gage and 2-3 mm deep) will alter the characteristics of the plug. New and smaller strain gages were glued just beneath the void and the wires were replaced with more elastic ones. The measurement series '4Test-3' was carried out. The value obtained was substantially lower than the previously recorded and should be rejected due to bad measurement conditions.

Theory indicates the possibility of frequency dependence in saturated rocks (Equation 47) for frequencies higher than the limiting case $\omega \rightarrow 0$. By increasing the measurement time and the integration time t_c , and acquire with a better resolution in the range of interest, one will obtain a better idea of where this region should start. Paffenholz et al. (1989) found frequency dependence on water saturated samples from 0.1 Hz (Limestone) to 100 Hz (Sandstone). Young's modulus in saturated samples was substantially lower than in dry samples, and could explain to some extent the effects seen in the Pierre shale.

Steel Steel was measured to the range of 180 ~ 200 GPa at strain values down to $2 \cdot 10^{-8}$, but since the settings required for those measurements are very different than what is needed in the other applications, steel has been omitted for further discussion.

Static modulus Several authors (Section 2.3.3) have made comparative studies of dynamic and static measurements. The RockHard setup could also be used for that purpose. Some static tests were done on the samples with this in mind, but due to instrumental error on a multichannel strain gage reader, the results need to be postponed.

General trends To have a direct numerical value-to-value comparison to literature is hard due to scarce amounts of published material and different ambient conditions for measuring. Spencer (1981) found a negligible attenuation and frequency dependence (modulus dispersion) in vacuum-dry rocks. Spencer (1981) used strain amplitudes near 10^{-7} . This observation is confirmed by the RockHard measurements both at the strains of Spencer (1981) and about a magnitude below. The presence of fluids was shown by Gordon et al. (1968), Tittmann et al. (1976) (in the kHz range!) and Spencer (1981) to dramatically

lower the Young's modulus and increase their attenuation. This could explain the very low value of Young's modulus measured in the Pierre shale, which was the only saturated sample in this experiment. Bautmanns (2009) suggested a decay in the Young's modulus for higher stress. For the clastic rocks this seems to be confirmed. On aluminium there is no frequency dependence as expected.

Adam et al. (2009) made use of the Lock In amplifier for their measurements of carbonate samples. Carbonates in general have very different properties than sandstones and cannot be directly compared.

10 Conclusion

A new setup for measuring both the Young's modulus E and the attenuation $1/Q$ at seismic frequencies has successfully been created. Strain value limits are among the lowest found in published data reaching an interim limit of about $2 \cdot 10^{-8}$ for measurement series of $200 \rightarrow 300$ seconds and time constants of $3 \rightarrow 30$ seconds on materials with $E \in \{2, 70\}$ GPa. Effort was made making the system user friendly and well documented with an easy to understand interface in both LabVIEW for acquiring data, and MATLAB for interpreting the data.

Heavy into-the-box shielding was necessary to obtain reproducible data. At low strain levels ($< 5 \cdot 10^{-8}$) soft samples showed the best response. Attenuation was more susceptible to noise than the absolute Young's modulus. For high strains (10^{-7}) the full complex Young's modulus was easily recorded. As literature suggests, an amplitude dependence to propagated stress was prominent in the sandstone samples. The softer the material, the lesser the dependence. The setup was verified to great accuracy by measuring samples of known elastic properties such as PEEK and aluminium.

Elastic theory correlates well with the samples showing no prominent frequency dependence for dry sandstone samples in Young's modulus. Saturated Pierre shale was found to increase rapidly in value of E during testing. One possible explanation is the increased consolidation from the applied static uniaxial stress (5MPa). Another suggestion is the drying of the sample. The effect seems too great to be solemnly caused by drying, and a combination with increased consolidation is considered more plausible. A frequency dependence has yet to be settled on the water saturated shale. A suggestion is to go even lower in frequency (sub Hertz), and use a strong driving perturbation to obtain clean unambiguous signals (strains in 10^{-7}). Amplitude dependence due to the drive must also be addressed. It would be beneficial to have better insight in the time lapse consolidation effects before attacking the frequency/amplitude dependence on the Pierre shale.

A more extensive comparative study of the numerical results would benefit from having measured the Poisson's ratio together with the Young's modulus. The best way of implementing this into the setup is to synchronize it with the measurement of the Young's modulus. This requires another dual channel input implemented in the LabVIEW program, and one more high quality lock in amplifier. Section 10.1 contains more ideas about the way ahead.

10.1 Further work

The RockHard setup has been continuously evolving. Hopes are that the setup will continue to improve and get even better. There are numerous issues facing the setup. Both when it comes to other means of operation, and improvement of the existing features. Items mentioned can be overlapping or closely related. Bautmans (2009) addressed some of the issues mentioned in his report dealing with a similar setup.

10.1.1 Hardware

1. Add a confining pressure vessel around sample
2. Add a fluid container to saturate the sample
3. Add a pre-amplifier between the Wheatstone bridge and the lock-in amplifier on the strain signal. It should have a perfect linear gain in the range sub-hertz to a couple of hundred hertz
4. Replace the signal generator with one capable of lower, more accurate output (< 10 mV)
5. Add more lock-in amplifiers to record also the lateral expansion
6. Do simultaneous ultrasonic measurements
7. Change strain gage configuration to 4 strain gages 90 degrees apart
8. Try semiconductor strain gages to get a higher gain value
NB! This may cause the measurements to go off scale (Bautmans, 2009)
9. Balance the Wheatstone bridge at static load
10. Use higher resolution on frequency and/or amplitude (measure more frequencies/amplitudes within the range)
11. Replace the Scitec lock-in amplifier with one of better specifications.
12. Put the computer in the rack and attach the screen to one of the sides

10.1.2 Software

1. HSE: Add further restrictions on all outputs to avoid malfunctioning and possible damage.
2. Simplify the code and clean up the structure

3. Avoid doing the same calculation more than once to increase the speed of post processing of data.
4. Enhance backwards compatibility
5. Better the user interface and make it more intuitive.
6. Automate more settings and make the system independent on the 3.5" floppy drive.

10.1.3 Chemical

1. Investigate the effect of the different adhesives: Is it stiff enough? Does it transfer all the strain?
2. Investigate how the epoxy stiffens the rock: How far does it intrude? Is it frequency dependent?

10.1.4 Other

1. Do static tests of all samples to compare their value of Young's modulus and attenuation
2. Increase the length of the sample: Look for dimensional impact on the measurements. Is it possible that the cutoff frequency is actually a geometrical property of the sample? Compare to the 2" plug.
3. Deliberately misalign the sample and check how this impacts the measurements (Bautmans, 2009)
4. Increase the width of the sample: Look for dimensional impacts on the measurements. Is it possible that the cutoff frequency is actually a geometrical property of the sample? Compare to the 1" plug.
5. Recalibrate the force sensor to a lower range (the smallest range is currently 100N, it is sufficient, but usually the measurements are well below 10N). NB! Be aware that any drift in the load frame may cause the meter to go off scale if the scale is set too narrow!

11 References

1. Adam, L., Batzle, M. I. Brevik (2006). Gassmann's fluid substitution and shear modulus variability in carbonates at laboratory seismic and ultrasonic frequencies. *Geophysics*, VOL. 71, NO. 6 nov-dec 2006; P. F173F183 doi:10.1190/1.2358494
2. Adam, L., Batzle, M., and Lewallen, K. (2009). Seismic wave attenuation in carbonates. *Journal of Geophysical Research*, VOL. 114, B06208, doi:10.1029/2008JB005890,
3. Aldrich, J. (1998). Doing Least Squares: Perspectives from Gauss and Yule". *International Statistical Review* 66 (1): 6181
4. Al-Tahini, A. M., C. H., Sondergeld, and C. S. Rai, 2004, The effect of cementation on static and dynamic properties in Jauf and Unayzah formations at Saudi Arabia: SPE Annual Conference and Exhibition, SPE, SPE number 90448.
5. Aluminum Standards and Data The Aluminum Association Inc, 818 Connecticut Ave. N.W, Washigton, D.C. 2006
6. Ament, W. S. (1953). Sound Propagation in Gross Mixtures. *J Acoust Soc Am*, 25(4), 638. doi:10.1121/1.1907156
7. Barkved, O. I., and Kristiansen, T. (2005). Seismic time-lapse effects and stress changes: Examples from a compacting reservoir. *The Leading Edge*, 24(12), 1244. doi:10.1190/1.2149636
8. Batzle, M., and Han, D. (2006). Fluid mobility and frequency-dependent seismic velocityDirect measurements. *Geophysics*.
9. Bautmans, P., (2009) Low frequency laboratory measurements of P-wave velocities, Master thesis, Katholieke Universiteit Leuven, The Netherlands
10. Biot, M. (1956). Theory of propagation of elastic waves in a fluid-saturated porous solid. II. Higher frequency range. *J Acoust Soc Am*.
11. Bøe, R. (2005): Mineralogical and petrophysical characterization of Pierre 1 shale, SINTEF Petroleum Research AS, 33.5384.00/01/05
12. Cheng, C. and Johnston D. H. (1981). Dynamic and static moduli. *Geophysical Research Letters*. Vol. 8. No. 1 Pages 39-42

13. Chen, YangQuan (July 17th 2003) Sinefit.m, Utah State University, Department of Electrical and Computer Engineering
14. Churcher, P., French, P., and Shaw, J. (1991). Rock properties of Berea sandstone, Baker dolomite, and Indiana limestone, SPE International Symposium on Oilfield Chemistry held in Anaheim, California, February 20-22,1991, SPE21044
15. Fintland, T. W. (2010): User Interface for Control and Data Acquisition in a Laboratory Setup for Small Rock Deformations/RockHard Deformations, NTNU, Trondheim, Norway, Department of Physics, Project work Complex Materials, December
16. Fjær, E., Holt, R. M., Horsrud, P., Raaen, A. M., and Risnes, R. (2008). Developments in Petroleum Science. Developments in Petroleum Science03767361 (Vol. 53, p. 175-218). Elsevier. doi:10.1016/S0376-7361(07)53005-0
17. Fjær, E., 1999, Static and dynamic moduli for weak sandstones, in B. Amadei, R. L. Kranz, G. A. Scott, and P. H. Smeallie, eds, Rock mechanics for industry, Balkema, 675-681.
18. Fjær, E. 2009. Static and dynamic moduli of a weak sandstone. Geophysics, 74(2), WA103WA112.
19. Gassmann, F. (1951). On Elasticity of Porous Media.
20. Gordon, R. B., and Davis, L. A. (1968). Velocity and Attenuation of Seismic Waves in Imperfectly Elastic Rock. Journal of Geophysical Research, 73(12), 39173935. American Geophysical Union. doi:10.1029/JB073i012p03917
21. Guyer, R. A., Rasolofosaon P. N. J. et al., (1995). Equation of state hysteresis and resonant bar measurements on rock, Rock Mechanics, Daeman and Shultz, Rotterdam, ISBN 90 5410 552 6
22. van Heerden, W. L., 1987, General Relatios between static and dynamic moduli of rocks: International Journal of Rock Mineral Science and Geomechanical Abstracts, 24, 381-385.
23. Holt, R. (2004). TPG4170, Rock Acoustics, Lecture Notes, NTNU, Trondheim
24. Hilterman, F. (1990). Is AVO the seismic signature of lithology? A case history of Ship Shoal-South Addition. The Leading Edge, 9(6), 15. doi:10.1190/1.1439744

-
25. Hofmann, R. (2006). Frequency Dependent Elastic and Anelastic Properties of Clastic Rocks, Colorado School of Mines, PhD thesis, crusher.mines.edu.
 26. Jeng, S. -, and Chen, S. -. (1997). The solidification characteristics of 6061 and a356 aluminum alloys and their ceramic particle-reinforced composites. *Acta Materialia*, 45(12), 4887-4899.
 27. Jizba, D., G. Mavko, and A. Nur, 1990, Static and dynamic moduli of tight gas sandstones: 60st Annual International Meeting, SEG, Expanded Abstracts, 827-829.
 28. Johnson, C.F. (1970). A Pulse Technique For The Direct Measurement Of Bar Velocity, The 12th U.S. Symposium on Rock Mechanics (USRMS), November 16 - 18, 1970 , Rolla, MO
 29. Johnson, P., and Zinszner, B. (1996). Resonance and elastic nonlinear phenomena in rock. *J geophys .*
 30. King, M. S. Static And Dynamic Elastic Moduli Of Rocks Under Pressure, The 11th U.S. Symposium on Rock Mechanics (USRMS), June 16 - 19, 1969 , Berkeley, CA, Paper nr: 69-0329
 31. KUO, M., TSAI, C., HUANG, J., and CHEN, M. (2005). PEEK composites reinforced by nano-sized SiO and AlO particulates. *Materials Chemistry and Physics*, 90(1), 185-195. doi:10.1016/j.matchemphys.2004.10.009
 32. Li, L. and Fjær E. (2008): Investigation of the stress-dependence of static and dynamic moduli of sandstones using a discrete element method, The 42nd U.S. Rock Mechanics Symposium (USRMS), June 29 - July 2, 2008 , San Francisco, CA, ARMA 08-191.
 33. Melo, J. D. D., and Radford, D. W. (2002). Elastic characterization of PEEK/IM7 using coefficients of thermal expansion. *Composites Part A: Applied Science and Manufacturing*, 33(11), 1505-1510.
 34. Montayeur, H., R. M. Graves, 1985, Prediction of static elastic/mechanical properties of consolidated and unconsolidated sands from acoustic measurements: 60th Annual Technical Conference and Exhibition, Society of Petroleum Engineers, SPE 14159.
 35. Olsen, C. (2007): Elastic and electric properties of North Sea Chalk. PhD Thesis. Institute of Environment & Resources. Technical University of Denmark, Kgs. Lyngby. pp. 27-33

36. Paffenholz, J. and H. Burkhard, (1989): Absorption and modulus measurements in the seismic frequency and strain range on partially saturated sedimentary rocks. *Journal of Geophysical Research*.
37. Platt, David K., (2003): *Engineering and High Performance Plastics Market Report*, ISBN-1859573800, 198p.
38. Plona, T. J., and J. M. Cook, 1995, Effects of stress cycles on static and dynamic Young's moduli in Castlegate sandstone, in *Proceedings of the 35th U. S. Symposium on Rock Mechanics*, J. J. K. Daemen and R. A. Schulz, eds., Balkema, 155-160
39. Rae, P. J., Brown, E. N., and Orlor, E. B. (2007). The mechanical properties of poly(ether-ether-ketone) (PEEK) with emphasis on the large compressive strain response. *Polymer*, 48(2), 598-615.
40. Ratner Buddy D. et al. eds., (1996): *Biomaterials Science: An Introduction to Materials in Medicine*, ISBN-0125824637, 864p.
41. Sarker, R., and Batzle, M. (2010). Anisotropic elastic moduli of the Mancos B Shale- An experimental study. *SEG Technical Program Expanded Abstracts*, 29(1), 26002605.
42. Searle, O. B., and Pfeiffer, R. H. (1985). Victrex poly(ethersulfone) (PES) and Victrex poly(etheretherketone) (PEEK). *Polymer Engineering and Science*, 25(8), 474-476. doi:10.1002/pen.760250808
43. Simmons, G., and Brace, W. F. (1965), Comparison of Static and Dynamic Measurements of Compressibility of Rocks, *J. Geophys. Res.*, 70(22), 56495656, doi:10.1029/JZ070i022p05649.
44. Spencer, J.W., 1981, Stress relaxations at low frequencies in fluid-saturated rocks, *Journal de physique, Colloque C5, supplément au n°10, Tome 42, octobre 1981*
45. Spencer, J., Jr, and Cates, M. (1994). Frame moduli of unconsolidated sands and sandstones. *Geophysics.*, VOL. 59, NO.9 (Sept 1994); P. 1352-136
46. Tittmann, B. R., L. Ahlberg, and J. Curnow, 1976, Internal friction and velocity measurements, *Lunar Science Conference, 7th, Houston, Tex., March 15-19, 1976, Proceedings. Volume 3. (A77-34651 15-91) New York, Pergamon Press, Inc., 1976, p. 3123-3132.*

47. Tutuncu, A. N., and M. M. Sharma, 1992, Relating Static and ultrasonic laboratory measurements to acoustic log measurements in tight gas sands: 67th Annual Technical Conference and Exhibition, Society of Petroleum Engineers, 299-311.
48. Tutuncu, A. N., A. L. Podio, and M. M. Sharma, 1994, Strain amplitude and stress dependence of static moduli in sandstones and limestones: in P. P. Nelson and S. E. Laubach., eds., Rock mechanics- Models and Measurements Challenges from Industry, Balkema, 489-496.
49. Tutuncu, A. N., A. L. Podio, and M. M. Sharma, 1998a, Nonlinear viscoelastic behavior of sedimentary rocks, Part I: Effect of frequency and strain amplitude: Geophysics, 63, 184-194.
50. Tsiklauri, D. (2001, September 4). Biot's theory of propagation of elastic waves in a fluid-saturated porous solid revisited: introduction of non-zero boundary slip velocity. arXiv.org.
51. Vienot, M., Neff, D., and Butler, E. (1998). Method for determining barriers to reservoir flow, US Patent 5,835,882
52. Wang, Z., 2000, Dynamic versus static elastic properties of reservoir rocks, in Z. Wang, and A. Nur, eds., Seismic and acoustic velocities in reservoir rocks volume 3 Recent developments, Geophysics reprint series No.19, 531-539.
53. Yale, D. P., J. A. Nieto, and S. P. Austin, 1995, The effect of cementation on the static and dynamic mechanical properties of the Rotliegendes sandstone, in Proceedings of the 35th U. S. Symposium on Rock Mechanics, J. J. K. Daemen and R. A. Schulz, eds., Balkema, 169-175.
54. Yale, D. P., and W. H. jr. Jamieson, 1994, Static and dynamic rock mechanical properties in the Hugoton and Panoma fields, Kansas: SPE Mid-Continent Gas Symposium, SPE, 209-219.
55. Zimmerman, J. (1968). Detection of electroseismic signal employing salt domes, US Patent 3,392,2327

11.1 Creative Commons' References

For images from the Creative Commons domain, the exact references are provided below.

1. User:Sigmund Date: June 18'th 2011, 11:42
Link: http://upload.wikimedia.org/wikipedia/commons/8/8e/Metal_yield.svg
Symbol Reference: Dieter, Mechanical Metallurgy, McGraw-Hill, 1986,
2. User:c.lingg, Date: June 17'th, 2011, 17:34
Link: http://upload.wikimedia.org/wikipedia/commons/d/d0/Shear_scherung.svg

A The Resistivity of a Strain Gage

To establish the relationship between linear extension and the change in resistance in a strain gage, one can consider the following

$$R = \rho \frac{L}{A},$$

where ρ is the conductivity of the material, L is the length, and A is the cross section. When stretching it

$$L \rightarrow L + \Delta L,$$

and if one assumes that the volume, V , is constant (may be subject to discussion)

$$A = \frac{V}{L},$$

one gets

$$R = \rho \frac{L}{A} = \rho \frac{L}{\frac{V}{L}} = \rho \frac{L^2}{V}.$$

Thus for a change in R

$$\begin{aligned} \Delta R &\approx \frac{\partial R(\rho, L)}{\partial L} \Delta L = \frac{\partial}{\partial L} \left(\rho \frac{L^2}{V} \right) \Delta L \\ &= \frac{1}{V} \left(\frac{\partial \rho}{\partial L} L^2 + 2\rho L \right) \Delta L, \end{aligned}$$

a factor of R is extracted from the parenthesis, and get

$$\Delta R = \left(\frac{1}{\rho} \frac{\partial \rho}{\partial L} R + \frac{2R}{L} \right) \Delta L.$$

Approximating the differentials by delta-values gives

$$\boxed{\frac{\Delta R}{R} = \left(\frac{\Delta \rho}{\rho} + 2 \frac{\Delta L}{L} \right)}.$$

If the piezo effect can be neglected (the resistivity of the material is constant), it can be simplified to

$$\boxed{\frac{\Delta R}{R} = k \frac{\Delta L}{L}},$$

where k is called the gage factor and is close to 2 for most metals.

B The Wheatstone Bridge

At first glance it may seem difficult to sense a small change in the resistivity of an ohmic sensor. To get an easy measurable quantity, one may convert it into a potential and measure the voltage. Even this may be difficult if the signal is strong and varies little. The Wheatstone bridge takes advantage of the ease of measure deviation from zero. From the principle of a voltage divider and

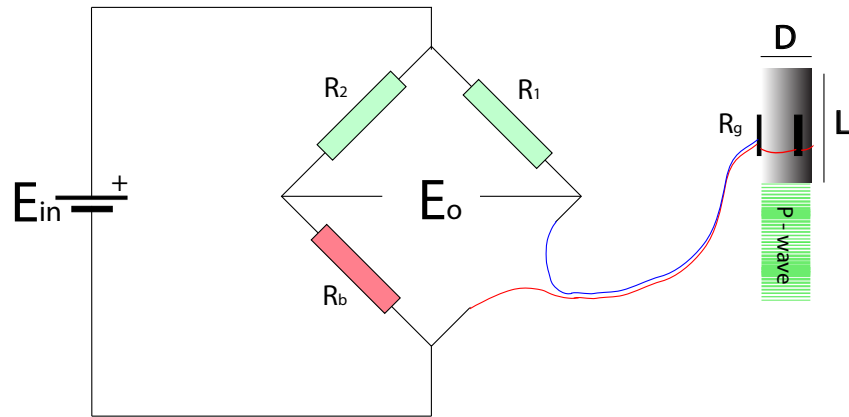


Figure 66: The Wheatstone bridge with supply voltage, V_s , bridge voltage, V_g , resistor;s R_A to R_D , length of sample, L , diameter, D , and one axial force F .

superposition one can reach the general expression for the potential between the two legs of the bridge,

$$\frac{V_g}{V_s} = \left(\frac{R_c}{R_c + R_D} - \frac{R_B}{R_A + R_B} \right),$$

where the names are according to Figure 66.

By expanding R_c with its differential ΔR and setting $R_a = R_B = R_C = R_D = R$ one obtains the result

$$\begin{aligned}
 \frac{V_g}{V_s} &= \left(\frac{R + \Delta R}{R + R + \Delta R} - \frac{R}{R + R} \right) \\
 &= \left(\frac{1 + X}{2(1 + \frac{1}{2}X)} - \frac{1}{2} \right) \\
 &\approx \left(\frac{(1 + X)(1 - \frac{1}{2}X)}{2} - \frac{1}{2} \right) \\
 &\approx \left(\frac{x}{4} - \frac{1}{4}x^2 \right),
 \end{aligned}$$

where $X = \Delta R/R$ and assuming that $|X| \ll 1$. By analyzing this expression one sees that the voltage is proportional to the relative change in ohmic resistance, $\Delta R/R$, by a quarter. As for the name ‘‘Quarter bridge’’. It can be equally shown that a half bridge would enhance the factor to $1/2$, thus doubling the sensitivity. In a full bridge (four times as sensitive) one is dependent on both compaction and expansion in counter phase. In brief the equation for the half bridge yields:

$$\begin{aligned}
 \frac{V_g}{V_s} &= \left(\frac{R + \Delta R}{R + R + \Delta R} - \frac{R}{R + R + \Delta R} \right) \\
 &= \left(\frac{1 + X}{2(1 + \frac{1}{2}X)} - \frac{1}{(2 + x)} \right) \\
 &\approx \left(\frac{x}{4} + \frac{1}{2} + \frac{x}{4} - \frac{1}{2} \right) \\
 &\approx \frac{x}{2},
 \end{aligned}$$

where R_A is replaced by the other strain gage and the same assumptions as earlier stated apply.

**C RockHard Scripts - rh* - Matlab scripts for
post processing of .tdms files**


```

dllfile='nilibddc.dll';
dllfolder='C:\RockHard\RockHardPostProcessing\Matlab\MATLAB TDM Example\dev\bin\32-
bit';
libname=strtok(dllfile, '.');
NI_TDM_DLL_Path=fullfile(dllfolder, dllfile);
hfile='nilibddc_m.h';
hfolder='C:\RockHard\RockHardPostProcessing\Matlab\MATLAB TDM
Example\dev\include\32-bit';
NI_TDM_H_Path=fullfile(hfolder, hfile);
clear dllfile dllfolder hfile hfolder;

%%Read the TDMS-file
%%The TDMS FILE CONTAINS 5 COLOUMNS
% 1 column: n/a
% 2 column: n/a
% 3 column: Strain measurement - Lock in X - "Green channel"
% 4 column: Force measurement - Lock in Y - "Brown channel"
% 5 column: Strain measurement - Scitec lock in - "Actuator sensor"
%
% ReadFile(pwd, fileName, libname, NI_TDM_DLL_Path, NI_TDM_H_Path);
ReadFile();
clear DDC_CHANNELGROUP_DESCRIPTION DDC_CHANNELGROUP_NAME DDC_CHANNEL_NAME
DDC_FILE_AUTHOR DDC_FILE_DATETIME DDC_FILE_DESCRIPTION DDC_FILE_NAME DDC_FILE_TITLE;
clear NI_TDM_DLL_Path NI_TDM_H_Path;
clear fileIn fileauthlen fileauthlenIn filedesclen filedesclenIn filenamelenIn
filetitlelen filetitlelenIn grpdesclen grpdesclenIn grpnamelenIn i j;
clear minute minuteIn month monthIn msecond msecondIn;
clear wkday wkdayIn year yearIn typeIn day dayIn second secondIn hour hourIn;
clear channamelenIn channames chanvals dummyVar err;
clear pchannamelenIn pchans pfilename pgrpname pgrps pvals vals;
clear numchansIn numgrpsIn numvalsIn type;
close all;

%%Sample details
master=getTDMS(filepath);

%Extract diameter from file name
crossArea=master.sample.crossArea; %Extracted from metadata - converted to
meters
lengthOfSample=master.sample.Length; %Extracted from metadata - converted to
meters
strainGaugeFactor=2.1; %[] from strain gauge
specifications
strainGaugeSupplyVoltage=10; %[V] to the Wheatstone bridge
NewtonPerVolt=10;
openLoop=1;

%%Sampling details
samplingFrequency=master.samplingRate;%input('Sampling frequency (Hz)[32Hz]: '); %Hz
if isempty(samplingFrequency)
    samplingFrequency=32;
end
samplingTime=length(MEASUREMENTS(:,3))/samplingFrequency;
% actualFrequency=input('Actual frequency (Hz)[79Hz]: '); %%%%%%%%%%%AS GIVEN ON
WAVE GENERATOR!!

```

```
%         if isempty(actualFrequency)
%             actualFrequency=79;
%         end

%%Amplifier details
    dummy=findstr(filepath, 'mV');
    dummy=dummy(3)-1;
    fullScaleForce=str2num(filepath(findstr(filepath, '_y')+2:dummy));
    clear dummy;
%     %0.01%0.5;%input('Full scale, force? (mV)[0.5] ');
%         if isempty(fullScaleForce)
%             fullScaleForce=0.5;
%         end
    fullScaleForce=fullScaleForce*10^(-3);

fullScaleStrainGauge=str2num(filepath(findstr(filepath, '_x')+2:findstr(filepath, '
'nV_')-1));

%     0.1%1;%input('Full scale, strain? (uV)[1] ');
%         if isempty(fullScaleStrainGauge)
%             fullScaleStrainGauge=1;
%         end
fullScaleStrainGauge=fullScaleStrainGauge*10^-9;

    fullScaleAmplitude=str2num(filepath(findstr(filepath, 'scitec')+6:findstr(filepath, '
'mV_')-1));
%     %30;%input('Full scale, amplitude? (mV)[30] ');
%         if isempty(fullScaleAmplitude)
%             fullScaleAmplitude=30;
%         end
fullScaleAmplitude=fullScaleAmplitude*10^-3;

actualFrequency=master.waveGenerator.frequency;
actualFrequency=str2num(filepath(findstr(filepath, 'mVpp_')+5:findstr(filepath, 'Hz_')
-1));

%%Saving the .mat file
    filepathMAT=[filepath(1:length(filepath)-5) '.mat'];
    save(filepathMAT);
clear filepath filepathMAT;

% %%Exporting to pdf-file
%     filePathPdfExport=[filepath(1:length(filepath)-5) '_analysis.pdf'];
%     print (1, '-dpdf', filePathPdfExport);

%%Looping
%onceMore=input('Once more? (1/0)[1]');
%     if isempty(onceMore)
%         onceMore=1;
%     end
%end
```



```

%
% NOTE: This script is not measuring the phase between Force and Strain!
%

close all;
%keep totalForce totalStrain totalAmplitude totalYoungsAmplitude totalYoungsStrain
listOfTDMSFiles mStartEndList numberOfFiles
screen_size = get(0, 'ScreenSize');

filefolder=pwd;
if exist('filepathMAT','var')==0
    [filepathMAT,filefolder]=uigetfile({'*.mat'},'Select the .mat file');
%else
    %filepathMAT=filepath_mat;
end
Data_PathMAT=fullfile(filefolder,filepathMAT);
load(Data_PathMAT, 'MEASUREMENTS', 'master', 'fullScaleAmplitude', 'fullScaleForce',
'NewtonPerVolt');
load(Data_PathMAT, 'fullScaleStrainGauge', 'strainGaugeFactor',
'strainGaugeSupplyVoltage', 'samplingFrequency');
load(Data_PathMAT, 'crossArea', 'lengthOfSample', 'openLoop', 'MEASUREMENTS');

%%System parameters
%%Scitec lock in settings
    %fullScaleAmplitude=30*10^-3;    %[V]
%%Force parameters
    %fullScaleForce=0.5;            %[V]    from lock in amplifier (upper right
corner)
    %NewtonPerVolt=10;              %[N/V]    from charge meter
%%Strain parameters
    %fullScaleStrainGauge=1*10^-6;  %[V]    from lock in amplifier (upper right
corner)
    %strainGaugeFactor=2.1;         %[]    from strain gauge specifications
    %strainGaugeSupplyVoltage=10;   %[V]    to the Wheatstone bridge
%%Sample parameters
    %crossArea=0.0005076;           %[m^2]
    %lengthOfSample=50.7*10^-3;     %[m]
        %Aluref03    =    0,0005070;
        %Peek03     =    0,0005076;
        %ML318_01_01=    0,0005062;
        %Steel      =    0,0005075;
%%Actuator-settings
    %openLoop=1;

%%Read the TDMS-file
%%The TDMS FILE CONTAINS 5 COLOUMNS
    % 1 column: n/a
    % 2 column: n/a
    % 3 column: Strain measurement - Lock in X - "Green channel"
    % 4 column: Force measurement - Lock in Y - "Brown channel"
    % 5 column: Strain measurement - Scitec lock in - "Actuator sensor"

% %%Sampling details
%     samplingFrequency=input('Sampling frequency (Hz)[256Hz]: '); %Hz

```

```

%   if isempty(samplingFrequency)
%       samplingFrequency=256;
%   end
%
%   samplingTime=length(MEASUREMENTS(:,3))/samplingFrequency;
% %   samplingTime=input('Sampling time (s)[7200s]: ');           %seconds (s)
% %   if isempty(samplingTime)
% %       samplingTime=7200;
% %   end
%   actualFrequency=input('Actual frequency (Hz)[79Hz]: '); %%%%%%%%%%%AS GIVEN ON ✓
WAVE GENERATOR!!
%   if isempty(actualFrequency)
%       actualFrequency=79;
%   end

%%Measuring details
    mStart=70;%input('Calculation starting from (percent)[25%]: '); %Hz
    if ~exist('mStart')
        mStart=70;
    end

    mEnd=100;%input('Calculation ending at (percent)[100%]: '); %Hz
    if ~exist('mEnd')
        mEnd=100;
    end

%%Making ready first figure.
f1 = figure(1);
set(f1, ...
    'Position', [0 0 screen_size(3) screen_size(4) ], ...
    'Name', 'Rock Hard Deformations - Post processing - Figure 1');
%   subplot(4,2,1:2); plot(MEASUREMENTS); legend(MEASUREMENTS_LEGEND), title ✓
(regexptranslate('escape', filepathMAT));
%   subplot(4,2,8); hist(ERRORLOG); title('Error log','Interpreter','latex');
orient('landscape');

%%Setting window for analysis
totalLengthOfMeasurements=length(MEASUREMENTS(:,4));
mStartMeasuringZone=floor(mStart/100*totalLengthOfMeasurements);
mEndMeasuringZone=floor(mEnd/100*totalLengthOfMeasurements);

%%Setting column factors of interpretation
thirdColumnFactor=16/3*2*sqrt(2)*fullScaleStrainGauge/(2.1 ✓
*strainGaugeSupplyVoltage*10); %<---Strain
%clear fullScaleStrainGauge strainGaugeSupplyVoltage;
fourthColumnFactor=2*sqrt(2)*NewtonPerVolt/10*fullScaleForce; ✓
%<---Force
%clear NewtonPerVolt fullScaleForce;
fifthColumnFactor=2*sqrt(2)*fullScaleAmplitude*1500; ✓
%<---Deformation

%%Making ready matrix for final measurements
timeForceStrainAmplitude=zeros((mEndMeasuringZone-mStartMeasuringZone+1),4);
timeForceStrainAmplitude(:,1)=mStartMeasuringZone/samplingFrequency; ✓

```

```

1/samplingFrequency:mEndMeasuringZone/samplingFrequency;

%%Converting into respective units and extracting max, avg and min values
    thirdColumn=MEASUREMENTS(mStartMeasuringZone:mEndMeasuringZone,3) ↵
*thirdColumnFactor;    %<--- Converting voltage to strain.
    strain(2)=mean(thirdColumn);
    strain(1)=min(thirdColumn);
    strain(3)=max(thirdColumn);
    strainstd=std(thirdColumn);
    timeForceStrainAmplitude(:,3)=thirdColumn;
    clear thirdColumn thirdColumnFactor;

    fourthColumn=MEASUREMENTS(mStartMeasuringZone:mEndMeasuringZone,4) ↵
*fourthColumnFactor;    %<--- Converting voltage to Newton.
    force(2)=mean(fourthColumn);
    force(1)=min(fourthColumn);
    force(3)=max(fourthColumn);
    forcestd=std(fourthColumn);
    timeForceStrainAmplitude(:,2)=fourthColumn;
    clear fourthColumn fourthColumnFactor;

    fifthColumn=MEASUREMENTS(mStartMeasuringZone:mEndMeasuringZone,5) ↵
*fifthColumnFactor;    %<--- Converting voltage to m.
    amplitude(2)=mean(fifthColumn);
    amplitude(1)=min(fifthColumn);
    amplitude(3)=max(fifthColumn);
    amplitudestd=std(fifthColumn);
    timeForceStrainAmplitude(:,4)=fifthColumn;
    clear fifthColumn fifthColumnFactor;

    youngsStrain(2)=force(2)/crossArea/strain(2)*10^-9;
    youngsStrain(3)=force(3)/crossArea/strain(1)*10^-9;
    youngsStrain(1)=force(1)/crossArea/strain(3)*10^-9;

    youngsAmplitude(2)=force(2)/crossArea/(amplitude(2)/lengthOfSample);
    youngsAmplitude(3)=force(3)/crossArea/(amplitude(1)/lengthOfSample);
    youngsAmplitude(1)=force(1)/crossArea/(amplitude(3)/lengthOfSample);

%%Saving the .mat file
    %filepath_mat=[filepath(1:length(filepath)-5) '.mat'];
    save(filepathMAT);

%%Plotting results
% Create textbox [xPositionOnLowerLeft yPositionOnLowerLeft xWidth yHeight]
    a1=annotation('textbox',...
    [0.372 0.30 0.26 0.19],...
    'Interpreter','latex',...
    'String',{...
    ['Deformation ($\rm{nm}_{pp}$): ' num2str(amplitude(2))],...
    ['Youngs Modulus SG(GPa): ' num2str(youngsStrain(2))] ['(' num2str(youngsStrain(1)) ↵
    ' to ' num2str(youngsStrain(3)) ')']...
    ['Youngs Modulus AMP(GPa): ' num2str(youngsAmplitude(2))] ['(' num2str ↵
    (youngsAmplitude(1)) ' to ' num2str(youngsAmplitude(3)) ')']...
    },...
    'FitBoxToText','off');

```

```

set(a1, 'FontSize', 16, 'HorizontalAlignment', 'center', 'VerticalAlignment', 'middle', 'BackgroundColor', [1 1 0.9]);

a2=annotation('textbox',...
[0.64 0.30 0.26 0.19],...
'Interpreter','latex',...
'String',{...
% 'Young's modulus:' num2str((Ahat_force/0.000507)/(Ahat_def*10^(-6)/0.05084)
*1/10^9) ...
% 'Youngs Modulus: ' num2str((brownChannel/0.000507)/strain) ...
['Strain: ' num2str(strain(2))] ['(' num2str(strain(1)) ' to ' num2str(strain(3))
)'] ...
['Force (N): ' num2str(force(2))] ['(' num2str(force(1)) ' to ' num2str(force(3))
)']...
},...
'FitBoxToText','off');
set(a2, 'FontSize', 14, 'HorizontalAlignment', 'center', 'VerticalAlignment', 'middle', 'BackgroundColor', [1 1 0.9]);

%%Coarsing the Measurements before plotting
if totalLengthOfMeasurements<1000
    coarseStep=1;
else
    coarseStep=floor(totalLengthOfMeasurements/1000);
end

%%Plotting the relative amplitudial behaviour
hold on;
plotTimeVector=0:1/samplingFrequency*coarseStep:(totalLengthOfMeasurements-1)
/samplingFrequency;
plot(plotTimeVector, MEASUREMENTS(1:coarseStep:totalLengthOfMeasurements,3)/max
(MEASUREMENTS(:,3)), 'g'); %<-- Strain
plot(plotTimeVector, MEASUREMENTS(1:coarseStep:totalLengthOfMeasurements,4)/max
(MEASUREMENTS(:,4)), 'r'); %<-- Force
plot(plotTimeVector, MEASUREMENTS(1:coarseStep:totalLengthOfMeasurements,5)/max
(MEASUREMENTS(:,5)), 'b'); %<-- Amplitude
title([regexprtranslate('escape', filepathMAT) 'STRAIN']);
legend('Strain', 'Force', 'Perturbation (p-p)');
vline(mStart/100*totalLengthOfMeasurements/samplingFrequency, 'r', 'Measurement
zone');
vline(mEnd/100*totalLengthOfMeasurements/samplingFrequency, 'r', 'Measurement
zone');
hold off;

%%If wanting to insert horizontal lines
% reffline(0, strain(3));
% reffline(0, strain(1));
% reffline(0, strain);
% vline(mStartMeasuringZone, 'r', 'Measurement zone');
% vline(mEndMeasuringZone, 'r', 'Measurement zone');

%%Exporting to pdf-file
filePathPdfExport=[filepathMAT(1:length(filepathMAT)-4) '_analysis.pdf'];
print (1, '-dpdf', filePathPdfExport);

```

```

clear filepath filefolder Data_Path;

% %%Looping
% onceMore=input('Once more? (1/0)[1]');
%     if isempty(onceMore)
%         onceMore=1;
%     end
% end

%%WHAT FOLLOWS HAS BEEN REMOVED FROM THE CODE, BUT IS LEFT HERE FOR LATER REFERENCE
% % %%The amplitude analysis is not needed because of column 5 analysis. I
% % %%leave it for later reference if it should be needed later on.
% %
% % t=0:1/samplingFrequency:samplingTime-1/samplingFrequency;
% % t=t(:); % To make t a column vector
% %
% % clear s0 Ahat_def Theta_def Omega_def RMS_def;
% %
% % analTime=5; %seconds
% % % s0=(MEASUREMENTS(samplingFrequency*1000:samplingFrequency*1030,5)-mean
(MEASUREMENTS(samplingFrequency*1000:samplingFrequency*1030,5)))';
% % s0=(MEASUREMENTS(3000:4000,5)-mean(MEASUREMENTS(3000:4000,5)))';
% %
% % [Ahat_def,Theta_def,Omega_def,RMS_def]=sinefit(s0,1/actualFrequency,0,1
/samplingFrequency);
% % title('Deformation (actuator)','Interpreter','latex');
% % set(get(gca,'YLabel'),'String','Relative position (um)','Interpreter','latex');
% % set(get(gca,'XLabel'),'String','Time (s)','Interpreter','latex');
% % totalDeformation=2000*Ahat_def;
% % orient('landscape');
% % title([regexpttranslate('escape', filepath) '_amplitude']);
% % filepath_amp=[y' filepath(1:length(filepath)-5) '_amplitude.tdms'];
% % print (1, '-dpdf', strrep(filepath_amp, '.tdms', '.pdf'));
% % close
%
%
% f1 = figure(1);
% set(f1, ...
%     'Position', [0 0 screen_size(3) screen_size(4) ], ...
%     'Name', 'Rock Hard Deformations - Post processing');
%
% % %%Deformation (actuator)
% % clear s0 Ahat Theta Omega RMS;
% % s0=(MEASUREMENTS(:,5)-mean(MEASUREMENTS(:,5)))';
% % subplot(4,2,5);
% % %sinefit(raw_data, period on the original signal (1/10 if 10Hz), start-time (0),
time-period of sampling( if 200Hz-> 1/200, if 1000Hz-> 1/1000))
% % [Ahat_def,Theta_def,Omega_def,RMS_def]=sinefit(s0,1/actualFrequency,0,1
/samplingFrequency);
% % title('Deformation (actuator)','Interpreter','latex');
% % set(get(gca,'YLabel'),'String','Relative position (um)','Interpreter','latex');
% % set(get(gca,'XLabel'),'String','Time (s)','Interpreter','latex');

```

```

%
%
% _____          _____          _____          _____
% / \  \ / \          / \  \ / \          / \  \ / \          / \  \ / \
% \ /  / \ / \        \ /  / \ / \        \ /  / \ / \        \ /  / \ / \
% \ /  / \ / \        \ /  / \ / \        \ /  / \ / \        \ /  / \ / \
% \ /  / \ / \        \ /  / \ / \        \ /  / \ / \        \ /  / \ / \
% \ /  / \ / \        \ /  / \ / \        \ /  / \ / \        \ /  / \ / \
% \ /  / \ / \        \ /  / \ / \        \ /  / \ / \        \ /  / \ / \
% \ /  / \ / \        \ /  / \ / \        \ /  / \ / \        \ /  / \ / \
% \ /  / \ / \        \ /  / \ / \        \ /  / \ / \        \ /  / \ / \
% \ /  / \ / \        \ /  / \ / \        \ /  / \ / \        \ /  / \ / \
% \ /  / \ / \        \ /  / \ / \        \ /  / \ / \        \ /  / \ / \
%
%%%%%%%%%%%%%%%%%%%%%%%%%%%%%%%%%%%%%%%%%%%%%%%%%%%%%%%%%%%%%%%%%%%%%%%%
%%%%%%%%%%%%%%%%%%%%%%%%%%%%%%%%%%%%%%%%%%%%%%%%%%%%%%%%%%%%%%%%%%%%%%%%
%%%%%%%%%%%%%%%%%%%%%%%%%%%%%%%%%%%%%%%%%%%%%%%%%%%%%%%%%%%%%%%%%%%%%%%%
%                          Trygve Westlye Fintland          %
%%%%%%%%%%%%%%%%%%%%%%%%%%%%%%%%%%%%%%%%%%%%%%%%%%%%%%%%%%%%%%%%%%%%%%%%
%                          Sintef Petroleum Research and NTNU    %
%%%%%%%%%%%%%%%%%%%%%%%%%%%%%%%%%%%%%%%%%%%%%%%%%%%%%%%%%%%%%%%%%%%%%%%%
%                          2011                                  %
%%%%%%%%%%%%%%%%%%%%%%%%%%%%%%%%%%%%%%%%%%%%%%%%%%%%%%%%%%%%%%%%%%%%%%%%
%%%%%%%%%%%%%%%%%%%%%%%%%%%%%%%%%%%%%%%%%%%%%%%%%%%%%%%%%%%%%%%%%%%%%%%%
%                          Rock Hard Deformations              %
%                          Post processing of data              %
%                          Step 2                               %
%%%%%%%%%%%%%%%%%%%%%%%%%%%%%%%%%%%%%%%%%%%%%%%%%%%%%%%%%%%%%%%%%%%%%%%%
%%%%%%%%%%%%%%%%%%%%%%%%%%%%%%%%%%%%%%%%%%%%%%%%%%%%%%%%%%%%%%%%%%%%%%%%
%
% This script (rh2phase.m) will ask for a '.mat' file if the variables
% filepath and filefolder are not present. If 'filepath' variable exists,
% it will run the script on the value given. It will then select the
% measurement zone based on mStart (which is given in percent [1-100]) and
% mEnd [2-100]. If mStart and/or mEnd is not provided, default values of 70
% and 100 are assumed.
%
% If running 'rh2phase.m' through 'rh2all.m' the mStart and mEnd are
% extracted from the '.csv' file present in measurement folder (it is
% generated with default values if not present).
%
% Based on the measurement zone the stress, strain, Young's modulus, and
% perturbation values are calculated and displayed. All values are
% 'peak-to-peak' even though in the raw code some may appear with names
% such as 'amplitude'.
%
% The values calculated are stored in the source file (.mat file). A graph
% showing the signals relative to their maximum values (and the measurement
% zone) is displayed and saved with the extension '_analysis.pdf'
%
% Input: '.mat' file (or 'filepath' and 'filefolder')
% Output: '.mat' file and '_analysis.pdf' file
%
% The file should be run in the same folder as where the .tdms files are
% located.
%
% Use rh2all.m to run on all .tdms files in folder (after date of creation)
% The script should only be used on files containing BOTH magnitude AND
% phase measurements. The script may not be completely backwards
% compatible, but should support measurement series from '4TestSeries'.
%
%
%

```

```

close all;
screen_size = get(0, 'ScreenSize');

filefolder=pwd;
if exist('filepathMAT','var')==0
    [filepathMAT,filefolder]=uigetfile({'*.mat'},'Select the .mat file');
end
Data_PathMAT=fullfile(filefolder,filepathMAT);
load(Data_PathMAT);

%System parameters
    %Scitec lock in settings
        %fullScaleAmplitude=30*10^-3;    %[V]
    %Force parameters
        %fullScaleForce=0.5;            %[V]    from lock in amplifier (upper right ↙
corner)
%    NewtonPerVolt=10;                %[N/V]    from charge meter <-- to rh1
    %Strain parameters
        %fullScaleStrainGauge=1*10^-6;    %[V]    from lock in amplifier (upper right ↙
corner)
%    strainGaugeFactor=2.1;            %[]    from strain gauge specifications <-- ↙
to rh1
%    strainGaugeSupplyVoltage=10;    %[V]    to the Wheatstone bridge <-- to rh1
    %Sample parameters
%    crossArea=0.0005076;            %[m^2] <-- to rh1
%    lengthOfSample=50.7*10^-3;    %[m]<-- to rh1
        %Aluref03    =    0,0005070;
        %Peek03     =    0,0005076;
        %ML318_01_01=    0,0005062;
        %Steel      =    0,0005075;
    %Actuator-settings

%%Read the TDMS-file
%The TDMS FILE CONTAINS 5 COLOUMNS
% 1 column: phase Force
% 2 column: phase Strain
% 3 column: Strain measurement - Lock in X - "Green channel"
% 4 column: Force measurement - Lock in Y - "Brown channel"
% 5 column: Strain measurement - Scitec lock in - "Actuator sensor"

% %%Sampling details
%    samplingFrequency=input('Sampling frequency (Hz)[256Hz]: '); %Hz
%    if isempty(samplingFrequency)
%        samplingFrequency=256;
%    end
%
%    samplingTime=length(MEASUREMENTS(:,3))/samplingFrequency;
%    samplingTime=input('Sampling time (s)[7200s]: ');    %seconds (s)
%    if isempty(samplingTime)
%        samplingTime=7200;
%    end
%    actualFrequency=input('Actual frequency (Hz)[79Hz]: '); %%%%%%%%%%%AS GIVEN ON ↙
WAVE GENERATOR!!
%    if isempty(actualFrequency)

```

```

%         actualFrequency=79;
%     end

%%Measuring details
    mStart=70;%input('Calculation starting from (percent)[25%]: '); %Hz
    if isempty(mStart)
        mStart=70;
    end

    mEnd=100;%input('Calculation ending at (percent)[100%]: '); %Hz
    if isempty(mEnd)
        mEnd=100;
    end

%%Making ready first figure.
f1 = figure(1);
set(f1, ...
    'Position', [0 0 screen_size(3) screen_size(4) ], ...
    'Name', 'Rock Hard Deformations - Post processing - Figure 1');
%     subplot(4,2,1:2); plot(MEASUREMENTS); legend(MEASUREMENTS_LEGEND), title
(regexprtranslate('escape', filepathMAT));
%     subplot(4,2,8); hist(ERRORLOG); title('Error log','Interpreter','latex');
orient('landscape');

%%Setting window for analysis
totalLengthOfMeasurements=length(MEASUREMENTS(:,4));
mStartMeasuringZone=floor(mStart/100*totalLengthOfMeasurements);
mEndMeasuringZone=floor(mEnd/100*totalLengthOfMeasurements);

%%Setting column factors of interpretation
firstColumnFactor=18;

secondColumnFactor=18;

thirdColumnFactor=16/3*2*sqrt(2)*fullScaleStrainGauge/(2.1
*strainGaugeSupplyVoltage*10); %<---Strain
%clear fullScaleStrainGauge strainGaugeSupplyVoltage;
fourthColumnFactor=2*sqrt(2)*NewtonPerVolt/10*fullScaleForce;
%<---Force
%clear NewtonPerVolt fullScaleForce;
fifthColumnFactor=2*sqrt(2)*fullScaleAmplitude*1500;
%<---Deformation

%%Making ready matrix for final measurements
timeForceStrainAmplitude=zeros((mEndMeasuringZone-mStartMeasuringZone+1),4);
timeForceStrainAmplitude(:,1)=mStartMeasuringZone/samplingFrequency:
1/samplingFrequency:mEndMeasuringZone/samplingFrequency;

%%Converting into respective units and extracting max, avg and min values
firstColumn=MEASUREMENTS(mStartMeasuringZone:mEndMeasuringZone,1)
*firstColumnFactor;
forcePhase(2)=mean(firstColumn);
forcePhase(1)=min(firstColumn);
forcePhase(3)=max(firstColumn);

```



```

timeForceStrainAmplitude(:,6)=firstColumn;
clear firstColumn firstColumnFactor;

secondColumn=MEASUREMENTS(mStartMeasuringZone:mEndMeasuringZone,2) ↙
*secondColumnFactor;
strainPhase(2)=mean(secondColumn);
strainPhase(1)=min(secondColumn);
strainPhase(3)=max(secondColumn);
timeForceStrainAmplitude(:,5)=secondColumn;
clear secondColumn secondColumnFactor;

thirdColumn=MEASUREMENTS(mStartMeasuringZone:mEndMeasuringZone,3) ↙
*thirdColumnFactor;    %<--- Converting voltage to strain.
strain(2)=mean(thirdColumn);
strain(1)=min(thirdColumn);
strain(3)=max(thirdColumn);
timeForceStrainAmplitude(:,3)=thirdColumn;
clear thirdColumn thirdColumnFactor;

fourthColumn=MEASUREMENTS(mStartMeasuringZone:mEndMeasuringZone,4) ↙
*fourthColumnFactor;  %<--- Converting voltage to Newton.
force(2)=mean(fourthColumn);
force(1)=min(fourthColumn);
force(3)=max(fourthColumn);
timeForceStrainAmplitude(:,2)=fourthColumn;
clear fourthColumn fourthColumnFactor;

fifthColumn=MEASUREMENTS(mStartMeasuringZone:mEndMeasuringZone,5) ↙
*fifthColumnFactor;   %<--- Converting voltage to m.
amplitude(2)=mean(fifthColumn);
amplitude(1)=min(fifthColumn);
amplitude(3)=max(fifthColumn);
timeForceStrainAmplitude(:,4)=fifthColumn;
clear fifthColumn fifthColumnFactor;

youngsStrain(2)=force(2)/crossArea/strain(2)*10^-9;
youngsStrain(3)=force(3)/crossArea/strain(1)*10^-9;
youngsStrain(1)=force(1)/crossArea/strain(3)*10^-9;

youngsAmplitude(2)=force(2)/crossArea/(amplitude(2)/lengthOfSample);
youngsAmplitude(3)=force(3)/crossArea/(amplitude(1)/lengthOfSample);
youngsAmplitude(1)=force(1)/crossArea/(amplitude(3)/lengthOfSample);

%%Saving the .mat file
%filepath_mat=[filepath(1:length(filepath)-5) '.mat'];
save(filepathMAT);

%%Plotting results
% Create textbox [xPositionOnLowerLeft yPositionOnLowerLeft xWidth yHeight]
a1=annotation('textbox',...
[0.372 0.30 0.26 0.19],...
'Interpreter','latex',...
'String',{...
['Deformation ($\rm{nm}_{pp}$): ' num2str(amplitude(2))]}...

```

```

    ['Youngs Modulus SG(GPa): ' num2str(youngsStrain(2))] ['(' num2str(youngsStrain(1))
' to ' num2str(youngsStrain(3)) ')']...
    ['Youngs Modulus AMP(GPa): ' num2str(youngsAmplitude(2))] ['(' num2str
(youngsAmplitude(1)) ' to ' num2str(youngsAmplitude(3)) ')']...
    },...
    'FitBoxToText','off');

    set(a1, 'FontSize', 16, 'HorizontalAlignment', 'center', 'VerticalAlignment',
'middle', 'BackgroundColor', [1 1 0.9]);

    a2=annotation('textbox',...
    [0.64 0.30 0.26 0.19],...
    'Interpreter','latex',...
    'String',{...
    % 'Young's modulus:' num2str((Ahat_force/0.000507)/(Ahat_def*10^(-6)/0.05084)
*1/10^9) ...
    % 'Youngs Modulus: ' num2str((brownChannel/0.000507)/strain) ...
    ['Strain: ' num2str(strain(2))] ['(' num2str(strain(1)) ' to ' num2str(strain(3))
')'] ...
    ['Force (N): ' num2str(force(2))] ['(' num2str(force(1)) ' to ' num2str(force(3))
')']...
    },...
    'FitBoxToText','off');
    set(a2, 'FontSize', 14, 'HorizontalAlignment', 'center', 'VerticalAlignment',
'middle', 'BackgroundColor', [1 1 0.9]);

%%Coarsing the Measurements before plotting
if totalLengthOfMeasurements<1000
    coarseStep=1;
else
    coarseStep=floor(totalLengthOfMeasurements/1000);
end

%%Plotting the relative amplitudial behaviour
hold on;
    plotTimeVector=0:1/samplingFrequency*coarseStep:(totalLengthOfMeasurements-1)
/samplingFrequency;
    plot(plotTimeVector, MEASUREMENTS(1:coarseStep:totalLengthOfMeasurements,3)/max
(MEASUREMENTS(:,3)), 'g'); %<-- Strain
    plot(plotTimeVector, MEASUREMENTS(1:coarseStep:totalLengthOfMeasurements,4)/max
(MEASUREMENTS(:,4)), 'r'); %<-- Force
    plot(plotTimeVector, MEASUREMENTS(1:coarseStep:totalLengthOfMeasurements,5)/max
(MEASUREMENTS(:,5)), 'b'); %<-- Amplitude
    title([regexpttranslate('escape', filepathMAT) 'STRAIN']);
    legend('Strain', 'Force', 'Perturbation (P-P)');
    vline(mStart/100*totalLengthOfMeasurements/samplingFrequency, 'r', 'Measurement
zone');
    vline(mEnd/100*totalLengthOfMeasurements/samplingFrequency, 'r', 'Measurement
zone');
    hold off;

%%If wanting to insert horizontal lines
% refline(0, strain(3));
% refline(0, strain(1));
% refline(0, strain);

```

```

    % vline(mStartMeasuringZone, 'r', 'Measurement zone');
    % vline(mEndMeasuringZone, 'r', 'Measurement zone');
filepathMAT
%%Exporting to pdf-file
    filePathPdfExport=[filepathMAT(1:length(filepathMAT)-4) '_analysis.pdf'];
    print (1, '-dpdf', filePathPdfExport);

% %%Looping
% onceMore=input('Once more? (1/0)[1]');
%     if isempty(onceMore)
%         onceMore=1;
%     end
% end

%%WHAT FOLLOWS HAS BEEN REMOVED FROM THE CODE, BUT IS LEFT HERE FOR LATER REFERENCE
% % %%The amplitude analysis is not needed because of column 5 analysis. I
% % %%leave it for later reference if it should be needed later on.
% %
% % t=0:1/samplingFrequency:samplingTime-1/samplingFrequency;
% % t=t(:); % To make t a column vector
% %
% % clear s0 Ahat_def Theta_def Omega_def RMS_def;
% %
% % analTime=5; %seconds
% % % s0=(MEASUREMENTS(samplingFrequency*1000:samplingFrequency*1030,5)-mean
(MEASUREMENTS(samplingFrequency*1000:samplingFrequency*1030,5)))';
% % s0=(MEASUREMENTS(3000:4000,5)-mean(MEASUREMENTS(3000:4000,5)))';
% %
% % [Ahat_def,Theta_def,Omega_def,RMS_def]=sinefit(s0,1/actualFrequency,0,1
/samplingFrequency);
% % title('Deformation (actuator)','Interpreter','latex');
% % set(get(gca,'YLabel'),'String','Relative position (um)','Interpreter','latex');
% % set(get(gca,'XLabel'),'String','Time (s)','Interpreter','latex');
% % totalDeformation=2000*Ahat_def;
% % orient('landscape');
% % title([regexprtranslate('escape', filepath) '_amplitude']);
% % filepath_amp=['y' filepath(1:length(filepath)-5) '_amplitude.tdms'];
% % print (1, '-dpdf', strrep(filepath_amp, '.tdms', '.pdf'));
% % close
%
%
% f1 = figure(1);
% set(f1, ...
%     'Position', [0 0 screen_size(3) screen_size(4) ], ...
%     'Name', 'Rock Hard Deformations - Post processing');
%
% % %%Deformation (actuator)
% % clear s0 Ahat Theta Omega RMS;
% % s0=(MEASUREMENTS(:,5)-mean(MEASUREMENTS(:,5)))';
% % subplot(4,2,5);
% % %sinefit(raw_data, period on the original signal (1/10 if 10Hz), start-time (0),
time-period of sampling( if 200Hz-> 1/200, if 1000Hz-> 1/1000))
% % [Ahat_def,Theta_def,Omega_def,RMS_def]=sinefit(s0,1/actualFrequency,0,1

```

```

%
%
% _____
% / \  _ \      / \  _ \      / \  _ \      / \  _ \
% \ \ / L \    / \ / \ / \  / \ / \ / \  / \ / \ / \
% \ \ / \ / \  / \ / \ / \  / \ / \ / \  / \ / \ / \
% \ \ / \ / \  / \ / \ / \  / \ / \ / \  / \ / \ / \
% \ \ / \ / \  / \ / \ / \  / \ / \ / \  / \ / \ / \
% \ \ / \ / \  / \ / \ / \  / \ / \ / \  / \ / \ / \
%
%
%%%%%%%%%%%%%%%%%%%%%%%%%%%%%%%%%%%%%%%%%%%%%%%%%%%%%%%%%%%%%%%%%%%%%%%%
%%%%%%%%%%%%%%%%%%%%%%%%%%%%%%%%%%%%%%%%%%%%%%%%%%%%%%%%%%%%%%%%%%%%%%%%
%%%%%%%%%%%%%%%%%%%%%%%%%%%%%%%%%%%%%%%%%%%%%%%%%%%%%%%%%%%%%%%%%%%%%%%%
% Trygve Westlye Fintland
% Sintef Petroleum Research and NTNU
%%%%%%%%%%%%%%%%%%%%%%%%%%%%%%%%%%%%%%%%%%%%%%%%%%%%%%%%%%%%%%%%%%%%%%%%
%%%%%%%%%%%%%%%%%%%%%%%%%%%%%%%%%%%%%%%%%%%%%%%%%%%%%%%%%%%%%%%%%%%%%%%%
%%%%%%%%%%%%%%%%%%%%%%%%%%%%%%%%%%%%%%%%%%%%%%%%%%%%%%%%%%%%%%%%%%%%%%%%
% Rock Hard Deformations
% Post processing of data
% Step 2
%%%%%%%%%%%%%%%%%%%%%%%%%%%%%%%%%%%%%%%%%%%%%%%%%%%%%%%%%%%%%%%%%%%%%%%%
%%%%%%%%%%%%%%%%%%%%%%%%%%%%%%%%%%%%%%%%%%%%%%%%%%%%%%%%%%%%%%%%%%%%%%%%
%%%%%%%%%%%%%%%%%%%%%%%%%%%%%%%%%%%%%%%%%%%%%%%%%%%%%%%%%%%%%%%%%%%%%%%%
%
% Please make sure that you run post processing with the right settings!
% At least you need to make the following adjustments:
% In code:
% - full scale of the lock in amplifiers and the charge meter (V and N/V)
% - dimentions of sample (m and m^2)
% At runtime:
% - sampling frequency (Hz)
% - actual frequency (Hz)
% - range for measurement (given i percent!)
%
% This file runs the rh2() over all frequencies in the frequency grid.
% The measurement zones are specified in the 'mStartEndList.csv' that
% should be present in the measurements folder. If not, standard values are
% assumed.
%
close all;
clear;
listOfMATFiles=dir(['RockHard_' '*.mat']);
% If measurements go overnight one may need sorting on time of creation.
[unused, order] = sort([listOfMATFiles(:).datenum]);
listOfMATFiles= listOfMATFiles(order);

%Not in use!
% datenumlist=listOfMATFiles.datenum;
% [dummy, index] = sort(datenumlist);
% listOfMATFiles=listOfMATFiles(index);
%listOfMATFiles(1).name

totalForce=[0 0 0];
totalStrain=[0 0 0];
totalAmplitude=[0 0 0];
totalYoungsAmplitude=[0 0 0];

```

```
totalYoungsStrain=[0 0 0];

%%Defining the measurement range from .csv file
if exist('mStartEndList.csv', 'file')
    %Import measurement range file
    importfile('mStartEndList.csv');
else
    %If the file does not exist - create it with standard values of 70% and 100% for
    all present frequencies!
    a=dir('RockHard*.mat');
    x=zeros(length(a),3);
    for teller=1:length(a)
        filepath=a(teller).name;
        x(teller,1)=str2num(filepath(findstr(filepath, 'mVpp_')+5:findstr(filepath,
'Hz_')-1));
        x(teller,2)=70;
        x(teller,3)=100;
    end
    x=x';
    %Write it to file
    fid=fopen('mStartEndList.csv', 'w+');
    fprintf(fid, '%6.2f; %12.2f; %12.2f;\n', x);
    fclose(fid);
    clear x fid;
    importfile('mStartEndList.csv');
end

%%
%frequencyGrid=[10 19 29 39 49 59 69 79 89 99 109 129 139 149 159 179 209 245 309 409
509 609 709 809 909 1009 1509 2009 3009 4009 5009 6009 7009 8009];
%sort(listOfMATFiles.name)

%%Number of files are given to output
numberOfFiles=length(listOfMATFiles)

%Reorganize list
for counter1=1:numberOfFiles-1
    filepathMAT=listOfMATFiles(counter1,1).name;
    load([pwd '\ ' filepathMAT], 'MEASUREMENTS', 'lengthOfSample', 'crossArea',
'strainGaugeFactor', 'openLoop', 'NewtonPerVolt', 'strainGaugeSupplyVoltage',
'fullScaleStrainGauge', 'fullScaleForce', 'fullScaleAmplitude', 'samplingFrequency',
'filepath');

    if exist('mStartEndList.csv', 'file')
        actualFrequency=mStartEndList(counter1,1);
        mStart=mStartEndList(counter1,2);
        mEnd=mStartEndList(counter1,3);

    else
        mStart=70;
        mEnd=100;
        frequency=frequencyGrid(counter1);
    end
end
```

```
rh2();  
close all;
```

```
end  
clear counter1 mStart mEnd frequency;
```

```

%
%
%   _ _ _ _ _
%  / \  \  \          / \  \          / \  \          / \  \
%  \ \  \L\ \        / \  \  \  \    / \  \  \  \    / \  \  \
%  \ \  \ , / \      / \  \  \  \  \  / \  \  \  \  / \  \  \
%  \ \  \ \ \ \ \   / \  \L\ \ \ \ \ \ \ \ \ \ \ \ \ \ \ \ \ \
%  \ \  \ \ \ \ \ \ \ \ \ \ \ \ \ \ \ \ \ \ \ \ \ \ \ \ \ \ \ \ \ \
%  \ \  \ \ \ \ \ \ \ \ \ \ \ \ \ \ \ \ \ \ \ \ \ \ \ \ \ \ \ \ \ \
%  \ \  \ \ \ \ \ \ \ \ \ \ \ \ \ \ \ \ \ \ \ \ \ \ \ \ \ \ \ \ \ \
%

```

```

%%%%%%%%%%%%%%%%%%%%%%%%%%%%%%%%%%%%%%%%%%%%%%%%%%%%%%%%%%%%%%%%%%%%%%%%
%%%%%%%%%%%%%%%%%%%%%%%%%%%%%%%%%%%%%%%%%%%%%%%%%%%%%%%%%%%%%%%%%%%%%%%%
%%%%%%%%%%%%%%%%%%%%%%%%%%%%%%%%%%%%%%%%%%%%%%%%%%%%%%%%%%%%%%%%%%%%%%%%
Trygve Westlye Fintland
%%%%%%%%%%%%%%%%%%%%%%%%%%%%%%%%%%%%%%%%%%%%%%%%%%%%%%%%%%%%%%%%%%%%%%%%
Sintef Petroleum Research and NTNU
%%%%%%%%%%%%%%%%%%%%%%%%%%%%%%%%%%%%%%%%%%%%%%%%%%%%%%%%%%%%%%%%%%%%%%%%
2011
%%%%%%%%%%%%%%%%%%%%%%%%%%%%%%%%%%%%%%%%%%%%%%%%%%%%%%%%%%%%%%%%%%%%%%%%
%%%%%%%%%%%%%%%%%%%%%%%%%%%%%%%%%%%%%%%%%%%%%%%%%%%%%%%%%%%%%%%%%%%%%%%%
Rock Hard Deformations
Post processing of data
Step 3
%%%%%%%%%%%%%%%%%%%%%%%%%%%%%%%%%%%%%%%%%%%%%%%%%%%%%%%%%%%%%%%%%%%%%%%%
%%%%%%%%%%%%%%%%%%%%%%%%%%%%%%%%%%%%%%%%%%%%%%%%%%%%%%%%%%%%%%%%%%%%%%%%
%%%%%%%%%%%%%%%%%%%%%%%%%%%%%%%%%%%%%%%%%%%%%%%%%%%%%%%%%%%%%%%%%%%%%%%%
%

```

```

%+-NB!-----+
% | THIS SCRIPT HAS BEEN REPLACED BY 'rh3phase.m' FROM '4TestSeries'. |
% | IT IS KEPT MAINLY FOR BACKWARDS COMPABILITY IN '3TestSeries'! |
% | ANY NEW MEASUREMENT INTERPRETATION SHOULD BE DONE BY: |
% | 'rh3phase.m' |
% +-----+
%

```

```

% Collects the .mat files and displays the data. The plotting depends
% on the frequency grid as the x-axis. The grid goes: 10Hz -> 8009Hz with
% 34 steps of quazilogarithmic distribution.
%
% The plots display the stress, the strain and the two Young's moduli as
% sub-plots. The amplitude of the actuator in itself is not plotted but is
% used for calculations. The output goes to the file: 'summary.pdf'.
%
% Input: 'RockHard*.mat'
% Output: 'summary.pdf', variables left in workspace
%
% Pre assumptions: Calculations have been done in previous files. This is
% collect and display. The x-values are all frequencies from either the
% .csv file or the frequency grid. If # of .mat files is smaller than
% frequency grid, it will cut the higher frequencies.
%

```

```

listOfMATFiles=dir('RockHard*.mat');
%[unused, order] = sort([listOfMATFiles(:).datenum]);
%listOfMATFiles = listOfMATFiles(order);
% datenumlist=listOfMATFiles.datenum;
% [dummy, index] = sort(datenumlist);
% listOfMATFiles=listOfMATFiles(index);
%listOfMATFiles(1).name

```

```

%easy(listOfMATFiles(1).name, 256, 7200, 79);
mLength=length(listOfMATFiles);
totalForce=zeros(3,mLength);
totalStrain=zeros(3,mLength);
totalAmplitude=zeros(3,mLength);
totalYoungsAmplitude=zeros(3,mLength);
totalYoungsStrain=zeros(3,mLength);
totalFrequency=zeros(1, mLength);
%crossArea=5.07E-4;

close all

if exist('mStartEndList.csv', 'file')
    importfile('mStartEndList.csv');
    xValues=mStartEndList(:,1)
    xValues=xValues'
else
frequencyGrid=[10 19 29 39 49 59 69 79 89 99 109 129 139 149 159 179 209 245 309 409
509 609 709 809 909 1009 1509 2009 3009 4009 5009 6009 7009 8009];
%sort(listOfMATFiles.name)
xValues=frequencyGrid(1:mLength);
end

%Reorganize list
for counter2=1:mLength

    name2=listOfMATFiles(counter2, 1).name;
    frequency=name2(strfind(name2, 'mVpp_')+5:strfind(name2, 'Hz_')-1);

    load(name2, 'force', 'strain', 'crossArea', 'amplitude', 'youngsAmplitude',
'youngsStrain');
    %totalFrequency(1, counter2)=frequency;
    totalForce(:,counter2)=force;
    totalStrain(:,counter2)=strain(:);
    totalAmplitude(:,counter2)=amplitude(:);
    totalYoungsAmplitude(:,counter2)=youngsAmplitude;
    totalYoungsStrain(:,counter2)=youngsStrain;

%    totalYoungsStrain(2, i)=force(2,i)/strain(2,i)/crossArea/10^9;
%    totalYoungsStrain(1, i)=totalForce(1,i)/totalStrain(3,i)/crossArea/10^9;
%    totalYoungsStrain(3, i)=totalForce(3,i)/totalStrain(1,i)/crossArea/10^9;
%    totalYoungsStrain(1, i)=totalYoungsStrain(1, i)-totalYoung(i);
%    totalYoungsStrain(3, i)=totalYoungsStrain(3, i)-totalYoung(i);
    %easy(listOfMATFiles(i).name, 256, 7200, 79);
end
%totalAll=struct(frequency, totalForce, totalStrain, totalYoungsStrain, totalAmplitude,
totalYoungsAmplitude);

subplot(3,2,1);
hold on;

errorbar(xValues, totalForce(2,:), totalForce(1,:)-totalForce(2,:), totalForce(3,:)-
totalForce(2,:));%, totalMaxForce-totalForce);
title('Average force', 'Interpreter', 'latex');
set(get(gca, 'YLabel'), 'String', 'Force', 'Interpreter', 'latex');

```



```
set(get(gca, 'XLabel'), 'String', '$\rm{mV_{pp}}$ or f\rm{(Hz)}$', 'Interpreter', 'latex');

subplot(3,2,2);
errorbar(xValues, totalStrain(2,:), totalStrain(1,:)-totalStrain(2,:), totalStrain(3,:) -
totalStrain(2,:));
title('Average strain', 'Interpreter', 'latex');
set(get(gca, 'YLabel'), 'String', 'Strain', 'Interpreter', 'latex');
set(get(gca, 'XLabel'), 'String', '$\rm{mV_{pp}}$ or $f\rm{(Hz)}$', 'Interpreter', 'latex');

subplot(3,2,3:4);
errorbar(xValues, totalYoungsAmplitude(2,:), totalYoungsAmplitude(1,:)-
totalYoungsAmplitude(2,:), totalYoungsAmplitude(3,:)-totalYoungsAmplitude(2,:));
hold off;
title('Average Youngs module amplitude', 'Interpreter', 'latex');
set(get(gca, 'YLabel'), 'String', 'Youngs module indirect (Act)', 'Interpreter', 'latex');
axis([min(xValues)-10 max(xValues)+10 0 max(totalYoungsAmplitude(2,:))+2]);
set(get(gca, 'XLabel'), 'String', '$\rm{mV_{pp}}$ or $f\rm{(Hz)}$', 'Interpreter', 'latex');

subplot(3,2,5:6);
errorbar(xValues, totalYoungsStrain(2,:), totalYoungsStrain(1,:)-totalYoungsStrain
(2,:), totalYoungsStrain(3,:)-totalYoungsStrain(2,:));
hold off;
title('Average Youngs module strain gauge', 'Interpreter', 'latex');
set(get(gca, 'YLabel'), 'String', 'Youngs module direct (SG)', 'Interpreter', 'latex');
axis([min(xValues)-10 max(xValues)+10 0 max(totalYoungsStrain(2,:))+10]);
set(get(gca, 'XLabel'), 'String', '$\rm{mV_{pp}}$ or $f\rm{(Hz)}$', 'Interpreter', 'latex');
% set(get(h, 'Parent'), 'XScale', 'log');

screen_size = get(0, 'ScreenSize');
print (1, '-dpdf', 'summary.pdf');

% files = dir(...);
% filenames = {files.name};
% [dummy, index] = sort(filenames);
% % re-index the files array:
% files = files(index);
```

```

%
% _____
% \  _  \   \          / \  \          / \  \          / \  \
% \  \  \L\ \    ___  / \  \  \  / \  \  \  \  / \  \  \  \
% \  \ , / \ / \  \ / \  \  \  \ , < / \  \  \ / \  \  \  \
% \  \ \ \ \ \ \  \L\ \ \  \  \  \  \  \  \  \  \ \ \  \  \  \
% \  \ \  \  \  \  \  \  \  \  \  \  \  \  \  \  \  \  \  \
% \  \ \ /  / \  \ /  \  \ \ / \ / \  \ \ / \ / \  \ \ / \ /
%
%%%%%%%%%%%%%%%%%%%%%%%%%%%%%%%%%%%%%%%%%%%%%%%%%%%%%%%%%%%%%%%%%%%%%%%%
%%%%%%%%%%%%%%%%%%%%%%%%%%%%%%%%%%%%%%%%%%%%%%%%%%%%%%%%%%%%%%%%%%%%%%%%
%%%%%%%%%%%%%%%%%%%%%%%%%%%%%%%%%%%%%%%%%%%%%%%%%%%%%%%%%%%%%%%%%%%%%%%%
%                               Trygve Westlye Fintland          %
%%%%%%%%%%%%%%%%%%%%%%%%%%%%%%%%%%%%%%%%%%%%%%%%%%%%%%%%%%%%%%%%%%%%%%%%
%           Sintef Petroleum Research and NTNU                    %
%%%%%%%%%%%%%%%%%%%%%%%%%%%%%%%%%%%%%%%%%%%%%%%%%%%%%%%%%%%%%%%%%%%%%%%%
%                                 2011                             %
%%%%%%%%%%%%%%%%%%%%%%%%%%%%%%%%%%%%%%%%%%%%%%%%%%%%%%%%%%%%%%%%%%%%%%%%
%%%%%%%%%%%%%%%%%%%%%%%%%%%%%%%%%%%%%%%%%%%%%%%%%%%%%%%%%%%%%%%%%%%%%%%%
%                               Rock Hard Deformations            %
%                               Post processing of data            %
%                               Step 3                             %
%%%%%%%%%%%%%%%%%%%%%%%%%%%%%%%%%%%%%%%%%%%%%%%%%%%%%%%%%%%%%%%%%%%%%%%%
%%%%%%%%%%%%%%%%%%%%%%%%%%%%%%%%%%%%%%%%%%%%%%%%%%%%%%%%%%%%%%%%%%%%%%%%
%
% Collects the .mat files and displays the data. Extracts the x values from
% the .csv file. If the file is not present the x grid goes: 10Hz -> 8009Hz
% with 34 steps of quazilogarithmic distribution.
%
% The plots display the stress, the strain and the two Young's moduli as
% sub-plots. The perturbation of the actuator in itself is not plotted but
% is used for calculations. The output goes to the file: 'summary.pdf', but
% is not saved.
%
% Input: 'RockHard_*.mat'
% Output: 'summary.pdf', variables left in workspace
%
% Pre assumptions: Calculations have been done in previous files. This is
% collect and display. This file must run before rh4*.
%

listOfTDMSFiles=dir('RockHard*.mat');
%[unused, order] = sort([listOfTDMSFiles(:).datenum]);
%listOfTDMSFiles = listOfTDMSFiles(order);
% datenumlist=listOfTDMSFiles.datenum;
% [dummy, index] = sort(datenumlist);
% listOfTDMSFiles=listOfTDMSFiles(index);
%listOfTDMSFiles(1).name
%easy(listOfTDMSFiles(1).name, 256, 7200, 79);
mLength=length(listOfTDMSFiles);
totalForce=zeros(3,mLength);
totalStrain=zeros(3,mLength);
totalForcePhase=zeros(3,mLength);
totalStrainPhase=zeros(3,mLength);
totalAmplitude=zeros(3,mLength);
totalYoungsAmplitude=zeros(3,mLength);
totalYoungsStrain=zeros(3,mLength);
totalFrequency=zeros(1, mLength);

```

```

%crossArea=5.07E-4;

close all

if exist('mStartEndList.csv', 'file')
    importfile('mStartEndList.csv');
    xValues=mStartEndList(:,1);
    xValues=xValues';
else
    %This line is kept for backwards compatibility
    frequencyGrid=[10 19 29 39 49 59 69 79 89 99 109 129 139 149 159 179 209 245 309 409
509 609 709 809 909 1009 1509 2009 3009 4009 5009 6009 7009 8009];
    %sort(listOfTDMSFiles.name)
    xValues=frequencyGrid(1:mLength);
end

%Reorganize list
for counter2=1:mLength

    name2=listOfTDMSFiles(counter2, 1).name;
    frequency=name2(strfind(name2, 'mVpp_')+5:strfind(name2, 'Hz_')-1);

    load(name2, 'force', 'forcePhase', 'strain', 'strainPhase', 'crossArea',
'amplitude', 'youngsAmplitude', 'youngsStrain');
    %totalFrequency(1, counter2)=frequency;
    totalForce(:,counter2)=force;
    totalForcePhase(:,counter2)=forcePhase;
    totalStrain(:,counter2)=strain(:);
    totalStrainPhase(:,counter2)=strainPhase(:);
    totalAmplitude(:,counter2)=amplitude(:);
    totalYoungsAmplitude(:,counter2)=youngsAmplitude;
    totalYoungsStrain(:,counter2)=youngsStrain;

    %    totalYoungsStrain(2, i)=force(2,i)/strain(2,i)/crossArea/10^9;
    %    totalYoungsStrain(1, i)=totalForce(1,i)/totalStrain(3,i)/crossArea/10^9;
    %    totalYoungsStrain(3, i)=totalForce(3,i)/totalStrain(1,i)/crossArea/10^9;
    %    totalYoungsStrain(1, i)=totalYoungsStrain(1, i)-totalYoung(i);
    %    totalYoungsStrain(3, i)=totalYoungsStrain(3, i)-totalYoung(i);
    %easy(listOfTDMSFiles(i).name, 256, 7200, 79);
end

%totalAll=struct(frequency, totalForce, totalStrain, totalYoungsStrain, totalAmplitude,
totalYoungsAmplitude);

f3 = figure(3);
screen_size = get(0, 'ScreenSize');
set(f3, ...
    'Position', [0 0 screen_size(3)/2 screen_size(4)/2 ], ...
    'Name', 'Rock Hard Deformations - Summary on linear scale');
%    subplot(4,2,1:2); plot(MEASUREMENTS); legend(MEASUREMENTS_LEGEND), title
(regexptranslate('escape', filepathMAT));
%    subplot(4,2,8); hist(ERRORLOG); title('Error log','Interpreter','latex');
orient('landscape');

subplot(3,2,1);

```

```

hold on;

errorbar(xValues, totalForce(2,:), totalForce(1, :)-totalForce(2, :), totalForce(3, :)-
totalForce(2, :));%, totalMaxForce-totalForce);
title('Average force', 'Interpreter', 'latex');
set(get(gca, 'YLabel'), 'String', 'Force', 'Interpreter', 'latex');
set(get(gca, 'XLabel'), 'String', '$\rm{mV_{pp}}$ or $f\rm{(Hz)}$', 'Interpreter', 'latex');

subplot(3,2,2);
errorbar(xValues, totalStrain(2,:), totalStrain(1, :)-totalStrain(2, :), totalStrain(3, :)-
-totalStrain(2, :));
title('Average strain', 'Interpreter', 'latex');
set(get(gca, 'YLabel'), 'String', 'Strain', 'Interpreter', 'latex');
set(get(gca, 'XLabel'), 'String', '$\rm{mV_{pp}}$ or $f\rm{(Hz)}$', 'Interpreter', 'latex');

subplot(3,2,3:4);
errorbar(xValues, totalYoungsAmplitude(2,:), totalYoungsAmplitude(1, :)-
totalYoungsAmplitude(2, :), totalYoungsAmplitude(3, :)-totalYoungsAmplitude(2, :));
hold off;
title('Average Youngs module indirect from perturbation', 'Interpreter', 'latex');
set(get(gca, 'YLabel'), 'String', 'Youngs module', 'Interpreter', 'latex');
axis([min(xValues)-10 max(xValues)+10 0 max(totalYoungsAmplitude(2, :))+2]);
set(get(gca, 'XLabel'), 'String', '$\rm{mV_{pp}}$ or $f\rm{(Hz)}$', 'Interpreter', 'latex');

subplot(3,2,5:6);
errorbar(xValues, totalYoungsStrain(2,:), totalYoungsStrain(1, :)-totalYoungsStrain
(2, :), totalYoungsStrain(3, :)-totalYoungsStrain(2, :));
hold off;
title('Average Youngs module direct from strain gauge', 'Interpreter', 'latex');
set(get(gca, 'YLabel'), 'String', 'Youngs module', 'Interpreter', 'latex');
axis([min(xValues)-10 max(xValues)+10 0 max(totalYoungsStrain(2, :))+10]);
set(get(gca, 'XLabel'), 'String', '$\rm{mV_{pp}}$ or $f\rm{(Hz)}$', 'Interpreter', 'latex');
% set(get(h, 'Parent'), 'XScale', 'log');

print (3, '-dpdf', 'summary.pdf');

%temphead='frequency', 'E-min', 'E-mean', 'E-max', 'Phase-Force-min', 'Phase-Force-
mean', 'Phase-Force-max'
temp1=xValues';
temp2=totalYoungsStrain';
temp3=totalForcePhase';
temp4=totalStrainPhase';
temp5=totalAmplitude';
temptot=[temp1 temp2 temp3 temp4 temp5];
save('Raw_data_xVal_3Young_3ForcePh_3StrPh_3amp.txt', 'temptot', '-ascii', '-double');
%save('Raw_data_xVal_3Young_3ForcePh_3StrPh_3amp.txt', 'xValues', 'totalYoungsStrain',
'totalForcePhase', 'totalStrainPhase', 'totalAmplitude', '-ascii', '-double');
clear temp1 temp2 temp3 temp4 temp5;

% files = dir(...);
% filenames = {files.name};
% [dummy, index] = sort(filenames);
% % re-index the files array:

```

```
% files = files(index);
```



```
[ax, h1, h2]=plotyy(xValues, totalYoungsAmplitude(2,:), xValues, totalAmplitude(2,:),  
'semilogx', 'semilogx');  
  
set(ax(1), 'YColor', 'k', 'YTick', [0:(y1Max/10):y1Max], 'YLim', [0, y1Max]);  
set(ax(2), 'YColor', 'r', 'YTick', [0:(y2Max/10):y2Max], 'YLim', [0,y2Max]);  
xlabel('Frequency (Hz)');  
  
set(get(ax(1), 'Ylabel'), 'String', 'Youngs modulus (GPa)');  
set(get(ax(2), 'Ylabel'), 'String', 'Perturbation (\rm{nm}_{pp})');  
set(h2,'LineStyle','.', 'Color', 'r');  
set(h1, 'LineStyle','-','Marker', '.', 'Color', [0 0.6, 0]);  
  
title({'Frequency and amplitude response in Youngs modulus', pwd});  
legend('Youngs modulus direct (SG)', 'Youngs modulus indirect (Act)', 'Perturbation p-  
p');  
% semilogx(xValues, totalYoungsStrain(2,:), ax(1));  
  
print (4, '-dpdf', 'frequencyDependence');  
% ax(2) = axes('Parent',4,'YTick',[0 5 10 15 20],...  
% 'YAxisLocation','right',...  
% 'YColor',[0.5 0 0],...  
% 'XScale','log',...  
% 'XMinorTick','on',...  
% 'ColorOrder',[0 0.5 0;1 0 0;0 0.75 0.75;0.75 0 0.75;0.75 0.75 0;0.25 0.25 0.25;0  
0 1],...  
% 'Color','none');  
  
% pause;  
% close 4;
```



```

% semilogx(xValues, totalYoungsAmplitude(2,:));
% ax1=gca;
% set(ax1,'XColor','k','YColor','k')
%
% ax2 = axes('Position',get(ax1,'Position'),...
%           'XAxisLocation','top',...
%           'YAxisLocation','right',...
%           'XColor','r','YColor','r');
%
% semilogx(xValues, totalAmplitude(2,:), 4, ax2);
hold on;
[ax, h1, h2]=plotyy(xValues(1:plotLimit), totalYoungsAmplitude(2,1:plotLimit), xValues(1:plotLimit), totalAmplitude(2,1:plotLimit), 'plot', 'plot');

set(ax(1), 'YColor', 'k', 'YTick', [0:(y1Max/10):y1Max], 'YLim', [0, y1Max]);
set(ax(2), 'YColor', 'r', 'YTick', [0:(y2Max/10):y2Max], 'YLim', [0, y2Max]);
xlabel('Frequency (Hz)');

set(get(ax(1), 'Ylabel'), 'String', 'Youngs modulus (GPa)');
set(get(ax(2), 'Ylabel'), 'String', 'Perturbation (nm_{pp})');
set(h2, 'LineStyle', '.', 'Color', 'r');
set(h1, 'LineStyle', '-', 'Marker', '.', 'Color', [0 0.6, 0]);

title({'Frequency and amplitude response in Youngs modulus', pwd});
legend('Youngs modulus from SG', 'Youngs modulus from Act', 'Perturbation (p-p)');
% semilogx(xValues, totalYoungsStrain(2,:), ax(1));

print (5, '-dpdf', 'frequencyDependence_small');
% ax(2) = axes('Parent',4,'YTick',[0 5 10 15 20],...
%           'YAxisLocation','right',...
%           'YColor',[0.5 0 0],...
%           'XScale','log',...
%           'XMinorTick','on',...
%           'ColorOrder',[0 0.5 0;1 0 0;0 0.75 0.75;0.75 0 0.75;0.75 0.75 0;0.25 0.25 0.25;0
0 1],...
%           'Color','none');

% pause;
% close 4;

% %%Plotting results
% % Create textbox [xPositionOnLowerLeft yPositionOnLowerLeft xWidth yHeight]
% a1=annotation('textbox',...
% [0.3 0.20 0.26 0.19],...
% 'Interpreter','latex',...
% 'String',{'...
% 'Act-value: ' num2str(mean(totalYoungsAmplitude(2,1:plotLimit)))...
% 'Ratio: ' num2str(mean(totalYoungsStrain(2,3:plotLimit))/mean
(totalYoungsAmplitude(2,3:plotLimit)))...
% },...
% 'FitBoxToText','off');

```



```

% hold all;
% semilogx(xValues, totalStrainPhase(2,:));
% ax1=gca;
% set(ax1,'XColor','k','YColor','k')
%
% ax2 = axes('Position',get(ax1,'Position'),...
%           'XAxisLocation','top',...
%           'YAxisLocation','right',...
%           'XColor','r','YColor','r');
%
% semilogx(xValues, totalAmplitude(2,:), 4, ax2);
hold on;
[ax, h1, h2]=plotyy(xValues(1:plotLimit), totalStrainPhase(2,1:plotLimit), xValues(1:
plotLimit), totalAmplitude(2,1:plotLimit), 'plot', 'plot');

set(ax(1), 'YColor', 'k', 'YTick', [-180:(y1Max/10):y1Max], 'YLim', [-180, y1Max]);
set(ax(2), 'YColor', 'r', 'YTick', [0:(y2Max/10):y2Max], 'YLim', [0,y2Max]);
xlabel('Frequency (Hz)');

set(get(ax(1), 'Ylabel'), 'String', 'Angle (deg.)');
set(get(ax(2), 'Ylabel'), 'String', 'Perturbation (nm_{pp})');
set(h2, 'LineStyle', '.', 'Color', 'r');
set(h1, 'LineStyle', '-', 'Marker', '.', 'Color', [0 0.6, 0]);

title({'Phase plot - Rock Hard Deformations', pwd});
legend('Phase Force', 'Phase Strain', 'Amplitude');
% semilogx(xValues, totalForcePhase(2,:), ax(1));

print (6, '-dpdf', 'frequencyDependence_small_phase');

f7=figure(7);
h0=errorbar(xValues(1:plotLimit), totalForcePhase(2,1:plotLimit)-totalStrainPhase(2,1:
plotLimit), totalForcePhase(1,1:plotLimit)-totalForcePhase(2,1:plotLimit)-
(totalStrainPhase(1,1:plotLimit)-totalStrainPhase(2,1:plotLimit)), totalForcePhase(3,1:
plotLimit)-totalForcePhase(2,1:plotLimit)-(totalStrainPhase(3,1:plotLimit)-
totalStrainPhase(2,1:plotLimit)), 'b.-');
title({'Absolute difference in phase plot - Rock Hard Deformations', pwd});
%legend('Phase Force', 'Phase Strain', 'Amplitude');
xlabel('Frequency (Hz)');
ylabel('Angle (deg.)');

print (7, '-dpdf', 'frequencyDependence_small_phase_diff');

attenuation(2,:)=tand(totalForcePhase(2,1:plotLimit)-totalStrainPhase(2,1:plotLimit));
attenuation(1,:)=tand(totalForcePhase(1,1:plotLimit)-totalForcePhase(2,1:plotLimit)-
(totalStrainPhase(1,1:plotLimit)-totalStrainPhase(2,1:plotLimit)));
attenuation(3,:)=tand(totalForcePhase(3,1:plotLimit)-totalForcePhase(2,1:plotLimit)-
(totalStrainPhase(3,1:plotLimit)-totalStrainPhase(2,1:plotLimit)));

f8=figure(8);
h0=errorbar(xValues(1:plotLimit), attenuation(2,:), attenuation(1,:),attenuation(3,:) ,
'b.-');
%h0=errorbar(xValues(1:plotLimit), totalForcePhase(2,1:plotLimit)-totalStrainPhase(2,1:
plotLimit), totalForcePhase(1,1:plotLimit)-totalForcePhase(2,1:plotLimit)-
(totalStrainPhase(1,1:plotLimit)-totalStrainPhase(2,1:plotLimit)), totalForcePhase(3,1:

```

```
plotLimit)-totalForcePhase(2,1:plotLimit)-(totalStrainPhase(3,1:plotLimit)-  
totalStrainPhase(2,1:plotLimit)), 'b.-');  
title({'Attenuation in rock - 1/Q', pwd});  
%legend('Phase Force', 'Phase Strain', 'Amplitude');  
xlabel('Frequency (Hz)');  
ylabel('1/Q');  
  
print (8, '-dpdf', 'frequencyDependence_small_phase_attenuation');  
clear y1Max y2Max plotLimit;  
  
clear y1Max y2Max plotLimit;  
  
% ax(2) = axes('Parent',4,'YTick',[0 5 10 15 20],...  
% 'YAxisLocation','right',...  
% 'YColor',[0.5 0 0],...  
% 'XScale','log',...  
% 'XMinorTick','on',...  
% 'ColorOrder',[0 0.5 0;1 0 0;0 0.75 0.75;0.75 0 0.75;0.75 0.75 0;0.25 0.25 0.25;0  
0 1],...  
% 'Color','none');  
  
% pause;  
% close 4;  
  
% %%Plotting results  
% % Create textbox [xPositionOnLowerLeft yPositionOnLowerLeft xWidth yHeight]  
% a1=annotation('textbox',...  
% [0.3 0.20 0.26 0.19],...  
% 'Interpreter','latex',...  
% 'String',{'...  
% 'Act-value: ' num2str(mean(totalStrainPhase(2,1:plotLimit)))...  
% 'Ratio: ' num2str(mean(totalForcePhase(2,3:plotLimit))/mean(totalStrainPhase(2,3:  
plotLimit)))...  
% },...  
% 'FitBoxToText','off');
```

D RockHard Functions - get* - Matlab functions for post processing of .tdms files


```
pos=-1;
rawString='-1';
end
```

```
% %%Search for end of number
%
%
% %b=~ismember(rawTDMSTextFile(dummyPos+7:dummys+11), ↵
'abcdefghijklmnopqrstuvwxyzABCDEFGHIJKLMNOPQRSTUVWXYZ1234567890.,!?!_<>*^~\`'}] ↵
[{'$£@|§!"#%&/()=?`' )
% rawString=rawTDMSTextFile(dummyPos+7:dummys+7+d-2)
% pos=dummys;
%
```



```
master.comments=getChar(a, 'Comments');

%%Sampling details
master.samplingRate=getNum(a, 'Samplingrate(Hz)');
master.samplingTime=getNum(a, 'Samplingtime(s)');
master.samplingTimeout=getNum(a, 'Samplingtimeout(s)');

%%Settings Wave generator
master.waveGenerator.Vpp=getChar(a, 'AmplitudeVpp');
master.waveGenerator.frequency=getChar(a, 'Frequency(0-1000Hz)');
master.waveGenerator.DCOffset=getChar(a, 'DC-offset(V)');
master.waveGenerator.waveFormFunction=getChar(a, 'WaveformFunction(1:Sine)');
%waveGenerator=struct(waveGeneratorVpp, waveGeneratorFrequency, waveGeneratorDCOffset, ↵
waveFormFunction);

%%Settings Charge Meter
%chargeMeterUnit=getChar(a, 'Unit');
master.chargeMeter.Sensor=getNum(a, 'Sensor');
master.chargeMeter.Range=getNum(a, 'Range');
master.chargeMeter.FSO=getChar(a, 'FSO');
master.chargeMeter.LPFilter=getNum(a, 'LPFilter');
master.chargeMeter.Ordnung=getChar(a, 'Ordnung');
master.chargeMeter.HPFilter=getChar(a, 'HPFilter');
%Input=getChar(a, 'Input');
master.chargeMeter.Sens.Unit=getChar(a, 'Sens.Unit');
master.chargeMeter.UnitMetr=getChar(a, 'UnitMetr');
%chargeMeter.Mode=getChar(a, 'Mode');
%chargeMeter.Lock=getChar(a, 'Lock');

%%Calculate crossArea
if 0<master.sample.Diameter&&master.sample.Diameter<=1
    %%Assume meters
    master.sample.crossArea=(master.sample.Diameter/2)^2*pi;
elseif 1<master.sample.Diameter&&master.sample.Diameter<100
    %%Assume mm
    master.sample.Diameter=master.sample.Diameter*10^(-3);
    master.sample.crossArea=(master.sample.Diameter/2)^2*pi;
elseif master.sample.Diameter>=100
    %%Assume micrometers
    master.sample.Diameter=master.sample.Diameter*10^(-6);
    master.sample.crossArea=(master.sample.Diameter/2)^2*pi;
else
    %%Assume standard value
    master.sample.Diameter=input('No diameter found! Enter value in mm or hit enter ↵
for one inch: ');
    if isempty(master.sample.Diameter)
        master.sample.Diameter=25.4;
    end
    master.sample.Diameter=master.sample.Diameter*10^(-3);
    master.sample.crossArea=(master.sample.Diameter/2)^2*pi;
end

%%Calculate length
if 0<master.sample.Length&&master.sample.Length<=1
```

```

    %%Assume mm
    master.sample.Length=master.sample.Length;
elseif 1<master.sample.Length&&master.sample.Length<=100
    %%Assume mm
    master.sample.Length=master.sample.Length*10^(-3);
elseif master.sample.Diameter>=100
    %%Assume micrometers
    master.sample.Length=master.sample.Length*10^(-6);
else
    %%Assume standard value
    master.sample.Length=50.64E-3;%input('No length found! Enter value in mm or hit ↵
enter for two inch: ');
    if isempty(master.sample.Length)
        master.sample.Length=50.8*10^(-3);
    end
end

clear a;

% =getChar(a, '')
% =getChar(a, '')
% =getChar(a, '')
% =getChar(a, '')
% =getChar(a, '')
% =getChar(a, '')
% =getChar(a, '')
% =getChar(a, '')
%
% %%Locate frequency
% %Frequency (0-1000 Hz) 000 00011,000000
% frequency=getNum(a, 'Frequency(0-1000Hz)', max(size('Frequency(0-1000Hz)')+14)
%
% %%Locate sampling rate
% %Sampling rate (Hz) 000 00032,000000
% samplingFrequency=getChar(a, 'Samplingrate(Hz)')
%
% %%Locate sample diameter
% %Sample diameter (mm) 000000025,4
% %on 550 with number at 568:581
% diameter=getNum(a, 'Samplediameter(mm)', 31)
%
% %%Locate sample length
% %Sample length (mm) 000000025,4
% length=getNum(a, 'Samplelength', 31)
%
% %%Locate Sample field
% %Sample field 0000000Sintef0000
% sampleField=getChar(a, 'Samplefield')
%
% %%Locate Sample ML#
% %Sample ML# 00000003180000
% sampleML=getChar(a, 'SampleML#')

```

E Other Scripts Modified by author - Matlab

```
%  
% This script was developed by National Instruments but  
% was modified by Trygve Westlye Fintland in the project Rock Hard  
% Deformations, Spring 2011.  
%  
%  
%  
%function []=ReadFile(filepath, filefolder, libname, NI_TDM_DLL_Path, NI_TDM_H_Path)  
%ReadFile(pwd, fileName, libname, NI_TDM_DLL_Path, hfolder, NI_TDM_H_Path)  
clc;  
  
%Recreate needed property constants defined in nilibddc_m.h  
DDC_FILE_NAME = 'name';  
DDC_FILE_DESCRIPTION = 'description';  
DDC_FILE_TITLE = 'title';  
DDC_FILE_AUTHOR = 'author';  
DDC_FILE_DATETIME = 'datetime';  
DDC_CHANNELGROUP_NAME = 'name';  
DDC_CHANNELGROUP_DESCRIPTION = 'description';  
DDC_CHANNEL_NAME = 'name';  
  
%Check if the paths to 'nilibddc.dll' and 'nilibddc_m.h' have been  
%selected. If not, prompt the user to browse to each of the files.  
if exist('NI_TDM_DLL_Path','var')==0  
    [dllfile,dllfolder]=uigetfile('*dll','Select nilibddc.dll');  
    libname=strtok(dllfile, '.');  
    NI_TDM_DLL_Path=fullfile(dllfolder,dllfile);  
end  
if exist('NI_TDM_H_Path','var')==0  
    [hfile,hfolder]=uigetfile('*h','Select nilibddc_m.h');  
    NI_TDM_H_Path=fullfile(hfolder,hfile);  
end  
  
%Prompt the user to browse to the path of the TDM or TDMS file to read  
  
if exist('filepath','var')==0  
    [filepath,filefolder]=uigetfile({'*.tdms'; '*.tdm'},'Select a TDM or TDMS file');  
    Data_Path=fullfile(filefolder,filepath);  
end  
    Data_Path=fullfile(filefolder,filepath);  
  
%Load nilibddc.dll (Always call 'unloadlibrary(libname)' after finished using the  
library)  
loadlibrary(NI_TDM_DLL_Path,NI_TDM_H_Path);  
  
%Open the file (Always call 'DDC_CloseFile' when you are finished using a file)  
fileIn = 0;  
[err,dummyVar,dummyVar,file]=calllib(libname, 'DDC_OpenFileEx',Data_Path, ',,1,fileIn);  
  
%Read and display file name property  
filenamelenIn = 0;  
%Get the length of the 'DDC_FILE_NAME' string property  
[err,dummyVar,filenamelen]=calllib(libname, 'DDC_GetFileStringLength',file,↵  
DDC_FILE_NAME,filenamelenIn);
```

```
if err==0 %Only proceed if the property is found
    %Initialize a string to the length of the property value
    pfilename=libpointer('stringPtr',blanks(filenamelen));
    [err,dummyVar,filename]=calllib(libname,'DDC_GetFileProperty',file,DDC_FILE_NAME,↵
pfilename,filenamelen+1);
    setdatatype(filename,'int8Ptr',1,filenamelen);
    disp(['File Name: ' char(filename.Value)]);
end

%Read and display file description property
filedesclenIn = 0;
%Get the length of the 'DDC_FILE_DESCRIPTION' string property
[err,dummyVar,filedesclen]=calllib(libname,'DDC_GetFileStringPropertyLength',file,↵
DDC_FILE_DESCRIPTION,filedesclenIn);
if err==0 %Only proceed if the property is found
    %Initialize a string to the length of the property value
    pfiledesc=libpointer('stringPtr',blanks(filedesclen));
    [err,dummyVar,filedesc]=calllib(libname,'DDC_GetFileProperty',file,↵
DDC_FILE_DESCRIPTION,pfiledesc,filedesclen+1);
    setdatatype(filedesc,'int8Ptr',1,filedesclen);
    disp(['File Description: ' char(filedesc.Value)]);
end

%Read and display file title property
filetitlelenIn = 0;
%Get the length of the 'DDC_FILE_TITLE' string property
[err,dummyVar,filetitlelen]=calllib(libname,'DDC_GetFileStringPropertyLength',file,↵
DDC_FILE_TITLE,filetitlelenIn);
if err==0 %Only proceed if the property is found
    %Initialize a string to the length of the property value
    pfiletitle=libpointer('stringPtr',blanks(filetitlelen));
    [err,dummyVar,filetitle]=calllib(libname,'DDC_GetFileProperty',file,DDC_FILE_TITLE,↵
pfiletitle,filetitlelen+1);
    setdatatype(filetitle,'int8Ptr',1,filetitlelen);
    disp(['File Title: ' char(filetitle.Value)]);
end

%Read and display file author property
fileauthlenIn = 0;
%Get the length of the 'DDC_FILE_AUTHOR' string property
[err,dummyVar,fileauthlen]=calllib(libname,'DDC_GetFileStringPropertyLength',file,↵
DDC_FILE_AUTHOR,fileauthlenIn);
if err==0 %Only proceed if the property is found
    %Initialize a string to the length of the property value
    pfileauth=libpointer('stringPtr',blanks(fileauthlen));
    [err,dummyVar,fileauth]=calllib(libname,'DDC_GetFileProperty',file,DDC_FILE_AUTHOR,↵
pfileauth,fileauthlen+1);
    setdatatype(fileauth,'int8Ptr',1,fileauthlen);
    disp(['File Author: ' char(fileauth.Value)]);
end

%Read and display file timestamp property
yearIn = 0;
monthIn = 0;
dayIn = 0;
```

```

hourIn = 0;
minuteIn = 0;
secondIn = 0;
msecondIn = 0;
wkdayIn = 0;
[err,dummyVar,year,month,day,hour,minute,second,msecond,wkday]=calllib
(libname,'DDC_GetFilePropertyTimestampComponents',file,DDC_FILE_DATETIME,yearIn,
monthIn,dayIn,hourIn,minuteIn,secondIn,msecondIn,wkdayIn);
if err==0 %Only proceed if the property is found
    disp(['File Timestamp: ' num2str(month) '/' num2str(day) '/' num2str(year) ', '
num2str(hour) ':' num2str(minute) ':' num2str(second) ':' num2str(msecond)]);
end

%Get channel groups
%Get the number of channel groups
numgrpsIn = 0;
[err,numgrps]=calllib(libname,'DDC_GetNumChannelGroups',file,numgrpsIn);
%Get channel groups only if the number of channel groups is greater than zero
if numgrps>0
    %Initialize an array to hold the desired number of groups
    pgrps=libpointer('int32Ptr',zeros(1,numgrps));
    [err,grps]=calllib(libname,'DDC_GetChannelGroups',file,pgrps,numgrps);
end
for i=1:numgrps %For each channel group
    %Get channel group name property
    grpnamelenIn = 0;
    [err,dummyVar,grpnamelen]=calllib
(libname,'DDC_GetChannelGroupStringPropertyLength',grps(i),DDC_CHANNELGROUP_NAME,
grpnamelenIn);
    if err==0 %Only proceed if the property is found
        %Initialize a string to the length of the property value
        pgrpname=libpointer('stringPtr',blanks(grpnamelen));
        [err,dummyVar,grpname]=calllib(libname,'DDC_GetChannelGroupProperty',grps(i),
DDC_CHANNELGROUP_NAME,pgrpname,grpnamelen+1);
        setdatatype(grpname,'int8Ptr',1,grpnamelen);
    else
        grpname=libpointer('stringPtr','');
    end

    %Get channel group description property
    grpdesclenIn = 0;
    [err,dummyVar,grpdesclen]=calllib
(libname,'DDC_GetChannelGroupStringPropertyLength',grps(i),
DDC_CHANNELGROUP_DESCRIPTION,grpdesclenIn);
    if err==0 %Only proceed if the property is found
        %Initialize a string to the length of the property value
        pgrpdesc=libpointer('stringPtr',blanks(grpdesclen));
        [err,dummyVar,grpdesc]=calllib(libname,'DDC_GetChannelGroupProperty',grps(i),
DDC_CHANNELGROUP_DESCRIPTION,pgrpdesc,grpdesclen+1);
    end

    % figure('Name',char(grpname.Value));
    hold on;

    %Get channels

```

```

numchansIn = 0;
%Get the number of channels in this channel group
[err,numchans]=calllib(libname,'DDC_GetNumChannels',grps(i),numchansIn);
%Get channels only if the number of channels is greater than zero
if numchans>0
    %Initialize an array to hold the desired number of channels
    pchans=libpointer('int32Ptr',zeros(1,numchans));
    [err,chans]=calllib(libname,'DDC_GetChannels',grps(i),pchans,numchans);
end

channames=cell(1,numchans);

for j=1:numchans %For each channel in the channel group
    %Get channel name property
    channamelenIn = 0;
    [err,dummyVar,channamelen]=calllib(
(libname,'DDC_GetChannelStringPropertyLength',chans(j),DDC_CHANNEL_NAME,channamelenIn);
    if err==0 %Only proceed if the property is found
        %Initialize a string to the length of the property value
        pchanname=libpointer('stringPtr',blanks(channamelen));
        [err,dummyVar,channame]=calllib(libname,'DDC_GetChannelProperty',chans(j),
DDC_CHANNEL_NAME,pchanname,channamelen+1);
        setdatatype(channame,'int8Ptr',1,channamelen);
        channames{j}=char(channame.Value);
    else
        channames{j}='';
    end

    %Get channel data type
    typeIn = 0;
    [err,type]=calllib(libname,'DDC_GetDataType',chans(j),typeIn);

    %Get channel values if data type of channel is double (DDC_Double = 10)
    if strcmp(type,'DDC_Double')
        numvalsIn = 0;
        [err,numvals]=calllib(libname,'DDC_GetNumDataValues',chans(j),numvalsIn);
        %Initialize an array to hold the desired number of values
        pvals=libpointer('doublePtr',zeros(1,numvals));
        [err,vals]=calllib(libname,'DDC_GetDataValues',chans(j),0,numvals,pvals);
        setdatatype(vals,'doublePtr',1,numvals);

        %Add channel values to a matrix. The comment, #ok<AGROW>, at
        %the end of the line prevents warnings about the matrix needing
        %to allocate more memory for the added values.
        chanvals(:,j)=(vals.Value); %#ok<AGROW>
    end
end

end

if i==1
    MEASUREMENTS=chanvals;
    MEASUREMENTS_LEGEND=channames;
elseif i>=2
    ERRORLOG=chanvals;
    ERRORLOG_LEGEND=channames;
end

```


end

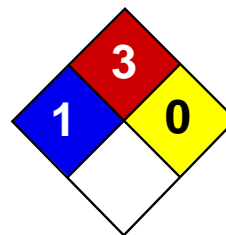
```
%Plot Data from channels in this group
%plot(chanvals);
chanvals=0;
channames=0;
%legend(channames);
```

end

```
%Close file
err = calllib(libname, 'DDC_CloseFile', file);

%Unload nilibddc.dll
unloadlibrary(libname);
```

F Chemical Data Sheets



Health	2
Fire	3
Reactivity	0
Personal Protection	H

Material Safety Data Sheet Acetone MSDS

Section 1: Chemical Product and Company Identification

Product Name: Acetone

Catalog Codes: SLA3502, SLA1645, SLA3151, SLA3808

CAS#: 67-64-1

RTECS: AL3150000

TSCA: TSCA 8(b) inventory: Acetone

CI#: Not applicable.

Synonym: 2-propanone; Dimethyl Ketone; Dimethylformaldehyde; Pyroacetic Acid

Chemical Name: Acetone

Chemical Formula: C₃H₆O

Contact Information:

Sciencelab.com, Inc.

14025 Smith Rd.

Houston, Texas 77396

US Sales: **1-800-901-7247**

International Sales: **1-281-441-4400**

Order Online: ScienceLab.com

CHEMTREC (24HR Emergency Telephone), call:

1-800-424-9300

International CHEMTREC, call: 1-703-527-3887

For non-emergency assistance, call: 1-281-441-4400

Section 2: Composition and Information on Ingredients

Composition:

Name	CAS #	% by Weight
Acetone	67-64-1	100

Toxicological Data on Ingredients: Acetone: ORAL (LD50): Acute: 5800 mg/kg [Rat]. 3000 mg/kg [Mouse]. 5340 mg/kg [Rabbit]. VAPOR (LC50): Acute: 50100 mg/m 8 hours [Rat]. 44000 mg/m 4 hours [Mouse].

Section 3: Hazards Identification

Potential Acute Health Effects:

Hazardous in case of skin contact (irritant), of eye contact (irritant), of ingestion, of inhalation. Slightly hazardous in case of skin contact (permeator).

Potential Chronic Health Effects:

CARCINOGENIC EFFECTS: A4 (Not classifiable for human or animal.) by ACGIH. MUTAGENIC EFFECTS: Not available. TERATOGENIC EFFECTS: Not available. DEVELOPMENTAL TOXICITY: Classified Reproductive system/toxin/female, Reproductive system/toxin/male [SUSPECTED]. The substance is toxic to central nervous system (CNS). The substance may be toxic to kidneys, the reproductive system, liver, skin. Repeated or prolonged exposure to the substance can produce target organs damage.

Section 4: First Aid Measures

Eye Contact:

Check for and remove any contact lenses. Immediately flush eyes with running water for at least 15 minutes, keeping eyelids open. Cold water may be used. Get medical attention.

Skin Contact:

In case of contact, immediately flush skin with plenty of water. Cover the irritated skin with an emollient. Remove contaminated clothing and shoes. Cold water may be used. Wash clothing before reuse. Thoroughly clean shoes before reuse. Get medical attention.

Serious Skin Contact:

Wash with a disinfectant soap and cover the contaminated skin with an anti-bacterial cream. Seek medical attention.

Inhalation:

If inhaled, remove to fresh air. If not breathing, give artificial respiration. If breathing is difficult, give oxygen. Get medical attention if symptoms appear.

Serious Inhalation:

Evacuate the victim to a safe area as soon as possible. Loosen tight clothing such as a collar, tie, belt or waistband. If breathing is difficult, administer oxygen. If the victim is not breathing, perform mouth-to-mouth resuscitation. Seek medical attention.

Ingestion:

Do NOT induce vomiting unless directed to do so by medical personnel. Never give anything by mouth to an unconscious person. Loosen tight clothing such as a collar, tie, belt or waistband. Get medical attention if symptoms appear.

Serious Ingestion: Not available.

Section 5: Fire and Explosion Data

Flammability of the Product: Flammable.

Auto-Ignition Temperature: 465°C (869°F)

Flash Points: CLOSED CUP: -20°C (-4°F). OPEN CUP: -9°C (15.8°F) (Cleveland).

Flammable Limits: LOWER: 2.6% UPPER: 12.8%

Products of Combustion: These products are carbon oxides (CO, CO₂).

Fire Hazards in Presence of Various Substances: Highly flammable in presence of open flames and sparks, of heat.

Explosion Hazards in Presence of Various Substances:

Risks of explosion of the product in presence of mechanical impact: Not available. Slightly explosive in presence of open flames and sparks, of oxidizing materials, of acids.

Fire Fighting Media and Instructions:

Flammable liquid, soluble or dispersed in water. SMALL FIRE: Use DRY chemical powder. LARGE FIRE: Use alcohol foam, water spray or fog.

Special Remarks on Fire Hazards: Vapor may travel considerable distance to source of ignition and flash back.

Special Remarks on Explosion Hazards:

Forms explosive mixtures with hydrogen peroxide, acetic acid, nitric acid, nitric acid + sulfuric acid, chromic anhydride, chromyl chloride, nitrosyl chloride, hexachloromelamine, nitrosyl perchlorate, nitryl perchlorate, permonosulfuric acid, thiodiglycol + hydrogen peroxide, potassium ter-butoxide, sulfur dichloride, 1-methyl-1,3-butadiene, bromoform, carbon, air, chloroform, thitriazylperchlorate.

Section 6: Accidental Release Measures

Small Spill:

Dilute with water and mop up, or absorb with an inert dry material and place in an appropriate waste disposal container.

Large Spill:

Flammable liquid. Keep away from heat. Keep away from sources of ignition. Stop leak if without risk. Absorb with DRY earth, sand or other non-combustible material. Do not touch spilled material. Prevent entry into sewers, basements or confined areas; dike if needed. Be careful that the product is not present at a concentration level above TLV. Check TLV on the MSDS and with local authorities.

Section 7: Handling and Storage

Precautions:

Keep locked up.. Keep away from heat. Keep away from sources of ignition. Ground all equipment containing material. Do not ingest. Do not breathe gas/fumes/ vapor/spray. Wear suitable protective clothing. In case of insufficient ventilation, wear suitable respiratory equipment. If ingested, seek medical advice immediately and show the container or the label. Avoid contact with skin and eyes. Keep away from incompatibles such as oxidizing agents, reducing agents, acids, alkalis.

Storage:

Store in a segregated and approved area (flammables area) . Keep container in a cool, well-ventilated area. Keep container tightly closed and sealed until ready for use. Keep away from direct sunlight and heat and avoid all possible sources of ignition (spark or flame).

Section 8: Exposure Controls/Personal Protection

Engineering Controls:

Provide exhaust ventilation or other engineering controls to keep the airborne concentrations of vapors below their respective threshold limit value. Ensure that eyewash stations and safety showers are proximal to the work-station location.

Personal Protection:

Splash goggles. Lab coat. Vapor respirator. Be sure to use an approved/certified respirator or equivalent. Gloves.

Personal Protection in Case of a Large Spill:

Splash goggles. Full suit. Vapor respirator. Boots. Gloves. A self contained breathing apparatus should be used to avoid inhalation of the product. Suggested protective clothing might not be sufficient; consult a specialist BEFORE handling this product.

Exposure Limits:

TWA: 500 STEL: 750 (ppm) from ACGIH (TLV) [United States] TWA: 750 STEL: 1000 (ppm) from OSHA (PEL) [United States] TWA: 500 STEL: 1000 [Australia] TWA: 1185 STEL: 2375 (mg/m3) [Australia] TWA: 750 STEL: 1500 (ppm) [United Kingdom (UK)] TWA: 1810 STEL: 3620 (mg/m3) [United Kingdom (UK)] TWA: 1800 STEL: 2400 from OSHA (PEL) [United States] Consult local authorities for acceptable exposure limits.

Section 9: Physical and Chemical Properties

Physical state and appearance: Liquid.

Odor: Fruity. Mint-like. Fragrant. Ethereal

Taste: Pungent, Sweetish

Molecular Weight: 58.08 g/mole

Color: Colorless. Clear

pH (1% soln/water): Not available.

Boiling Point: 56.2°C (133.2°F)

Melting Point: -95.35 (-139.6°F)

Critical Temperature: 235°C (455°F)

Specific Gravity: 0.79 (Water = 1)

Vapor Pressure: 24 kPa (@ 20°C)

Vapor Density: 2 (Air = 1)

Volatility: Not available.

Odor Threshold: 62 ppm

Water/Oil Dist. Coeff.: The product is more soluble in water; $\log(\text{oil/water}) = -0.2$

Ionicity (in Water): Not available.

Dispersion Properties: See solubility in water.

Solubility: Easily soluble in cold water, hot water.

Section 10: Stability and Reactivity Data

Stability: The product is stable.

Instability Temperature: Not available.

Conditions of Instability: Excess heat, ignition sources, exposure to moisture, air, or water, incompatible materials.

Incompatibility with various substances: Reactive with oxidizing agents, reducing agents, acids, alkalis.

Corrosivity: Non-corrosive in presence of glass.

Special Remarks on Reactivity: Not available.

Special Remarks on Corrosivity: Not available.

Polymerization: Will not occur.

Section 11: Toxicological Information

Routes of Entry: Absorbed through skin. Dermal contact. Eye contact. Inhalation.

Toxicity to Animals:

WARNING: THE LC50 VALUES HEREUNDER ARE ESTIMATED ON THE BASIS OF A 4-HOUR EXPOSURE. Acute oral toxicity (LD50): 3000 mg/kg [Mouse]. Acute toxicity of the vapor (LC50): 44000 mg/m³ 4 hours [Mouse].

Chronic Effects on Humans:

CARCINOGENIC EFFECTS: A4 (Not classifiable for human or animal.) by ACGIH. DEVELOPMENTAL TOXICITY: Classified Reproductive system/toxin/female, Reproductive system/toxin/male [SUSPECTED]. Causes damage to the following organs: central nervous system (CNS). May cause damage to the following organs: kidneys, the reproductive system, liver, skin.

Other Toxic Effects on Humans:

Hazardous in case of skin contact (irritant), of ingestion, of inhalation. Slightly hazardous in case of skin contact (permeator).

Special Remarks on Toxicity to Animals: Not available.

Special Remarks on Chronic Effects on Humans:

May affect genetic material (mutagenicity) based on studies with yeast (*S. cerevisiae*), bacteria, and hamster fibroblast cells. May cause reproductive effects (fertility) based upon animal studies. May contain trace amounts of benzene and formaldehyde which may cause cancer and birth defects. Human: passes the placental barrier.

Special Remarks on other Toxic Effects on Humans:

Acute Potential Health Effects: Skin: May cause skin irritation. May be harmful if absorbed through the skin. Eyes: Causes eye irritation, characterized by a burning sensation, redness, tearing, inflammation, and possible corneal injury. Inhalation: Inhalation at high concentrations affects the sense organs, brain and causes respiratory tract irritation. It also may affect the Central Nervous System (behavior) characterized by dizziness, drowsiness, confusion, headache, muscle weakness, and possibly motor incoordination, speech abnormalities, narcotic effects and coma. Inhalation may also affect the gastrointestinal tract (nausea, vomiting). Ingestion: May cause irritation of the digestive (gastrointestinal) tract (nausea, vomiting). It may also

affect the Central Nervous System (behavior), characterized by depression, fatigue, excitement, stupor, coma, headache, altered sleep time, ataxia, tremors as well as the blood, liver, and urinary system (kidney, bladder, ureter) and endocrine system. May also have musculoskeletal effects. Chronic Potential Health Effects: Skin: May cause dermatitis. Eyes: Eye irritation.

Section 12: Ecological Information

Ecotoxicity:

Ecotoxicity in water (LC50): 5540 mg/l 96 hours [Trout]. 8300 mg/l 96 hours [Bluegill]. 7500 mg/l 96 hours [Fathead Minnow]. 0.1 ppm any hours [Water flea].

BOD5 and COD: Not available.

Products of Biodegradation:

Possibly hazardous short term degradation products are not likely. However, long term degradation products may arise.

Toxicity of the Products of Biodegradation: The product itself and its products of degradation are not toxic.

Special Remarks on the Products of Biodegradation: Not available.

Section 13: Disposal Considerations

Waste Disposal:

Waste must be disposed of in accordance with federal, state and local environmental control regulations.

Section 14: Transport Information

DOT Classification: CLASS 3: Flammable liquid.

Identification: : Acetone UNNA: 1090 PG: II

Special Provisions for Transport: Not available.

Section 15: Other Regulatory Information

Federal and State Regulations:

California prop. 65: This product contains the following ingredients for which the State of California has found to cause reproductive harm (male) which would require a warning under the statute: Benzene California prop. 65: This product contains the following ingredients for which the State of California has found to cause birth defects which would require a warning under the statute: Benzene California prop. 65: This product contains the following ingredients for which the State of California has found to cause cancer which would require a warning under the statute: Benzene, Formaldehyde Connecticut hazardous material survey.: Acetone Illinois toxic substances disclosure to employee act: Acetone Illinois chemical safety act: Acetone New York release reporting list: Acetone Rhode Island RTK hazardous substances: Acetone Pennsylvania RTK: Acetone Florida: Acetone Minnesota: Acetone Massachusetts RTK: Acetone Massachusetts spill list: Acetone New Jersey: Acetone New Jersey spill list: Acetone Louisiana spill reporting: Acetone California List of Hazardous Substances (8 CCR 339): Acetone TSCA 8(b) inventory: Acetone TSCA 4(a) final test rules: Acetone TSCA 8(a) IUR: Acetone

Other Regulations:

OSHA: Hazardous by definition of Hazard Communication Standard (29 CFR 1910.1200). EINECS: This product is on the European Inventory of Existing Commercial Chemical Substances.

Other Classifications:

WHMIS (Canada):

CLASS B-2: Flammable liquid with a flash point lower than 37.8°C (100°F). CLASS D-2B: Material causing other toxic effects (TOXIC).

DSCL (EEC):

R11- Highly flammable. R36- Irritating to eyes. S9- Keep container in a well-ventilated place. S16- Keep away from sources of ignition - No smoking. S26- In case of contact with eyes, rinse immediately with plenty of water and seek medical advice.

HMIS (U.S.A.):

Health Hazard: 2

Fire Hazard: 3

Reactivity: 0

Personal Protection: h

National Fire Protection Association (U.S.A.):

Health: 1

Flammability: 3

Reactivity: 0

Specific hazard:

Protective Equipment:

Gloves. Lab coat. Vapor respirator. Be sure to use an approved/certified respirator or equivalent. Wear appropriate respirator when ventilation is inadequate. Splash goggles.

Section 16: Other Information**References:**

-Material safety data sheet issued by: la Commission de la Sant  et de la S curit  du Travail du Qu bec. -The Sigma-Aldrich Library of Chemical Safety Data, Edition II. -Hawley, G.G.. The Condensed Chemical Dictionary, 11e ed., New York N.Y., Van Nostrand Reinold, 1987. LOLI, RTECS, HSDB databases. Other MSDSs

Other Special Considerations: Not available.

Created: 10/10/2005 08:13 PM

Last Updated: 11/01/2010 12:00 PM

The information above is believed to be accurate and represents the best information currently available to us. However, we make no warranty of merchantability or any other warranty, express or implied, with respect to such information, and we assume no liability resulting from its use. Users should make their own investigations to determine the suitability of the information for their particular purposes. In no event shall ScienceLab.com be liable for any claims, losses, or damages of any third party or for lost profits or any special, indirect, incidental, consequential or exemplary damages, howsoever arising, even if ScienceLab.com has been advised of the possibility of such damages.



Hysol[®] 3430[™]

March 2008

PRODUCT DESCRIPTION

Hysol[®] 3430[™] provides the following product characteristics:

Technology	Epoxy
Chemical Type	Epoxy
Appearance (Resin)	Ultra clear
Appearance (Hardener)	Ultra clear
Appearance (Mixed)	Ultra clear, Transparent ^{LMS}
Components	Two part - Resin & Hardener
Mix Ratio, by volume - Resin : Hardener	1 : 1
Mix Ratio, by weight - Resin : Hardener	100 : 100
Cure	Room temperature cure after mixing
Application	Bonding

Hysol[®] 3430[™] is a two component, clear epoxy adhesive which cures rapidly at room temperature after mixing. It is a general purpose adhesive which develops high strength on a wide range of substrates. The gap filling properties make this adhesive system suitable for rough and poorly fitting surfaces made from metal, ceramic, rigid plastics or wood.

TYPICAL PROPERTIES OF UNCURED MATERIAL

Resin Properties

Specific Gravity @ 25 °C 1.14 to 1.2
 Viscosity @ 25 °C, Cone & Plate Rheometer, mPa·s (cP):
 Shear Rate: 10 s⁻¹ 18,000 to 28,000
 Flash Point - See MSDS

Hardener Properties

Specific Gravity @ 25 °C 1.14 to 1.2
 Viscosity @ 25 °C, Cone & Plate Rheometer, mPa·s (cP):
 Shear Rate: 10 s⁻¹ 18,000 to 28,000
 Flash Point - See MSDS

Mixed Properties

Specific Gravity @ 25 °C 1.14 to 1.2^{LMS}
 Viscosity @ 25 °C, Cone & Plate Rheometer, mPa·s (cP):
 Shear Rate: 10 s⁻¹ 18,000 to 28,000^{LMS}
 Gel Time @ 25 °C, minutes:
 5 g resin / 5 g hardener 5 to 10^{LMS}

TYPICAL CURING PERFORMANCE

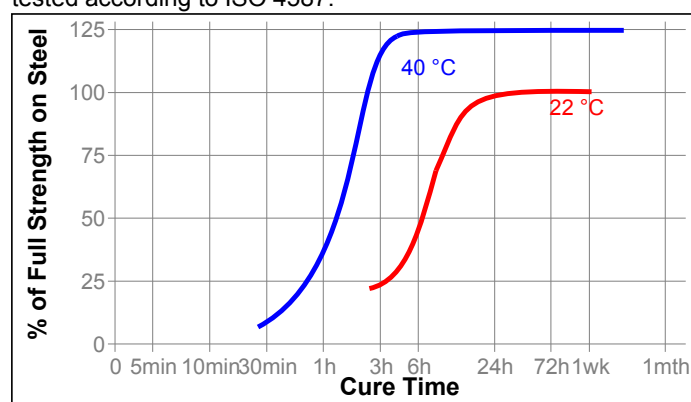
Fixture Time

Fixture time is defined as the time to develop a shear strength of 0.1 N/mm².

Fixture Time, mixed, minutes 15

Cure Speed vs. Time, Temperature

The rate of cure will depend on the ambient temperature, elevated temperatures may be used to accelerate the cure. The graph below shows shear strength developed with time at various temperatures on grit blasted steel lap shears and tested according to ISO 4587.



TYPICAL PROPERTIES OF CURED MATERIAL

Cured for 7 days @ 22 °C, 4 mm thick samples.

Physical Properties:

Coefficient of Thermal Expansion ISO 11359-2, K⁻¹:
 Temperature Range: 10 °C to 40 °C 53×10⁻⁶

Cured for 7 days @ 22 °C, 1.2 mm thick samples

Physical Properties:

Coefficient of Thermal Conductivity, ISO 8302, W/(m·K) 0.3
 Tensile Strength, ISO 527-3 N/mm² 36 (psi) (5,220)
 Tensile Modulus, ISO 527-3 N/mm² 3,210 (psi) (465,500)
 Compressive Strength, ISO 604 N/mm² 65 (psi) (9,420)
 Elongation, ISO 527-3,% 2
 Shore Hardness, ISO 868, Durometer D 70
 Glass Transition Temperature, ASTM E 1640, °C 58

Electrical Properties:

Dielectric Breakdown Strength, IEC 60243-1, kV/mm 25
 Volume Resistivity, IEC 60093, Ω·cm 3×10¹⁵
 Surface Resistivity, IEC 60093, Ω 0.2×10¹⁸



Dielectric Constant / Dissipation Factor, IEC 60250:	
1 kHz	3.07 / 0.04
1 MHz	3.26 / 0.04
10 MHz	3.57 / 0.01

TYPICAL PERFORMANCE OF CURED MATERIAL

Adhesive Properties

Cured for 7 days @ 22 °C

Lap Shear Strength , ISO 4587:

Mild steel (grit blasted)	N/mm ²	22
	(psi)	(3,200)
Stainless steel	N/mm ²	15
	(psi)	(2,175)
Aluminum (Isopropanol wiped)	N/mm ²	7
	(psi)	(1,010)
Aluminum (abraded)	N/mm ²	14
	(psi)	(2,030)
Zinc dichromate	N/mm ²	16
	(psi)	(2,320)
Polycarbonate	N/mm ²	4
	(psi)	(580)
ABS	N/mm ²	5
	(psi)	(725)
PVC	N/mm ²	5
	(psi)	(725)
GRP (polyester resin matrix)	N/mm ²	3
	(psi)	(435)
Softwood (Deal)	N/mm ²	8
	(psi)	(1,160)
Hardwood (Teak)	N/mm ²	11
	(psi)	(1,600)

180° Peel Strength, ISO 8510-2:

Steel (grit blasted)	N/mm	3
	(lb/in)	(17)

Impact Strength , ISO 9653, J/m²

3

TYPICAL ENVIRONMENTAL RESISTANCE

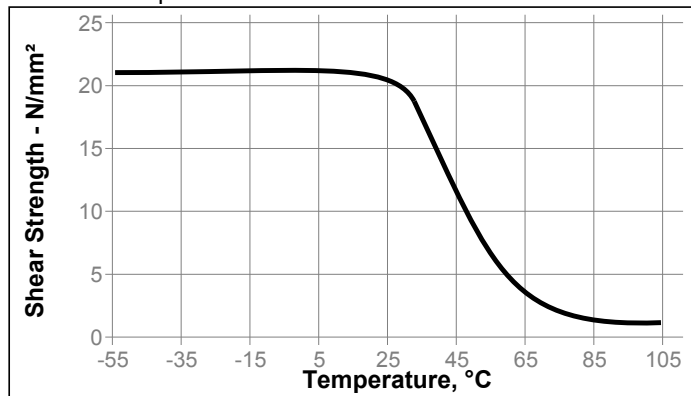
Cured for 7 days @ 22 °C (0.05 mm bond gap).

Lap Shear Strength , ISO 4587:

Mild steel (grit blasted)

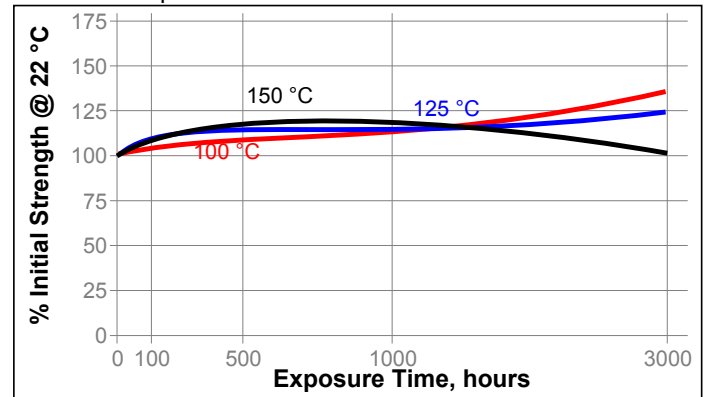
Hot Strength

Tested at temperature



Heat Aging

Stored at temperatures indicated and tested at 22°C.



Chemical/Solvent Resistance

Aged under conditions indicated and tested at 22 °C

Environment	°C	% of initial strength		
		500 h	1000 h	3000 h
Water	60	55	50	45
Water	90	50	40	20
Motor oil	22	85	75	75
Unleaded gasoline	22	95	90	75
Water/glycol 50/50	87	25	20	20
98% RH	40	95	85	85
Sodium Chloride, 7.5%	22	95	95	80
Acetone	22	85	75	75
Acetic Acid, 10%	22	85	75	50
Sodium hydroxide, 4%	22	90	85	80

GENERAL INFORMATION

This product is not recommended for use in pure oxygen and/or oxygen rich systems and should not be selected as a sealant for chlorine or other strong oxidizing materials.

For safe handling information on this product, consult the Material Safety Data Sheet, (MSDS).

Where aqueous washing systems are used to clean the surfaces before bonding, it is important to check for compatibility of the washing solution with the adhesive. In some cases these aqueous washes can affect the cure and performance of the adhesive.

Directions for use

1. For best performance surfaces for bonding should be clean, dry and free of grease. For high strength structural bonds, special surface treatments can increase the bond strength and durability.
2. To use, resin and hardener must be blended. Product can be applied directly from dual cartridges by dispensing through the mixer head supplied. Discard the first 3 to 8 cm of bead dispensed. Using twin cartridges or bulk containers, mix thoroughly by weight or volume in the proportions specified in the Product Description Matrix. For hand mixing, weigh or measure out the desired amount of resin and hardener and mix thoroughly. Mix approximately 15 seconds after uniform color is obtained.
3. **Do not mix quantities greater than 20 g in mass as excessive heat build-up can occur. Mixing smaller quantities will minimize the heat build-up.**
4. Apply the adhesive as quickly as possible after mixing to one surface to be joined. For maximum bond strength apply adhesive evenly to both surfaces. Parts should be assembled immediately after mixed adhesive has been applied.
5. Working life of the mixed adhesive is ≤ 4 minutes @ 22 °C. Higher temperature and larger quantities will shorten this working time.
6. Keep the assembled parts from moving during cure. The joint should be allowed to develop full strength before subjecting to any service loads.
7. Excess uncured adhesive can be wiped away with organic solvent (e.g. Acetone).
8. After use and before adhesive hardens, mixing and application equipment should be cleaned with hot soapy water.

Storage

Store product in the unopened container in a dry location. Storage information may be indicated on the product container labeling.

Optimal Storage: 8 °C to 21 °C. Storage below 8 °C or greater than 28 °C can adversely affect product properties.

Material removed from containers may be contaminated during use. Do not return product to the original container. Henkel Corporation cannot assume responsibility for product which has been contaminated or stored under conditions other than those previously indicated. If additional information is required, please contact your local Technical Service Center or Customer Service Representative.

Loctite Material Specification^{LMS}

LMS dated August 03, 2007. Test reports for each batch are available for the indicated properties. LMS test reports include selected QC test parameters considered appropriate to specifications for customer use. Additionally, comprehensive controls are in place to assure product quality and consistency. Special customer specification requirements may be coordinated through Henkel Quality.

Conversions

$(^{\circ}\text{C} \times 1.8) + 32 = ^{\circ}\text{F}$
 $\text{kV/mm} \times 25.4 = \text{V/mil}$
 $\text{mm} / 25.4 = \text{inches}$
 $\text{N} \times 0.225 = \text{lb}$
 $\text{N/mm} \times 5.71 = \text{lb/in}$
 $\text{N/mm}^2 \times 145 = \text{psi}$
 $\text{MPa} \times 145 = \text{psi}$
 $\text{N}\cdot\text{m} \times 8.851 = \text{lb}\cdot\text{in}$
 $\text{N}\cdot\text{m} \times 0.738 = \text{lb}\cdot\text{ft}$
 $\text{N}\cdot\text{mm} \times 0.142 = \text{oz}\cdot\text{in}$
 $\text{mPa}\cdot\text{s} = \text{cP}$

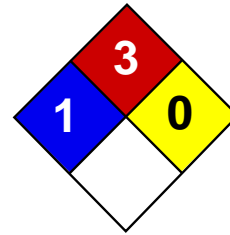
Note

The data contained herein are furnished for information only and are believed to be reliable. We cannot assume responsibility for the results obtained by others over whose methods we have no control. It is the user's responsibility to determine suitability for the user's purpose of any production methods mentioned herein and to adopt such precautions as may be advisable for the protection of property and of persons against any hazards that may be involved in the handling and use thereof. In light of the foregoing, **Henkel Corporation specifically disclaims all warranties expressed or implied, including warranties of merchantability or fitness for a particular purpose, arising from sale or use of Henkel Corporation's products. Henkel Corporation specifically disclaims any liability for consequential or incidental damages of any kind, including lost profits.** The discussion herein of various processes or compositions is not to be interpreted as representation that they are free from domination of patents owned by others or as a license under any Henkel Corporation patents that may cover such processes or compositions. We recommend that each prospective user test his proposed application before repetitive use, using this data as a guide. This product may be covered by one or more United States or foreign patents or patent applications.

Trademark usage

Except as otherwise noted, all trademarks in this document are trademarks of Henkel Corporation in the U.S. and elsewhere. ® denotes a trademark registered in the U.S. Patent and Trademark Office.

Reference 2.1



Health	2
Fire	3
Reactivity	0
Personal Protection	H

Material Safety Data Sheet Isopropyl alcohol MSDS

Section 1: Chemical Product and Company Identification

Product Name: Isopropyl alcohol

Catalog Codes: SLI1153, SLI1579, SLI1906, SLI1246, SLI1432

CAS#: 67-63-0

RTECS: NT8050000

TSCA: TSCA 8(b) inventory: Isopropyl alcohol

CI#: Not available.

Synonym: 2-Propanol

Chemical Name: isopropanol

Chemical Formula: C3-H8-O

Contact Information:

Sciencelab.com, Inc.

14025 Smith Rd.

Houston, Texas 77396

US Sales: **1-800-901-7247**

International Sales: **1-281-441-4400**

Order Online: ScienceLab.com

CHEMTREC (24HR Emergency Telephone), call:

1-800-424-9300

International CHEMTREC, call: 1-703-527-3887

For non-emergency assistance, call: 1-281-441-4400

Section 2: Composition and Information on Ingredients

Composition:

Name	CAS #	% by Weight
Isopropyl alcohol	67-63-0	100

Toxicological Data on Ingredients: Isopropyl alcohol: ORAL (LD50): Acute: 5045 mg/kg [Rat]. 3600 mg/kg [Mouse]. 6410 mg/kg [Rabbit]. DERMAL (LD50): Acute: 12800 mg/kg [Rabbit].

Section 3: Hazards Identification

Potential Acute Health Effects:

Hazardous in case of eye contact (irritant), of ingestion, of inhalation. Slightly hazardous in case of skin contact (irritant, sensitizer, permeator).

Potential Chronic Health Effects:

Slightly hazardous in case of skin contact (sensitizer). CARCINOGENIC EFFECTS: A4 (Not classifiable for human or animal.) by ACGIH, 3 (Not classifiable for human.) by IARC. MUTAGENIC EFFECTS: Not available. TERATOGENIC EFFECTS: Not available. DEVELOPMENTAL TOXICITY: Classified Reproductive system/toxin/female, Development toxin [POSSIBLE]. The substance may be toxic to kidneys, liver, skin, central nervous system (CNS). Repeated or prolonged exposure to the substance can produce target organs damage.

Section 4: First Aid Measures

Eye Contact:

Check for and remove any contact lenses. In case of contact, immediately flush eyes with plenty of water for at least 15 minutes. Cold water may be used. Get medical attention.

Skin Contact:

Wash with soap and water. Cover the irritated skin with an emollient. Get medical attention if irritation develops. Cold water may be used.

Serious Skin Contact: Not available.

Inhalation:

If inhaled, remove to fresh air. If not breathing, give artificial respiration. If breathing is difficult, give oxygen. Get medical attention if symptoms appear.

Serious Inhalation:

Evacuate the victim to a safe area as soon as possible. Loosen tight clothing such as a collar, tie, belt or waistband. If breathing is difficult, administer oxygen. If the victim is not breathing, perform mouth-to-mouth resuscitation. Seek medical attention.

Ingestion:

Do NOT induce vomiting unless directed to do so by medical personnel. Never give anything by mouth to an unconscious person. Loosen tight clothing such as a collar, tie, belt or waistband. Get medical attention if symptoms appear.

Serious Ingestion: Not available.

Section 5: Fire and Explosion Data

Flammability of the Product: Flammable.

Auto-Ignition Temperature: 399°C (750.2°F)

Flash Points: CLOSED CUP: 11.667°C (53°F) - 12.778 deg. C (55 deg. F) (TAG)

Flammable Limits: LOWER: 2% UPPER: 12.7%

Products of Combustion: These products are carbon oxides (CO, CO₂).

Fire Hazards in Presence of Various Substances:

Highly flammable in presence of open flames and sparks, of heat. Flammable in presence of oxidizing materials. Non-flammable in presence of shocks.

Explosion Hazards in Presence of Various Substances:

Risks of explosion of the product in presence of mechanical impact: Not available. Explosive in presence of open flames and sparks, of heat.

Fire Fighting Media and Instructions:

Flammable liquid, soluble or dispersed in water. SMALL FIRE: Use DRY chemical powder. LARGE FIRE: Use alcohol foam, water spray or fog.

Special Remarks on Fire Hazards:

Vapor may travel considerable distance to source of ignition and flash back. CAUTION: MAY BURN WITH NEAR INVISIBLE FLAME. Hydrogen peroxide sharply reduces the autoignition temperature of Isopropyl alcohol. After a delay, Isopropyl alcohol ignites on contact with dioxigenyl tetrafluoroborate, chromium trioxide, and potassium tert-butoxide. When heated to decomposition it emits acrid smoke and fumes.

Special Remarks on Explosion Hazards:

Secondary alcohols are readily autooxidized in contact with oxygen or air, forming ketones and hydrogen peroxide. It can become potentially explosive. It reacts with oxygen to form dangerously unstable peroxides which can concentrate and explode during distillation or evaporation. The presence of 2-butanone increases the reaction rate for peroxide formation. Explosive in the form of vapor when exposed to heat or flame. May form explosive mixtures with air. Isopropyl alcohol + phosgene forms isopropyl chloroformate and hydrogen chloride. In the presence of iron salts, thermal decomposition can occur, which in some cases can become explosive. A homogeneous mixture of concentrated peroxides + isopropyl alcohol are capable of detonation by shock or heat. Barium perchlorate + isopropyl alcohol gives the highly explosive alkyl perchlorates.

It forms explosive mixtures with trinitormethane and hydrogen peroxide. It produces a violent explosive reaction when heated with aluminum isopropoxide + crotonaldehyde. Mixtures of isopropyl alcohol + nitroform are explosive.

Section 6: Accidental Release Measures

Small Spill:

Dilute with water and mop up, or absorb with an inert dry material and place in an appropriate waste disposal container.

Large Spill:

Flammable liquid. Keep away from heat. Keep away from sources of ignition. Stop leak if without risk. Absorb with DRY earth, sand or other non-combustible material. Do not touch spilled material. Prevent entry into sewers, basements or confined areas; dike if needed. Be careful that the product is not present at a concentration level above TLV. Check TLV on the MSDS and with local authorities.

Section 7: Handling and Storage

Precautions:

Keep away from heat. Keep away from sources of ignition. Ground all equipment containing material. Do not ingest. Do not breathe gas/fumes/ vapor/spray. Avoid contact with eyes. Wear suitable protective clothing. In case of insufficient ventilation, wear suitable respiratory equipment. If ingested, seek medical advice immediately and show the container or the label. Keep away from incompatibles such as oxidizing agents, acids.

Storage:

Store in a segregated and approved area. Keep container in a cool, well-ventilated area. Keep container tightly closed and sealed until ready for use. Avoid all possible sources of ignition (spark or flame).

Section 8: Exposure Controls/Personal Protection

Engineering Controls:

Provide exhaust ventilation or other engineering controls to keep the airborne concentrations of vapors below their respective threshold limit value. Ensure that eyewash stations and safety showers are proximal to the work-station location.

Personal Protection:

Splash goggles. Lab coat. Vapor respirator. Be sure to use an approved/certified respirator or equivalent. Gloves.

Personal Protection in Case of a Large Spill:

Splash goggles. Full suit. Vapor respirator. Boots. Gloves. A self contained breathing apparatus should be used to avoid inhalation of the product. Suggested protective clothing might not be sufficient; consult a specialist BEFORE handling this product.

Exposure Limits:

TWA: 983 STEL: 1230 (mg/m³) [Australia] TWA: 200 STEL: 400 (ppm) from ACGIH (TLV) [United States] [1999] TWA: 980 STEL: 1225 (mg/m³) from NIOSH TWA: 400 STEL: 500 (ppm) from NIOSH TWA: 400 STEL: 500 (ppm) [United Kingdom (UK)] TWA: 999 STEL: 1259 (mg/m³) [United Kingdom (UK)] TWA: 400 STEL: 500 (ppm) from OSHA (PEL) [United States] TWA: 980 STEL: 1225 (mg/m³) from OSHA (PEL) [United States] Consult local authorities for acceptable exposure limits.

Section 9: Physical and Chemical Properties

Physical state and appearance: Liquid.

Odor:

Pleasant. Odor resembling that of a mixture of ethanol and acetone.

Taste: Bitter. (Slight.)

Molecular Weight: 60.1 g/mole

Color: Colorless.

pH (1% soln/water): Not available.

Boiling Point: 82.5°C (180.5°F)

Melting Point: -88.5°C (-127.3°F)

Critical Temperature: 235°C (455°F)

Specific Gravity: 0.78505 (Water = 1)

Vapor Pressure: 4.4 kPa (@ 20°C)

Vapor Density: 2.07 (Air = 1)

Volatility: Not available.

Odor Threshold:

22 ppm (Sittig, 1991) 700 ppm for unadapted panelists (Verschuren, 1983).

Water/Oil Dist. Coeff.: The product is equally soluble in oil and water; $\log(\text{oil/water}) = 0.1$

Ionicity (in Water): Not available.

Dispersion Properties: See solubility in water, methanol, diethyl ether, n-octanol, acetone.

Solubility:

Easily soluble in cold water, hot water, methanol, diethyl ether, n-octanol, acetone. Insoluble in salt solution. Soluble in benzene. Miscible with most organic solvents including alcohol, ethyl alcohol, chloroform.

Section 10: Stability and Reactivity Data

Stability: The product is stable.

Instability Temperature: Not available.

Conditions of Instability: Heat, Ignition sources, incompatible materials

Incompatibility with various substances: Reactive with oxidizing agents, acids, alkalis.

Corrosivity: Non-corrosive in presence of glass.

Special Remarks on Reactivity:

Reacts violently with hydrogen + palladium combination, nitroform, oleum, COCl₂, aluminum triisopropoxide, oxidants
Incompatible with acetaldehyde, chlorine, ethylene oxide, isocyanates, acids, alkaline earth, alkali metals, caustics, amines, crotonaldehyde, phosgene, ammonia. Isopropyl alcohol reacts with metallic aluminum at high temperatures. Isopropyl alcohol attacks some plastics, rubber, and coatings. Vigorous reaction with sodium dichromate + sulfuric acid.

Special Remarks on Corrosivity: May attack some forms of plastic, rubber and coating

Polymerization: Will not occur.

Section 11: Toxicological Information

Routes of Entry: Absorbed through skin. Dermal contact. Eye contact. Inhalation.

Toxicity to Animals:

WARNING: THE LC50 VALUES HEREUNDER ARE ESTIMATED ON THE BASIS OF A 4-HOUR EXPOSURE. Acute oral toxicity (LD50): 3600 mg/kg [Mouse]. Acute dermal toxicity (LD50): 12800 mg/kg [Rabbit]. Acute toxicity of the vapor (LC50): 16000 8 hours [Rat].

Chronic Effects on Humans:

CARCINOGENIC EFFECTS: A4 (Not classifiable for human or animal.) by ACGIH, 3 (Not classifiable for human.) by IARC.
DEVELOPMENTAL TOXICITY: Classified Reproductive system/toxin/female, Development toxin [POSSIBLE]. May cause damage to the following organs: kidneys, liver, skin, central nervous system (CNS).

Other Toxic Effects on Humans:

Hazardous in case of ingestion, of inhalation. Slightly hazardous in case of skin contact (irritant, sensitizer, permeator).

Special Remarks on Toxicity to Animals: Not available.

Special Remarks on Chronic Effects on Humans:

May cause adverse reproductive/teratogenic effects (fertility, fetotoxicity, developmental abnormalities(developmental toxin)) based on animal studies. Detected in maternal milk in human.

Special Remarks on other Toxic Effects on Humans:

Acute Potential Health Effects: Skin: May cause mild skin irritation, and sensitization. Eyes: Can cause eye irritation. Inhalation: Breathing in small amounts of this material during normal handling is not likely to cause harmful effects. However, breathing large amounts may be harmful and may affect the respiratory system and mucous membranes (irritation), behavior and brain (Central nervous system depression - headache, dizziness, drowsiness, stupor, incoordination, unconsciousness, coma and possible death), peripheral nerve and sensation, blood, urinary system, and liver. Ingestion: Swallowing small amounts during normal handling is not likely to cause harmful effects. Swallowing large amounts may be harmful. Swallowing large amounts may cause gastrointestinal tract irritation with nausea, vomiting and diarrhea, abdominal pain. It also may affect the urinary system, cardiovascular system, sense organs, behavior or central nervous system (somnolence, generally depressed activity, irritability, headache, dizziness, drowsiness), liver, and respiratory system (breathing difficulty). Chronic Potential Health Effects: May cause defatting of the skin and dermatitis and allergic reaction. May cause adverse reproductive effects based on animal data (studies).

Section 12: Ecological Information

Ecotoxicity: Ecotoxicity in water (LC50): 100000 mg/l 96 hours [Fathead Minnow]. 64000 mg/l 96 hours [Fathead Minnow].

BOD5 and COD: Not available.

Products of Biodegradation:

Possibly hazardous short term degradation products are not likely. However, long term degradation products may arise.

Toxicity of the Products of Biodegradation: The product itself and its products of degradation are not toxic.

Special Remarks on the Products of Biodegradation: Not available.

Section 13: Disposal Considerations

Waste Disposal:

Waste must be disposed of in accordance with federal, state and local environmental control regulations.

Section 14: Transport Information

DOT Classification: CLASS 3: Flammable liquid.

Identification : Isopropyl Alcohol UNNA: 1219 PG: II

Special Provisions for Transport: Not available.

Section 15: Other Regulatory Information

Federal and State Regulations:

Connecticut hazardous material survey.: Isopropyl alcohol Illinois toxic substances disclosure to employee act: Isopropyl alcohol Rhode Island RTK hazardous substances: Isopropyl alcohol Pennsylvania RTK: Isopropyl alcohol Florida: Isopropyl alcohol Minnesota: Isopropyl alcohol Massachusetts RTK: Isopropyl alcohol New Jersey: Isopropyl alcohol New Jersey spill list: Isopropyl alcohol Director's list of Hazardous Substances: Isopropyl alcohol Tennessee: Isopropyl alcohol TSCA 8(b) inventory: Isopropyl alcohol TSCA 4(a) final testing order: Isopropyl alcohol TSCA 8(a) IUR: Isopropyl alcohol TSCA 8(d) H

and S data reporting: Isopropyl alcohol: Effective date: 12/15/86 Sunset Date: 12/15/96 TSCA 12(b) one time export: Isopropyl alcohol SARA 313 toxic chemical notification and release reporting: Isopropyl alcohol

Other Regulations:

OSHA: Hazardous by definition of Hazard Communication Standard (29 CFR 1910.1200). EINECS: This product is on the European Inventory of Existing Commercial Chemical Substances.

Other Classifications:

WHMIS (Canada):

CLASS B-2: Flammable liquid with a flash point lower than 37.8°C (100°F). CLASS D-2B: Material causing other toxic effects (TOXIC).

DSCL (EEC):

R11- Highly flammable. R36- Irritating to eyes. S7- Keep container tightly closed. S16- Keep away from sources of ignition - No smoking. S24/25- Avoid contact with skin and eyes. S26- In case of contact with eyes, rinse immediately with plenty of water and seek medical advice.

HMIS (U.S.A.):

Health Hazard: 2

Fire Hazard: 3

Reactivity: 0

Personal Protection: h

National Fire Protection Association (U.S.A.):

Health: 1

Flammability: 3

Reactivity: 0

Specific hazard:

Protective Equipment:

Gloves. Lab coat. Vapor respirator. Be sure to use an approved/certified respirator or equivalent. Wear appropriate respirator when ventilation is inadequate. Splash goggles.

Section 16: Other Information

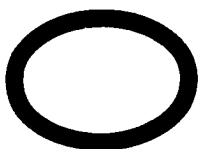
References: Not available.

Other Special Considerations: Not available.

Created: 10/09/2005 05:53 PM

Last Updated: 11/01/2010 12:00 PM

The information above is believed to be accurate and represents the best information currently available to us. However, we make no warranty of merchantability or any other warranty, express or implied, with respect to such information, and we assume no liability resulting from its use. Users should make their own investigations to determine the suitability of the information for their particular purposes. In no event shall ScienceLab.com be liable for any claims, losses, or damages of any third party or for lost profits or any special, indirect, incidental, consequential or exemplary damages, howsoever arising, even if ScienceLab.com has been advised of the possibility of such damages.



ESSO PETROLEUM COMPANY LIMITED

PRODUCT HEALTH AND SAFETY DATA

PAGE 1

1. IDENTIFICATION OF THE SUBSTANCE/PREPARATION

PRODUCT: MARCOL 52
PRODUCT #: U-3151
PHSD #: 61-4060000
DATE OF ISSUE: DECEMBER 1992

ESSO PETROLEUM COMPANY LIMITED
ESSO HOUSE
ERMYN WAY
LEATHERHEAD
SURREY KT22 8UX

IN AN EMERGENCY PLEASE CONTACT:
01372 223131

2. COMPOSITION/INFORMATION ON INGREDIENTS

Ingredients present at or above 0.1 wt% (classified as toxic or very toxic) or 1 wt% (classified as harmful, irritant or corrosive).

HAZARDOUS INGREDIENT	APPROXIMATE CONCENTRATION
----------------------	---------------------------

-----	-----
None	

3. HAZARD IDENTIFICATION

This product contains a highly refined base oil and is not considered to present any hazard during normal use, although the OEL for oil mist should be observed.

4. FIRST AID

INHALATION:

At ambient/normal handling temperatures (0-38 deg. C), no adverse effects due to inhalation of vapour are expected.

SKIN CONTACT:

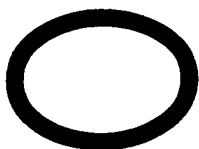
No adverse effects due to skin contact are expected.

EYE CONTACT:

No adverse effects due to eye contact are expected.

INGESTION:

DO NOT induce vomiting since it is important that no amount of the material should enter the lungs (aspiration). Keep at rest. Get prompt medical attention.



ESSO PETROLEUM COMPANY LIMITED

PRODUCT HEALTH AND SAFETY DATA

PAGE 2

PRODUCT: MARCOL 52

5. FIRE-FIGHTING MEASURES

EXTINGUISHING MEDIA:

Foam, dry chemical powder, carbon dioxide.

FIRE AND EXPLOSION HAZARDS:

Combustible material, low hazard. The product can form flammable mixtures or can burn only on heating above the flash point. However, minor contamination by hydrocarbons of higher volatility may increase the hazard.

SPECIAL FIRE-FIGHTING PROCEDURES:

Water fog or spray, to cool fire-exposed surfaces (e.g. containers) and to protect personnel, should only be used by personnel trained in fire fighting.

Cut off "fuel"; depending on circumstances, either allow the fire to burn out under controlled conditions or use foam or dry chemical powder to extinguish the fire.

Respiratory and eye protection required for fire fighting personnel exposed to fumes or smoke.

HAZARDOUS COMBUSTION PRODUCTS:

Smoke, and carbon monoxide may be formed in the event of incomplete combustion.

6. ACCIDENTAL RELEASE MEASURES

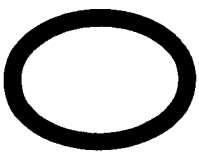
PERSONAL PRECAUTIONS: See Section 8.

LAND SPILL:

Shut off source taking normal safety precautions. Prevent liquid from entering sewers, water courses or low lying areas; advise the relevant authorities if it has, or if it contaminates soil/vegetation. Take measures to minimise the effects on ground water.

Recover by skimming or pumping using explosion-proof equipment, or contain spilled liquid with booms, sand, or other suitable absorbent and remove mechanically into containers.

If necessary, dispose of adsorbed residues as directed in Section 13.



ESSO PETROLEUM COMPANY LIMITED

PRODUCT HEALTH AND SAFETY DATA

PAGE 3

PRODUCT: MARCOL 52

6. ACCIDENTAL RELEASE MEASURES (Continued)

WATER SPILL:

Confine the spill immediately with booms. Warn other shipping. Notify port and other relevant authorities.

Remove from the surface by skimming or with suitable absorbents. Disperse the residue in unconfined waters, if permitted by local authorities and environmental agencies.

7. HANDLING AND STORAGE

Store the product in cool, well ventilated surroundings, well away from sources of ignition.

Provide suitable mechanical equipment for the safe handling of drums and heavy packages.

Electrical equipment and fittings must comply with local regulations regarding fire prevention with this class of product.

LOAD/UNLOAD TEMPERATURE deg. C: Ambient to max. 50 C

STORAGE TEMPERATURE deg. C: 0 C to max. 40 C

SPECIAL PRECAUTIONS:

Take extreme care to avoid contamination by other products and materials.

Keep containers closed when not in use.

Prevent small spills and leakages to avoid slip hazard.

8. EXPOSURE CONTROLS AND PERSONAL PROTECTION

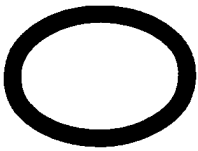
OCCUPATIONAL EXPOSURE LIMIT:

5 mg/m³ for oil mists (TWA, 8h - workday) recommended based upon the ACGIH TLV (Analysis according to US NIOSH Method 5026, NIOSH Manual of Analytical Methods, 3rd Ed.).

PERSONAL PROTECTION:

In open systems where contact is likely, wear safety glasses with side shields.

When concentrations in air may exceed the occupational exposure limit, and where engineering, work practices, or other means of exposure reduction are not adequate, approved respirators may be required.



ESSO PETROLEUM COMPANY LIMITED

PRODUCT HEALTH AND SAFETY DATA

PAGE 4

PRODUCT: MARCOL 52

9. PHYSICAL AND CHEMICAL PROPERTIES

APPEARANCE / ODOUR:

Clear colourless liquid, neutral odour.

DENSITY, g/ml: 0.84 at 15 deg. C (range 0.82 - 0.84)

BOILING RANGE: 316.0 deg. C IBP.

VISCOSITY, mm²/S: 6.9 at 40 deg. C Range 6.8 - 7.9

VAPOUR PRESSURE, kPa: at 20 deg. C max. 0.01

VAPOUR DENSITY AT 1 BAR (Air=1): Data not available.

EVAPORATION RATE (n-butyl acetate=1): <0.01

SOLUBILITY IN WATER: 20 deg. C Negligible

pH: Not Applicable.

FLASH POINT: > 148 deg. C METHOD: COC

FLAMMABILITY LIMITS IN AIR, % BY VOL:

LEL: 1.0 UEL: 6.0 Approx.

AUTOIGNITION TEMPERATURE: Data not available.

PARTITION COEFFICIENT n-octanol/water: Data not available.

10. STABILITY AND REACTIVITY

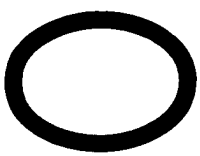
STABILITY (THERMAL, LIGHT, ETC): Stable

CONDITIONS TO AVOID:

Keep away from heat sources, open flames and other sources of ignition.

INCOMPATIBLE MATERIALS:

Avoid contact with strong oxidants such as liquid chlorine and concentrated oxygen.



**ESSO PETROLEUM COMPANY LIMITED
PRODUCT HEALTH AND SAFETY DATA**

PAGE 5

PRODUCT: MARCOL 52

10. STABILITY AND REACTIVITY (Continued)

HAZARDOUS DECOMPOSITION PRODUCTS:

Product does not decompose at ambient temperature.

11. TOXICOLOGICAL INFORMATION

EFFECTS OF OVER EXPOSURE:

INHALATION:

No hazard in normal industrial use.

SKIN CONTACT:

Not considered to be a hazard.

EYE CONTACT:

Not considered to be a hazard.

INGESTION:

No hazard in normal industrial use.

Minute amounts aspirated into the lungs during ingestion or vomiting may cause severe pulmonary injury and death.

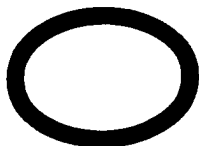
CHRONIC:

Contains lubricating oil base stocks. Base oils of similar composition and refining history have exhibited no carcinogenic activity in laboratory animals.

TOXICITY DATA:

ACUTE:

No test data are available for this product. The potential health hazards were therefore derived from what is known of the toxicity of base oils in general. The general effects of base oils of this type are well known and are described in numerous publications including CONCAWE Report 5/87 "Health Aspects of Lubricants".



ESSO PETROLEUM COMPANY LIMITED
PRODUCT HEALTH AND SAFETY DATA

PAGE 6

PRODUCT: MARCOL 52

11. TOXICOLOGICAL INFORMATION (Continued)

CHRONIC:

Although there is no specific test data on the base oil components, the base oil would not be expected to exhibit carcinogenic potential based upon what is known of the toxicity of base oils in general.

12. ECOLOGICAL INFORMATION

In the absence of specific environmental data for this product, this assessment is based on information for general hydrocarbon components found in lubricant mineral oils. Lubricant mineral oils, immediately following a release into the environment, will remain largely on the soil surface, and in water, will remain largely on the water surface. Based on chemical/physical information from the literature for this product category, no harmful effects to terrestrial or aquatic habitats would be expected. This product is expected to be resistant to biodegradation and to persist in the environment. This product may contain additives for which no environmental data is available. Hence, the above assessment concerns the base oil(s) only.

13. DISPOSAL CONSIDERATIONS

Collect and dispose of waste product at an authorised disposal facility, in conformance with national and local regulations, and in accordance with EEC Directives on the disposal of waste oil.

14. TRANSPORT INFORMATION

USUAL SHIPPING CONTAINERS:

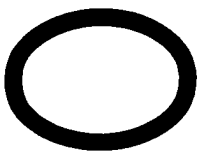
Rail cars, tank trucks, drums.

TRANSPORT TEMPERATURE deg. C: Ambient to max. 40 C

15. REGULATORY INFORMATION

EC DANGEROUS SUBSTANCES/PREPARATIONS CLASSIFICATION:

Not Regulated



**ESSO PETROLEUM COMPANY LIMITED
PRODUCT HEALTH AND SAFETY DATA**

PAGE 7

PRODUCT: **MARCOL 52**

15. REGULATORY INFORMATION (Continued)

Refer to your national legislation implementing the EC Directive 91/155/EC

16. OTHER INFORMATION

PRODUCT TYPE / USES:

White oil meets US and European Pharmacopoeia requirements;
complies with FDA regulations 21 CFR 172.878 and 178.3620(a)

SOURCE OF KEY DATA:

The recommendations presented in this Material Safety Data Sheet were compiled from actual test data (when available), comparison with similar products, component information from suppliers and from recognised codes of good practice.

The information and recommendations contained herein are, to the best of Exxon's knowledge and belief, accurate and reliable as of the date issued, but are offered without guarantee or warranty. They relate to the specific material designated and may not be valid for such material used in combination with any other materials or in any process. Conditions of use of the material are under the control of the user; therefore, it is the user's responsibility to satisfy himself as to the suitability and completeness of such information for his own particular use.



MATERIAL SAFETY DATA SHEET

SECTION 1: CHEMICAL PRODUCT AND COMPANY IDENTIFICATION

PRODUCT: M-Bond 200 Adhesive

August 17, 2007

Vishay Micro-Measurements
Post Office Box 27777
Raleigh, NC 27611

MSDS # MGM007T

919-365-3800

CHEMTREC 1-800-424-9300 (U.S.)
703-527-3887 (Outside U.S.)

NOTE: CHEMTREC numbers to be used only in the event of chemical emergencies involving a spill, leak, fire, exposure or accident involving chemicals.

SECTION 2: HAZARDOUS INGREDIENTS / IDENTITY INFORMATION

NOTE: This material is purchased from a number of suppliers and distributed by Vishay Micro-Measurements. To ensure that you have the appropriate information, cross-reference the following data with the manufacturer's label on the product you purchased.

CAS NUMBER	CHEMICAL IDENTITY	%
Methyl Cyanoacrylate Adhesive MC-100 (Chemence, Inc.)		
137-05-3	Methyl 2-Cyanoacrylate	90-95
9011-14-7	Poly Methyl Methacrylate	5-10
123-31-9	Hydroquinone	0.1-0.5
Cyberbond APOLLO 2010 (Cyberbond, L.L.C.)		
7085-85-0	Ethyl 2 Cyanoacrylate	80-90
9011-14-7	Poly Methyl Methacrylate	10-20
SI 120 Cyanoacrylate Adhesive (Adhesive Systems, Inc.)		
7085-85-0	Ethyl Cyanoacrylate	86-99.99

M-Bond 200 Adhesive

MSDS # MGM007T

414 Superbond (Henkle Loctite Corporation)

7085-85-0

Ethyl Cyanoacrylate

60-100

Instabond S-100 (Accrabond Inc.)

7085-85-0

Ethyl Cyanoacrylate

70-100

SECTION 3: HEALTH HAZARD DATA

Routes of Entry:

Inhalation: YES **Skin:** YES **Ingestion:** Accidental

Health Hazards (Acute and Chronic): Bonds skin rapidly and strongly.

Carcinogenicity:

NTP:	Not listed
IARC Monographs:	Not listed
OSHA Regulated:	Not listed

Signs and Symptoms of Exposure:

INHALATION: Vapor is irritating to nose and bronchial passages. Prolonged and repeated over-exposure to vapors may produce allergic reactions with asthma-like symptoms in sensitive individuals.

EYE CONTACT: Cyanoacrylates may bond eyelid to eyelid and/or eye.

SKIN CONTACT: Cyanoacrylates bond skin rapidly and strongly. A large drop may cause burn upon solidification.

INGESTION: It is almost impossible to swallow cyanoacrylates. The adhesive solidifies and adheres in mouth. Lips may become stuck together.

Conditions Generally Aggravated by Exposure: None known.

SECTION 4: EMERGENCY AND FIRST AID PROCEDURES

Information for first aid and casualty on treatment for adhesion of human skin to itself if caused by cyanoacrylate adhesives.

Cyanoacrylate adhesive is a very fast setting and strong adhesive. It bonds human tissue including skin in seconds. Experience has shown that accidents due to cyanoacrylates are handled best by passive, non-surgical first aid. Treatment of specific types of accidents are given below.

SKIN CONTACT: Remove excess adhesive. Soak in warm, soapy water. The adhesive will come loose from the skin in several hours. Dried adhesive does not present a health hazard even when bonded to the skin. Avoid contact with clothes, fabric, rags or tissue. Contact with these materials may cause polymerization. The polymerization of large amounts of adhesive will generate heat causing smoke, skin burns, and strong, irritating vapors. Wear rubber or polyethylene gloves and an apron when handling large amounts of adhesive.

SKIN ADHESION: First, immerse the bonded surface in warm soapy water. Peel or roll the surfaces apart with the aid of a blunt edge, e.g. a spatula or a teaspoon handle; then remove adhesive from the skin with soap and water. Do not try to pull surfaces apart with a direct opposing action.

EYELID TO EYELID OR EYEBALL ADHESION: In the event that eyelids are stuck together or bonded to the eyeball, wash thoroughly with warm water and apply a gauze patch. The eye will open without further action, typically in 1 - 4 days. There will be no residual damage. Do not try to open the eyes by manipulation.

ADHESIVE ON THE EYEBALL: Cyanoacrylate introduced into the eyes will attach itself to the eye protein and will disassociate from it over an indeterminable period, generally covering several hours. This will cause periods of weeping until clearance is achieved. During the period of contamination, double vision may be experienced together with a lachrymatory effect, and it is important to understand the cause and realize that disassociation will normally occur within a matter of hours, even with gross contamination.

MOUTH: If lips are accidentally stuck together, apply lots of warm water to the lips and encourage maximum wetting and pressure from saliva inside the mouth. Peel or roll lips apart. Do not try to pull the lips with direct opposing action.

It is almost impossible to swallow cyanoacrylate. The adhesive solidifies and adheres in the mouth. Saliva will lift the adhesive in 1/2 to 2 days. In case a lump forms in the mouth, position the patient to prevent ingestion of the lump when it detaches.

INGESTION: Saliva should lift the adhesive in 12 to 48 hours. Do not force removal. Do not swallow the adhesive when it loosens.

BURNS: Cyanoacrylates give off heat on solidification. In rare cases a large drop will increase in temperature enough to cause a burn.

Burns should be treated normally after the lump of cyanoacrylate is released from the tissue as described above.

SURGERY: It should never be necessary to use such a drastic method to separate accidentally bonded skin.

INHALATION: Move to fresh air. If symptoms persist, call a physician.

SECTION 5: FIRE AND EXPLOSION HAZARD DATA

Flash Point (Method Used): 150°F - 200°F Tag Closed Cup

Flammable limits: LEL: Not determined UEL: Not determined

Extinguishing Media: Carbon dioxide, foam, dry chemical.

Special Firefighting Procedures: Firefighters should wear proper protective clothing and self-contained breathing apparatus.

Unusual Fire and Explosion Hazards: Vapors exceeding the flash point will ignite when exposed to flame.

SECTION 6: ACCIDENTAL RELEASE MEASURES

Steps to be taken if material is released or spilled: Flood with water to polymerize cyanoacrylate adhesive and to control product vapors. Soak up with an inert absorbent or scrape up cured product.

SECTION 7: EXPOSURE CONTROLS -- PERSONAL PROTECTION

Respiratory Protection: Use fresh air breathing apparatus or solvent filter mask when exposed to large quantities.

Ventilation: Positive down-draft exhaust ventilation should be provided to maintain vapor concentration below TLV.

Local Exhaust: Keep below TLV.

Mechanical: Keep below TLV.

Special: N/A

Other: N/A

Protective Gloves: Polyethylene gloves recommended. Do not use cotton gloves.

Eye Protection: Safety glasses or goggles.

Other Protective Clothing or Equipment: Polyethylene apron recommended.

Work / Hygienic Practices: Wash hands thoroughly after using product.

SECTION 8: HANDLING AND STORAGE

Precautions to be taken in handling and storing: Store at or below 75°F to maximize shelf life. Avoid contact with skin and eyes. Avoid breathing vapors.

Other Precautions: None.

SECTION 9: PHYSICAL AND CHEMICAL PROPERTIES
--

Boiling Point:	>300°F (149°C)
Vapor Pressure (mmHg):	<0.2 @ 75°F (24°C)
Vapor Density (Air = 1):	>1
Specific Gravity (H₂O = 1):	1.09
Melting Point:	Not determined
Evaporation Rate (BuAc = 1):	Not determined
Volatile Organic Compounds:	≈ 1000 g/liter

Solubility in Water: Insoluble; polymerized by water.

Appearance and Odor: Clear liquid with sharp, pungent odor.

SECTION 10: STABILITY AND REACTIVITY DATA
--

Stability: Stable.

Conditions to Avoid: High temperatures.

Incompatibility (Materials to Avoid): Water, alcohols, amines, alkalies, peroxides, cotton and wool.

Hazardous Decomposition or By-products: None known.

Hazardous Polymerization: Will not occur.

SECTION 11: TOXICOLOGICAL INFORMATION
--

Methyl Cyanoacrylate

OSHA PEL:	Not Established
ACGIH TLV:	2 ppm TWA Estimated
OTHER:	None

Ethyl Cyanoacrylate

OSHA PEL:	Not known
ACGIH TLV:	2 ppm TWA
ACGIH STEL:	4 ppm TWA
OTHER:	None

Poly Methyl Methacrylate

OSHA PEL:	None
ACGIH TLV:	None
OTHER:	None

Hydroquinone

OSHA PEL: 2 mg/M³ TWA
 ACGIH TLV: 2 mg/M³ TWA
 OTHER: 4 mg/m³ STEL

SECTION 12: DISPOSAL CONSIDERATIONS
--

Waste Disposal Method: Dispose of in accordance with local, state, and federal regulations.

SECTION 13: TRANSPORTATION INFORMATION

SHIPPING NAME	CLASS	UN NUMBER
---------------	-------	-----------

Not regulated.

SECTION 14: REGULATORY INFORMATION

SECTION 313 SUPPLIER NOTIFICATION:

This product contains a toxic chemical or chemicals (as listed below) subject to the reporting requirements of Section 313 Title III of the Superfund Amendment and Reauthorization Act of 1986 and 40 CFR Part 372.

CAS NUMBER	CHEMICAL NAME	% BY WEIGHT
123-31-9	Hydroquinone	0.1-0.5

TSCA NOTIFICATION:

All components of this product are listed in the Toxic Substance Control Act Chemical Substance Inventory (TSCA).

SECTION 15: OTHER INFORMATION

To the best of our knowledge, the information provided above meets the requirements of the United States Occupational Safety and Health Act and regulations established under 29 CFR 1910.1200 (g)(2)(c)(1)-(4) for a mixture of hazardous chemicals which has not been tested as a whole. The data provided on this Material Safety Data Sheet is from manufacturers of the original components. Vishay Micro-Measurements specifically disclaims any and all form of liability and/or responsibility for the application of this product.

=====
Product Identification
=====

MSDS NAME:M-BOND 200 CATALYST B
NIIN:00N063528
MSDS Number: BYXBS
=== Responsible Party ===
Company:MEASUREMENTS GROUP INC
Box:27777
City:RALEIGH
State:NC
ZIP:27611
Country:US
Info Phone Num:919-365-3800
Emergency Phone Num:800-424-9300 (CHEMTREC)
Preparer's Name:R.L. FRIDLEY
CAGE:88952

==== Contractor Identification ===

Company:MEASUREMENTS GROUP INC
Address:9517 US 64 HWY
Box:City:WENDELL
State:NC
ZIP:27591
Country:US
Phone:919-365-3800
CAGE:88952

=====
Composition/Information on Ingredients
=====

Name:ISOPROPYL ALCOHOL; (2-PROPANOL) (SARA 313) LD50: (ORAL,
RAT) 5840 MG/KG
CAS:67-63-0
RTECS #:NT8050000
Fraction by Wt: 98%
OSHA PEL:400 PPM
ACGIH TLV:400 PPM; 500 STEL

Name:ETHANOL, 2-(ETHYLPHENYLAMINO)-; (PHENYLETHYLETHANOLAMINE)
CAS:92-50-2
RTECS #:KL0878000
Fraction by Wt: 2%
OSHA PEL:N/K
ACGIH TLV:N/K

Name:VOLATILE ORGANIC COMPOUND: 98%
RTECS #:9999999V0

OSHA PEL:N/K
ACGIH TLV:N/K

=====
Hazards Identification
=====

LD50 LC50 Mixture:SEE INGREDIENT 1

Routes of Entry: Inhalation:YES Skin:YES Ingestion:YES

Reports of Carcinogenicity:NTP:NO IARC:NO OSHA:NO

Health Hazards Acute and Chronic:INHALATION: IRRITATION OF NOSE AND THROAT, HEADACHE, NAUSEA, VOMITING, DIZZINESS, DROWSINESS, IRRITATION OF UPPER RESPIRATORY TRACT, UNCONSCIOUSNESS. EYES: IRRITATION; MAY CAUSE TEMPORARY CORNEAL DAMA GE. SKIN: IRRITATION; PROLONGED CONTACTMAY CAUSE DERMATITIS. INGESTION: HEADACHE, NAUSEA, VOMITING, (EFTS OF OVEREXP)

Explanation of Carcinogenicity:NOT RELEVANT

Effects of Overexposure:HLTH HAZ: DIZZINESS, GASTROINTESTINAL IRRITATION.

Medical Cond Aggravated by Exposure:NONE KNOWN.

=====
First Aid Measures
=====

First Aid:INHALATION: REMOVE TO FRESH AIR. IF NOT BREATHING, GIVE ARTIFICIAL RESPIRATION. IF BREATHING IS DIFFICULT, GIVE OXYGEN. EYES: IMMEDIATELY FLUSH WITH PLENTY OF WATER FOR AT LEAST 15 MINUTES. INGESTION: CALL MD. IF SWALLOWED, IF CONSCIOUS, GIVE LARGE AMOUNTS OF WATER. INDUCE VOMITING. SKIN: FLUSH SKIN WITH WATER.

=====
Fire Fighting Measures
=====

Flash Point Method:CC

Flash Point:53.0F,11.7C

Lower Limits:2.0%

Upper Limits:12.0%

Extinguishing Media:ALCOHOL FOAM, DRY CHEMICAL, CARBON DIOXIDE.

Fire Fighting Procedures:USE NIOSH/MSHA APPROVED SCBA AND FULL PROTECTIVE EQUIPMENT .

Unusual Fire/Explosion Hazard:CLOSED CONTAINERS MAY EXPLODE IF EXPOSED TO HIGH HEAT.

=====
Accidental Release Measures
=====

Spill Release Procedures:WEAR SUITABLE PROT CLTHG. SHUT OFF IGNIT SOURCES, NO FLARES, SMOKING OR FLAMES IN AREA. STOP LEAK IF YOU CAN DO SO W/OUT RISK. USE WATER SPRAY TO REDUCE VAPS. TAKE UP W/SAND OR



MATERIAL SAFETY DATA SHEET

SECTION 1: CHEMICAL PRODUCT AND COMPANY IDENTIFICATION

PRODUCT: M-Prep Conditioner A

October 8, 2008

Vishay Micro-Measurements
Post Office Box 27777
Raleigh, NC 27611

MSDS # MGM046N

919-365-3800

CHEMTREC 1-800-424-9300 (U.S.)
703-527-3887 (Outside U.S.)

NOTE: CHEMTREC numbers to be used only in the event of chemical emergencies involving a spill, leak, fire, exposure or accident involving chemicals.

SECTION 2: HAZARDOUS INGREDIENTS / IDENTITY INFORMATION

CAS NUMBER	CHEMICAL IDENTITY	%
7664-38-2	Phosphoric Acid	5.0-6.0
7732-18-5	Distilled Water	93.5-94.9

SECTION 3: HEALTH HAZARD DATA

Routes of Entry:

Inhalation: YES **Skin:** YES **Ingestion:** Accidental

Health Hazards (Acute and Chronic): None known.

Carcinogenicity: NTP: Not listed
 IARC Monographs: Not listed
 OSHA Regulated: Not listed

Signs and Symptoms of Exposure:

INHALATION: May cause severe irritation of respiratory system. In confined areas, vapors in high concentrations are anesthetic. Over-exposure may result in light-headedness and staggering gait. Mist may cause coughing, sneezing, salivation, and difficult breathing.

EYE CONTACT: May cause severe irritation or burns.

SKIN CONTACT: May cause severe irritation or burns.

INGESTION: May cause burns to mouth, throat, and stomach.

Conditions Generally Aggravated by Exposure: None identified.

SECTION 4: EMERGENCY AND FIRST AID PROCEDURES

INHALATION: If inhaled, remove to fresh air. If not breathing, give artificial respiration. If breathing is difficult, give oxygen. Prompt action is essential.

EYE CONTACT: In case of eye contact, immediately flush with plenty of water for at least fifteen minutes. Seek medical aid.

SKIN CONTACT: In case of contact, immediately flush skin with plenty of water for at least fifteen minutes while removing contaminated clothing and shoes. Wash clothing before re-use.

INGESTION: CALL A PHYSICIAN. If swallowed, do NOT induce vomiting. If conscious, give water, milk, or milk of magnesia.

SECTION 5: FIRE AND EXPLOSION HAZARD DATA

Flash Point (Method Used): None

Flammable limits: LEL: N/A UEL: N/A

Extinguishing Media: Will not support combustion or burn.

Special Firefighting Procedures: If product is present in a fire, avoid exposure to skin and eyes from mists and splashes. Firefighters should wear standard protective clothing and adequate respiratory protection.

Unusual Fire and Explosion Hazards: May react with some metals including aluminum, magnesium, and zinc, resulting in evolution of hydrogen gas.

SECTION 6: ACCIDENTAL RELEASE MEASURES

Steps to be taken if material is released or spilled: Ventilate area. Absorb with absorbent material. Flush spill area with plenty of water.

SECTION 7: EXPOSURE CONTROLS -- PERSONAL PROTECTION

Respiratory Protection: Self-contained breathing apparatus is recommended for emergency use.

Ventilation:

Local Exhaust: Keep below TLV
Mechanical: Keep below TLV
Special: N/A
Other: N/A

Protective Gloves: Chemical resistant or rubber gloves recommended.

Eye Protection: Chemical safety glasses and faceshield recommended.

Other Protective Clothing or Equipment: Rubber apron or suitable protective clothing. Eye wash station and safety shower should be available in the work area.

Work / Hygienic Practices: Wash hands thoroughly after using and before eating, drinking or smoking.

SECTION 8: HANDLING AND STORAGE

Precautions to be taken in handling and storing: Store below 80°F (27°C). Keep containers tightly sealed. Avoid storing or mixing with materials containing chlorine.

Other Precautions: Avoid eye and skin contact. Avoid breathing mist.

SECTION 9: PHYSICAL AND CHEMICAL PROPERTIES

Boiling Point:	210°F to 212°F (99°C to 100°C)
Vapor Pressure (mmHg):	N/A
Vapor Density (Air = 1):	N/A
Specific Gravity (H₂O = 1):	≈ 1-1.1
Melting Point:	N/A
Evaporation Rate (BuAc = 1):	<1
Volatile Organic Compounds:	None
Solubility in Water:	Complete

Appearance and Odor: Clear to slightly turbid liquid; no odor.

SECTION 10: STABILITY AND REACTIVITY DATA

Stability: Stable under normal conditions of use and storage.

Conditions to Avoid: N/A

Incompatibility (Materials to Avoid): Alkaline materials and materials containing chlorine.

Hazardous Decomposition or By-products: Oxides of phosphorous.

Hazardous Polymerization: Will not occur.

SECTION 11: TOXICOLOGICAL INFORMATION
--

Phosphoric Acid

OSHA PEL:	1 mg/m ³ (TWA)
ACGIH TLV:	1 mg/m ³
OTHER:	N/A

Distilled Water

OSHA PEL:	Not established
ACGIH TLV:	Not established
OTHER:	Not established

SECTION 12: DISPOSAL CONSIDERATIONS
--

Waste Disposal Method: Dispose of in accordance with local, state, and federal environmental regulations.

SECTION 13: TRANSPORTATION INFORMATION

SHIPPING NAME	CLASS	PACKING GROUP	UN NUMBER
Corrosive Liquid, N.O.S. (Phosphoric Acid)	8	III	1760

SECTION 14: REGULATORY INFORMATION

SECTION 313 SUPPLIER NOTIFICATION:

This product contains a toxic chemical or chemicals (as listed below) subject to the reporting requirements of Section 313 Title III of the Superfund Amendment and Reauthorization Act of 1986 and 40 CFR Part 372.

CAS NUMBER	CHEMICAL NAME	% BY WEIGHT
7664-38-2	Phosphoric Acid	5.0-6.0

TSCA NOTIFICATION:

All components of this product are listed in the Toxic Substance Control Act Chemical Substance Inventory (TSCA).

SECTION 15: OTHER INFORMATION

To the best of our knowledge, the information provided above meets the requirements of the United States Occupational Safety and Health Act and regulations established under 29 CFR 1910.1200 (g)(2)(c)(1)-(4) for a mixture of hazardous chemicals which has not been tested as a whole. The data provided on this Material Safety Data Sheet is from manufacturers of the original components. Vishay Micro-Measurements specifically disclaims any and all form of liability and/or responsibility for the application of this product.



MATERIAL SAFETY DATA SHEET



SECTION 1: CHEMICAL PRODUCT AND COMPANY IDENTIFICATION

PRODUCT: M-Prep Neutralizer 5A

April 13, 2010

Vishay Measurements Group, Inc.
Post Office Box 27777
Raleigh, NC 27611

919-365-3800

CHEMTREC 1-800-424-9300 (U.S.)
703-527-3887 (Outside U.S.)

NOTE: CHEMTREC numbers to be used only in the event of chemical emergencies involving a spill, leak, fire, exposure or accident involving chemicals.

SECTION 2: HAZARDOUS INGREDIENTS / IDENTITY INFORMATION

CAS NUMBER	CHEMICAL IDENTITY	%
1336-21-6	Ammonium Hydroxide	<0.02
10101-89-0	Trisodium Phosphate	<0.05
12179-04-3	Sodium Tetraborate Pentahydrate	<0.01
7732-18-5	Distilled Water	99.92

SECTION 3: HEALTH HAZARD DATA

Routes of Entry:

Inhalation: YES **Skin:** YES **Ingestion:** Accidental

Health Hazards (Acute and Chronic): Ammonium hydroxide is irritating and corrosive to body tissues and a sensitized person may react to even dilute solutions.

Carcinogenicity: NTP: Not listed
 IARC Monographs: Not listed
 OSHA Regulated: Not listed

Signs and Symptoms of Exposure:

INHALATION: May cause headache, coughing, and possible lung damage (edema and difficulty in breathing). Excessive inhalation of vapors is irritating to the mucous membranes of the respiratory tract.

EYE CONTACT: May cause possible burning and reddening. Liquid contact to the eye can be severely damaging and can result in loss of vision.

SKIN CONTACT: May cause irritation, reddening, and possible burns.

INGESTION: May cause possible burning sensation. Ingestion is corrosive to the digestive tract.

Conditions Generally Aggravated by Exposure: Preclude from exposure anyone with eye or pulmonary disease.

SECTION 4: EMERGENCY AND FIRST AID PROCEDURES
--

INHALATION: Remove to fresh air. If breathing is difficult have a trained person administer oxygen. Keep warm and at rest, and contact physician promptly.

EYE CONTACT: Immediately flush with plenty of water for at least 15 minutes while holding the eyelids open. Contact physician, preferably an ophthalmologist.

SKIN CONTACT: Flush with plenty of water while removing contaminated clothing. Wash affected area with soap and water. Launder contaminated clothing before reuse. Seek medical aid if irritation persists.

INGESTION: If conscious, promptly give lots of water, dilute vinegar, or citrus juices to drink, followed by milk. Do NOT induce vomiting. Contact physician.

SECTION 5: FIRE AND EXPLOSION HAZARD DATA
--

Flash Point (Method Used): NONE

Flammable limits: LEL: N/A UEL: N/A

Extinguishing Media: Will not support combustion.

Special Firefighting Procedures: Use media appropriate to surrounding fire conditions. Use cold water spray to control vapors and cool fire exposed containers.

Unusual Fire and Explosion Hazards: When heated, material will emit anhydrous ammonia vapor which necessitates respiratory and eye protection for firefighting. Use protective clothing.

SECTION 6: ACCIDENTAL RELEASE MEASURES

Steps to be taken if material is released or spilled: Ventilate area. Absorb with absorbent material. Neutralize with dilute acid. Flush spill area with plenty of water.

SECTION 7: EXPOSURE CONTROLS -- PERSONAL PROTECTION

Respiratory Protection: For air contaminants above TLV or permissible limits use NIOSH approved respirator for organic vapors.

Ventilation:

Local Exhaust: Keep below TLV
Mechanical: Keep below TLV
Special: N/A
Other: N/A

Protective Gloves: Neoprene or rubber gloves are recommended.

Eye Protection: Full face shield or chemical safety goggles are recommended.

Other Protective Clothing or Equipment: Rubber apron is recommended. Safety shower and eyewash should be available in work area.

Work / Hygienic Practices: Use good housekeeping practices. Wash thoroughly after use.

SECTION 8: HANDLING AND STORAGE

Precautions to be taken in handling and storing: Store below 80°F (27°C) in dry place. Keep containers tightly sealed.

Other Precautions: Avoid breathing vapors and direct contact.

SECTION 9: PHYSICAL AND CHEMICAL PROPERTIES

Boiling Point: 212°F (100°C)
Vapor Pressure (mmHg): 760 mmHg @ 100°C
Vapor Density (Air = 1): 1.0
Specific Gravity (H₂O = 1): 1.0
Melting Point: 32°F (0°C)
Evaporation Rate (BuAc = 1): <1
Volatile Organic Compounds: 0%
Solubility in Water: 100%

Appearance and Odor: Colorless liquid; mild ammonia odor.

SECTION 10: STABILITY AND REACTIVITY DATA
--

Stability: Stable.

Conditions to Avoid: Adding Sodium Hydroxide to this material and/or heating will volatilize Ammonia.

Incompatibility (Materials to Avoid): Acids, peroxides, metallic copper, tin, zinc, and their alloys, halogenated compounds.

Hazardous Decomposition or By-products: None known.

Hazardous Polymerization: Will not occur.

SECTION 11: TOXICOLOGICAL INFORMATION
--

Ammonium Hydroxide

OSHA PEL:	35 ppm (STEL)
ACGIH TLV:	35 ppm (STEL)
OTHER:	N/A

Trisodium Phosphate

OSHA PEL:	Not established
ACGIH TLV:	Not established
OTHER:	N/A

Sodium Tetraborate Pentahydrate

OSHA PEL:	Not established
ACGIH TLV:	1 mg/m ³
OTHER:	N/A

Distilled Water

OSHA PEL:	Not established
ACGIH TLV:	Not established
OTHER:	N/A

SECTION 12: DISPOSAL CONSIDERATIONS
--

Waste Disposal Method: Neutralize absorbent material with dilute acid. Dispose of in accordance with local, state, and federal regulations.

SECTION 13: TRANSPORTATION INFORMATION

SHIPPING NAME	CLASS	PACKING GROUP	UN NUMBER
Corrosive Liquids, N.O.S. (Ammonium Hydroxide)	8	III	1760

SECTION 14: REGULATORY INFORMATION

SECTION 313 SUPPLIER NOTIFICATION:

This product contains a toxic chemical or chemicals (as listed below) subject to the reporting requirements of Section 313 Title III of the Superfund Amendment and Reauthorization Act of 1986 and 40 CFR Part 372.

CAS NUMBER	CHEMICAL NAME	% BY WEIGHT
------------	---------------	-------------

NONE

TSCA NOTIFICATION:

All components of this product are listed in the Toxic Substance Control Act Chemical Substance Inventory (TSCA).

SECTION 15: OTHER INFORMATION

To the best of our knowledge, the information provided above meets the requirements of the United States Occupational Safety and Health Act and regulations established under 29 CFR 1910.1200 (g)(2)(c)(1)-(4) for a mixture of hazardous chemicals which has not been tested as a whole. The data provided on this Material Safety Data Sheet is from manufacturers of the original components. Micro-Measurements specifically disclaims any and all form of liability and/or responsibility for the application of this product.

MATERIAL SAFETY DATA SHEET

DATE: 02/18/05

Revision #7 Page 1 of 2

Section 1

PACER TECHNOLOGY
9420 Santa Anita Avenue
Rancho Cucamonga, CA 91730

HAZARD RATING

2
1 x 1

For Chemical Emergency Only:

In the US & Canada (800) 424-9300
Int'l & Wash DC (COLLECT) (703) 527-3887
Telephone for Information:(909) 987-0550

PRODUCT IDENTIFICATION: ZAP-A-GAP CA+**Section 2 - HAZARDOUS INGREDIENTS INFORMATION:**

Hazardous Components (Common Names, CAS Number)	OSHA PEL	ACGIH TLV	OTHER LIMITS	% OPTION
Ethyl-2-Cyanoacrylate (7085-85-0)	NE	NE	0.2ppm TWA	60-100
Poly (Methyl Methacrylate) (9011-14-7)	NE	NE		10-30
Hydroquinone* (123-31-9)	2mg/m3	2mg/m3		0-1

*This ingredient is subject to the reporting requirements of Section 313 of Title III of the Superfund Amendments & Reauthorization Act of 1986 (SARA) and 40 CFR 372.

Section 3 - PHYSICAL/CHEMICAL CHARACTERISTICS:

Boiling Point: 365 F Specific Gravity (H2O=1): 1.06
 Vapor Density (Air=1): nil-NE Melting Point: NE
 Vapor Pressure (mm Hg): 1 @ 20 C Evaporation Rate (Butyl acetate=1): nil-NE
 Solubility in Water: Insoluble, material reacts to hardened mass for non-hazardous waste.
 Appearance & Odor: Transparent water-white to straw colored liquid with stimulative odor.

Section 4 - FIRE AND EXPLOSION HAZARD DATA:

Flash Point (Method Used): 185 F (TCC) Flammable Limits: LEL: NE UEL: NE
 Extinguishing Media: Flush with large amounts of water or dry chemical extinguisher.
 Special Fire Fighting Procedures: Fumes may be irritating if not burning and require air supply with goggles while applying large amounts of water or dry chemical extinguisher.
 Unusual Fire and Explosion Hazards: None. Combustible requiring the above procedures.

Section 5 - REACTIVITY DATA:

Stability: Stable XX Conditions to Avoid: Excessive heat above 176 F, moisture and alkalines. Stable up to 122 F. Store in a cool dry place.
 Incompatibility (Materials to Avoid): Polymerized by water, alcohol, amines, alkaline materials and direct UV.
 Hazardous Decomposition Products: Combustible by-products of carbon monoxide/dioxide.
 Hazardous Polymerization: May Not Occur XX

Section 6 - HEALTH HAZARD DATA:

Route(s) of Entry: Inhalation: Yes Skin: NO Ingestion: LD50 = 12.2cc/kg
 Health Hazards (Acute and Chronic): (mice)
 Acute - Irritates eyes, mucous membranes.
 Chronic - No residual effects of acute properties.

Carcinogenicity: NTP: No IARC Monographs: No OSHA Regulated: No

Signs and Symptoms of Exposure & First Aid Procedures:

Eye contact - Tearing from eye irritation. Remove to fresh air. Flush areas of contact with water. Adhesive will disassociate from eye/eyelids over time, usually within several hours. Temporary weeping of eyes/double vision may be experienced until clearance is achieved.

Skin contact - Immerse bonded areas in warm, soapy water. Peel or roll skin apart. Remove cured adhesive with several applications of warm, soapy water. Prolonged or repeated contact at elevated levels may cause dermatitis in sensitive individuals.

Inhalation - Irritation of mucous membranes/coughing. Remove to fresh air. Prolonged or repeated exposure at elevated levels may produce allergic reactions with asthma-like symptoms in sensitive individuals.

Ingestion - Lips may become stuck together: apply copious amounts of warm water & encourage wetting/pressure from saliva inside mouth. Peel or roll (do not pull) lips apart. It is almost impossible to swallow cyanoacrylate as adhesive solidifies upon contact with saliva & may adhere to inside of mouth. Saliva will lift adhesive in 1-2 days, avoid swallowing adhesive after detachment.

Medical Conditions Generally Aggravated by Exposure: Pre-existing skin, eye and respiratory disorders may be aggravated by exposure.

Section 7 - PRECAUTIONS FOR SAFE HANDLING AND USE:

Steps to Be Taken in Case Material is Released or Spilled: Polymerize with water. Solid material may be scraped from surface.

Waste Disposal Method: Incinerate solid combustible waste or dump as chemical waste according to local, state and federal regulations.

Precautions to Be Taken in Handling and Storing: Avoid contact with clothing as contact can cause burn. Avoid moisture, direct UV-sunlight and do not store above 25 C. Keep containers closed tightly when not in use. Ideal storage: 5-10 C.

Other Precautions: Avoid breathing vapor, contact with eyes/skin. Allow product to reach room temperature before use.

Section 8 - CONTROL MEASURES:

Respiratory Protection (Specify Type): A NIOSH-approved organic vapor canister may be used to maintain vapor concentration below TLV.

Ventilation: Local Exhaust: To maintain vapor concentration below TLV.

Mechanical (General): Large amounts used to 0.2ppm.

Protective Clothing or Equipment: Safety glasses with side shield, Vinyl (polyethylene) non-sticking gloves, rubber apron to protect clothing.

Work/Hygienic Practices: Soap and water helps remove adhesive from skin.

NE = Not established

The data contained herein is based upon information that Pacer Technology believes to be reliable. Users of this product have the responsibility to determine the suitability of use and to adopt all necessary precautions to ensure the safety and protection of property and persons involved in said use. All statements or suggestions are made without warranty, express or implied, regarding accuracy of the information, the hazards connected with the use of the material or the results to be obtained from the use thereof.

MATERIAL SAFETY DATA SHEET

DATE: 02/18/05

Revision #4 Page 1 of 2

Section 1

PACER TECHNOLOGY
9420 Santa Anita Avenue
Rancho Cucamonga, CA 91730

HAZARD RATING

3
2 x 0

For Chemical Emergency:

In the US & Canada (800) 424-9300
Int'l & Wash DC (COLLECT) (703) 527-3887
Telephone for Information: (909) 987-0550

PRODUCT IDENTIFICATION: ZIP KICKER ACCELERATOR FOR SUPER GLUES**Section 2 - HAZARDOUS INGREDIENTS INFORMATION:**

Hazardous Components (Common Names, CAS Number)	OSHA PEL	ACGIH TLV	OTHER LIMITS	% OPTION
Aliphatic Petroleum (64742-89-8)	300ppm	300ppm	TLV/STEL=400ppm	80-100%
Alkyl Toluidines (99-97-8)	NE	NE	NE	6-12%
Xylene (1330-20-7) *	100ppm	100ppm	TLV/STEL=150ppm	2-6%
Ethylbenzene (100-41-4) *	100ppm	100ppm	TLV/STEL-125ppm	1-3%

- This ingredient is subject to the reporting requirements of Section 313 of Title III of the Superfund Amendments & Reauthorization Act of 1986 (SARA) and 40 CFR 372.

Note: Product contains a bittering agent to discourage ingestion via drinking.

Section 3 - PHYSICAL/CHEMICAL CHARACTERISTICS:

Boiling Point: 235-284F	Specific Gravity (H2O=1):	0.77
Vapor Density (Air=1): 3.8	Melting Point:	NE
Vapor Pressure (mm Hg): 30 @ 100F	Evaporation Rate (Butyl Acetate=1):	1.2
Solubility in Water: Negligible	V.O.C.:	770 g/L
Appearance & Odor: Water-white to straw colored liquid with hydrocarbon odor.		

Section 4 - FIRE AND EXPLOSION HAZARD DATA:

Flash Point (Method Used): 57 F (TCC) Flammable Limits: LEL: 1.0 UEL: 7.0

Extinguishing Media: Water fog, foam, dry chemical or carbon dioxide. Do not use direct stream of water as product may reignite on surface of water.

Special Fire Fighting Procedures: Warning - FLAMMABLE! Clear fire area of unprotected personnel. Do not enter confined fire space without full bunker gear (helmet with face shield, bunker coats, gloves & rubber boots), inc. a positive pressure NIOSH-approved self-contained breathing apparatus. Cool fire exposed containers with water.

Unusual Fire and Explosion Hazards: Containers exposed to intense heat from fires should be cooled with water to prevent vapor pressure buildup, which could result in container rupture.

Section 5 - REACTIVITY DATA:

Stability: Unstable ___ Stable XX Conditions to Avoid: heat, sparks & open flames.

Incompatibility (Materials to Avoid): Avoid strong oxidizing agents.

Hazardous Decomposition Products: Carbon monoxide & unidentified organic compounds may be formed during combustion.

Hazardous Polymerization: May Occur ___ May Not Occur XX

Section 6 - HEALTH HAZARD DATA: Route(s) of Entry:

Inhalation: (rat)4hrLC50=3400ppm Skin: (rat)DermalLD50=>4ml/kg Ingestion: (rat)OralLD50=>8ml/kg

Health Hazards (Acute and Chronic):

Acute - mildly irritating to eyes & skin, nose, throat & respiratory tract, early to moderate CNS depression may cause giddiness, headache, dizziness & nausea.

Chronic - in extreme cases, unconsciousness, aspiration pneumonitis may be evidenced by coughing, labored breathing & cyanosis (bluish skin), in extreme-severe cases death may occur.

Carcinogenicity: NTP: No IARC Monographs: Yes OSHA Regulated: No
Ethylbenzene = 2B

WARNING: THIS PRODUCT CONTAINS A CHEMICAL KNOWN TO THE STATE OF CALIFORNIA TO CAUSE CANCER, BIRTH DEFECTS OR OTHER REPRODUCTIVE HARM.

Signs and Symptoms of Exposure & First Aid Procedures:

Eye contact -irritation upon direct contact. Immediately flush eyes with water for 15 min. Get medical attention.

Skin contact -irritation upon direct contact. Remove contaminated clothing and wash before reuse. Wash affected areas with water, followed by soap & water. If irritation occurs, get medical attention. Prolonged or repeated contact can cause dermatitis in sensitive individuals.

Inhalation -vapors may be irritating to nose, throat & respiratory tract. Remove to fresh air and provide oxygen if breathing is difficult. Give artificial respiration if not breathing. Get medical attention.

Ingestion -do not induce vomiting. If vomiting occurs, keep head below hips to prevent aspiration of liquid into the lungs. Get medical attention. Product contains a bittering agent to discourage ingestion via drinking.

NOTE TO PHYSICIAN: If more than 2.0ml/kg has been ingested & vomiting has not occurred, emesis should be induced with supervision. Keep victim's head below hips to prevent aspiration; if symptoms such as loss of gag reflex, convulsions or unconsciousness occur before emesis, gastric lavage using a cuffed endotracheal tube should be considered.

Medical Conditions Generally Aggravated by Exposure: Preexisting skin disorders.

Section 7 - PRECAUTIONS FOR SAFE HANDLING AND USE:

Steps to Be Taken in Case Material is Released or Spilled: Warning - flammable! Ventilate area and remove all sources of ignition. Remove all unprotected personnel from hazard area. Avoid skin contact & breathing of vapors by using appropriate respirator & protective safety equipment. Confine & remove with inert absorbent. Dispose of absorbed material & water run-off in accordance with applicable federal, state, and local regulations.

Waste Disposal Method: Dispose of water flush solutions & absorbed material in non-leaking containers as hazardous waste according to all applicable regulations.

Precautions to Be Taken in Handling and Storing: Keep liquid & vapor away from heat, sparks & flame. Do not store near any ignition sources. Keep containers closed when not in use & use with adequate ventilation. Use wires to ground all transfer containers & equipment.

Other Precautions: Static electricity may create a fire hazard: bond & ground all equipment. Dispose of used containers as hazardous waste.

Section 8 - CONTROL MEASURES:

Respiratory Protection (Specify Type): Use a NIOSH-approved respirator in absence of proper ventilated environment. If needed, use air-purifying respirator for organic vapors when exposure may exceed occupational exposure limits.

Ventilation: Local Exhaust: Good Mechanical (General): As needed

Protective Clothing or Equipment: Safety glasses/goggles, chemical-resistant (ie. nitrile or polyvinyl alcohol material) gloves and other safety equipment to minimize contact.

Work/Hygienic Practices: Avoid direct contact with liquid. Wear protective safety equipment as necessary. Wash hands with soap & water and air-dry then launder any contaminated clothing before reuse.

NE = Not established

The data contained herein is based upon information that Pacer Technology believes to be reliable. Users of this product have the responsibility to determine the suitability of use and to adopt all necessary precautions to ensure the safety and protection of property and persons involved in said use. All statements or suggestions are made without warranty, express or implied, regarding accuracy of the information, the hazards connected with the use of the material or the results to be obtained from the use thereof.

G Hardware Data Sheets

Line-R®
Automatisk spenningsregulator
Modellene LE600I og LE1200I

Takk for at du kjøpte APC sin Line-R automatiske spenningsregulator! Vennligst fyll ut og send registreringsformulæret for produktgarantien, eller fyll ut et formulær online på www.apc.com.

Line-R korrigerer automatisk spenningsreduksjoner (ved å øke lave spenninger) og overspenninger (ved å senke høye spenninger) i strømmettet til nivåer som er sikre for datamaskiner og annet sensitivt utstyr. Line-R-enheten fra APC gir den høyeste grad av beskyttelse mot spenningsreduksjoner og -økninger i strømmettet, og er konstruert for mange års pålitelig og vedlikeholdsfri drift.

Bruk

FORSIKTIG: Det totale strømforbruket for alt utstyr som er pluggert inn i Line-R-enheten må ikke overstige den nominelle ytelsen for "Maks. nytteeffekt" som fremgår av tabellen *Spesifikasjoner*. Dersom den totale lasten overstiger den nominelle ytelsen, utløses overlastbryteren.

Line-R-enheten er konstruert for bruk sammen med spenningssensitivt utstyr, slik som: datamaskin, skjerm, blekkstråleskriver, skanner eller faksmaskin. Den er også konstruert for bruk med elektronisk hjemmeutstyr (TV'er, stereo-systemer, CD-spillere osv.).

Apparater som ikke er egnet for bruk med Line-R-enheten er utstyr slik som kjøleskap, fryseskap/-bokser, el-verktøy, klimaanlegg, avfukningsapparater, mikser eller enhver annen innretning som bruker en vekselstrømsmotor. Skal ikke brukes sammen med overlevelsesutstyr og apparater med et effektbehov som overstiger den nominelle ytelsen for "Maks. nytteeffekt" som fremgår av tabellen *Spesifikasjoner*.

Egenskaper

- ✓ Lyser når inngangsspenningen er høy.
- ✓ Blinker når inngangsspenningen er over det nominelle inngangsspenningsområdet.
- ✓ Inngangsspenningen er normal.
- ✓ Lyser når inngangsspenningen er lav.
- ✓ Blinker når inngangsspenningen er under det nominelle inngangsspenningsområdet.

Med nettbryteren slås strømmen til Line-R-enheten på/av (I = PÅ) / (O = AV).

Nettbryter

Medfølgende strøm-kabel koples til en av utgangene og til det aktuelle apparatet

Apparatets løse strøm-kabel koples til her og til en veggkontakt

Vekselstrømskontakter (4) (Kople til utstyr her)

Innstillbar spenningsvender (Se Veig inngangsspenning)

Trykknapp for overlastbryter

Nettbryter

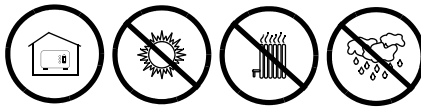
Line-R har en nettbryter (I = PÅ) / (O = AV) på frontpanelet som fungerer som hovedbryter for Line-R samt alt utstyr som er tilkoppelt enheten.

Trykknapp for overlastbryter

Line-R har en trykknapp for overlastbryteren på bakpanelet for beskyttelse mot overlast. Hvis overlastbryteren utløses, kopler du fra enheten som ble koplet til enheten sist og trykker deretter knappen helt inn.

Installasjon

- **Plassering** - Installer Line-R-enheten i et beskyttet miljø fritt for overdrevent stov, mekanisk vibrasjon, antennebare gasser og eksplosive eller korroderende omgivelser.



Ikke blokker ventilasjonsåpningene på toppen eller sidene av enheten. La det være minimum 2,5 cm klaring ved åpningene.



- **Veig inngangsspenning** - Line-R har en trepunkts innstillbar spenningsvender for tilpasning til den regionale inngangsspenningen der apparatet benyttes (eksempel: Russland - 220V, Danmark - 230V, Storbritannia - 240V). Skriv venderen for å velge korrekt spenning for ditt område.

- **Kople Line-R til en veggkontakt** - Trekk ut datamaskinens strøm-kabel fra baksiden på datamaskinen og bruk kabelen for å kople Line-R-enheten til veggkontakten. Bruk en av de to strøm-kablene som ble levert sammen med Line-R-enheten for å kople datamaskinen til en av de fire utgangene på baksiden av Line-R. Line-R-enheten bør kun benyttes i bygninger som har korrekt jording og på en kurs som er beskyttet med sikring eller overlastbryter.

- **Kople til utstyr** - Kople utstyret til utgangene på bakpanelet på Line-R og slå deretter utstyret PÅ. Utstyret blir ikke tilført nettspenning for Line-R-enheten slås PÅ.

- **FORSIKTIG:** Det totale strømforbruket for alt utstyr som er pluggert inn i Line-R-enheten må ikke overstige de nominelle ytelsene som fremgår av tabellen *Spesifikasjoner* nedenfor. Dersom den totale lasten overstiger den nominelle ytelsen, utløses trykknappen for overlastbryteren.

- **Slå PÅ Line-R** - Trykk nettbryteren på frontpanelet til posisjonen (I). Denne bryteren kan benyttes som hovedbryter for enheten samt alt tilkoppelt utstyr.

Spesifikasjoner

Merkedata	Modell LE600I	Modell LE1200I
Maks. nytteeffekt	600 W eller 600 VA	1200 W eller 1200 VA
Nominell utgangsspenning	220, 230, eller 240 V (innstillbar)	
Nominell inngangsstrøm	2,6 A	5,2 A
Nominell inngangsspenning	250 V vekselspenning	
Tillatt inngangsspenningstoleranse	160 - 270 V (vender satt til 220V) 166 - 280 V (vender satt til 230V) 170 - 290 V (vender satt til 240V)	
Maks. tillatt inngangsspenning	300 V	
Strømtet	300 joule	
Utgangsstilling	+6%/-12%	
Reaksjonstid	< 2 vekselstrømsyklus	
Nytteeffekt	>92%	
Nominell frekvens	47 - 63 Hz	
Antall utganger	4	
Drifttemperatur	0 - 40°C	
Relativ fuktighet	0 - 95% ikke-kondenserende	
Mål	118 x 214 x 141 mm	
Vekt	3,1 kg	4,2 kg

Begrenset garanti

Vanlig garanti gjelder i to (2) år fra kjøpsdato. APC sin standardprosedyre er å bytte den originale enheten med en fabrikkoverhalt enhet. Kunder som er avhengige av å få tilbake den originale enheten grunnet gjenstandsmerking og avskrivingsruiner, må angi dette ved første kontakt med representanten fra tekniske support hos APC. APC vil sende bytteenheten straks den defekte enheten er mottatt på verkstedsavdelingen, eventuelt sende den umiddelbart mot at du oppgir et gyldig kredittkortnummer. Kunden betaler for forsendelsen av enheten til APC. APC betaler ordinære transportkostnader for forsendelse av bytteenheten til kundens adresse.

APC Kontaktinformasjon

Online teknisk support	http://support.apc.com
Internett	www.apc.com
USA/Canada	800 800 4272
Hele verden	+1 401 789 5735
India	1 800 4254 877 272
Europa, Midtøsten, Afrika	+35391 702020

LM35

Precision Centigrade Temperature Sensors

General Description

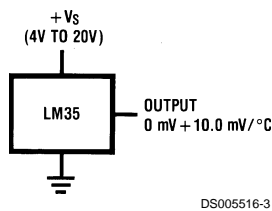
The LM35 series are precision integrated-circuit temperature sensors, whose output voltage is linearly proportional to the Celsius (Centigrade) temperature. The LM35 thus has an advantage over linear temperature sensors calibrated in ° Kelvin, as the user is not required to subtract a large constant voltage from its output to obtain convenient Centigrade scaling. The LM35 does not require any external calibration or trimming to provide typical accuracies of $\pm 1/4^\circ\text{C}$ at room temperature and $\pm 3/4^\circ\text{C}$ over a full -55 to $+150^\circ\text{C}$ temperature range. Low cost is assured by trimming and calibration at the wafer level. The LM35's low output impedance, linear output, and precise inherent calibration make interfacing to readout or control circuitry especially easy. It can be used with single power supplies, or with plus and minus supplies. As it draws only $60\ \mu\text{A}$ from its supply, it has very low self-heating, less than 0.1°C in still air. The LM35 is rated to operate over a -55° to $+150^\circ\text{C}$ temperature range, while the LM35C is rated for a -40° to $+110^\circ\text{C}$ range (-10° with improved accuracy). The LM35 series is available pack-

aged in hermetic TO-46 transistor packages, while the LM35C, LM35CA, and LM35D are also available in the plastic TO-92 transistor package. The LM35D is also available in an 8-lead surface mount small outline package and a plastic TO-220 package.

Features

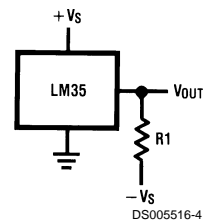
- Calibrated directly in ° Celsius (Centigrade)
- Linear + 10.0 mV/°C scale factor
- 0.5°C accuracy guaranteeable (at +25°C)
- Rated for full -55° to $+150^\circ\text{C}$ range
- Suitable for remote applications
- Low cost due to wafer-level trimming
- Operates from 4 to 30 volts
- Less than $60\ \mu\text{A}$ current drain
- Low self-heating, 0.08°C in still air
- Nonlinearity only $\pm 1/4^\circ\text{C}$ typical
- Low impedance output, $0.1\ \Omega$ for 1 mA load

Typical Applications



DS005516-3

FIGURE 1. Basic Centigrade Temperature Sensor (+2°C to +150°C)



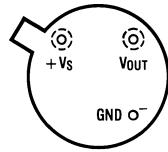
DS005516-4

Choose $R_1 = -V_S/50\ \mu\text{A}$
 $V_{\text{OUT}} = +1,500\ \text{mV}$ at $+150^\circ\text{C}$
 $= +250\ \text{mV}$ at $+25^\circ\text{C}$
 $= -550\ \text{mV}$ at -55°C

FIGURE 2. Full-Range Centigrade Temperature Sensor

Connection Diagrams

**TO-46
Metal Can Package***



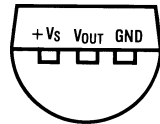
BOTTOM VIEW
DS005516-1

*Case is connected to negative pin (GND)

Order Number LM35H, LM35AH, LM35CH, LM35CAH or LM35DH

See NS Package Number H03H

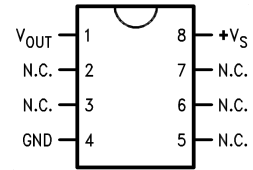
**TO-92
Plastic Package**



BOTTOM VIEW
DS005516-2

**Order Number LM35CZ,
LM35CAZ or LM35DZ**
See NS Package Number Z03A

**SO-8
Small Outline Molded Package**

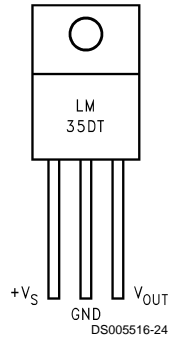


DS005516-21

N.C. = No Connection

**Top View
Order Number LM35DM
See NS Package Number M08A**

**TO-220
Plastic Package***



DS005516-24

*Tab is connected to the negative pin (GND).

Note: The LM35DT pinout is different than the discontinued LM35DP.

**Order Number LM35DT
See NS Package Number TA03F**

Absolute Maximum Ratings (Note 10)

If Military/Aerospace specified devices are required, please contact the National Semiconductor Sales Office/Distributors for availability and specifications.

Supply Voltage	+35V to -0.2V
Output Voltage	+6V to -1.0V
Output Current	10 mA
Storage Temp.:	
TO-46 Package,	-60°C to +180°C
TO-92 Package,	-60°C to +150°C
SO-8 Package,	-65°C to +150°C
TO-220 Package,	-65°C to +150°C
Lead Temp.:	
TO-46 Package, (Soldering, 10 seconds)	300°C

TO-92 and TO-220 Package, (Soldering, 10 seconds)	260°C
SO Package (Note 12)	
Vapor Phase (60 seconds)	215°C
Infrared (15 seconds)	220°C
ESD Susceptibility (Note 11)	2500V
Specified Operating Temperature Range: T_{MIN} to T_{MAX} (Note 2)	
LM35, LM35A	-55°C to +150°C
LM35C, LM35CA	-40°C to +110°C
LM35D	0°C to +100°C

Electrical Characteristics

(Notes 1, 6)

Parameter	Conditions	LM35A			LM35CA			Units (Max.)
		Typical	Tested Limit (Note 4)	Design Limit (Note 5)	Typical	Tested Limit (Note 4)	Design Limit (Note 5)	
Accuracy (Note 7)	$T_A = +25^\circ\text{C}$	±0.2	±0.5		±0.2	±0.5		°C
	$T_A = -10^\circ\text{C}$	±0.3			±0.3		±1.0	°C
	$T_A = T_{MAX}$	±0.4	±1.0		±0.4	±1.0		°C
	$T_A = T_{MIN}$	±0.4	±1.0		±0.4		±1.5	°C
Nonlinearity (Note 8)	$T_{MIN} \leq T_A \leq T_{MAX}$	±0.18		±0.35	±0.15		±0.3	°C
Sensor Gain (Average Slope)	$T_{MIN} \leq T_A \leq T_{MAX}$	+10.0	+9.9, +10.1		+10.0		+9.9, +10.1	mV/°C
Load Regulation (Note 3) $0 \leq I_L \leq 1$ mA	$T_A = +25^\circ\text{C}$	±0.4	±1.0		±0.4	±1.0		mV/mA
	$T_{MIN} \leq T_A \leq T_{MAX}$	±0.5		±3.0	±0.5		±3.0	mV/mA
Line Regulation (Note 3)	$T_A = +25^\circ\text{C}$	±0.01	±0.05		±0.01	±0.05		mV/V
	$4V \leq V_S \leq 30V$	±0.02		±0.1	±0.02		±0.1	mV/V
Quiescent Current (Note 9)	$V_S = +5V, +25^\circ\text{C}$	56	67		56	67		µA
	$V_S = +5V$	105		131	91		114	µA
	$V_S = +30V, +25^\circ\text{C}$	56.2	68		56.2	68		µA
	$V_S = +30V$	105.5		133	91.5		116	µA
Change of Quiescent Current (Note 3)	$4V \leq V_S \leq 30V, +25^\circ\text{C}$	0.2	1.0		0.2	1.0		µA
	$4V \leq V_S \leq 30V$	0.5		2.0	0.5		2.0	µA
Temperature Coefficient of Quiescent Current		+0.39		+0.5	+0.39		+0.5	µA/°C
Minimum Temperature for Rated Accuracy	In circuit of <i>Figure 1</i> , $I_L = 0$	+1.5		+2.0	+1.5		+2.0	°C
Long Term Stability	$T_J = T_{MAX}$, for 1000 hours	±0.08			±0.08			°C

Electrical Characteristics

(Notes 1, 6)

Parameter	Conditions	LM35			LM35C, LM35D			Units (Max.)
		Typical	Tested Limit (Note 4)	Design Limit (Note 5)	Typical	Tested Limit (Note 4)	Design Limit (Note 5)	
Accuracy, LM35, LM35C (Note 7)	$T_A = +25^\circ\text{C}$	± 0.4	± 1.0		± 0.4	± 1.0		$^\circ\text{C}$
	$T_A = -10^\circ\text{C}$	± 0.5			± 0.5		± 1.5	$^\circ\text{C}$
	$T_A = T_{\text{MAX}}$	± 0.8	± 1.5		± 0.8		± 1.5	$^\circ\text{C}$
	$T_A = T_{\text{MIN}}$	± 0.8		± 1.5	± 0.8		± 2.0	$^\circ\text{C}$
Accuracy, LM35D (Note 7)	$T_A = +25^\circ\text{C}$				± 0.6	± 1.5		$^\circ\text{C}$
	$T_A = T_{\text{MAX}}$				± 0.9		± 2.0	$^\circ\text{C}$
	$T_A = T_{\text{MIN}}$				± 0.9		± 2.0	$^\circ\text{C}$
Nonlinearity (Note 8)	$T_{\text{MIN}} \leq T_A \leq T_{\text{MAX}}$	± 0.3		± 0.5	± 0.2		± 0.5	$^\circ\text{C}$
Sensor Gain (Average Slope)	$T_{\text{MIN}} \leq T_A \leq T_{\text{MAX}}$	+10.0	+9.8, +10.2		+10.0		+9.8, +10.2	mV/ $^\circ\text{C}$
Load Regulation (Note 3) $0 \leq I_L \leq 1$ mA	$T_A = +25^\circ\text{C}$	± 0.4	± 2.0		± 0.4	± 2.0		mV/mA
	$T_{\text{MIN}} \leq T_A \leq T_{\text{MAX}}$	± 0.5		± 5.0	± 0.5		± 5.0	mV/mA
Line Regulation (Note 3)	$T_A = +25^\circ\text{C}$	± 0.01	± 0.1		± 0.01	± 0.1		mV/V
	$4\text{V} \leq V_S \leq 30\text{V}$	± 0.02		± 0.2	± 0.02		± 0.2	mV/V
Quiescent Current (Note 9)	$V_S = +5\text{V}, +25^\circ\text{C}$	56	80		56	80		μA
	$V_S = +5\text{V}$	105		158	91		138	μA
	$V_S = +30\text{V}, +25^\circ\text{C}$	56.2	82		56.2	82		μA
	$V_S = +30\text{V}$	105.5		161	91.5		141	μA
Change of Quiescent Current (Note 3)	$4\text{V} \leq V_S \leq 30\text{V}, +25^\circ\text{C}$	0.2	2.0		0.2	2.0		μA
	$4\text{V} \leq V_S \leq 30\text{V}$	0.5		3.0	0.5		3.0	μA
Temperature Coefficient of Quiescent Current		+0.39		+0.7	+0.39		+0.7	$\mu\text{A}/^\circ\text{C}$
Minimum Temperature for Rated Accuracy	In circuit of <i>Figure 1</i> , $I_L = 0$	+1.5		+2.0	+1.5		+2.0	$^\circ\text{C}$
Long Term Stability	$T_J = T_{\text{MAX}}$, for 1000 hours	± 0.08			± 0.08			$^\circ\text{C}$

Note 1: Unless otherwise noted, these specifications apply: $-55^\circ\text{C} \leq T_J \leq +150^\circ\text{C}$ for the LM35 and LM35A; $-40^\circ\text{C} \leq T_J \leq +110^\circ\text{C}$ for the LM35C and LM35CA; and $0^\circ\text{C} \leq T_J \leq +100^\circ\text{C}$ for the LM35D. $V_S = +5\text{Vdc}$ and $I_{\text{LOAD}} = 50 \mu\text{A}$, in the circuit of *Figure 2*. These specifications also apply from $+2^\circ\text{C}$ to T_{MAX} in the circuit of *Figure 1*. Specifications in **boldface** apply over the full rated temperature range.

Note 2: Thermal resistance of the TO-46 package is $400^\circ\text{C}/\text{W}$, junction to ambient, and $24^\circ\text{C}/\text{W}$ junction to case. Thermal resistance of the TO-92 package is $180^\circ\text{C}/\text{W}$ junction to ambient. Thermal resistance of the small outline molded package is $220^\circ\text{C}/\text{W}$ junction to ambient. Thermal resistance of the TO-220 package is $90^\circ\text{C}/\text{W}$ junction to ambient. For additional thermal resistance information see table in the Applications section.

Note 3: Regulation is measured at constant junction temperature, using pulse testing with a low duty cycle. Changes in output due to heating effects can be computed by multiplying the internal dissipation by the thermal resistance.

Note 4: Tested Limits are guaranteed and 100% tested in production.

Note 5: Design Limits are guaranteed (but not 100% production tested) over the indicated temperature and supply voltage ranges. These limits are not used to calculate outgoing quality levels.

Note 6: Specifications in **boldface** apply over the full rated temperature range.

Note 7: Accuracy is defined as the error between the output voltage and $10\text{mV}/^\circ\text{C}$ times the device's case temperature, at specified conditions of voltage, current, and temperature (expressed in $^\circ\text{C}$).

Note 8: Nonlinearity is defined as the deviation of the output-voltage-versus-temperature curve from the best-fit straight line, over the device's rated temperature range.

Note 9: Quiescent current is defined in the circuit of *Figure 1*.

Note 10: Absolute Maximum Ratings indicate limits beyond which damage to the device may occur. DC and AC electrical specifications do not apply when operating the device beyond its rated operating conditions. See Note 1.

Note 11: Human body model, 100 pF discharged through a 1.5 k Ω resistor.

Note 12: See AN-450 "Surface Mounting Methods and Their Effect on Product Reliability" or the section titled "Surface Mount" found in a current National Semiconductor Linear Data Book for other methods of soldering surface mount devices.

Datenblatt / Data Sheet

030893

**Materialprüfmaschine MTS 2/M
modernisiert mit der digitalen Zwick
Elektronik ZMART.PRO-testControl
Fmax 10 kN
Gebraucht**

**Materials Testing Machine MTS 2/M
modernized with the digital Zwick
electronics ZMART.PRO-testControl
Nominal Load 10 kN
Pre-owned**

bestehend aus**consisting of****MTS 2/M**

Beanspruchungseinheit 10 kN
Prüfraumbreite 440 mm
Traversenhub 1200 mm
Kraftaufnehmer 10 kN
Tischmodell
Anschlussbolzen Ø 20 mm
Faltenbalg
2 Kugelumlaufspindeln
2 Säulen

Load frame 10 kN
Width of testing area 440 mm
Crosshead travel max. 1200 mm
Load cell 10 kN
Table model
Mounting stud Ø 20 mm
Bellows cover
2 ball lead screws
2 columns

BZ1-MMFR010

Modernisierungseinheit
ZMART.PRO bestehend aus
testControl Elektronik mit 2
Steckplätzen, Antrieb 300 W

Modernization Unit ZMART.PRO
consisting of testControl electronics with
2 slots, drive 300 W

Änderungen vorbehalten / Subject to alterations

PZT5A & 5H Materials Technical Data (Typical Values)

Property	Symbol	Units	Material Type				
			3195STD	3195HD	3221HD	3203STD	3203HD
Dielectric Constant (1KHz)	K^T_{33}		1800	1900	3450	3250	3800
Dielectric Loss Factor (1KHz)	$\tan\delta_e$	%	1.8	1.8		2.0	2.0
Density	ρ	g/cm ³	7.7	7.8	7.87	7.7	7.87
Curie Point	T_c	°C	350	350	242	235	225
Mechanical Quality Factor	Q_m		80	80		30	30
Coercive Field (Measured < 1 Hz)	E_c	kV/cm	14.9	12.0	8.8	10.6	8.0
Remanent Polarization	P_r	μCoul/cm ²	39.2	39.0		37.2	39.0
Coupling Coefficients	k_p		0.63	0.65		0.69	0.75
	k_{33}		0.70	0.72	0.78	0.73	0.75
	k_{31}		0.35	0.36	0.44	0.41	0.43
	k_t		0.49	0.48	0.55	0.53	0.55
	k_{15}			0.59	0.78		0.78
Piezoelectric Charge (Displacement Coefficient)	d_{31}	Coul/N x 10 ⁻¹² (or) m/V x 10 ⁻¹²	-175	-190	-300	-275	-320
	d_{33}		350	390	595	550	650
Piezoelectric Voltage Coefficient (Voltage Coefficient)	g_{33}	V•m/N x 10 ⁻³	24.2	24.0	19.9	19.0	19.0
	g_{31}		-11.0	-11.3	-10.2	-9.6	-9.5
Elastic Modulus	Y^E_{11}	N/m ² x 10 ¹⁰	6.9	6.7	6.2	6.3	6.2
	Y^E_{33}		5.5	5.3	5.1	5.0	4.9
Frequency Constants Radial	N_r	KHz•cm	202			192	
Resonant Thickness	N_{tr}	KHz•cm	204	211	202	191	202
Anti-Resonant Thickness	N_{ta}	KHz•cm	229	236	235	222	236
Thermal Expansion (Perpendicular to poling)	α	ppm/°C		3.0			3.5
Specific Heat	C_p	J/kg•°C		440			420
		J/mol•°C		145			138
Thermal Conductivity with Au Electrodes	K_d	W/cm•°C		1.9-2.3			1.9-2.3
		W/m•°K		1.2			1.2
		W/m•°K		1.45			1.45
Poisson's Ratio	ν			0.31			0.31
Elastic Constants Short Circuit	S^E_{11}	x 10 ⁻¹² m ² /N		16.2	16.0		16.6
	S^E_{33}			18.6	19.8		21.0
Elastic Constants Open Circuit	S^D_{11}	x 10 ⁻¹² m ² /N		14.6	13.0		13.9
	S^D_{33}			9.6	7.7		8.8
Elastic Constants Short Circuit	Y^E_{11}	x 10 ¹⁰ N/m ²		6.7	6.2		6.2
	Y^E_{33}			5.3	5.1		4.9
Elastic Constants Open Circuit	Y^D_{11}	x 10 ¹⁰ N/m ²		6.8	7.8		7.0
	Y^D_{33}			10.6	13.0		11.0

Formulas	
Disc Capacitance	$(d^2 \cdot K^T_{33}) / (5.67 \cdot t)$
Plate Capacitance	$(l \cdot w \cdot K^T_{33}) / (4.45 \cdot t)$
Disc K^T_{33}	$(5.662 \cdot \text{Cap} \cdot t) / d^2$
Plate K^T_{33}	$(4.447 \cdot \text{Cap} \cdot t) / (l \cdot w)$
f_r (radial)	$N_r / (2.54 \cdot d)$
f_r (length)	$N_{31r} / (2.54 \cdot l)$
f_r (width)	$N_{31r} / (2.54 \cdot w)$
f_t (thickness)	$N_t / (2.54 \cdot t)$

Formula length, width, and diameter are for electroded area only.

Definitions			
$\tan\delta_e$	Dielectric Loss Factor	C	Capacitance (nF)
ρ	Mass Density of Ceramic	l	Length (in.)
T_c	Curie Point	w	Width (in.)
d_{33}	Direct Charge Coefficient	d	Diameter (in.)
d_{31}	Transverse Charge Coefficient	t	Thickness (10 ⁻³ in.)
E_c	Coercive Field	k_{33}	Direct Electromechanical Coupling Coefficient
g_{33}	Direct Voltage Coefficient	k_{31}	Transverse Electromechanical Coupling Coefficient
g_{31}	Transverse Voltage Coefficient	K^T_{33}	Free Dielectric Constant Measured Along Poling Axis
k_p	Planar Electromechanical Coupling Coefficient		
		N_r	Radial Frequency Constant
		N_t	Thickness Mode Frequency Constant
		P_r	Remanent Polarization
		Q_m	Mechanical Q (Quality Factor)
		Y^E_{33}	Direct Young's Modulus
		Y^E_{11}	Elastic Modulus
		f_r	Resonant Frequency
		f_a	Anti-Resonant Frequency

Model 420 Dual Phase Analogue Lock-in Amplifier

Feature

Scitec Instruments Model 420 is a dual phase analogue lock-in amplifier. Both single phase Model 410 and dual phase Model 420 are suitable for making amplitude and phase measurements but it is significantly easier with the Model 420.

- Dual phase instrument
- Differential or single-ended input
- Gain settings from 3 μ V to 1 V
- 10 Hz to 100 kHz
- High performance wide bandwidth input gain stage
- Analogue meter for display of output signals
- Output offset controls
- Output time constants from 100 μ s to 30 s
- 1F and 2F reference signal operation
- 90° step and fine phase control



Specifications

Input Signal Channel : The input signal channel amplifies the input signal to a level suitable for the demodulator. High performance, low-noise, broad-band amplifiers are used throughout. The input circuitry can accept a differential or single-ended input via the front panel signal input BNC.

- Input : High or low impedance differential or single ended via front panel BNC
- Sensitivity : 3 μ V to 1 V (for 1 V output) switched in 1, 3, 10 steps
- Input Impedance : 10^{12} W//1 nF, dc coupled
- Frequency : 10 Hz to 100 kHz
- Maximum Inputs : ± 16 V before input protection circuitry comes into operation. The input BNC has been tested for electrostatic discharge damage
- Input Noise Voltage : Other lock-in amplifier manufacturers give input noise values but without providing any definition of this specification. Indeed there is no meaningful definition of this specification in relation to lock-in amplifiers. As such, Scitec Instruments does not provide noise values and other manufacturers data sheets are considered misleading. Further details about input noise are available on request
- Gain Accuracy : 1%
- Gain Stability : 200 ppm/°C
- Dynamic Reserve : 60 dB limited by a maximum signal input noise voltage of 10 V

Demodulator : The output of the signal input stage is processed using two very high bandwidth demodulators each operating 90° apart from each other to produce the X and Y signals.

Low Pass Filter : The X and Y outputs from the demodulators are passed through two first order low pass filters and then amplified. The X and Y signals are combined to produce R, the modulus signal, where $R=(X^2+Y^2)^{1/2}$ before output via a front panel BNC.

- Time Constant : 100 μs to 30 s in 1, 3, 10 steps
- All Outputs : +/-1 V output corresponds to full scale input. Short circuit protection included
- Front Panel Output: X, Y or R switchable output
- Rear Panel Outputs: X, Y and R separate outputs
- Offset : Up to 1x full scale for both X and Y channels, switchable on or off

Reference Channel

- Frequency : 10 Hz to 100 kHz
- Input Impedance : 5.6 M ac coupled
- Trigger : Sine - 100 mV rms min (15 V max.) Pulse - 5 V, 95% mark/space ratio min.
- Acquisition Time : 10 s max.
- Phase Control : 90° steps + fine shift in range 0° - 100°
- Phase Drift : 0.1°/°C

General

- Power : 115 Vac, 230 Vac ; 50-60 Hz ; 10 VA max.
- Mechanical : 440(W) x 87(H) x 190(D) mm
- Temperature range : 0-50°C
- Warranty : 2 years from date of shipment

Standards

- Electrostatic Discharge : BS EN 61000-4-2 Level 2
- Surge : BS EN 61000-4-5 Level 3
- Burst & Transient : BS EN 61000-4-4 Level 2
- RF Emissions : BS EN 50081-2
- RF Immunity : BS EN 61000-4-3 / BS EN 50082-2
- Low Voltage Directive : BS EN 61010-1



VISHAY MICRO-MEASUREMENTS & SR-4

General Purpose
STRAIN GAGES

FOR COMPLETE TECHNICAL DATA, VISIT WWW.VISHAY.COM/REF/STRAINAGAGES

GRID RESISTANCE IN OHMS TC OF GAGE FACTOR, %/100°C
350.0±0.3% **(+1.2±0.2)**

GRID	GAGE FACTOR @ 24°C	TRANSVERSE SENSITIVITY
1		
2		
3		
NOM	2.11 NOM	(+0.4 ±0.2)%

ORDER	THERMAL OUTPUT COEFFICIENTS FOR 1018 STEEL	
	FAHRENHEIT	CELSIUS
0	-1.64E+2	-5.84E+1
1	+4.28E+0	+4.28E+0
2	-3.33E-2	-8.44E-2
3	+7.83E-5	+4.20E-4
4	-4.90E-8	-5.14E-7

FOIL LOT NUMBER
A66AD931

BATCH NUMBER
VF413677

ITEM CODE
17090

QUANTITY
5

CODE
171117



MADE IN UNITED STATES



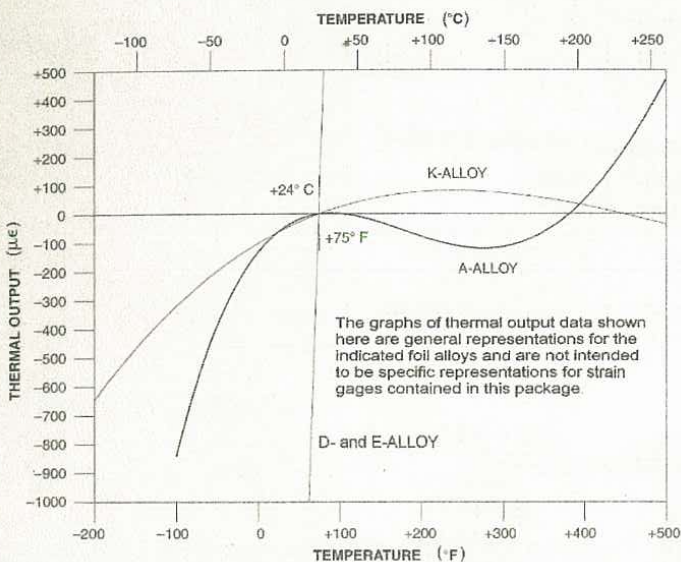
CEA-06-250WQ-350

TEMPERATURE COEFFICIENT OF RESISTANCE FOR BONDABLE RESISTORS

NICKEL - Pure nickel has the highest resistance-versus-temperature sensitivity of the three most commonly used materials and is normally selected for span-versus-temperature compensation of transducers. The temperature coefficient of resistance is +0.33% per deg Fahrenheit (+0.59% deg Celsius) over a temperature range of +50 to +150 deg Fahrenheit (+10 to +65 deg Celsius).

BALCO - With a lower temperature coefficient of resistance (TCR) and a higher resistivity than nickel, Balco yields higher resistance values more easily. The TCR for Balco is +0.24% per deg Fahrenheit (+0.43% per deg Celsius) over the temperature range of +50 to +150 deg Fahrenheit (+10 to +65 deg Celsius).

COPPER - Pure copper has the lowest and most linear TCR, as well as the lowest resistivity of the three materials, making it ideal for smaller scale temperature compensations in transducers. The TCR for pure copper is +0.20% per deg Fahrenheit (+0.36% per deg Celsius).



CALCULATION OF THERMAL OUTPUT FOR STRAIN GAGES

The thermal output of the gages contained in this package can be calculated from the following polynomial expression

$$a_0 + a_1 \cdot T + a_2 \cdot T^2 + a_3 \cdot T^3 + a_4 \cdot T^4$$

where a_N are the coefficients and T is temperature to the N th power.

The coefficients for both Celsius and Fahrenheit temperature scales are provided on the data label affixed to this package for strain gages.

A-Alloy, D-Alloy, and E-Alloy will generally use all five coefficients (a_0 to a_4) but K-Alloy will generally use only the first four coefficients (a_0 to a_3) with the fifth (a_4) being zero.

TEMPERATURE COEFFICIENT OF RESISTANCE FOR TEMPERATURE SENSORS

The temperature characteristics for all Vishay Micro-Measurements temperature sensors is provided in Tech Note TN-500. This document is available in PDF format at www.vishay.com/doc?11056.



VISHAY MICRO-MEASUREMENTS & SR-4

General Purpose
STRAIN GAGES

FOR COMPLETE TECHNICAL DATA, VISIT WWW.VISHAY.COM/REF/STRAINGAGES

GRID RESISTANCE IN OHMS	TC OF GAGE FACTOR, %/100°C
350.0±0.3%	(+1.2±0.2)

GRID	GAGE FACTOR @ 24°C	TRANSVERSE SENSITIVITY
1	2.100±0.5%	(-0.3 ±0.2)%
2		
3		
NOM		

ORDER	THERMAL OUTPUT COEFFICIENTS FOR 1018 STEEL	
	FAHRENHEIT	CELSIUS
0	-1.64E+2	-6.01E+1
1	+4.18E+0	+4.27E+0
2	-3.16E-2	-8.08E-2
3	+7.23E-5	+3.90E-4
4	-4.30E-8	-4.51E-7

FOIL LOT NUMBER
A66AD893

BATCH NUMBER
CF385612

ITEM CODE
3271

QUANTITY
5

CODE
162215



MADE IN UNITED STATES



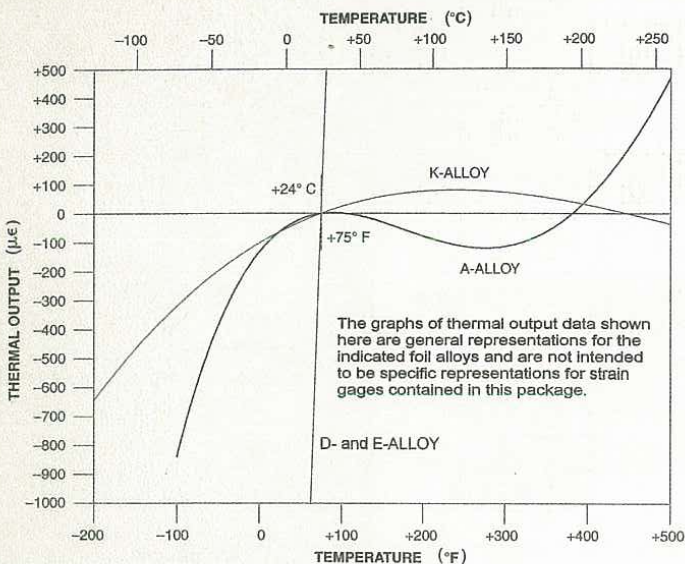
CEA-06-500UW-350

TEMPERATURE COEFFICIENT OF RESISTANCE FOR BONDABLE RESISTORS

NICKEL - Pure nickel has the highest resistance-versus-temperature sensitivity of the three most commonly used materials and is normally selected for span-versus-temperature compensation of transducers. The temperature coefficient of resistance is +0.33% per deg Fahrenheit (+0.59% deg Celsius) over a temperature range of +50 to +150 deg Fahrenheit (+10 to +65 deg Celsius).

BALCO - With a lower temperature coefficient of resistance (TCR) and a higher resistivity than nickel, Balco yields higher resistance values more easily. The TCR for Balco is +0.24% per deg Fahrenheit (+0.43% per deg Celsius) over the temperature range of +50 to +150 deg Fahrenheit (+10 to +65 deg Celsius).

COPPER - Pure copper has the lowest and most linear TCR, as well as the lowest resistivity of the three materials, making it ideal for smaller scale temperature compensations in transducers. The TCR for pure copper is +0.20% per deg Fahrenheit (+0.36% per deg Celsius).



CALCULATION OF THERMAL OUTPUT FOR STRAIN GAGES

The thermal output of the gages contained in this package can be calculated from the following polynomial expression

$$a_0 + a_1*T + a_2*T^2 + a_3*T^3 + a_4*T^4$$

where a_N are the coefficients and T^N is temperature to the Nth power.

The coefficients for both Celsius and Fahrenheit temperature scales are provided on the data label affixed to this package for strain gages.

A-Alloy, D-Alloy, and E-Alloy will generally use all five coefficients (a_0 to a_4) but K-Alloy will generally use only the first four coefficients (a_0 to a_3) with the fifth (a_4) being zero.

TEMPERATURE COEFFICIENT OF RESISTANCE FOR TEMPERATURE SENSORS

temperature characteristics for all Vishay Micro Measurements temperature sensors is provided in Tech Note TN-11056. This document is available in PDF format at www.vishay.com/doc?11056.



Strain Gage Installations with M-Bond 200 Adhesive

INTRODUCTION

Vishay Micro-Measurements Certified M-Bond 200 is an excellent general-purpose laboratory adhesive because of its fast room-temperature cure and ease of application. When properly handled and used with the appropriate strain gage, M-Bond 200 can be used for high-elongation tests in excess of 60 000 microstrain, for fatigue studies, and for one-cycle proof tests to over +200 °F [+95 °C] or below -300 °F [-185°C]. The normal operating temperature range is -25° to +150°F [-30° to +65°C]. M-Bond 200 is compatible with all Vishay Micro-Measurements strain gages and most common structural materials. When bonding to plastics, it should be noted that for best performance the adhesive flowout should be kept to a minimum. For best reliability, it should be applied to surfaces between the temperatures of +70° and +85°F [+20° to +30°C], and in a relative humidity environment of 30% to 65%.

M-Bond 200 catalyst has been specially formulated to control the reactivity rate of this adhesive. The catalyst should be used sparingly for best results. Excessive catalyst can contribute many problems; e.g., poor bond strength, age-embrittlement of the adhesive, poor glue-line thickness control, extended solvent evaporation time requirements, etc.

Since M-Bond 200 bonds are weakened by exposure to high humidity, adequate protective coatings are essential. This adhesive will gradually become harder and more brittle with time, particularly if exposed to elevated temperatures. For these reasons, M-Bond 200 is not generally recommended for installations exceeding one or two years.

For proper results, the procedures and techniques presented here should be used with qualified Vishay Micro-Measurements installation accessory products (refer to Catalog A-110). Those used in this procedure are:

- CSM Degreaser or GC-6 Isopropyl Alcohol
- Silicon Carbide Paper
- M-Prep Conditioner A
- M-Prep Neutralizer 5A
- GSP-1 Gauze Sponges
- CSP-1 Cotton Applicators
- PCT- 2M Gage Installation Tape

SHELF AND STORAGE LIFE

M-Bond 200 adhesive has a shelf life of three months at +75°F [+24°C] after opening and with the cap placed back onto the bottle immediately after each use.

Note: To ensure the cap provides a proper seal, the bottle spout should be wiped clean and dry before replacing the cap.

Unopened M-Bond 200 adhesive may be stored up to three months at +75°F [+24°C] or six months at +40°F [+5°C].

HANDLING PRECAUTIONS

M-Bond 200 is a modified alkyl cyanoacrylate compound. Immediate bonding of eye, skin or mouth may result upon contact. Causes irritation. The user is cautioned to: (1) avoid contact with skin; (2) avoid prolonged or repeated breathing of vapors; and (3) use with adequate ventilation. For additional health and safety information, consult the Material Safety Data Sheet, which is available upon request.

Note: Condensation will rapidly degrade adhesive performance and shelf life; after refrigeration the adhesive must be allowed to reach room temperature before opening, and refrigeration after opening is not recommended.

GAGE APPLICATION TECHNIQUES

The installation procedure presented on the following pages is somewhat abbreviated and is intended only as a guide in achieving proper gage installation with M-Bond 200. Vishay Micro-Measurements Application Note B-129 presents recommended procedures for surface preparation, and lists specific considerations which are helpful when working with most common structural materials.

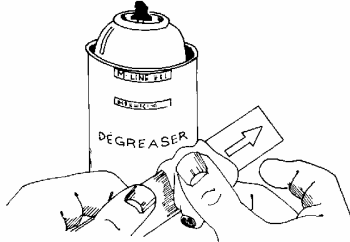
Strain Gage Installations with M-Bond 200 Adhesive



Instruction Bulletin B-127-14

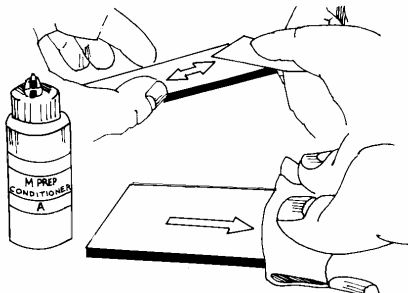
Vishay Micro-Measurements

Step 1



Thoroughly degrease the gaging area with solvent, such as CSM Degreaser or GC-6 Isopropyl Alcohol. The former is preferred, but there are some materials (e.g., titanium and many plastics) that react with strong solvents. In these cases, GC-6 Isopropyl Alcohol should be considered. All degreasing should be done with uncontaminated solvents—thus the use of “one-way” containers, such as aerosol cans, is highly advisable.

Step 2

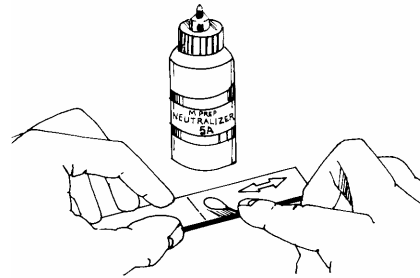


Preliminary dry abrading with 220- or 320-grit silicon-carbide paper is generally required if there is any surface scale or oxide. Final abrading is done by using 320-grit silicon-carbide paper on surfaces thoroughly wetted with M-Prep Conditioner A; this is followed by wiping dry with a gauze sponge. Repeat this wet abrading process with 400-grit silicon-carbide paper, then dry by slowly wiping through with a gauze sponge.

Using a 4H pencil (on aluminum) or a ballpoint pen (on steel), burnish (do not scribe) whatever alignment marks are needed on the specimen. Repeatedly apply M-Prep Conditioner A and scrub with cotton-tipped applicators until a clean tip is no longer discolored. Remove all residue

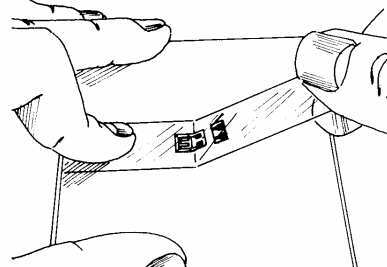
and Conditioner by again slowly wiping through with a gauze sponge. Never allow any solution to dry on the surface because this invariably leaves a contaminating film and reduces chances of a good bond.

Step 3



Now apply a liberal amount of M-Prep Neutralizer 5A and scrub with a cotton-tipped applicator. With a single, slow wiping motion of a gauze sponge, carefully dry this surface. Do not wipe back and forth because this may allow contaminants to be redeposited.

Step 4



Using tweezers to remove the gage from the transparent envelope, place the gage (bonding side down) on a chemically clean glass plate or gage box surface. If a solder terminal will be used, position it on the plate adjacent to the gage as shown. A space of approximately 1/16 in [1.6 mm] or more where space allows or application requires should be left between the gage backing and terminal. Place a 4- to 6-in [100- to 150-mm] piece of Vishay Micro-Measurements PCT-2M gage installation tape over the gage and terminal. Take care to center the gage on the tape. Carefully lift the tape at a shallow angle (about 45 degrees to specimen surface), bringing the gage up with the tape as illustrated above.

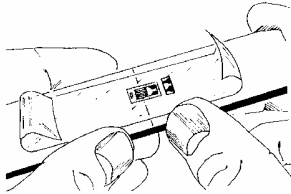
Strain Gage Installations with M-Bond 200 Adhesive



Instruction Bulletin B-127-14

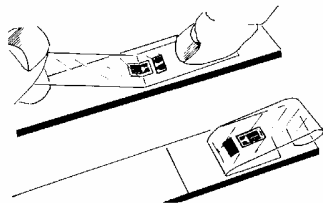
Vishay Micro-Measurements

Step 5



Position the gage/tape assembly so that the triangle alignment marks on the gage are over the layout lines on the specimen. If the assembly appears to be misaligned, lift one end of the tape at a shallow angle until the assembly is free of the specimen. Realign properly, and firmly anchor at least one end of the tape to the specimen. Realignment can be done without fear of contamination by the tape mastic if Vishay Micro-Measurements PCT-2M gage installation tape is used, because this tape will retain its mastic when removed.

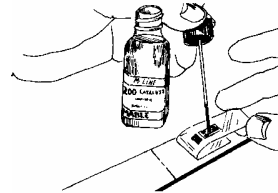
Step 6



Lift the gage end of the tape assembly at a shallow angle to the specimen surface (about 45 degrees) until the gage and terminal are free of the specimen surface. Continue lifting the tape until it is free from the specimen approximately 1/2 in [10 mm] beyond the terminal. Tuck the loose end of the tape under and press to the specimen surface so that the gage and terminal lie flat, with the bonding surface exposed.

Note: Vishay Micro-Measurements gages have been treated for optimum bonding conditions and require no pre-cleaning before use unless contaminated during handling. If contaminated, the back of any gage can be cleaned with a cotton-tipped applicator slightly moistened with M-Prep Neutralizer 5A.

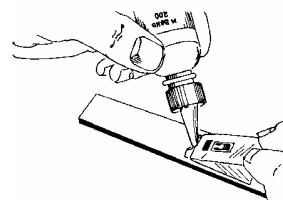
Step 7



M-Bond 200 catalyst can now be applied to the bonding surface of the gage and terminal. M-Bond 200 adhesive will harden without the catalyst, but less quickly and reliably. Very little catalyst is needed, and it should be applied in a thin, uniform coat. Lift the brush-cap out of the catalyst bottle and wipe the brush approximately 10 strokes against the inside of the neck of the bottle to wring out most of the catalyst. Set the brush down on the gage and swab the gage backing. Do not stroke the brush in a painting style, but slide the brush over the entire gage surface and then the terminal. Move the brush to the adjacent tape area prior to lifting from the surface. Allow the catalyst to dry at least one minute under normal ambient conditions of +75°F [+24°C] and 30% to 65% relative humidity before proceeding.

Note: The next three steps must be completed in the sequence shown, within 3 to 5 seconds. Read Steps 8, 9, and 10 before proceeding.

Step 8



Lift the tucked-under tape end of the assembly, and, holding in the same position, apply one or two drops of M-Bond 200 adhesive at the fold formed by the junction of the tape and specimen surface. This adhesive application should be approximately 1/2 in [13 mm] outside the actual gage installation area. This will insure that local polymerization that takes place when the adhesive comes in contact with the specimen surface will not cause unevenness in the gage glue line.

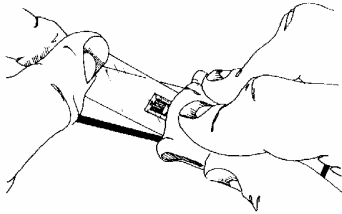
Strain Gage Installations with M-Bond 200 Adhesive



Instruction Bulletin B-127-14

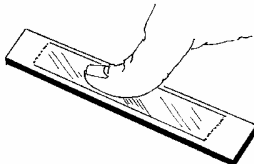
Vishay Micro-Measurements

Step 9



Immediately rotate the tape to approximately a 30-degree angle so that the gage is bridged over the installation area. While holding the tape slightly taut, slowly and firmly make a single wiping stroke over the gage/tape assembly with a piece of gauze bringing the gage back down over the alignment marks on the specimen. Use a firm pressure with your fingers when wiping over the gage. A very thin, uniform layer of adhesive is desired for optimum bond performance.

Step 10

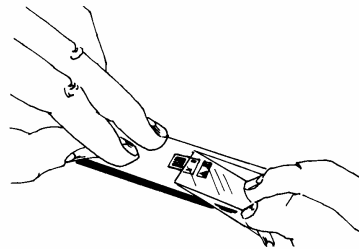


Immediately upon completion of wipe-out of the adhesive, firm thumb pressure must be applied to the gage and terminal area. This pressure should be held for at least one minute. In low-humidity conditions (below 30%), or if the ambient temperature is below +70°F [+20°C], this pressure application time may have to be extended to several minutes.

Where large gages are involved, or where curved surfaces such as fillets are encountered, it may

be advantageous to use preformed pressure padding during the operation. Pressure-application time should again be extended due to the lack of "thumb heat" which helps to speed adhesive polymerization. Wait two minutes before removing tape.

Step 11



The gage and terminal strip are now solidly bonded in place. It is not necessary to remove the tape immediately after gage installation. The tape will offer mechanical protection for the grid surface and may be left in place until it is removed for gage wiring. To remove the tape, pull it back directly over itself, peeling it slowly and steadily off the surface. This technique will prevent possible lifting of the foil on open-faced gages or other damage to the installation.

FINAL INSTALLATION PROCEDURE

1. Referring to Vishay Micro-Measurements Catalog A-110, select appropriate solder and attach leadwires. Prior to any soldering operations, open-faced gage grids should be masked with PDT-1 drafting tape to prevent possible damage.
2. Remove the solder flux with Rosin Solvent, RSK-1.
3. Select and apply protective coating according to the protective coating selection chart found in Catalog A-110.

Strain Gage Installations with M-Bond 200 Adhesive

Document No.: 11127

Page 4 of 4

Revision 17-Jan-05

INTERTECHNOLOGY
1-800-465-1600 INC.

1 Scarsdale Road
Don Mills, ON M3B 2R2

Tel: 416-445-5500
Fax: 416-445-1170
E-Mail: sales@intertechnology.com




**APC Smart-UPS 750VA USB RM 2U
230V**

Part Number: SUA750RMI2U



Output

Output Power Capacity	480 Watts / 750 VA
Max Configurable Power	480 Watts / 750 VA
Nominal Output Voltage	230V
Output Voltage Note	Configurable for 220 : 230 or 240 nominal output voltage
Output Voltage Distortion	Less than 5% at full load
Output Frequency (sync to mains)	47 - 53 Hz for 50 Hz nominal, 57 - 63 Hz for 60 Hz nominal
Waveform Type	Sine wave
Output Connections	(4) IEC 320 C13 
	(2) IEC Jumpers

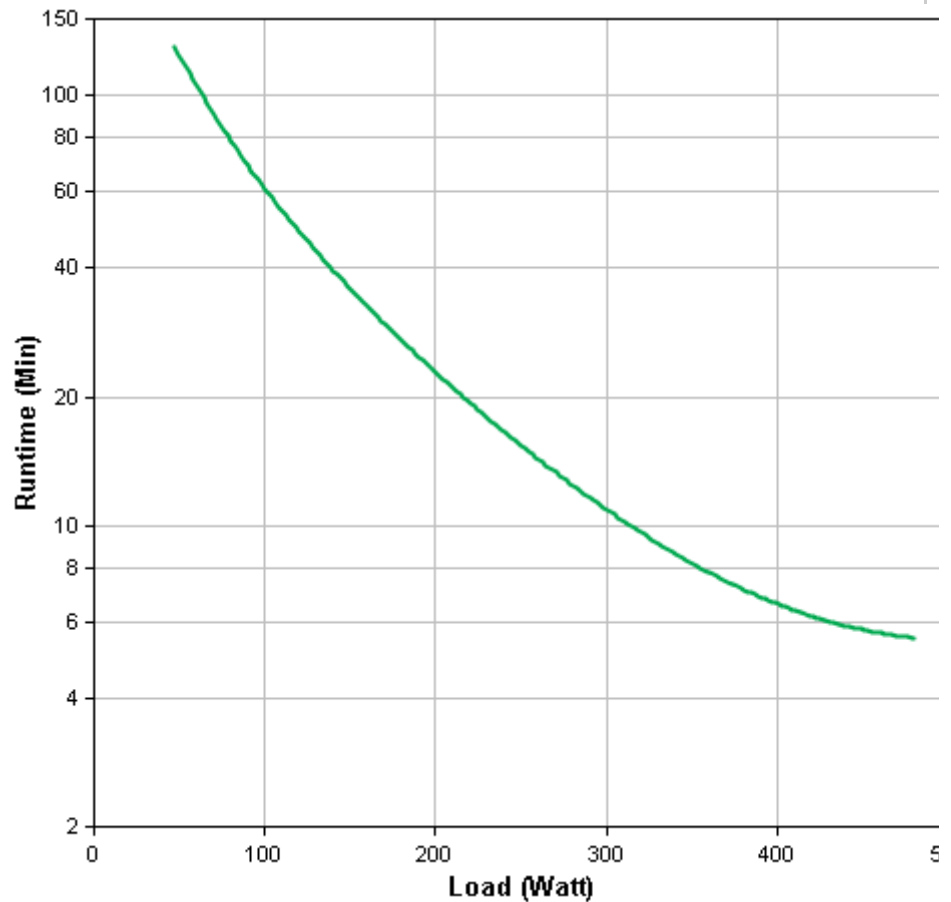
Input

Nominal Input Voltage	230V
Input Frequency	50/60 Hz +/- 3 Hz (auto sensing)
Input Connections	IEC-320 C14
Input voltage range for main operations	160 - 286V
Input voltage adjustable range for mains operation	151 - 302V

Batteries & Runtime

Battery Type	Maintenance-free sealed Lead-Acid battery with suspended electrolyte : leakproof
Typical recharge time	3 hour(s)
Replacement Battery	RBC22

Runtime Graph



Hover over the line on the graph above to view the runtime at any desired load

Curve fit to measured runtime data. All measurements taken with new, full charged batteries, at typical environmental conditions, with no electrical input and balanced resistive load (PF = 1.0) output.

[View Enlarged Graph](#)

[View Runtime Chart](#)

Communications & Management

Interface Port(s)	DB-9 RS-232, SmartSlot, USB
Available SmartSlot™	1
Interface Quantity	
Control panel	LED status display with load and battery bar-graphs and On Line : On Battery : Replace Battery : and Overload Indicators
Audible Alarm	Alarm when on battery : distinctive low battery alarm : configurable delays
Emergency Power Off (EPO)	Optional

Surge Protection and Filtering

Surge energy rating	480 Joules
Filtering	Full time multi-pole noise filtering : 0.3% IEEE surge let-through : zero clamping response time : meets UL 1449

Physical

Maximum Height	89.00 mm
Maximum Width	432.00 mm
Maximum Depth	457.00 mm
Rack Height	2U
Net Weight	21.82 KG
Shipping Weight	25.11 KG
Shipping Height	254.00 mm
Shipping Width	594.00 mm
Shipping Depth	603.00 mm
Color	Black
Units per Pallet	16.00

Environmental

Operating Environment	0 - 40 °C
Operating Relative Humidity	0 - 95%
Operating Elevation	0-3000 meters
Storage Temperature	-15 - 45 °C
Storage Relative Humidity	0 - 95%
Storage Elevation	0-15000 meters
Audible noise at 1 meter from surface of unit	36.00 dBA
Online Thermal Dissipation	68.00 BTU/hr

Conformance

Regulatory Approvals	C-tick,CE,EN 50091-1,EN 50091-2,TUV,VDE
Standard Warranty	2 years repair or replace
Environmental Compliance	RoHS 7b Exemption,China RoHS

**The time to recharge to 90% of full battery capacity following a discharge to shutdown using a load rated for 1/2 the full load rating of the UPS.

[Copyright](#) © American Power Conversion Corp., all rights reserved

For additional hardware specifications the author refers to research of December 2010 on the same project (Fintland, 2010).